ESABASE2/Debris Release 12.1

Technical Description

Contract No:	16852/02/NL/JA
Title:	PC Version of DEBRIS Impact Analysis Tool
ESA Technical Officer:	Mark Millinger
Prime Contractor:	FEV etamax GmbH
Authors:	A. Miller
Date:	2024-02-19
Reference:	R077-231rep_01_11_Debris_Technical Description.docx
Revision:	1.11
Status:	Final
Confidentiality:	public

FEV etamax GmbH

Phone: +49 (0)531.866688.0

Fax: +49 (0)531.866688.99

http://www.etamax.de

Table of Contents

Project: ESABASE2/Debris Release 12.1	Date:	2024-02-19
Technical Description	Revision:	1.11
Reference: R077-231rep_01_11_Debris_Technical Description.docx	Status:	Final

FEV etamax GmbH   Page 2 / 173

Project: ESABASE2/Debris Release 12.1	Date:	2024-02-19
Technical Description	Revision:	1.11
Reference: R077-231rep_01_11_Debris_Technical Description.docx	Status:	Final

FEV etamax GmbH   Page 3 / 173

Project: ESABASE2/Debris Release 12.1	Date:	2024-02-19
Technical Description	Revision:	1.11
Reference: R077-231rep_01_11_Debris_Technical Description.docx	Status:	Final

Document Information

I. Release Note

	Name	**Function**	**Date**	**Signature**
Prepared by:	A. Miller	PE	2024-02-19	*signed A. Miller*
Approved by:	Thomas Schenk	PM	2024-02-19	*signed T. Schenk*

II. Revision History

Revision	Date	Initials	Changed	Reason for Revision
1.0	2009-07-03	AG		New CI, content of r040_rep025_02_00_01_Technical Description.doc copied, description of Master2005 and MEM appended
1.1	2010-03-02	KB	section 2.2.1	ESTEC comments included
1.2	2012-11-27	AM	chapter 1, 2 and section 5.3.1	Description of MASTER 2009
1.3	2013-04-24	AM	chapter 1, 2, 5, 6, 7, 8	Introducing the extension for lunar orbit analysis, LunarMEM and trajectory file handling
1.3.1	2013-07-05	AM	Section 2.2.12.4, sections 2.1.3.3, 2.1.5.2, 2.1.6.2	Corrected G_k equation ('-' instead of '+'), p. 74, clarification of the used date for MASTER population snapshots
1.4	2014-03-19	AM	Chapter 1, 6, 8, Section 3.2	Introduction of the extension for Earth L1/L2 orbit analysis. Revised McHugh&Richardson BLE preconfiguration.
1.5	2014-07-25	AM	various	Description of ORDEM 3.0, correction of ESA Triple
1.6	2015-12-16	AM	chapter 1, 2 and section 5.3.1	Description of MEMr2
1.7	2017-09-14	AM	Section 5.4	Formula correction
1.8	2019-09-24	AM	chapter 1, 2 and section 5.3.1	Description of MASTER 8
1.9	2021-04-13	AM/MTR	Chapter 1 and sections 2.2.1 , 2.2.7, 2.2.8, 2.2.9, 5.5, 6.2, 6.3, 6.4, 6.6, 7.2, 7.3	Extended for use in interplanetary missions and MEM 3
1.10	2021-07-07	AM	Chapter 1 and sections	Include comments from ESA
1.11	2024-02-19	AM/TSC	various	Description of ORDEM 3.2 and change of company name

Project: ESABASE2/Debris Release 12.1		Date:	2024-02-19
Technical Description		Revision:	1.11
Reference: R077-231rep_01_11_Debris_Technical Description.docx		Status:	Final

FEV etamax GmbH   Page 5 / 173

III. Distribution List

Company (Dept.)	Name	Comment
ESA/ESTEC/TEC-EES	M. Millinger	
etamax	ESABASE2/Debris developers	
various	ESABASE2/Debris users	pdf

Project: ESABASE2/Debris Release 12.1		Date:	2024-02-19
Technical Description		Revision:	1.11
Reference: R077-231rep_01_11_Debris_Technical Description.docx		Status:	Final

FEV etamax GmbH

Page 6 / 173

IV. References

/1/   Drolshagen, G. and Borde, J., ESABASE/Debris, Meteoroid / Debris Impact Analysis, Technical Description, ESABASE-GD-01/1, 1992

/2/   Mandeville, J.C. , Enhanced Debris/Micrometeoroid Environment Models and 3-D Tools, Technical Note 3 - 452200: Numerical simulations and selected MLI damage equations, CERT/ONERA, August 1997

/3/   Anderson, B.J., Review of Meteoroids / Orbital Debris Environment, NASA SSP 30425, Revision A ,1991

/4/   Grün, E., Zook, H.A., Fechtig, H., Giese, R.H., Collisional Balance of the Meteoritic Complex, ICARUS 62, pp 244-277, 1985

/5/   Jenniskens, P., Meteor Stream Activity I, The annual streams, J. Astron. Astrophys. 287, 990-1013, 1994

/6/   McBride, N. et al. Asymmetries in the natural meteoroid population as sampled by LDEF, Planet. Space Sci.,43,757-764, 1995

/7/   Kessler, D.J, Zhang, J., Matney, M.J., Eichler, P., Reynolds, R.C., Anz-Meador, P.D. and Stansbery, E.G.; A Computer Based Orbital Debris Environment Model for Spacecraft Design and Observations in low Earth Orbit, NASA Technical Memorandum, NASA JSC, March 1996 (referenced to as NASA 96 Model)

/8/   Sdunnus, H., Meteoroid and Space Debris Terrestrial Environment Reference Model "MASTER" , Final Report of ESA/ESOC Contract 10453/93/D/CS, 1995

/9/   McBride, N. and McDonnell, J.A.M. Characterisation of Sporadic Meteoroids for Modelling, UNISPACE KENT, 23 April 1996

/10/   Taylor, A.D. The Harvard Radio Meteor Project meteor velocity distribution reappraised, Icarus, 116: 154-158, 1995

/11/   Cour-Palais, B.G.; Meteoroid environment model - 1969, NASA SP-8013, 1969

/12/   Taylor, A.D., Baggaley,W.J. and Steel,D.I.; Discovery of interstellar dust entering the Earth's atmosphere, Nature, Vol. 380, March 1996, pp 323-325

/13/   McBride, N., The Importance of the Annual Meteoroid Streams to Spacecraft and Their Detectors, Unit of Space Sciences and Astrophysics, The Physics Lab., The University, Canterbury UK, October 1997, presented at COSPAR 1997

/14/   S-50/95-SUM-HTS 1/2, HTS AG, August 1998 - ESABASE/Debris Enhanced Debris/Micro-meteoroid environment 3D software tools - Software User Manual

/15/   S-50/95-TN3-HTS 1/1, ACM, G.Scheifele, HTS AG, C. Lemcke - ESABASE/Debris Enhanced Debris/Micro-meteoroid environment 3D software tools - Technical Note 3

/16/   Mandeville, J.C. and M. Rival, Enhanced Debris/Micrometeoroid Environment Models and 3-D Tools, Review and Selection of a Model for ejecta Characterisation - Technical Note 2, CERT/ONERA, May 1996 - partial report 452200/01

/17/   Pauvert, C. , Enhanced Debris/Micrometeoroid Environment Models and 3-D Tools, Implementation of the Ejecta Model into ESABASE/Debris - Technical Note 4, ESA contract 11540/95/NL/JG MMS, October 1996 - DSS/CP/NT/056.96

/18/   Bunte, K.D.; Analytical Flux Model for High Altitudes, Technical Note of WP6 in ESA Contract 13145/98/NL/WK 'Update of Statistical Meteoroid/Debris Models for GEO', etamax space, Oct 2000

/19/   Kessler, D.J.; Matney, M.J.; A Reformulation of Divine's Interplanetary Model, Physics, Chemistry, and Dynamics of Interplanetary Dust, ASP Conference Series, Vol. 104, 1996

/20/   Wegener, P.; Bendisch, J.; Bunte, K.D.; Sdunnus, H.; Upgrade of the ESA MASTER Model; Final Report of ESOC/TOS-GMA contract 12318/97/D/IM; May 2000

/21/   Divine, N.; Five Populations of Interplanetary Meteoroids, Journal Geophysical Research 98, 17, 029 - 17, 048 1993

Project: ESABASE2/Debris Release 12.1	Date:	2024-02-19
Technical Description	Revision:	1.11
Reference: R077-231rep_01_11_Debris_Technical Description.docx	Status:	Final

FEV etamax GmbH   Page 7 / 173

/22/ Staubach, P., Numerische Modellierung von Mikrometeoriden und ihre Bedeutung für interplanetare Raumsonden und geozentrische Satelliten, Theses at the University of Heidelberg, April 1996

/23/ Bendisch, J., K. D. Bunte, S. Hauptmann, H. Krag, R. Walker, P. Wegener, C. Wiedemann, Upgrade of the ESA MASTER Space Debris and Meteoroid Environment Model – Final Report, ESA/ESOC Contract 14710/00/D/HK, Sep 2002

/24/ Mandeville, J.C., Upgrade of ESABASE/Debris, Upgrade of the Ejecta Model - Note, ONERA/DESP, Toulouse, August 2002

/25/ ESABASE/DEBRIS, Release 3, Software User Manual, ref. R033_r020_SUM, Version 1.0, etamax space, 09/2002

/26/ ESABASE2/DEBRIS, Release 1.2, Software User Manual, ref. R040-024rep_SUM, Rel. 1.0, etamax space, 06/2006

/27/ Liou, J.-C., M.J. Matney, P.D. Anz-Meador, D. Kessler, M. Jansen, J.R. Theall; The New NASA Orbital Debris Engineering Model ORDEM2000; NASA/TP-2002-210780, NASA, May 2002

/28/ Hörz, F., et al., Preliminary analysis of LDEF instrument A0187-1 "Chemistry of micrometeoroid experiment.", In LDEF-69 months in space: First post-retrieval symposium (A.S. Levine, Ed.), NASA CP-3134, 1991

/29/ Hörz, F., et al., Preliminary analysis of LDEF instrument A0187-1, the chemistry of micrometeoroid experiment (CME), In Hypervelocity Impacts in Space (J.A.M. McDonnell, Ed.), University of Kent at Canterbury Press., 1992

/30/ Humes, D.H., Large craters on the meteoroid and space debris impact experiment, In LDEF-69 months in space: First post-retrieval symposium (A.S. Levine, Ed.), NASA CP-3134, 1991

/31/ Humes, D.H., Small craters on the meteoroid and space debris impact experiment, In LDEF-69 months in space: Third post-retrieval symposium (A.S. Levine, Ed.), NASA CP-3275, 1993

/32/ Krisko, P.H., et al., EVOLVE 4.0 User's Guide and Handbook, LMSMSS-33020, 2000

/33/ Hauptmann, S., A. Langwost, ESABASE2/Debris Design Definition File, Ref. R040_r019, Rel. 1.5 (Draft), ESA/ESTEC Contract 16852/02/NL/JA "PC Version of Debris Impact Analysis Tool", etamax space, Jan 2004

/34/ Oswald, M.; Stabroth, S.; Wegener, P.; Wiedemann, C.; Martin, C.; Klinkrad, H. Upgrade of the MASTER Model. Final Report of ESA contract 18014/03/D/HK(SC), M05/MAS-FR, 2006.

/35/ Stabroth, S.; Wegener, P.; Klinkrad, H. MASTER 2005., Software User Manual, M05/MAS-SUM, 2006.

/36/ Jones, J. Meteoroid Engineering Model – Final Report, SEE/CR-2004-400, University of Western Ontario, London, Ontario, 28/06/2004

/37/ McNamara, H., et al. METEOROID ENGINEERING MODEL (MEM): A meteoroid model for the inner solar system

/38/ Flegel, S.; Gelhaus, J.; Möckel, M.; Wiedemann, C.; Kempf, D.; Krag, H. Maintenance of the ESA MASTER Model, Final Report of ESA contract 21705/08/D/HK, M09/MAS-FR, June 2011

/39/ Flegel, S.; Gelhaus, J.; Möckel, M.; Wiedemann, C.; Kempf, D.; Krag, H. MASTER-2009 Software User Manual, M09/MAS-SUM, June 2011

/40/ ESABASE Reference Manual, ESABASE/GEN-UM-061, Issue 2, Mathematics & Software Division, ESTEC, March 1994

/41/ Seidelmann P.K. et al., „Report of the IAU/IAG Working Group on cartographic coordinates and rotational elements: 2006", Celestial Mech. Dyn. Astr. 98: 155 – 180, 2007

/42/ Simon J.L. et al, "Numerical expression for precession formulae and mean elements for the Moon and the planets.", Astronomy and Astrophysics, vol. 282, no. 2, p. 663 – 683

/43/ Vallado D.A., "Fundamentals of Astrodynamics and Applications", Third Edition, Microcosm press and Springer, 2007

/44/ K. Ruhl, K.D. Bunte, ESABASE2/Debris software user manual, R077-232rep, ESA/ESTEC Contract 16852/02/NL/JA "PC Version of DEBRIS Impact Analysis Tool", etamax space, 2009

/45/ R.R. Bate, D.D. Mueller, J.E. White, "Fundamentals of Astrodynamics", 1971

/46/ http://naif.jpl.nasa.gov/naif/, 2012-10-01

/47/ NASA Orbital Debris Engineering Model ORDEM 3.0 – User's Guide, Orbital Debris Program Office, NASA/TP-2014-217370, April 2014

/48/ NASA Meteoroid Engineering Model Release 2.0 – User's Guide, Meteoroid Environment Office, George C. Marshall Space Flight Center, Huntsville, January 2013

/49/ Horstmann, A.; Hesselbach, S.; Kebschull, C.; Lorenz, J.; Wiedemann, C. Software User Manual - MASTER, M2018/MAS-SUM, May 2019

/50/ NASA NAIF: SPICE – An Observation Geometry System for Space Science Missions, https://naif.jpl.nasa.gov/naif/ (visited on 2019-06-20)

/51/ V. Dikarev et al., "Towards a New Model of the Interplanetary Meteoroid Environment", Adv. Space Res. 2002, 29 (28) pp. 1171–1175, https://www.sciencedirect.com/science/article/pii/S0273117702001345

/52/ A. Mints and V.Dikarev, IMEM 1.1 User manual, 2012

/53/ Soja, R. et al. (2019). IMEM2: A meteoroid environment model for the inner solar system. Astronomy & Astrophysics. 628. 10.1051/0004-6361/201834892

/54/ Interplanetary Meteoroid Environment Model 2 (IMEM2), Design Description of the Model and Implementation of observational Data, IRS, University of Stuttgart, IRS-2018-007IMEM2-V1.2, Contract No. 4000114513/15/NL/HK, March 2019

/55/ P. Strub, "The IMEM2 command line tool", Nov. 2019

/56/ Interplanetary Meteoroid Environment Model 2 (IMEM2), User Manual for the IMEM2 User Interface, IRS, University of Stuttgart, IRS-2017-011IMEM2-V1.0, Contract No. 4000114513/15/NL/HK, December 2017

/57/ CCSDS: *Orbit Data Messages*, Recommended Standard, CCSDS 502.0-B-2 Cor. 1, May 2012. https://public.ccsds.org/Pubs/502x0b2c1.pdf (visited on 2019-06-20)

/58/ https://naif.jpl.nasa.gov/pub/naif/utilities/PC_Windows_64bit/oem2spk.ug (visited on 2019-06-20)

/59/ Feldman, Dima & Shavitt, Yuval. (2007). An Optimal Median Calculation Algorithm for Estimating Internet Link Delays from Active Measurements. Fifth IEEE/IFIP Workshop on End-to-End Monitoring Techniques and Services, E2EMON'07. 1 - 7. 10.1109/E2EMON.2007.375318.

/60/ A.V.Moorhead et al., "NASA Meteoroid Engineering Model (MEM) version 3", July 22, 2019

/61/ NASA Orbital Debris Engineering Model ORDEM 3.1 – Software User Guide, Orbital Debris Program Office, NASA/TP-2019-220448, December 2019 (included in ORDEM 3.2 distribution)

V. List of Abbreviations

Abbreviation	Description
API	Application Program Interface
AU	Astronomical Unit (mean distance Sun – Earth)
CCSDS	Consultative Committee for Space Data Systems
ESA	European Space Agency
ESOC	European Space Operations Centre
ESTEC	European Space Research and Technology Centre
FAME	Fast Algorithm for Median Estimation
GEO	Geostationary Orbit
GTO	Geostationary Transfer Orbit
GUI	Graphical User Interface
ISS	International Space Station
L1/L2	Sun-Earth libration points L1 or L2, respectively
LEO	Low Earth Orbit
LDEF	Long Duration Exposure Facility
MASTER	Meteoroid and Space Debris Terrestrial Environment Reference (Model)
MEM	Meteoroid Engineering Model
MLI	Multi-layer Insulation
NAIF	Navigation and Ancillary Information Facility
NASA	National Astronautic and Space Administration
OEM	Orbit Ephmeris Message
ORDEM	Orbital Debris Engineering Model
PCHIP	Piecewise Cubic Hermite Interpolating Polynomials
RORSAT	Radar Ocean Reconnaissance Satellite
SIMT	Study Information Management Tool
SOI	Sphere Of Influence
STENVI	Standard Environment Interface
STS	Space Transportation System
USSTRATCOM	United States Strategic Command

Project: ESABASE2/Debris Release 12.1	Date:	2024-02-19
Technical Description	Revision:	1.11
Reference: R077-231rep_01_11_Debris_Technical Description.docx	Status:	Final

FEV etamax GmbH   Page 10 / 173

VI. List of Figures

Project: ESABASE2/Debris Release 12.1		Date:	2024-02-19
Technical Description		Revision:	1.11
Reference: R077-231rep_01_11_Debris_Technical Description.docx		Status:	Final

Project: ESABASE2/Debris Release 12.1		Date:	2024-02-19
Technical Description		Revision:	1.11
Reference: R077-231rep_01_11_Debris_Technical Description.docx		Status:	Final

Project: ESABASE2/Debris Release 12.1		Date:	2024-02-19
Technical Description		Revision:	1.11
Reference: R077-231rep_01_11_Debris_Technical Description.docx		Status:	Final

Project: ESABASE2/Debris Release 12.1	Date:	2024-02-19
Technical Description	Revision:	1.11
Reference: R077-231rep_01_11_Debris_Technical Description.docx	Status:	Final

VII. List of Tables

1 Introduction

In this document, the physical models and technical background of the space debris and meteoroid environment modelling and risk analysis on which the enhanced ESABASE2/Debris software tool is built are described.

The software architecture and design itself is described in the design definition file /33/, the software handling in the software user manual /26/.

In Chapter 2 all debris and meteoroid models which have been implemented in the enhanced version of the ESABASE2/Debris software tool are described.

Eight debris models are available within the ESABASE2/Debris simulation software:

- The NASA 90 model, which provides a simple and very fast debris flux calculation, but does not fully reflect the current knowledge of the Earth's debris environment, in particular the existence of a large number of particles on eccentric orbits. Additional shortcomings: the population is described by a small number of equations; the model is restricted to orbital altitudes below 1000km, and finally the age of the model.

- The NASA 96 model (also known as ORDEM 96) is the successor of the NASA 90 model and was implemented in former ESABASE/Debris versions. It is outdated and thus no longer included in ESABASE2/Debris.

- The MASTER 2001 model is based on numerical modelling of all known fragmentation events, SRM firings, NaK droplet releases, the Westford needles experiments, the generation of paint flakes by surface degradation effects, as well as the generation of ejecta particles and subsequent propagation of the particle orbits. The model provides realistic yearly population snapshots for the past and the future. The flux calculation is based on the analytic evaluation of the distributions of the size and the orbital elements of the particle population (MASTER 2001 Standard application). The model considers the population asymmetry induced by the asymmetric distribution of the particle orbits argument of perigee.

- The ORDEM2000 model describes the orbital debris environment in the low Earth orbit region between 200 and 2,000 km altitude. The model is appropriate for those engineering solutions requiring knowledge and estimates of the orbital debris environment (debris spatial density, flux, etc.). Incorporated in the model is a large set of observational data (both in-situ and ground-based), covering the object size range from 10 μm to 10 m and employing a new analytical technique utilizing a maximum likelihood estimator to convert observations into debris population probability distribution functions. These functions then form the basis of debris populations. ORDEM2000 uses a finite element model to process the debris populations to form the debris environment.

- The MASTER 2005 model is the successor of MASTER 2001. The model provides realistic four population snapshots per year for the past and the future. Compared to MASTER2001 lots of features have been significantly updated or added.

- The MASTER 2009 model is the successor of MASTER 2005. The model provides the same features as MASTER 2005. For MASTER 2009 several features were significantly updated, the Multi-Layer Insulation as a new source and the STENVI as a new possible interface were introduced.

Project: ESABASE2/Debris Release 12.1		Date:	2024-02-19
Technical Description		Revision:	1.11
Reference: R077-231rep_01_11_Debris_Technical Description.docx		Status:	Final

FEV etamax GmbH   Page 16 / 173

- The MASTER 8 model is the successor of MASTER 2009. The model provides the same features as MASTER 2009, but several features were significantly updated. With Condensed population a possibility was introduced to consider all sources combined as one population, speeding up the analyses.

- The ORDEM 3.0 model describes the orbital debris environment in the Earth orbit region between 100 and 40,000 km altitude. The model is appropriate for those engineering solutions requiring knowledge and estimates of the orbital debris environment (debris spatial density, flux, etc.). Incorporated in the model is a large set of observational data (both in-situ and ground-based), covering the object size range from 10 µm to 10 m and employing the Bayesian statistical model for population derivation. OREDEM 3.0 uses a finite element model to process the debris populations to form the debris environment.

- The ORDEM 3.2 model is an update of ORDEM 3.0. It incorporates all the features of ORDEM 3.0, the main differences are the update of the sources to the time range 2016 to 2050 and the change of the interpolation approach for the used reference data points in ORDEM 3.1. The latter change is the main reason of including and considering ORDEM 3.2 as an individual model in ESABASE2.

For meteoroids the omni-directional Grün model is maintained. It is described in this document.

Additionally, seven further meteoroid models are implemented in ESABASE2/Debris, Divine-Staubach, MEM, MEMr2, LunarMEM, MEM 3, IMEM and IMEM2.

- The Divine-Staubach meteoroid model is part of the MASTER 8 model. The model is based on the size and orbital element distributions of five meteoroid sub-populations, and thus provides directional information in the same way as the MASTER 8 debris model.

- The MEM meteoroid model, developed by The University of Western Ontario, is a parametric model of the spatial distribution of sporadic meteoroids by taking their primary source to be short-period comets with aphelia less than 7 AU. It considers the contribution to the sporadic meteor complex from long-period comets and includes the effects of the gravitational shielding and focussing of the planets.

- LunarMEM is a version of MEM which is tailored to the vicinity of the Moon and therefore applicable only up to a radius of ca. 66000 km around the Moon.

- MEM Release 2.0 (MEMr2) is the successor of the MEM model(s). It comprises three individual environment sub-models: for Earth Orbiting S/C; for Moon Orbiting S/C; and for Interplanetary S/C, that describe the background meteoroid environment for spacecraft in orbit around the Earth, Moon, and in interplanetary space.

- MEM 3 is the successor of the MEMr2 model. It drops the concept of individual environment sub-models but considers internally for the effect of the S/C being in the vicinity of a celestial body. Thus, MEM 3 describes the background meteoroid environment for spacecraft in the inner solar system considering the effects of the vicinity of the following celestial bodies: Earth, Moon, Mercury, Venus and Mars.

- IMEM models the orbits of particles from Jupiter-family comets and asteroids and was fitted largely to in situ data and infrared brightness measurements /51/, /52//51/.

Project: ESABASE2/Debris Release 12.1	Date:	2024-02-19
Technical Description	Revision:	1.11
Reference: R077-231rep_01_11_Debris_Technical Description.docx	Status:	Final

FEV etamax GmbH | Page 17 / 173

- IMEM2 is the follow-up approach of ESA's IMEM to model meteoroids in the Solar system. IMEM2 contains a dynamical engineering model of the dust component of the space environment using state-of-the-art knowledge of dust cloud constituents and their development under dynamical and physical effects /53/.

An enhanced stream model by Jenniskens, which is based on observation data gathered over a 10 year period, is available for the flux and damage analysis. This model includes directional information on the streams.

Further, in case of Grün, directional information is obtained by attempting to separate the β - meteoroids, which are driven away from the Sun into hyperbolic orbits by radiation pressure, from the α - meteoroids. An apex enhancement of the α - meteoroids and interstellar streams may introduce further directional information.

The meteoroid velocity distribution according to Taylor is available in ESABASE2/Debris for Grün model. This distribution is altitude enhanced for gravitational effects.

In the Chapter 3 the damage equations used in the software are described. A parametric approach has been chosen, allowing for flexibility in the usage of the damage equations. A new hole equation has been introduced, based on the latest research performed in this field at the University of Kent.

The behaviour of MLI as micro-particle debris shield was also investigated during the study. It was found that MLI can be characterised by the available parametric ballistic limit equations, either as single wall or multiple wall, depending on the analysis objectives.

In the Chapter 4, the Ejecta model is described. This feature of the ESABASE2/Debris software is based on a model developed by CERT/ONERA in Toulouse. The ejecta model has been updated, allows simulating the debris particle ejected from a primary impact with ray tracing.

In Chapter 5 the techniques used for the damage and risk analysis using ray tracing technique is lined out. The new tool relies entirely on ray tracing for the computation of impact fluxes, failure fluxes and cratering fluxes. The ray tracing scheme which is implemented also allows accounting for Earth shielding and flux enhancements due to spacecraft motion (also known as the K factor). The full implementation of ray tracing allowed a smooth implementation of the enhanced directional effects of the environment models. Additionally, the FAME algorithm used for the calculation of weak spots data in the simulation results is explained.

In Chapter 6 the extensions of the orbit generation techniques are described, which allow to apply the SAPRE propagator to lunar orbits. Also, the generation techniques of the L1/L2 orbits and interplanetary trajectories are described. For interplanetary trajectories, the technique relies on data from SPICE kernels and optionally OEM files.

Project: ESABASE2/Debris Release 12.1	Date:	2024-02-19
Technical Description	Revision:	1.11
Reference: R077-231rep_01_11_Debris_Technical Description.docx	Status:	Final

In Chapter 7 the modifications of the pointing facility are introduced that were performed for the application to lunar orbits and interplanetary trajectories.

Finally, in Chapter 8 the trajectory file handling process is outlined.

2 Environment Models

This chapter describes the environment models which are implemented in the ESABASE2/Debris software. In this document, environment refers to the micro-particle environment of micro-meteoroids (natural particles) and space debris (man-made particles).

Due to their different characteristics, the two environments are presented separately.

2.1 The Space Debris Environment Models

2.1.1 Introduction

ESABASE/Debris, release 2 contained three debris flux models. While the ***NASA 96*** and the ***MASTER 96 Hybrid model*** provided flux results including directional information, the ***NASA 90*** model describes the debris environment by means of a set of analytical equations.

For release 3 of ESABASE/Debris the MASTER 96 model has been replaced by the ***MASTER 2001 model***, which represents the state-of-the-art of debris modelling and offers some new features, which are available within ESABASE/Debris for the first time.

A major upgrade of the ESABASE software was performed in the framework of the "PC Version of Debris Impact Analysis Tool" contract. ESABASE/Debris was ported to the Windows PC platform. The ESABASE data model has been completely revised, a geometry modeller with basic CAD features was implemented and a state-of-the-art graphical user interface was developed. Additionally, NASA's ORDEM2000 debris model was implemented. Due to the major changes and to distinguish between the Unix and the PC version of ESABASE, the PC version is called ***ESABASE2***.

The following debris models are available in the latest release of ESABASE2/Debris:

NASA 90 Model (section 2.1.2)

This model has been the first more or less detailed description of the Earth's debris environment. It provides very fast, but less detailed debris flux analysis capabilities and is restricted to altitudes below 1000 km. The NASA 90 model has been maintained as an option and it is therefore briefly described in this document.

MASTER 2001 Model (Section 2.1.3)

The MASTER 2001 release (Ref. /23/) of the European MASTER model is based on a consequent upgrade and extension of the MASTER concept (Ref. /8/). The MASTER reference population as of May 1., 2001 now includes the population sources listed in Table 1:

Name	Origin	Particle size range
launch and mission related objects	all trackable objects except those generated by simulated fragmentation events	0.5 mm ... 4 mm (Westford Needles)

Name	Origin	Particle size range
	such as explosions or collisions (corresponds to the catalogued objects/TLE background population of MASTER '99); includes the Westford needles, which were released during two American experiments (MIDAS 4 & 6) in the early sixties	and 10 cm ... 10 m
fragments	resulting from and collisions	0.1 mm ... 10 m
NaK droplets	coolant droplets released by Russian RORSAT's	2 mm ... 4 cm
SRM slag particles	large particles released during the final phase of solid rocket motor firings	0.1 mm ... 3 cm
SRM Al$_2$O$_3$ dust	small particles released during solid rocket motor firings	1 µm ... 80 µm
paint flakes	resulting from surface degradation	2 µm ... 0.2 mm
ejecta	resulting from meteoroid and debris impacts on exposed surfaces	1 µm ... 5 mm

Table 1 Population sources considered in the MASTER model

One of the most demanding aspects of the recent upgrade of the MASTER model is its capability to allow for flux and spatial density analysis for the complete space age, which is based on 3-monthly population snapshots. Moreover, three future debris population scenarios are provided by means of the corresponding yearly population snapshots (Ref. /23/). These future sub-populations include all particles larger than 1mm. Due to its large relevance for the future debris population evolution, the fragments are sub-divided to explosion fragments and collision fragments.

Two flux analysis applications are offered by MASTER, the Analyst application and the Standard application. Since the database of the Analyst application is too big to be implemented into ESABASE2/Debris, the MASTER 2001 Standard application has been selected for the implementation.

ORDEM2000 Model (Section 2.1.4)

ORDEM2000 is NASA's debris engineering model and the successor of ORDEM96 (called NASA96 in ESABASE2/Debris). It is mainly based on measurement data originating from in-situ measurements, the examination of retrieved hardware and from ground based radar and optical observations. Auxiliary modelling with respect to the future space debris population was performed. The debris population data (spatial density, velocity distribution, inclination distribution) is provided by means of a so called Finite Element Model of the LEO Environment, and is provided by a set of pre-processed data files. For this purpose the region between 200-

Project: ESABASE2/Debris Release 12.1		Date:	2024-02-19
Technical Description		Revision:	1.11
Reference: R077-231rep_01_11_Debris_Technical Description.docx		Status:	Final

FEV etamax GmbH Page 21 / 173

and 2000-km altitudes is divided into (5 deg × 5 deg × 50 km) cells in longitude, latitude, and altitude, respectively.

To calculate the flux on an orbiting spacecraft, the orbit of the spacecraft has to be specified. The model divides the orbit of the spacecraft into the specified number of segments in equal mean longitude (i.e., equal time) and then calculates the flux, from particles of six different sizes (10 µm to 1 m), on the spacecraft at each segment. The output results are stored in a flux table. It includes the altitude and latitude of the spacecraft at each segment and the fluxes from particles of six different sizes at that location. At the end of the table, fluxes averaged over the number of segments are given.

MASTER 2005 Model (Section 2.1.5)

The latest release (Ref. /34/) of the European MASTER model is the successor of MASTER 2001. Compared to the previous version, the following features have been significantly updated or added in the MASTER 2005 release:

- Upgrade of the debris source models.

- Update of the reference population.

- Unified flux and spatial density computation concept.

- Implementation of damage laws.

- Flux and spatial density analysis for historic and future epochs.

In difference to MASTER 2001 now only one unified analysis application is offered with MASTER 2005.

MASTER 2009 Model (Section 2.1.6)

The latest release (Ref. /38/) of ESA's reference model − MASTER − is the successor of MASTER 2005. Compared to the previous version, the following improvements were done in the MASTER 2009 release:

- Population files for the time range 1957 − 2060.

- Consideration of future population down to 1 micrometer.

- Improvement of the small size region of fragmentation modelling for payloads and rocket bodies.

- Implementation of Multi-Layer Insulation as new debris source.

- Introducing of a Standard Environment Interface (STENVI).

- Possibility to overlay flux contributions from downloadable population clouds over background particulate environment.

- Introduction of a possibility to consider multiple target orbits.

In difference to MASTER 2005 an additional multidimensional distribution output (STENVI), which defines the cross-dependencies of the parameters in a better way, can be provided by MASTER 2009.

ORDEM 3.0 Model *(Section 2.1.7)*

ORDEM 3.0 is NASA's latest debris engineering model and the successor of ORDEM2000. It is mainly based on measurement data originating from in-situ measurements, the examination of retrieved hardware and from remote sensors (ground based radar and optical observations). The ORDEM 3.0 input debris populations are binned in quasi-orthogonal orbital elements. The bins vary with the parameter value and the bin sizes are chosen to complement actual population distributions. The final files are from the direct yearly input database of ORDEM 3.0.

ORDEM 3.0 provides a population brake down by type and material density in five populations: Intacts, Low-density fragments, Medium-density fragments and microdebris, High-density fragments and microdebris and RORSAT NaK coolant droplets. The populations are available for the time range from 2010 to 2035 and cover the Earth orbits from 100 km up to 40,000 km altitude.

To calculate the flux on an orbiting spacecraft, the orbit of the spacecraft has to be specified. The binned input populations are accessed via the spacecraft using the encounter igloo method for the computation of the flux. The resulting igloo distribution is provided for particles of the five types and eleven different sizes (10 µm to 1 m) for each type. The finest resolution of the igloo results is 10° in azimuth, 10° in elevation and 1 km/s in velocity. The output results are stored in a flux table, e.g. particle size vs. flux distribution with 501 size classes (10 µm to 1 m).

MASTER 8 Model *(Section 2.1.8)*

The MASTER 8 release (Ref. /49/) of ESA's reference model – MASTER – is the successor of MASTER 2009. Compared to the previous version, the following improvements were done in the MASTER 8 release:

- Implementation of uncertainty indicators in altitude and diameter spectra.
- Target orbit propagation.
- Model revisions and updates, e.g. MLI (including future projection), NaK, SRM firing list, fragmentation event database up to 2016-11-01.
- Upgrade of NASA breakup model implementation.
- Improvement of the small size region of fragmentation modelling for payloads and rocket bodies.
- Implementation of the Grün model.
- Meteoroid flux evaluation in Lagrange points.
- Flexible reference epoch based on available reference population data files.

- Introduction of a condensed population, including the space debris distribution of all man-made objects combined.

ORDEM 3.2 Model *(Section 2.1.9)*

ORDEM 3.2 is an update of NASA's ORDEM 3.0 model. It's functionalities and features basically correspond to ORDEM 3.0 with updated populations, thus please refer to the description of ORDEM 3.0. The updated populations are now available for the time range from 2016 to 2050.

2.1.2 NASA 90 Model

2.1.2.1 NASA 90 Flux Model

The NASA 90 flux model, as published in Ref. /3/, was implemented in the original ESABASE/Debris software (Ref. /1/). Since this debris model is more efficient than the MASTER 2001 model with respect to the execution time, it remains a useful option in the enhanced ESABASE2/Debris software. For completeness the corresponding equations are here recorded again, using the nomenclature of Ref. /1/.

The flux F, which is the cumulative number of impacts on a spacecraft in a *circular orbit* per m^2 and year on a randomly tumbling surface is defined as a function of the minimum debris *diameter d* [cm] , the target orbit *altitude h* [km] ($h \leq 1000$ km) , the target orbit *inclination I* [deg] , the *mission date t* [year] , and of the *solar radio flux S* (measured in the year prior to the mission).

$$F(d,h,i,t,S) = H(d)\ \Phi(h,S)\ \psi(i)\ [F_1(d)\ g_1(t,q) + F_2(d)\ g_2(t,p)]$$

$$H(d) = \left(10^{\exp\left[-\left(\log_{10} d - 0.78\right)^2/0.406\right]}\right)^{1/2}$$

$$F_1(d) = 1.22 \cdot 10^{-5}\ d^{-2.5}$$

$$F_2(d) = 8.1 \cdot 10^{10}\ (d+700)^{-6}$$

$$\Phi(h,S) = \Phi_1(h,S)\ (1 + \Phi_1(h,S))^{-1}$$

$$\Phi_1(h,S) = 10^{(h/200 - S/140 - 1.5)}$$

Project: ESABASE2/Debris Release 12.1	Date:	2024-02-19
Technical Description	Revision:	1.11
Reference: R077-231rep_01_11_Debris_Technical Description.docx	Status:	Final

FEV etamax GmbH   Page 24 / 173

The functions $g_1(t,q)$ and $g_2(t,p)$ with the assumed annual growth rate of mass in orbit, p (default $p = 0.05$) and with the assumed growth rate of fragments q (default $q = 0.02$, and 0.04 after 2011) become

$$g_1(t,q) \quad = \quad (1 + q)^{t - 1988}$$

$$g_2(t,p) \quad = \quad 1 + p\,(t - 1988)\ .$$

In ESABASE2/Debris the population growth is accounted for linearly over the mission duration.

Finally the inclination dependent function $\psi(i)$ is tabulated as follows:

i [°]	28.5	30	40	50	60	70	80	90	100	120
$\psi(i)$	0.91	0.92	0.96	1.02	1.09	1.26	1.71	1.37	1.78	1.18

For intermediate values of i, a linear interpolation in $\psi(i)$ is performed.

For the application of the ray tracing method to a fixed oriented plate the flux must be scaled by the cosine of the angle between the plate normal and the debris velocity arrival direction.
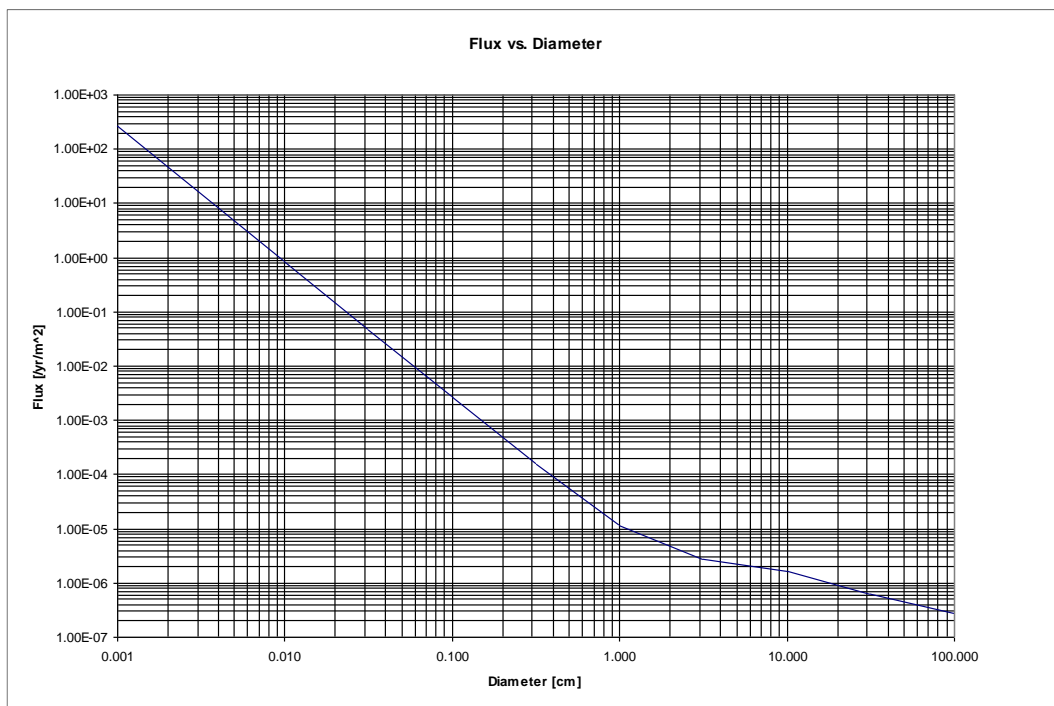
Figure 2-1   NASA 90 flux vs. diameter, 400 km / 51.6° orbit

Project: ESABASE2/Debris Release 12.1		Date:	2024-02-19
Technical Description		Revision:	1.11
Reference: R077-231rep_01_11_Debris_Technical Description.docx		Status:	Final

FEV etamax GmbH

Page 25 / 173
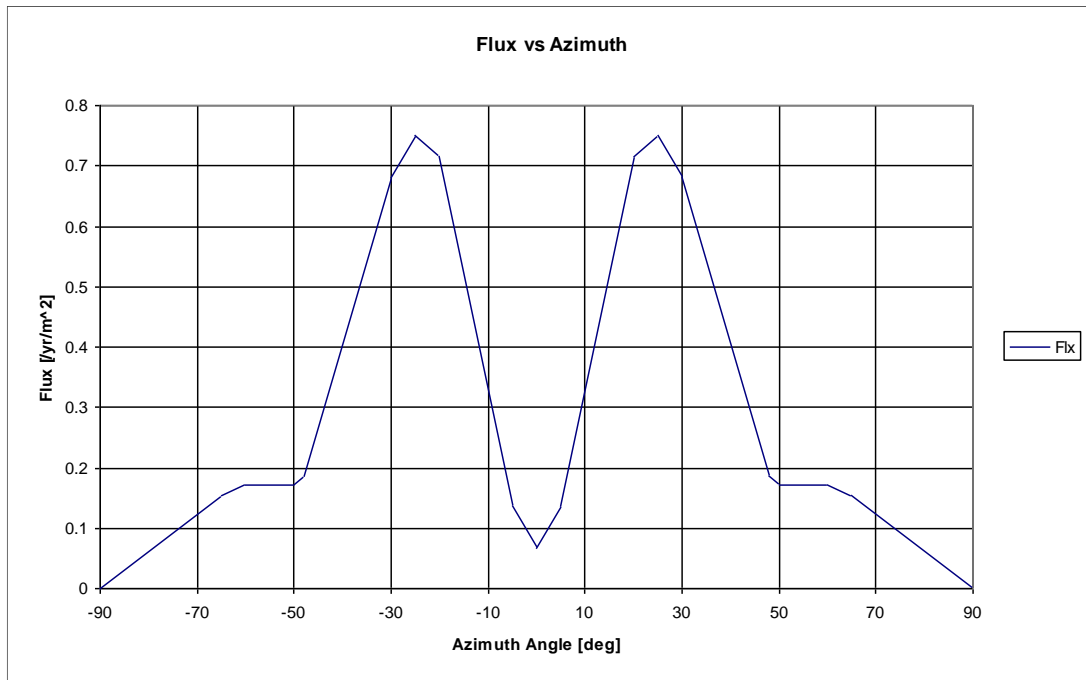
Figure 2-2   NASA 90 flux vs. azimuth, 400 km / 51.6° orbit

2.1.2.2 NASA 90 Velocity Distribution

The collision velocity distribution $g(v)$ which represents the number of impacts with velocities between v and $v + dv$ is expressed as a function of inclination i in Ref. /3/. Taking into account that the orbital circular velocity at altitude h, $v_0(h)$ is occurring in the expression, it may be interpreted as a function of altitude. Thus, according to Ref. /1/ , we may write

$$g(v,i,h) = v\,(2v_0 - v)\,\{g_1 \exp[-((v - 2.5v_0)\,/\,g_2\,v_0)^2] + g_3 \exp[-((v - g_4\,v_0)/g_5\,v_0))^2]\} + g_6\,v\,(4v_0 - v)$$

where the functions $g_1(i)$ to $g_6(i)$ are defined as follows, and $v_0(h)$ is the velocity at target orbit altitude h.

$$[G =] \quad g_1(i) = \begin{cases} 18.7 & i < 60° \\ 18.7 + 0.0298\,(i - 60)^3 & 60° \le i < 80° \\ 250 & i \ge 80° \end{cases}$$

$$[B =] \quad g_2(i) = \begin{cases} 0.5 & i < 60° \\ 0.5 - 0.01\,(i - 60) & 60° \le i < 80° \\ 0.3 & i \ge 80° \end{cases}$$

$$[F =] \quad g_3(i) = \begin{cases} 0.3 + 0.0008\,(i - 50)2 & i < 50° \\ 0.3 - 0.01\,(i - 50) & 50° \le i < 80° \\ 0 & i \ge 80° \end{cases}$$

Project: ESABASE2/Debris Release 12.1		Date:	2024-02-19
Technical Description		Revision:	1.11
Reference: R077-231rep_01_11_Debris_Technical Description.docx		Status:	Final

FEV etamax GmbH   Page 26 / 173

[D =]	$g_4(i)$	=	$1.3 - 0.01\,(i - 30)$

[E =]	$g_5(i)$	=	$0.55 + 0.005\,(i - 30)$

$$[H.C =] \quad g_6(i) \ = \ \begin{cases} 0.0125\,(1 - 0.0000757\,(i - 60)2) & i < 100° \\[2mm] [0.0125+0.00125(i-100)]\,[1-0.0000757(i-60)2] & i \geq 100° \end{cases}$$

$$v_0(i,h) \ = \ \begin{cases} v_0(h)\,.\ (7.25 + 0.015\,(i - 30))\,/\,7.7 & i < 60° \\[2mm] v_0(h) & i \geq 60° \end{cases}$$

(The notations which are used in the original Ref. /3/ for the inclination dependent functions are listed in square brackets for comparison purposes.)

Since only circular orbits are represented by the NASA 90 model all debris are assumed to arrive in a plane tangent to the Earth. By vector addition one obtains for the direction dependence of the impact velocity v_{imp}

$$v_{imp} = 2\,v_s\,\cos\alpha\ ,$$

where α is the angle between the satellite velocity vector and the debris arrival velocity vector. For a low Earth orbit $2\,v_s$ is typically on the order of 15.4 km/s .

For the ray tracing method however, the debris velocity vector must be used and the impact velocity vector follows from numerical vector subtraction (see chapter 5).

2.1.2.3 Particle Mass Density

For the NASA 90 model the particle mass density can be either set to a constant with default value of $\rho = 2.8$ g/cm^3 or the following dependency may be chosen:

$$\rho\,(d) \ = \ \frac{2.8}{d^{\,0.74}}\ \ [\text{g/cm}^3] \qquad \text{for} \qquad d \ \geq \ 0.62\ \text{cm}$$

$$\rho\,(d) \ = \ 4\ \text{g/cm}^3 \qquad\qquad \text{for} \qquad d \ < \ 0.62\ \text{cm}$$

with d as the particle diameter.

It is suggested to use the same values for the NASA 96 model and for the MASTER 2001 model.

The density option as implemented in the software tool is identical for all debris models.

Project: ESABASE2/Debris Release 12.1		Date:	2024-02-19
Technical Description		Revision:	1.11
Reference: R077-231rep_01_11_Debris_Technical Description.docx		Status:	Final

FEV etamax GmbH — Page 27 / 173

2.1.3 MASTER 2001 Model

2.1.3.1 Overview

As mentioned in section 2.1.1, the MASTER 2001 model has been implemented into ESABASE2/Debris by means of the Standard application.

The MASTER 2001 Standard application is an upgrade and extension of the MASTER '99 Standard application, which is described in detail in Ref. /20/. The approach is based on the mathematical theory used by N. Divine (Ref. /21/) to calculate meteoroid fluxes to detectors onboard probes in interplanetary space. After a thorough review, the theory has been adapted to spacecraft in Earth orbit.

The population data describing the Earth's debris environment is derived from the MASTER reference population using comprehensive statistical analysis to "translate" the population given by representative objects to a population description by means of probability density distributions of the orbital elements and of the diameter and mass distributions (cf. Ref. /23/).

2.1.3.2 Flux Calculation

The basics of the Divine approach are described in Ref. /21/, /19/, and /23/. Although these descriptions of the model are well known and easily accessible, a short compilation of the most important equations is given in this section.

For the calculation of space debris flux to an Earth satellite, an Earth-centred equatorial coordinate system has to be used instead of the sun-centred ecliptic system. Furthermore, all focussing, shielding, and detector related factors (η_F, η_S, F_S, Γ) can be set to 1.

After the introduction of these changes, the flux on a target at a specified position on its orbit is derived from

$$J_M = \frac{1}{4} \sum_{dir=1}^{4} \left[N_M \cdot \left(v_{imp} \right)_{dir} \right] \qquad\qquad (1)$$

where N_M is the spatial density

$$N_M = \frac{H_M}{\pi} \cdot \int_0^{\pi/2} N_1(\sin\chi)\,d\chi \cdot \int_{e_\chi}^1 \frac{p_e}{\sqrt{e - e_\chi}}\,de \cdot \int_{|\delta|}^{\pi-|\delta|} \frac{(\sin i)p_i}{\sqrt{\cos^2\delta - \cos^2 i}}\,di \quad . \qquad (2)$$

The impact velocity v_{imp} is the velocity difference

$$v_{imp} = \left| \vec{v}_{part} - \vec{v}_{tar} \right| , \qquad\qquad (3)$$

and the cumulative size distribution including the number of particles of the specified population is

Project: ESABASE2/Debris Release 12.1	Date:	2024-02-19
Technical Description	Revision:	1.11
Reference: R077-231rep_01_11_Debris_Technical Description.docx	Status:	Final

FEV etamax GmbH   Page 28 / 173

$$H_M = \int_m^\infty H_m dm \; .$$

<div align="right">(4)</div>

N_1, p_e and p_i are the differential distributions of the orbital elements of the particles. Integration over these distributions, using the auxiliary variable χ (s. /18/, equation (7)), gives the spatial density for all particles whose size exceeds the lower size threshold m. If the integration in equation (4) is carried out over a certain size range it gives the number of particles in this size range and thus flux or spatial density for this size range is evaluated. The limits of the integrals in equation (2) ensure, that only particle orbits are considered, which may reach the target position:

➢ The particle orbit perigee altitude has to be below the altitude of the target at its current position. This requirement is considered in the first integration (over the perigee radius distribution).

➢ The eccentricity of the particle's orbit must exceed a minimum value e_χ (s. /18/, equation (7)) to be able to reach the target. This is considered in the second integration (over the eccentricity distribution).

➢ The particle orbit inclination i has to be equal or larger than the declination $|\delta|$ of the target position, and less than or equal to $|180° - \delta|$. This is considered in the third integration (over the inclination distribution).

The summation in equation (1) takes into account, that due to the assumption of uniform distributions of the particle's right ascension of ascending node and argument of perigee four velocity directions are possible with the same probability.

In order to obtain correct results it became necessary to use so called 'textbook' distributions to describe the particles orbital elements (refer to /19/). Those 'textbook' distributions are probability density functions, which has to be transformed to the distributions used by Divine using the transformations given in Table 2:

distribution	symbol of 'textbook' distribution	condition for 'textbook' distribution	transformation
perigee radius R_1	D_1	$\int_0^\infty D_1(r_1)dr_1 = 1$	$N_1 = \dfrac{D_1}{r_1^{\,2}}$
eccentricity e	D_e	$\int_0^1 D_e(e)de = 1$	$p_e = (1-e)^{\frac{3}{2}} D_e$
inclination i	D_i	$\int_0^\pi D_i(i)di = 1$	$p_i = \dfrac{D_i}{2\pi^2 \sin i}$

Table 2   **Transformation from 'textbook' distributions to Divine's distributions**

Project: ESABASE2/Debris Release 12.1		Date:	2024-02-19
Technical Description		Revision:	1.11
Reference: R077-231rep_01_11_Debris_Technical Description.docx		Status:	Final

Some assumptions in the theory of the selected approach require a certain effort to make this solution applicable to the needs of a debris model:

➢ Different distributions of the orbital elements of particles of different size within one population (e.g. fragments) do not allow describing the population by only four distributions (mass or diameter, perigee radius, eccentricity, inclination).

➢ Cross-coupling effects between the orbital elements of the particles are not considered in the approach. This may lead to the calculation of flux contribution from objects, which are not existing in reality (e.g. in the SRM slag population).

➢ The assumption of symmetric particle distribution with respect to the equatorial plane and with respect to the Earth's rotation axis may result in an inaccurate description of some source populations, namely those, which do not fulfil the symmetry assumption (e.g. parts of the catalogued objects population, such as Molniya-type orbits).

These problems have been solved during the development of the MASTER 2001 Standard application:

➢ A population pre-processing tool – called pCube – has been developed, which automatically creates the Standard application population input files. The generation of the size and orbital element distributions is based on a comprehensive statistical analysis of the populations. So called cross-coupling effects between the size distribution and the orbital element distributions on one hand, and between the orbital element distributions on the other hand are identified using the statistical method of a cluster analysis.

➢ The approach to consider asymmetries in the population is based on the fact, that each of the four possible impact velocities (in case of population symmetry) can be related to a well defined particle nodal line position and perigee position. Thus, each impact velocity – and consequently flux value – may be "weighted" with a factor related to the distribution values of the right ascension of ascending node distribution and the argument of perigee distribution. Within ESABASE2/Debris, the described asymmetries are considered as follows:

  – right ascension of ascending node: Off for all sub-populations,

  – argument of perigee: On for all sub-populations except the SRM dust sub-population.

The results of the new Standard application have been verified against the reference results of the MASTER Analyst application (Ref. /23/).

2.1.3.3 Population Snapshots

The MASTER 2001 model provides realistic historic population snapshots from the beginning of spaceflight in 1957 until the reference epoch May 1st, 2001. Additionally, three different future population snapshots for each year from 2002 until 2050 are provided under the assumption of three different debris environment evolution scenarios.

Within the ESABASE2/Debris implementation of MASTER 2001, the following sub-sets of these population snapshots are available:

Historic populations from 1980 to 2001, one snapshot (May 1st) per year.

Future populations from 2002 to 2020, one snapshot per year, reference scenario (no future constellations, no mitigation, continuation of recent traffic).

| Project: ESABASE2/Debris Release 12.1 | Date: | 2024-02-19 |
| Technical Description | Revision: | 1.11 |
| Reference: R077-231rep_01_11_Debris_Technical Description.docx | Status: | Final |

FEV etamax GmbH   Page 30 / 173

Important note: Future populations comprise all objects ≥ 1 mm, while historic populations include all objects down to 1 µm in diameter.

Due to the fact, that ESABASE2/Debris does not contain a time loop, but considers population evolution during the mission duration by applying a population growth rate which is specified by the user, the debris analyser makes use of the population snapshot of the May 1st of the mission start year. The population growth factor is not considered, if the debris flux is calculated with the MASTER 2001 model.

If it is intended to analyse the debris risk as a function of time, subsequent ESABASE2/Debris runs have to be performed with different analysis time start epochs.

2.1.3.4 Results

This section provides a brief description of the MASTER 2001 model results, which are used for flux calculation and damage assessment within ESABASE2/Debris.

Four two-dimensional spectra, and one three-dimensional spectrum are generated by the model. The spectra definitions are given in Table 3:

Spectrum	min. value	max. value	number of steps
flux vs. diameter	as specified for the analysis		32
flux vs. impact velocity	0 km/s	40 km/s	80
flux vs. impact azimuth angle	−180°	180°	90
flux vs. impact elevation angle	−90°	90°	90
flux vs. impact velocity and impact azimuth angle	as specified for the corresponding 2D spectra		

<div align="center">

Table 3　　　　**MASTER 2001 flux spectra**

</div>

Figure 2-3 to Figure 2-7 provide the results (cross-sectional flux on a sphere) of the MASTER model for an ISS-like orbit. The diameter spectrum (Figure 2-3) is given for the complete size range of the MASTER model, while the other spectra are given for a lower diameter threshold of 0.1mm.
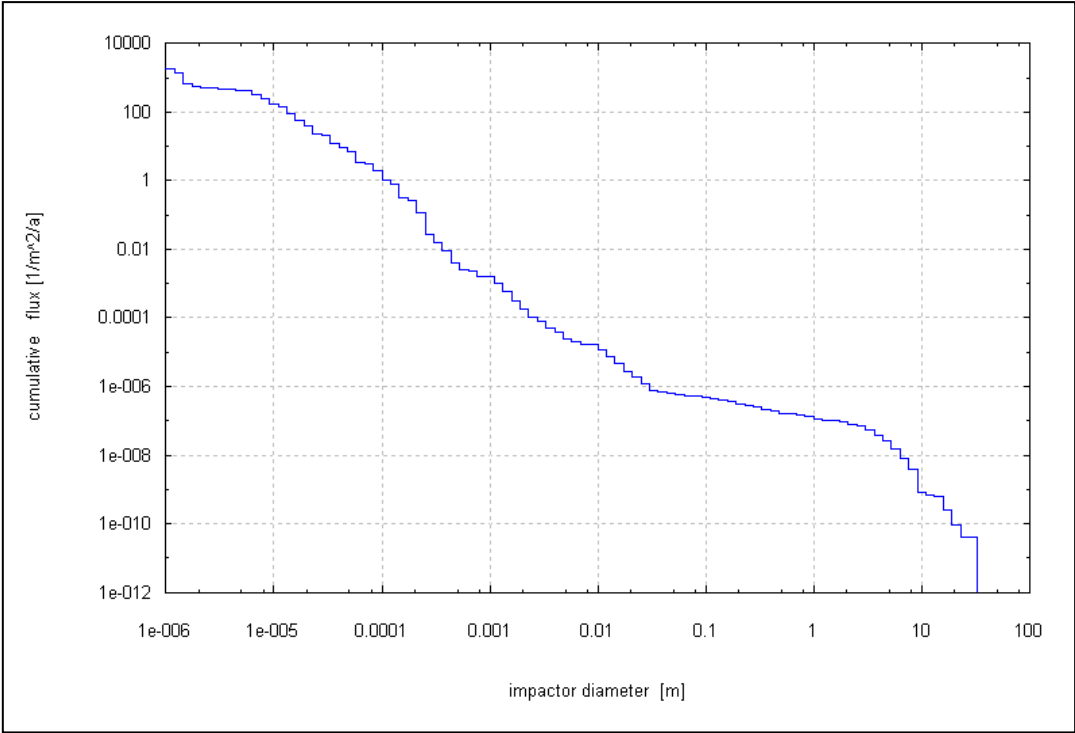
Figure 2-3   MASTER 2001 flux vs. particle diameter, 400 km / 51.6° orbit
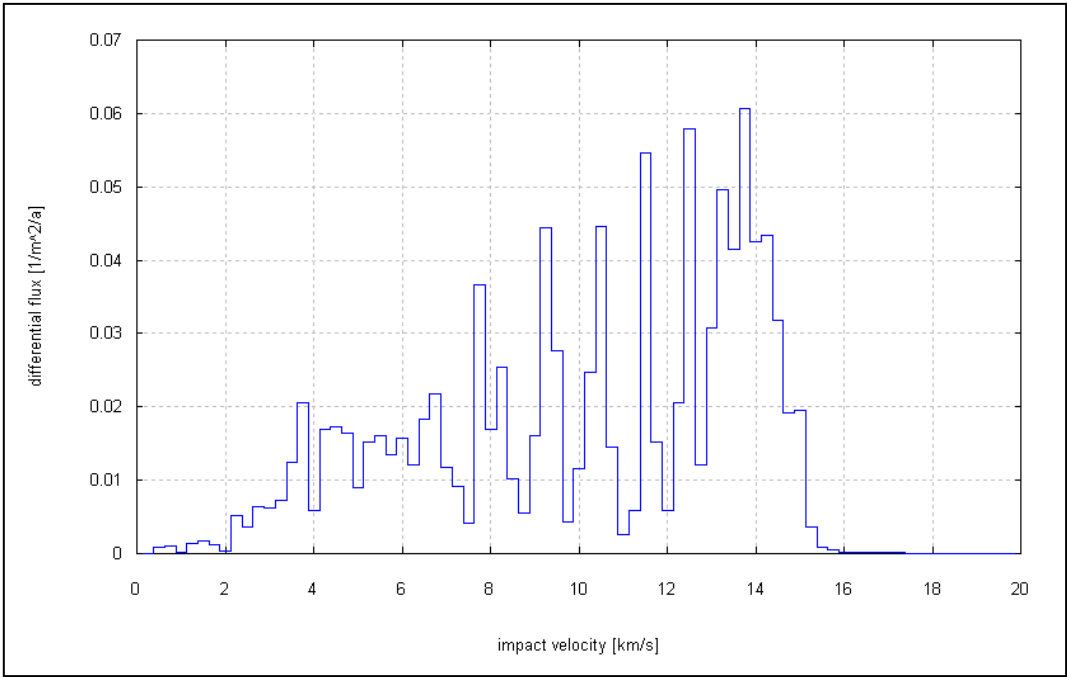
Figure 2-4   MASTER 2001 flux vs. impact velocity, 400 km / 51.6° orbit / d > 0.1 mm

Project: ESABASE2/Debris Release 12.1		Date:	2024-02-19
Technical Description		Revision:	1.11
Reference: R077-231rep_01_11_Debris_Technical Description.docx		Status:	Final

FEV etamax GmbH   Page 32 / 173
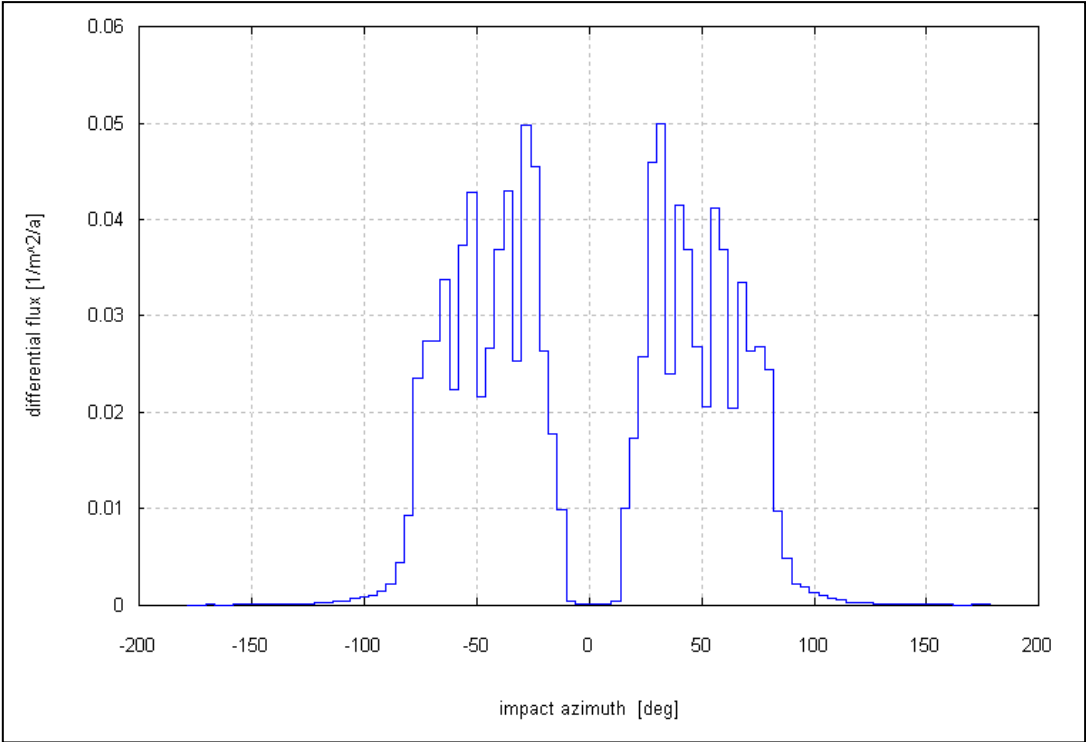
Figure 2-5   MASTER 2001 flux vs. azimuth, 400 km / 51.6° orbit / d > 0.1 mm
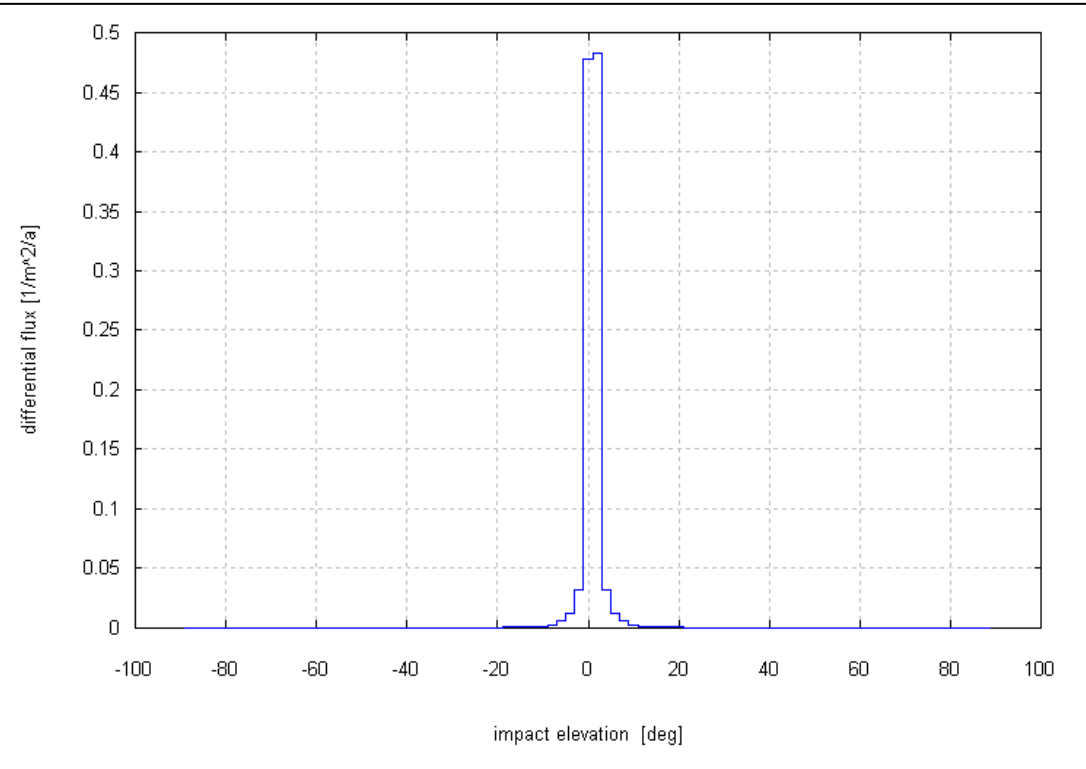
Figure 2-6   MASTER 2001 flux vs. elevation, 400 km / 51.6° orbit / d > 0.1 mm

Project: ESABASE2/Debris Release 12.1	Date:	2024-02-19
Technical Description	Revision:	1.11
Reference: R077-231rep_01_11_Debris_Technical Description.docx	Status:	Final

FEV etamax GmbH   Page 33 / 173
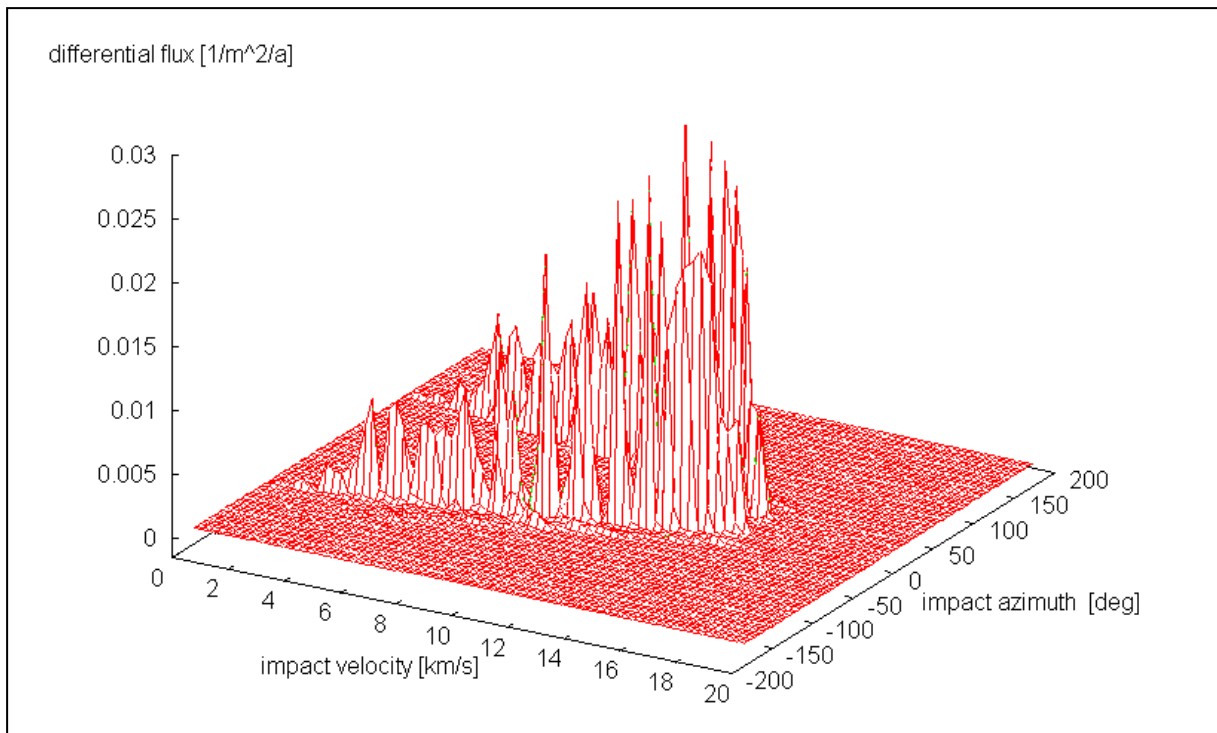
Figure 2-7   MASTER 2001 flux vs. velocity and azimuth, 400 km / 51.6° orbit / d > 0.1 mm

Although the spectra are displayed as differential distributions – except the diameter spectrum, which is cumulative – for compatibility with the results of the other debris models (see section 2.1.2.1), the distributions are provided and used in their cumulative form within the ESABASE2 analysis as described in chapter 5.

In ESABASE2/Debris the MASTER 2001 flux analysis is performed for single orbital points specified by the user. This differs from the previous ESABASE version, where the flux analysis was performed for orbital arcs centred around each orbital point so that the entire orbit is covered. This change might result in partly considerable difference in the analysis results. It became necessary to change the implementation to yield results comparable to those of ORDEM2000, where flux is always related to single orbital points instead of orbital arcs.

2.1.4 ORDEM2000 Model

2.1.4.1 Overview

With the establishment of the ORDEM2000 engineering model NASA implemented a completely different approach compared to the NASA90 and ORDEM96 (NASA96) models. Here, the debris population is described by the distributions of spatial density and velocity in space. Figure 2-8 outlines the different approaches of ORDEM2000 and ORDEM96.

Project: ESABASE2/Debris Release 12.1	Date:	2024-02-19
Technical Description	Revision:	1.11
Reference: R077-231rep_01_11_Debris_Technical Description.docx	Status:	Final

FEV etamax GmbH

Page 34 / 173
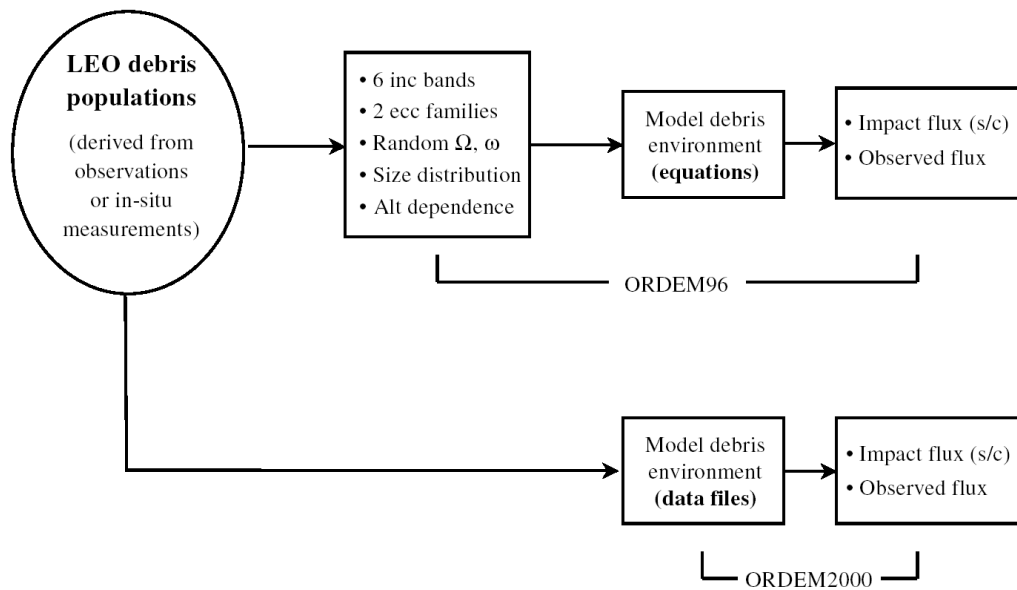
Figure 2-8   Comparison of the approaches of ORDEM2000 and ORDEM96 /27/

Once a debris population is derived from existing data, ORDEM96 simplifies the population into 6 inclination bands and 2 eccentricity families /7/. Objects within each inclination band are assumed to have the same inclination rather than a distribution of inclinations. The ORDEM2000 debris environment model describes the spatial density, velocity distribution, and inclination distribution of debris particles at different latitudes and altitudes. The debris environment is represented by a set of pre-processed data files. No assumptions regarding debris particles' inclinations, eccentricities, or orientations in space (longitudes of the ascending node and arguments of perigee) are required in this approach. However, ORDEM2000 uses a randomized distribution of the objects' right ascension of the ascending nodes.

2.1.4.2 Observation Data Sources and Modelling Approach

Table 4 represents a list of all observation data sources used in the establishment of the ORDEM2000 model. A detailed description of the data sources, processing and analysis can be found in /27/.

Project: ESABASE2/Debris Release 12.1		Date:	2024-02-19
Technical Description		Revision:	1.11
Reference: R077-231rep_01_11_Debris_Technical Description.docx		Status:	Final

FEV etamax GmbH   Page 35 / 173

	Size range	Altitude Range (km)	Inc. Range (degree)	Time of Collection
SSN	10 cm to 10 m	200 to 2000	All	up to Dec. 99
Haystack	0.3 cm to 10 m 0.5 cm to 10 m 0.5 cm to 10 m 0.5 cm to 10 m 1.0 cm to 10 m	350 to 1100 350 to 650 350 to 650 700 to 1100 1200 to 2100	40 to 140 28 to 152 32 to 148 32 to 148 40 to 140	91 to 99 91 to 99 91 to 94 94 to 98 93,94,96,97
HAX	1.0 cm to 10 m 0.8 cm to 10 m	450 to 1050 450 to 1050	40 to 140 40 to 140	94 to 97 98 to 99
LDEF[a]	0.01 to 1 mm	330 to 480	All	Apr. 84 to Jan. 90
HST-SA	0.01 to 1 mm	586 to 614	All	Apr. 90 to Dec. 93
EuReCa	0.005 to 0.5 mm	502 to 508	All	Aug. 92 to Jun. 93
Shuttle[b]	0.1 to 1 mm	300 to 400	All	95 to 98
SFU	10 μm to 1 mm	480	All	Mar. 95 to Jan. 96
Mir	10 to 100 μm	170 to 300	All	Mar. 96 to Oct. 97
Goldstone	2 mm to 2 cm	280 to 2000	32 to 148	Oct. 94 to Oct. 98

[a]LDEF: Space Debris Impact Experiment (/30/, /31/), Chemistry of Meteoroid Experiment (/28/, /29/), Interplanetary Dust Experiment (F. Singer), LDEF frame (M/D Special Investigation Group).

[b]Shuttle: STS-50, 56, 71, 72, 73, 75, 76, 77, 79, 80, 81, 84, 85, 86, 87, 88, 89, 91, 94, 95, 96.

Table 4   Data sources used in the establishment of ORDEM2000 /27/

The ORDEM2000 model is based on five pre-calculated debris populations. They correspond to objects of five different size thresholds: 10 μm and greater, 100 μm and greater, 1 cm and greater, 10 cm and greater, and 1 m and greater (hereafter referred to as 10-μm, 100-μm, 1-cm, 10-cm, and 1-m populations). The major sources

- SSN catalog (build the 1-m and 10-cm populations),
- Haystack radar data (build the 1-cm population),
- LDEF measurements (build the 10-μm and 100-μm populations),

were used to build the debris populations, while the other sources were used to verify and validate the model predictions.

Since no direct measurement at 1 mm is available, the 1-mm debris population in the model is based on an interpolation between the 100-μm and 1-cm populations. Goldstone radar data for the 3-mm objects are used to justify the interpolation.

The reference date for the debris populations was selected to be January 1, 1999. The SSN catalogue from the same reference date was used, and the Haystack debris detection from each year was projected to the reference date using the historical growth rate of the 1-cm population from the NASA orbital debris evolution model EVOLVE 4.0 (/32/). Then, the combined Haystack data was used to build the 1-cm population as of January 1, 1999. The LDEF debris impact data are first processed with a simple model that calculates the historical 10-μm and 100-μm debris populations, including the effects of atmospheric drag and solar radiation pressure. Then, the number of debris impacts detected during the LDEF mission (1984-1990) was scaled with the model prediction during the same period, and then projected to January 1, 1999.

2.1.4.3 The LEO Debris Environment Model

Figure 2-9 shows the subdivision of the region between 200 km and 2000 km altitude into 5 deg × 5 deg × 50 km cells in longitude (θ), latitude (90 deg-φ), and radius (r), respectively. The resident time of each (observed) debris particle within each cell is calculated using the fractional time that it spends in that cell. For example, if a debris particle spends 3% of its orbital period within a given cell, 0.03 "object" is assigned to that cell. Once the same procedure is completed for every debris particle in the population, the spatial density of this debris population within each cell is simply the sum of objects within that cell divided by its volume V_{cell}, where

$$V_{cell} = \iiint r^2 (\sin\varphi)\, \mathrm{d}r\, \mathrm{d}\varphi\, \mathrm{d}\theta \, ,$$

and r, φ, and θ are defined in Figure 2-9.

The velocity of a debris particle within a given cell is calculated in two steps. The first step is to convert its orbital elements to the velocity and position vectors in the geocentric equatorial system. The second step is to transfer the velocity components to a special local system via two coordinate transformations. The local system is a right-handed geocentric system where the x-axis points in the radial-outward direction, the y-axis points in the local east direction, and the z-axis points in the local north direction. The plane defined by the y-axis and z-axis is the local horizontal.
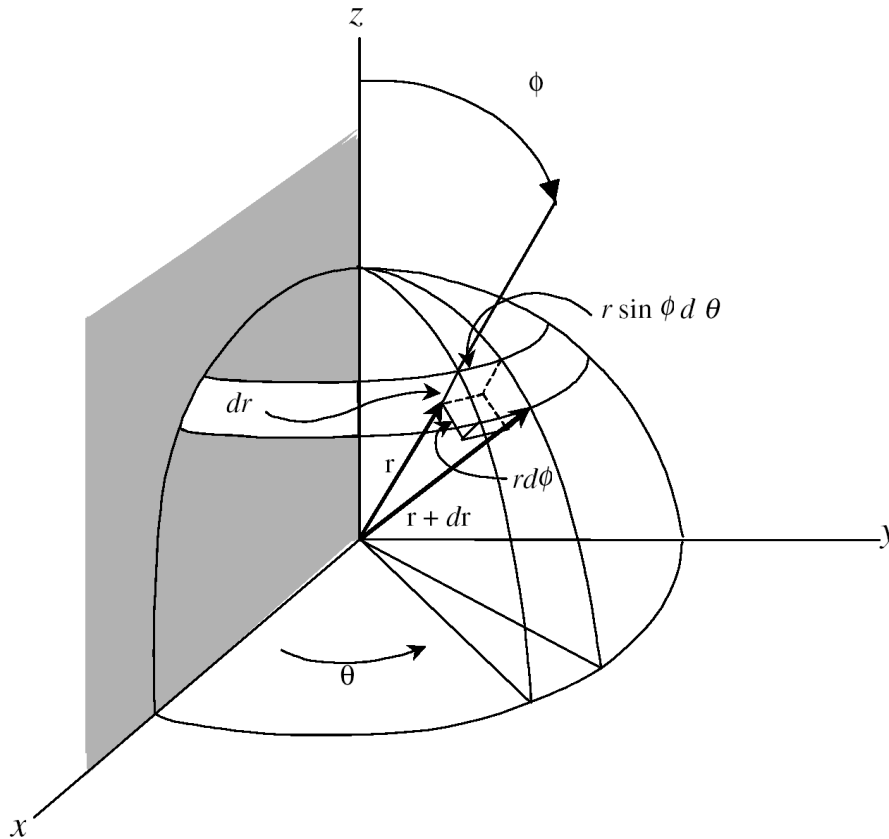
Figure 2-9 Definition of the cells /27/

Let (v_x, v_y, v_z) be the geocentric equatorial velocity components of a debris particle in a given cell. The components (v_{x2}, v_{y2}, v_{z2}) in the local system are calculated with the following two transformations:

$$v_{x1} = v_x \cos\theta + v_y \sin\theta$$

$$v_{y1} = -v_x \sin\theta + v_y \cos\theta$$

$$v_{z1} = v_z$$

and

$$v_{x2} = v_{x1} \cos(90°-\varphi) + v_{z1} \sin(90°-\varphi)$$

$$v_{y2} = v_{y1}$$

$$v_{z2} = -v_{x1} \sin(90°-\varphi) + v_{z1} \cos(90°-\varphi),$$

where θ and φ are defined in Figure 2-9.

The velocity distribution of debris particles within a given cell is calculated using all particles in the cell, weighted by their individual spatial densities. To reduce the size of the templates, only the velocity components in the local horizontal plane are recorded. This is justified since the radial velocity component is generally less than 0.1 km/s while the horizontal velocity component is about 6 km/s to 11 km/s. The velocity distribution within each cell is stored in a

magnitude-and-direction two-dimensional matrix, as shown in Figure 2-10. The magnitude ranges from 6 km/s to 11 km/s with an increment of 1 km/s while the direction ranges from 0 deg to 360 deg with an increment of 10 deg. Each element in the matrix gives the fraction of particles with a velocity within the magnitude and direction specified by the position of the element. For example, the 2% element in Figure 2-10 indicates that 2% of all particles in this three-dimensional cell have their orbital velocity (in the local horizontal plane) between 6 km/s and 7 km/s with a direction between the local east and 10 deg northward. The sum of all elements in a matrix is always 100%.
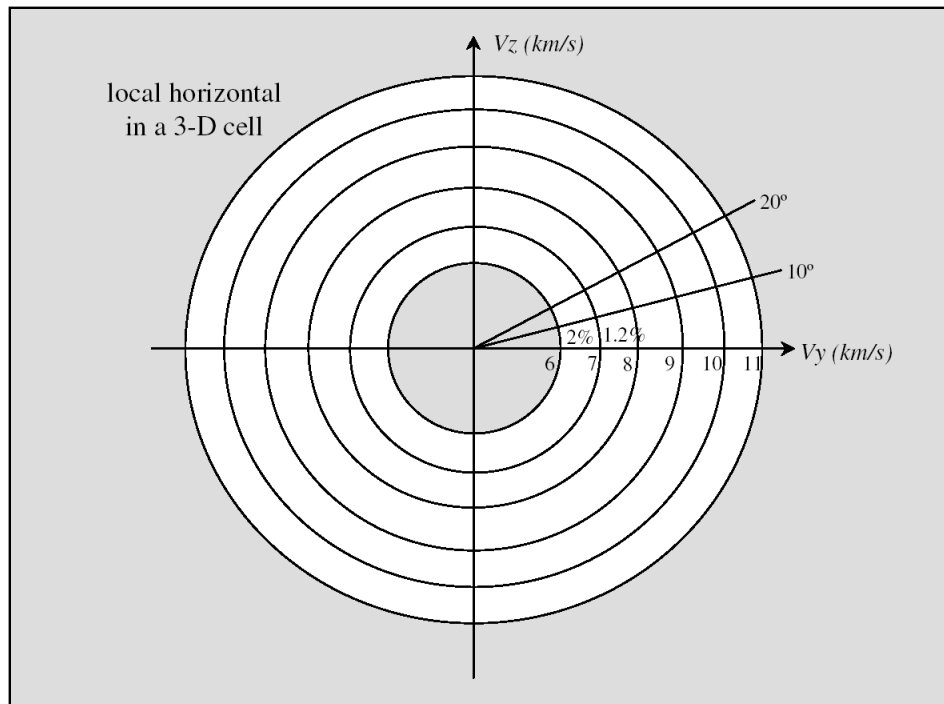
Figure 2-10   Velocity distribution matrix /27/

The inclination distribution of debris particles within each cell is also calculated and saved as part of the template files. The range is between 0 deg and 180 deg with an increment of 2 deg.

2.1.4.4 Results

Some exemplary results of ORDEM2000 are displayed in Figure 2-11 to Figure 2-13. Since the three-dimensional velocity vs. impact angle distribution of ORDEM2000 provides the percentage of debris objects coming from a particular direction with a particular velocity, and ESABASE2 requires the flux vs. impact velocity and impact azimuth angle distribution, the latter distributions have to be derived from the ORDEM2000 results. ORDEM2000 generates the 3D output for each analysed orbital point. Due to the fact that the flux vs. diameter distributions are also given for each orbital point, these can be considered in the generation of the 3D flux Vs. velocity and azimuth distribution used by ESABASE2.

Figure 2-11 gives the average flux vs. diameter. While ORDEM2000 performs a cubic spline interpolation, ESABASE2 interpolates linearly. This leads to differences in the 100 µm to 1 mm and in the 1 cm to 10 cm diameter ranges. However, these differences will become visible in the ESABASE2 output only, if the user selects a lower diameter threshold within the named diameter ranges, e.g. 300 µm or 2 cm.

Project: ESABASE2/Debris Release 12.1	Date:	2024-02-19
Technical Description	Revision:	1.11
Reference: R077-231rep_01_11_Debris_Technical Description.docx	Status:	Final

FEV etamax GmbH   Page 39 / 173
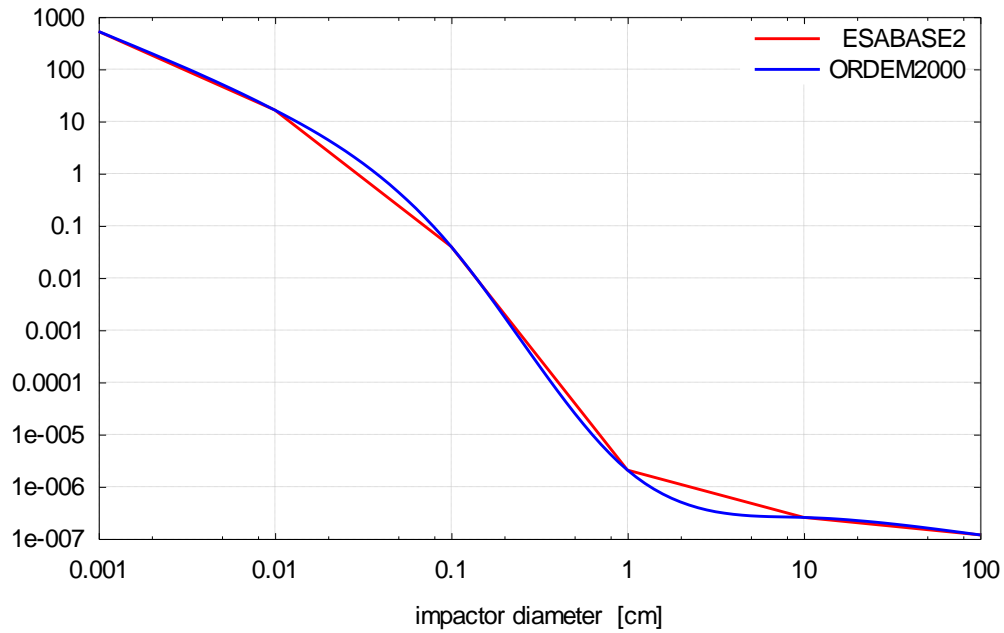
Figure 2-11   ORDEM2000 flux vs. diameter, ISS-like orbit

Figure 2-12a shows the relative flux vs. impact angle distribution, where the "impact" angle is not related to the spacecraft orbit or orientation, but to the horizontal plane of the cell corresponding to the spacecraft position (cp. Figure 2-10). 0 deg is the East direction, 90 deg North and so on.

a)   b)
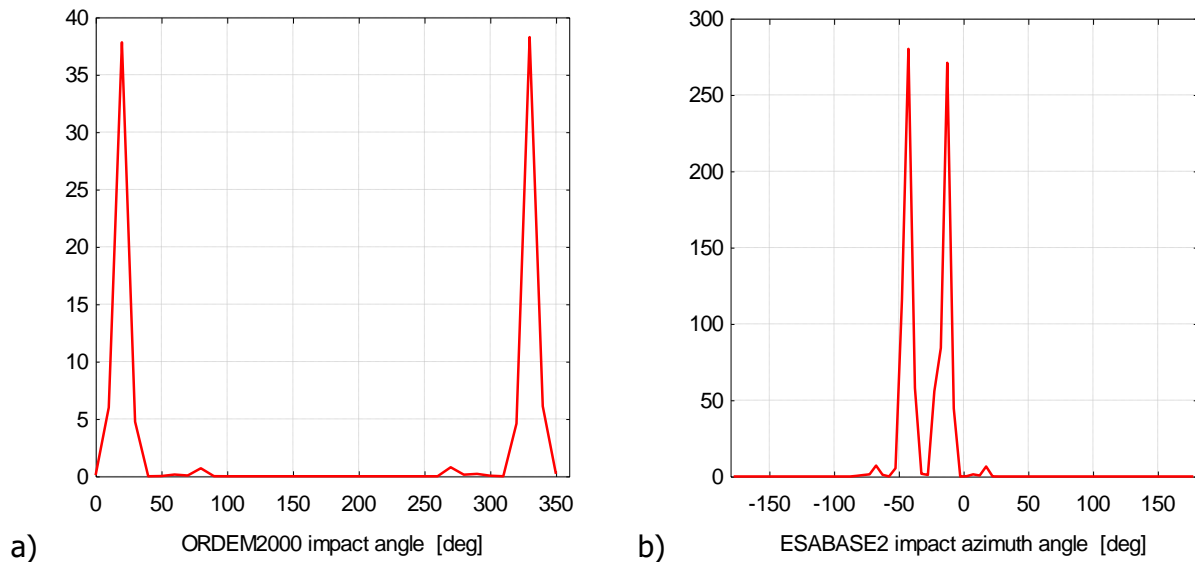
Figure 2-12   a) ORDEM2000 flux vs. impact angle,
b) corresponding ESABASE2 flux vs. impact azimuth angle,
ISS-like orbit at the ascending node, d > 10 µm

Consequently, the distribution given in Figure 2-12a has to be translated to an impact azimuth angle distribution which is used by ESABASE2 to derive the random ray directions. Figure 2-12b shows the impact azimuth angle distribution calculated from the ORDEM2000 impact angle

Project: ESABASE2/Debris Release 12.1		Date:	2024-02-19
Technical Description		Revision:	1.11
Reference: R077-231rep_01_11_Debris_Technical Description.docx		Status:	Final

distribution for a given size class (particle diameter: 10 µm). The "translation" has to be performed under consideration of the particle velocity distribution. The azimuth angle is the angle between the projection of the impact velocity vector to the local horizontal plane and the space craft velocity vector. It is positive if the particle arrives form the left side.

One can see that the peaks of the almost symmetric ORDEM2000 distribution are reflected in the azimuth distribution. This is underlined by Figure 2-13a and b: The peaks can be found in both distributions.

a)

b)
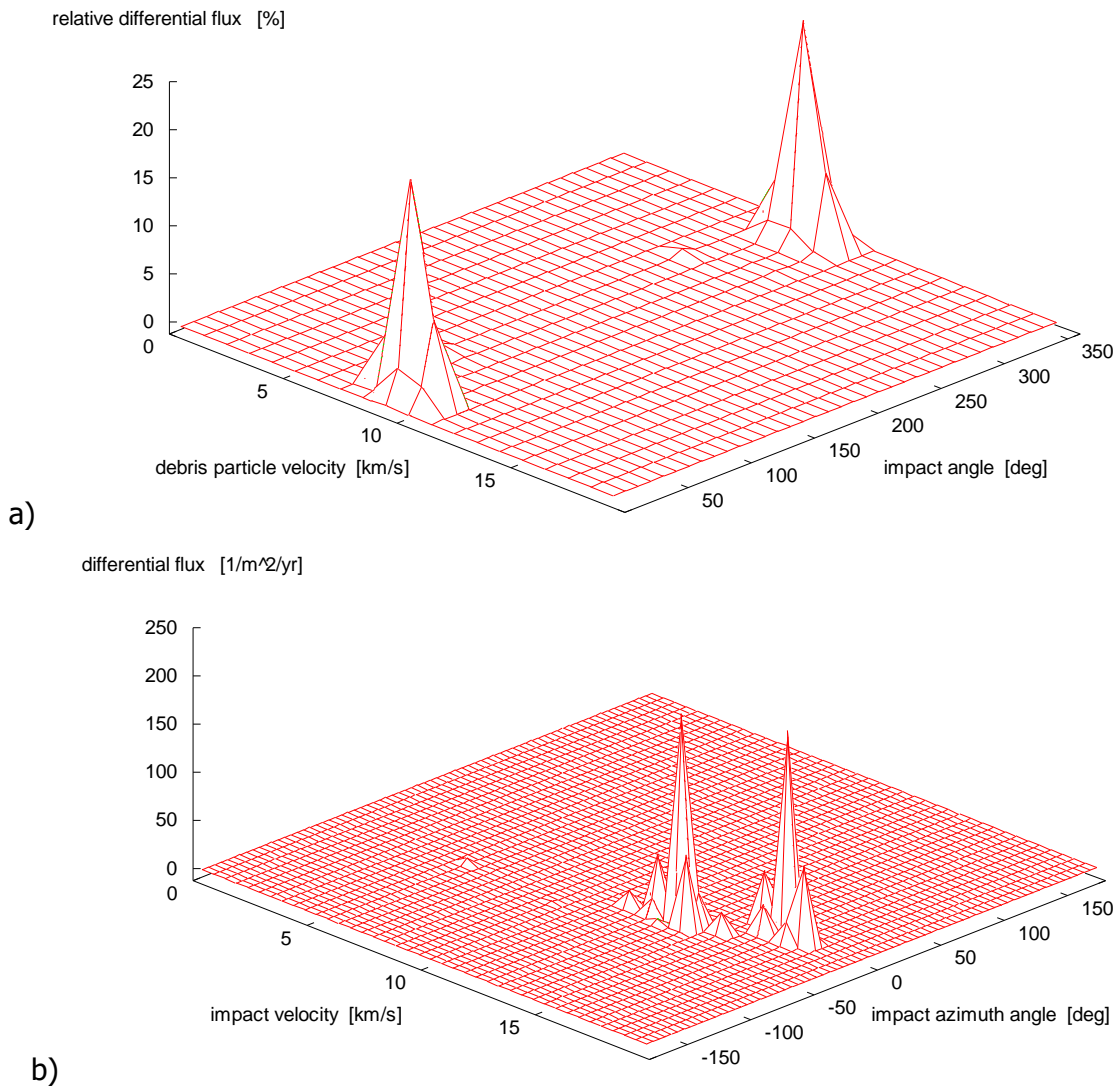
Figure 2-13 **a) ORDEM2000 flux vs. debris particle velocity and impact angle,**
b) corresponding ESABASE2 flux vs. impact velocity and impact azimuth angle,
ISS-like orbit at the ascending node, d > 10 µm

However, the almost symmetric distribution shown in Figure 2-13a becomes asymmetric when transferred to Figure 2-13b. This asymmetry is a consequence of the consideration of the particle and the spacecraft velocity vectors.

Project: ESABASE2/Debris Release 12.1	Date:	2024-02-19
Technical Description	Revision:	1.11
Reference: R077-231rep_01_11_Debris_Technical Description.docx	Status:	Final

2.1.4.5 Limitations

The applicability of ORDEM2000 within the ESABASE2/Debris application is limited by the following facts:

- The altitude range of ORDEM2000 is 200 km to 2000 km. Consequently, all orbits with higher orbital altitude (also in parts of the orbit, e.g. GTO) cannot be analysed with ORDEM2000. The MASTER 2001 model is currently the only debris model which allows the analysis of orbits up to 1000 km above GEO.
- ORDEM2000 includes debris particles in the size range from 10 μm to 1 m.

Eccentric debris particle orbits are not considered in the determination of the impact direction (velocity component in the local horizontal plane only), i.e. ORDEM2000 does not provide an impact elevation angle distribution. Consequently, similar to NASA90, no flux will be calculated on surfaces which are parallel to the local horizontal plane.

2.1.5 MASTER 2005 Model

2.1.5.1 Overview

Upgrade of the Debris Source Models

The following debris source models have been upgraded in MASTER 2005:

- The NASA break-up model has been revised for object sizes smaller 1 mm with a re-definition of the area-to-mass distribution and an increase of the delta velocity distribution.

- The size distribution parameter settings for SRM slag and dust, paint flakes, and ejecta have been revised based on newly available impact measurement data.

- The NaK droplet model is based on a physical description of the release mechanism. This includes new size, velocity, and directional distributions.

- The ejecta model has been thoroughly reviewed which results in major changes to the orbital distribution compared to the former MASTER release.

- The release model for surface degradation products (paint flakes) now depends on the changing atomic oxygen density environment near Earth due to the solar activity.

Update of the Reference Population

The processing of debris generation mechanisms (SRM firings, fragmentations, NaK release events, etc.) were considered and the resulting population propagated to the new reference epoch of May 1, 2005. The updated list of events now comprises 203 fragmentations, 1076 SRM firings, 16 NaK droplet releases, and 2 West Ford needle deployments. The update also includes processing of the ongoing generation of surface degradation products and ejecta.

Unified Flux and Spatial Density Computation Concept

The MASTER 2001 high precision flux prediction tool ANALYST was upgraded to provide the user with spatial density computations. This new MASTER application is the only flux browser on the user side of MASTER 2005. It combines a quick assessment of spatial density characteristics with high resolution flux results. The statistical flux determination approach based on probability tables for the object characteristics is now used for all debris sources.

Project: ESABASE2/Debris Release 12.1	Date:	2024-02-19
Technical Description	Revision:	1.11
Reference: R077-231rep_01_11_Debris_Technical Description.docx	Status:	Final

FEV etamax GmbH   Page 42 / 173

Flux and Spatial Density Analysis for Historic and Future Epochs

The storage needs for the probability tables enables the generation of population snapshots for the complete space age on a single DVD, ranging from 1957 to the future (2055). For future epochs the user may select between three different population evolution scenarios. The stand-alone version of MASTER 2005 allows a flux and spatial density analysis for any epoch within the mentioned time span. However, the user should be aware of the computation time, which may drastically increase subject to the analysis parameter settings (time interval, target orbit, number of populations to be considered, number of spectra to be generated, etc.).

2.1.5.2 Observation Data Sources

The debris environment of the Earth provided with MASTER 2005 contains different sources down to a particle diameter of 1 μm. Figure 2-14 shows the different debris sources and its corresponding size range.
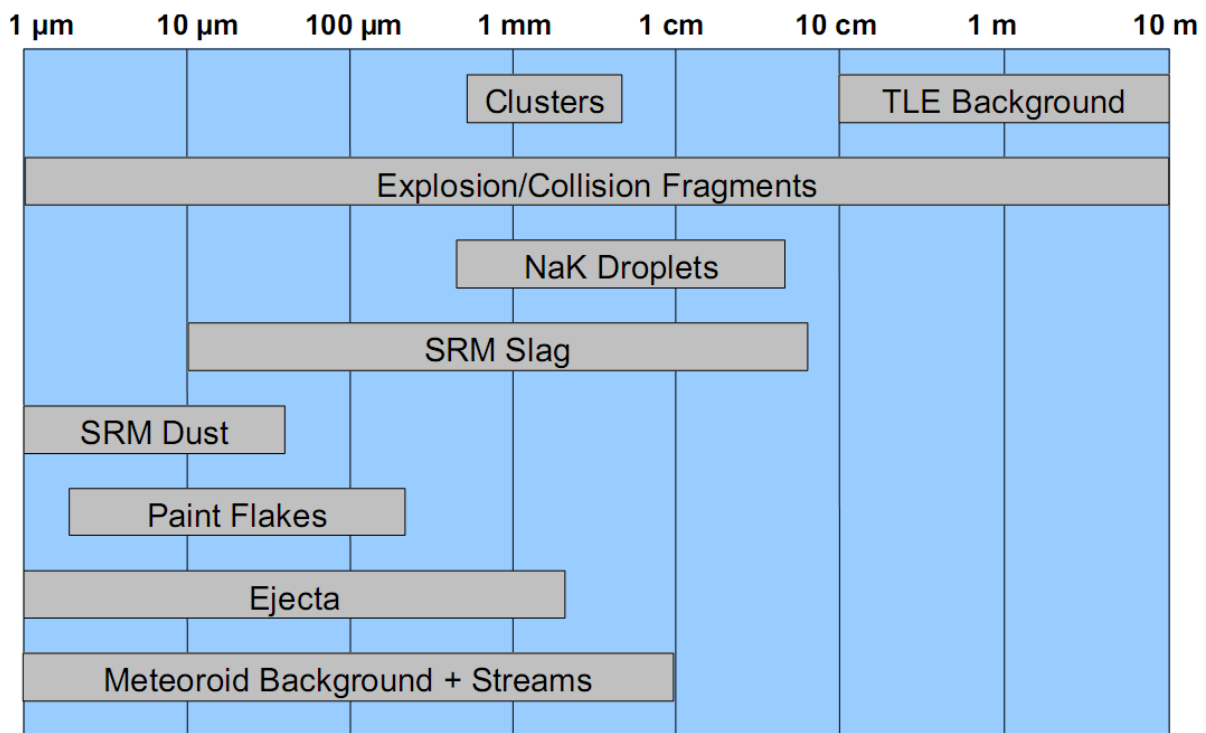
Figure 2-14:   Debris and meteoroid sources considered in MASTER 2005 model

The MASTER 2005 model provides realistic historic population snapshots (3-monthly) from the beginning of spaceflight in 1957 until the reference epoch May 1st, 2005. Additionally, three different future population snapshots for each year from 2006 until 2055 are provided under the assumption of three different debris environment evolution scenarios. Further details can be found in /34/.

Within the ESABASE2/Debris implementation of MASTER 2005, the following sub-sets of these population snapshots are available:

Historic populations from 1980 to 2005, one snapshot (May 1st) per year.

Project: ESABASE2/Debris Release 12.1		Date:	2024-02-19
Technical Description		Revision:	1.11
Reference: R077-231rep_01_11_Debris_Technical Description.docx		Status:	Final

Future populations from 2006 to 2020, one snapshot per year, reference scenario (no future constellations, no mitigation, continuation of recent traffic).

Important note: Future populations comprise all objects ≥ 1 mm, while historic populations include all objects down to 1 µm in diameter.

As for MASTER 2001 the debris analyser makes use of the population snapshot of the May 1st of the mission start year. The user specified population growth factor is not considered, if the debris flux is calculated with the MASTER 2005 model.

If it is intended to analyse the debris risk as a function of time, subsequent ESABASE2/Debris runs have to be performed with different analysis time start epochs.

2.1.5.3 Results

This section provides a brief description of the MASTER 2005 model results, which are used for flux calculation and damage assessment within ESABASE2/Debris.

Four two-dimensional spectra, and one three-dimensional spectrum are generated by the model. The spectra definitions are given in Table 5:

Spectrum	min. value	max. value	number of steps
flux vs. diameter	as specified for the analysis		≤ 32
flux vs. impact velocity	0 km/s	40 km/s	80
flux vs. impact azimuth angle	−180°	180°	90
flux vs. impact elevation angle	−90°	90°	90
flux vs. impact velocity and impact azimuth angle	as specified for the corresponding 2D spectra		

Table 5   MASTER 2005 flux spectra

Figure 2-15 to Figure 2-19 provide the results (cross-sectional flux on a sphere) of the MASTER model for an ISS-like orbit. All spectra are given for the complete size range of the MASTER model.

Project: ESABASE2/Debris Release 12.1	Date:	2024-02-19
Technical Description	Revision:	1.11
Reference: R077-231rep_01_11_Debris_Technical Description.docx	Status:	Final

FEV etamax GmbH   Page 44 / 173
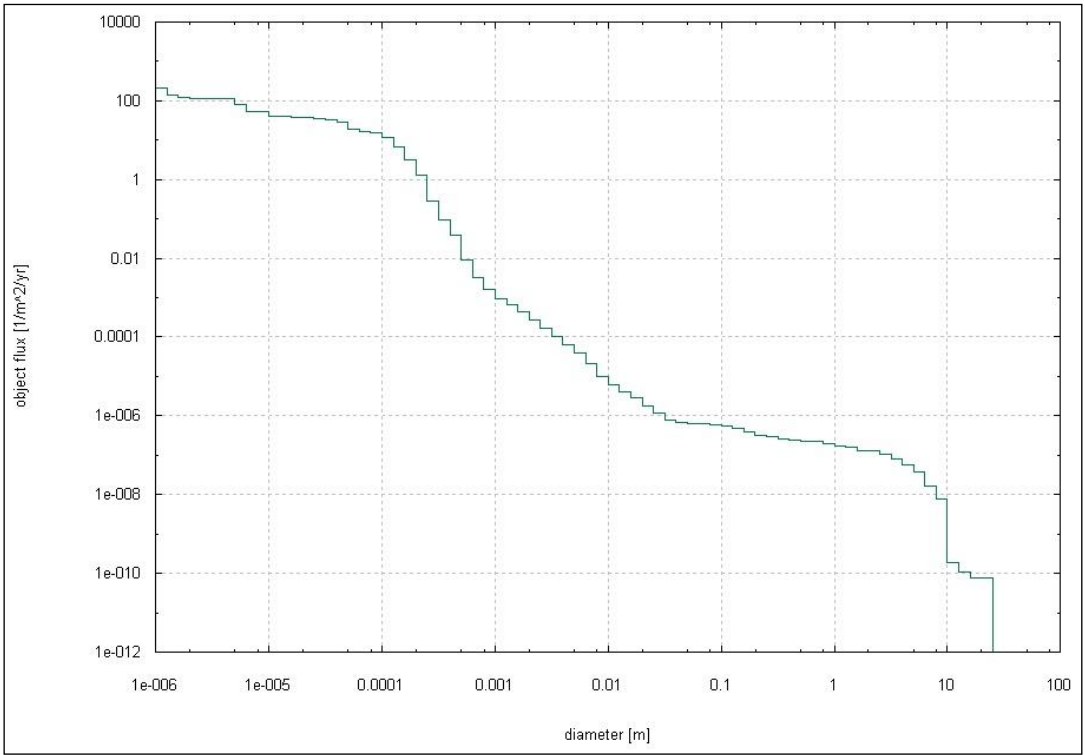
Figure 2-15   MASTER 2005 flux vs. particle diameter, 400 km / 51.6° orbit
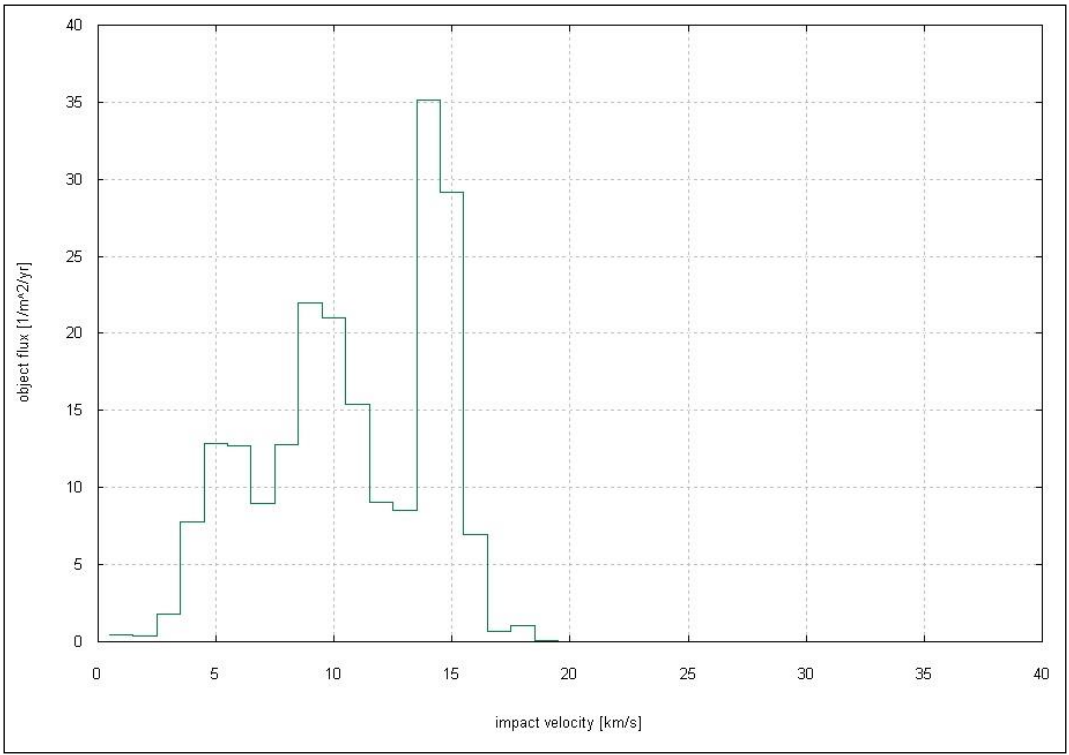
Figure 2-16   MASTER 2005 flux vs. impact velocity, 400 km / 51.6° orbit / d > 1 µm

Project: ESABASE2/Debris Release 12.1		Date:	2024-02-19
Technical Description		Revision:	1.11
Reference: R077-231rep_01_11_Debris_Technical Description.docx		Status:	Final
FEV etamax GmbH			Page 45 / 173

Figure 2-17   MASTER 2005 flux vs. azimuth, 400 km / 51.6° orbit / d > 1 µm
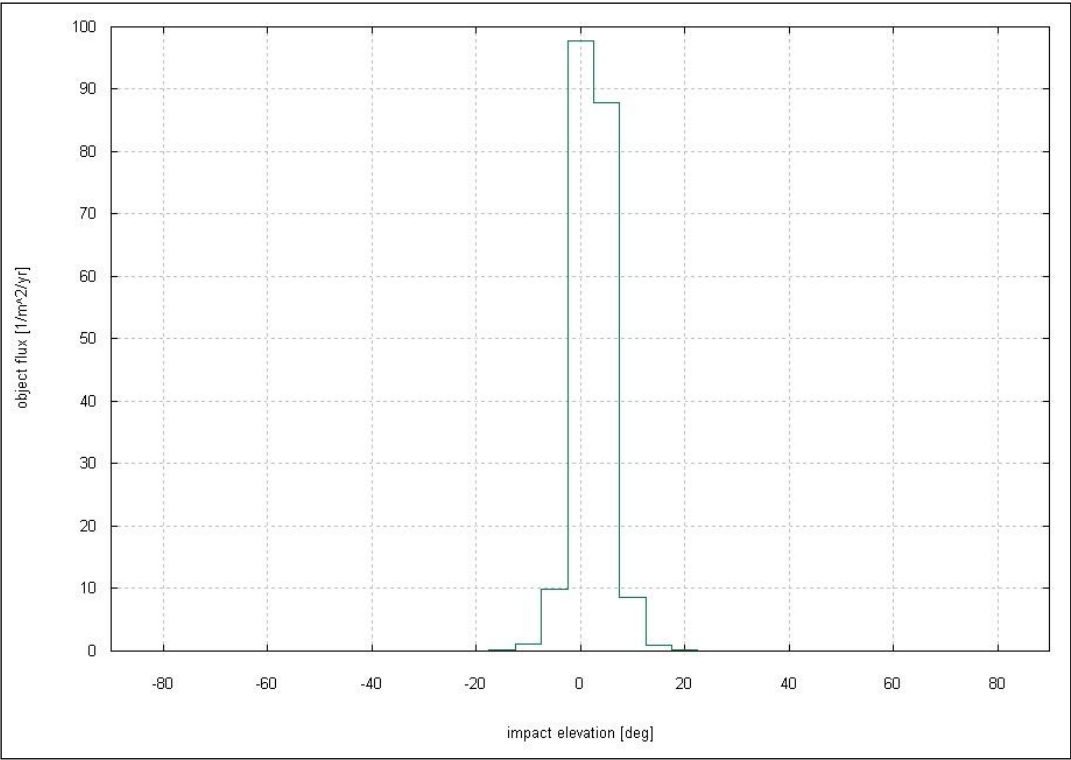
Figure 2-18   MASTER 2005 flux vs. elevation, 400 km / 51.6° orbit / d > 1 µm

Project: ESABASE2/Debris Release 12.1		Date:	2024-02-19
Technical Description		Revision:	1.11
Reference: R077-231rep_01_11_Debris_Technical Description.docx		Status:	Final

FEV etamax GmbH   Page 46 / 173
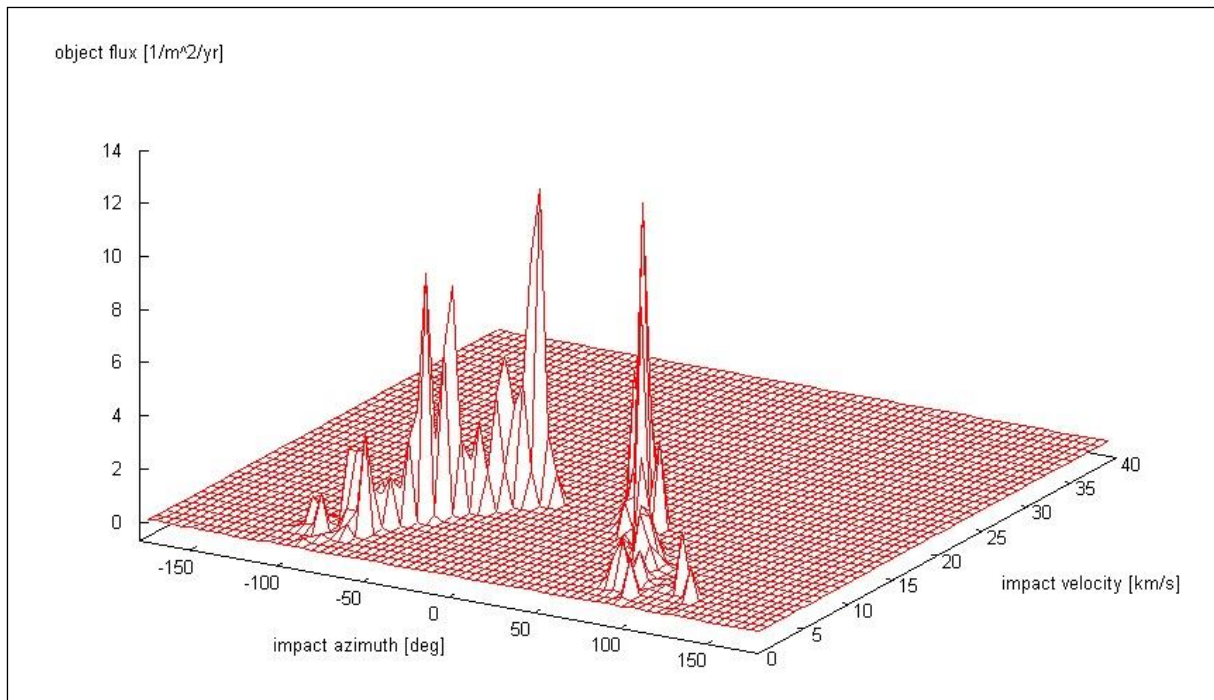
**Figure 2-19   MASTER 2005 flux vs. velocity and azimuth,
400 km / 51.6° orbit / d > 1 µm**

Although the spectra are displayed as differential distributions – except the diameter spectrum, which is cumulative – for compatibility with the results of the other debris models (see section 2.1.2.1), the distributions are provided and used in their cumulative form within the ESABASE2 analysis as described in chapter 5.

In ESABASE2/Debris the MASTER 2005 flux analysis is always performed for one complete orbit due to corresponding limitations of the MASTER 2005 flux analysis output. This results in identical analysis results for each orbital point in case of MASTER 2005, while in case of MASTER 2001 and ORDEM 2000 the flux analysis is performed for each orbital point.

2.1.6 MASTER 2009 Model

2.1.6.1 Overview

Upgrade of the Source Models

The following source models have been upgraded in MASTER 2009:

– The NASA break-up model has been revised for object sizes smaller 1 mm. Due to new data and findings, the area-to-mass distribution, in this size segment, is divided to consider for different materials of the fragments.

– A model for the new (historical, up to reference date) multi-layer insulation (MLI) population is introduced.

– The sodium-potassium (NaK) droplet model is revised and mathematical improvements are applied. Also observational data are considered. This leads to a lower released mass.

Project: ESABASE2/Debris Release 12.1	Date:	2024-02-19
Technical Description	Revision:	1.11
Reference: R077-231rep_01_11_Debris_Technical Description.docx	Status:	Final

FEV etamax GmbH   Page 47 / 173

- A possibility is introduced, that allows using flux contributions from downloadable population clouds as source and overlaying them over the background particulate environment.

Update of the Reference Population

During the processing of the historical population generation non-simulated and simulated objects are combined. 'Non-simulated objects' are objects, which are published (e.g. in USSTRATCOM's Space Catalogue) and propagated until the reference date. 'Simulated objects' are objects, which are simulated based on (known) events, e.g. explosions, collisions, SRM firings and NaK droplets releases, or on a theory, e.g. surface degradation (for paint flakes or for deterioration based MLI). The ejecta population is also simulated. Objects larger than 1 µm are considered. According to the process, the population is generated and propagated up to the reference epoch of May 1, 2009, providing quarterly population snapshots. The updated list of events now comprises 234 fragmentations (including 14 non-confirmed events), 1965 SRM firings, 16 NaK droplets releases, and 2 West Ford needle deployments.

STENVI (Standard Environment Interface) Output Files

The MASTER 2009 application introduces a possibility to activate the output of STENVI files. These files contain the flux results as a multi-dimensional distribution, with the available dimensions: impact azimuth, impact elevation, impact velocity, argument of true latitude, particle diameter and material density. One file is created for each considered debris source. The STENVI files provide a better description of the cross-dependencies of the parameters, compared to the 2D- or 3D-distributions, for the post processing of the data in the ESABASE2 analyses.

Multiple Target Orbit

The stand-alone version of MASTER 2009 allows the user to define multiple target orbits with individual time frames to simulate mission profiles with large orbit changes. The orbits are defined by sets of Keplerian orbital elements. The upper border of the MASTER control volume is r = 43164 km. If a part of the orbit exceeds this volume, it is ignored and only the part within the control volume is analysed. The lower border is r = 6564 km, thus if the defined perigee altitude is below 186 km it is automatically adjusted to 186 km.

Flux and Spatial Density Analysis for Historic and Future Epochs

The storage needs for the probability tables enables the generation of population snapshots for the complete space age on a single double-layer DVD, ranging from 1957 to the future (2060). For future epochs the user may select between three different population evolution scenarios. The stand-alone version of MASTER 2009 allows a flux and spatial density analysis for any epoch within the mentioned time span.

Note: Due to the improvement of the precision of the flux calculation in MASTER 2009, the simulation duration is increased. In particular cases (e.g. GTO) the duration increase can be up to 10 times compared with MASTER 2005.

2.1.6.2 Observation Data Sources

MASTER 2009 is a model of the debris environment of the Earth considering different sources and a particle diameter down to 1 µm. Figure 2-20 shows the considered debris sources and the corresponding size ranges.
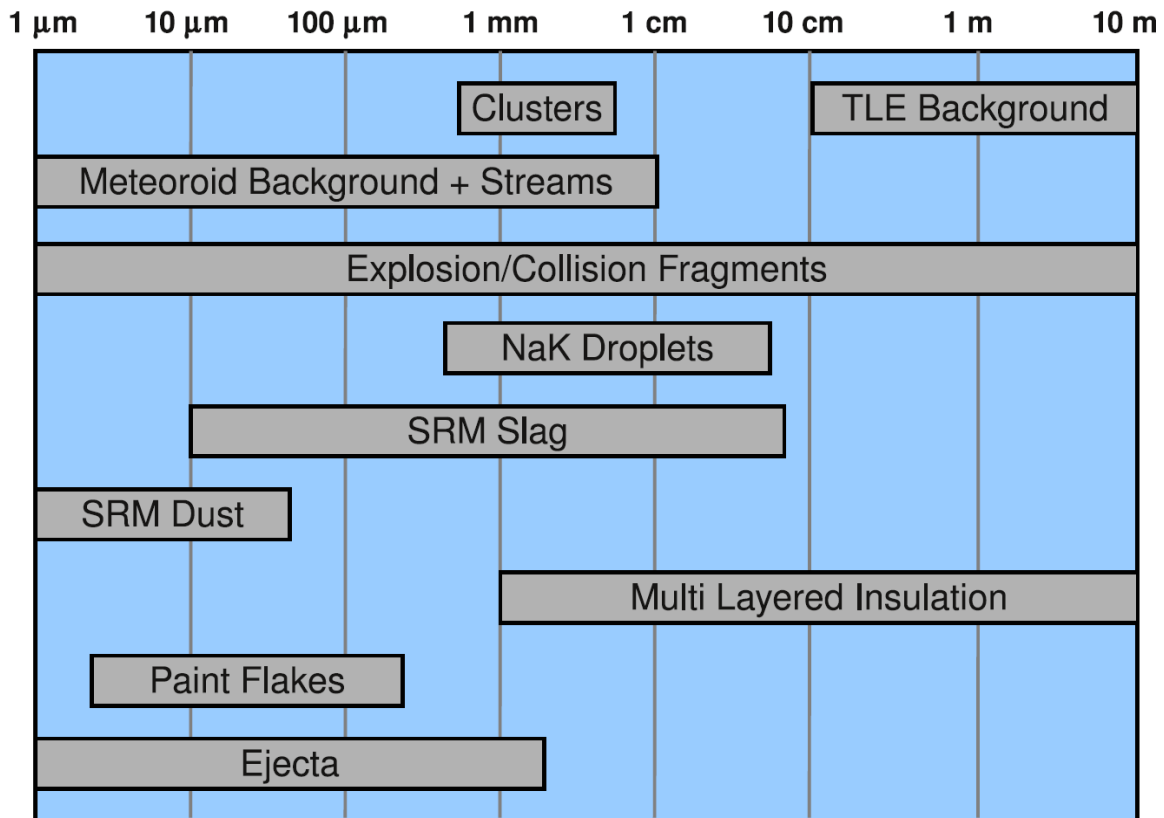
Figure 2-20:   Debris and meteoroid sources considered in MASTER 2009 model

The MASTER 2009 model provides realistic historic (quarterly) population snapshots from the beginning of spaceflight in 1957 until the reference epoch May 1st, 2009. Additionally, population snapshots for three different future scenarios for the years from 2010 until 2060 are provided. More information and the description of the scenarios can be found in /38/.

Within the ESABASE2/Debris implementation of MASTER 2009, the following sub-sets of these population snapshots are available:

Historic populations from 1980 to 2009, one snapshot (May 1st) per year.

Future populations from 2010 to 2025, one snapshot per year of the reference 'Business As Usual' scenario (no future constellations, no mitigation, continuation of recent traffic).

Note: *In contrary to MASTER 2005, the MASTER 2009 model both the future populations as well as the historic populations include all objects larger than 1 µm.*

Note: *Additional   population   snapshots   can   be   included   in   the "~|Solver\DEBRIS\Master2009\data" folder in the ESABASE2 installation from the MASTER 2009 DVD, if required.*

Project: ESABASE2/Debris Release 12.1	Date:	2024-02-19
Technical Description	Revision:	1.11
Reference: R077-231rep_01_11_Debris_Technical Description.docx	Status:	Final

FEV etamax GmbH   Page 49 / 173

As for MASTER 2001 and MASTER 2005 the debris analyser makes use of the population snapshot of the May 1st of the mission start year.

If it is intended to analyse the debris risk as a function of time, subsequent ESABASE2/Debris runs have to be performed with different analysis time start epochs.

2.1.6.3 Results

This section provides a brief description of the MASTER 2009 model results, which are used for flux calculation and damage assessment within ESABASE2/Debris.

The MASTER 2009 model still provides the four two-dimensional spectra, and the three-dimensional spectrum, as MASTER 2005 does. The spectra definitions are given in Table 6:

Spectra	min. value	max. value	number of steps
Flux vs. diameter	as specified for the analysis		≤ 16
Flux vs. impact velocity	0 km/s	20 km/s (60 km/s for meteoroids)	20 (60 for meteoroids)
Flux vs. impact azimuth angle	−180°	180°	72
Flux vs. impact elevation angle	−90°	90°	36
Flux vs. impact velocity and impact azimuth angle	as specified for the corresponding 2D spectra		

Table 6   MASTER 2009 flux spectra

Furthermore the MASTER 2009 model can provide a seven-dimensional spectrum, with the flux vs. impact azimuth, impact elevation, impact velocity, particle diameter, argument of true latitude and particle material density. The parameters are specified as for the 2D spectra. The additional parameter density is considered up to 5 g/cm³ without binning and the argument of true latitude is adjusted according to the calculated orbital point as one bin also. In this configuration a five-dimensional spectrum of flux vs. impact azimuth, impact elevation, impact velocity and diameter for a defined orbital arc is provided. This multi-dimensional spectrum is applied for the analysis purposes in ESABASE2/Debris.

Figure 2-21 to Figure 2-25 display the results (cross-sectional flux on a sphere) of the MASTER model for an ISS-like orbit. All spectra are given for the complete size range of the MASTER model.
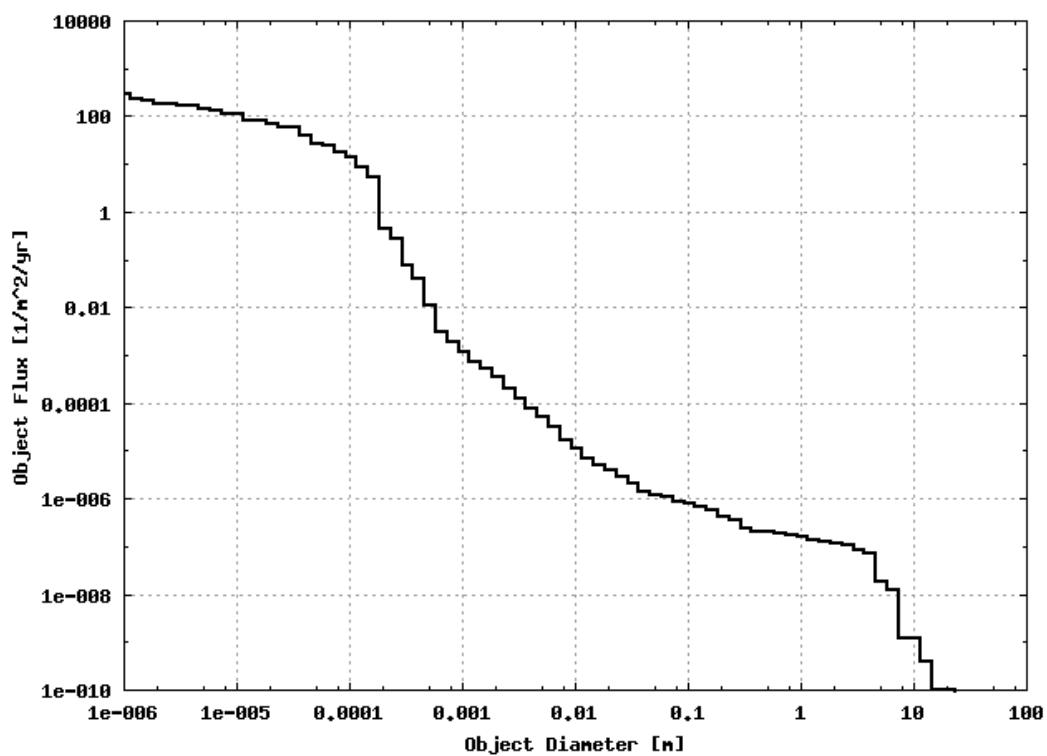
Figure 2-21   MASTER 2009 flux vs. object diameter, 400 km / 51.6° orbit / d > 1 µm
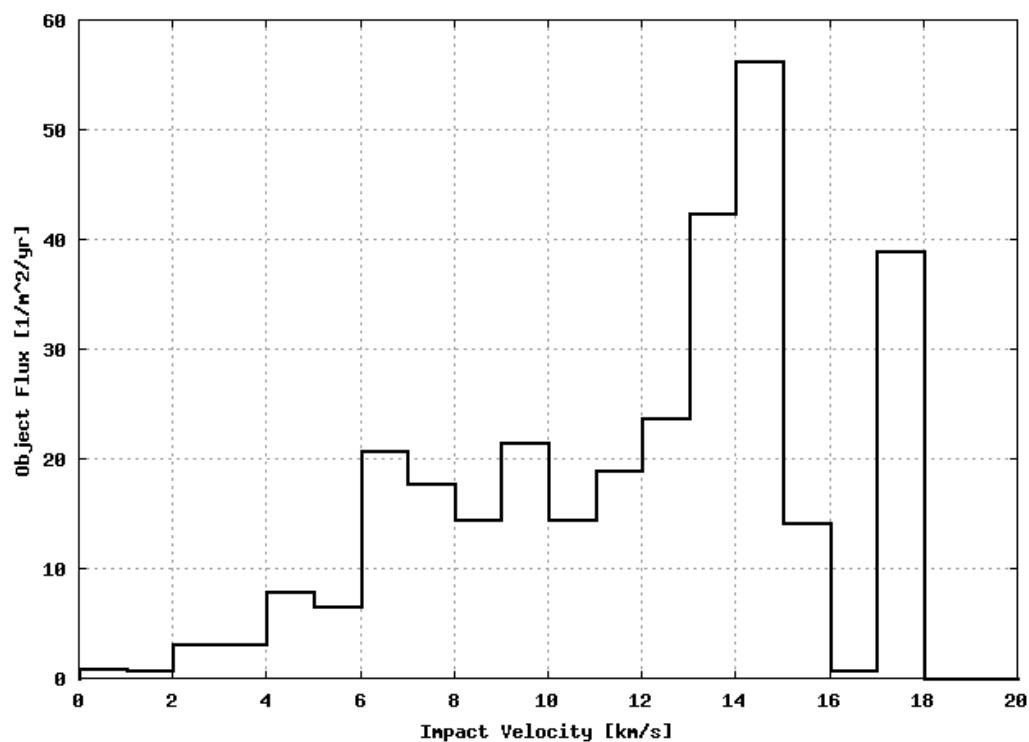
Figure 2-22   MASTER 2009 flux vs. impact velocity, 400 km / 51.6° orbit / d > 1 µm
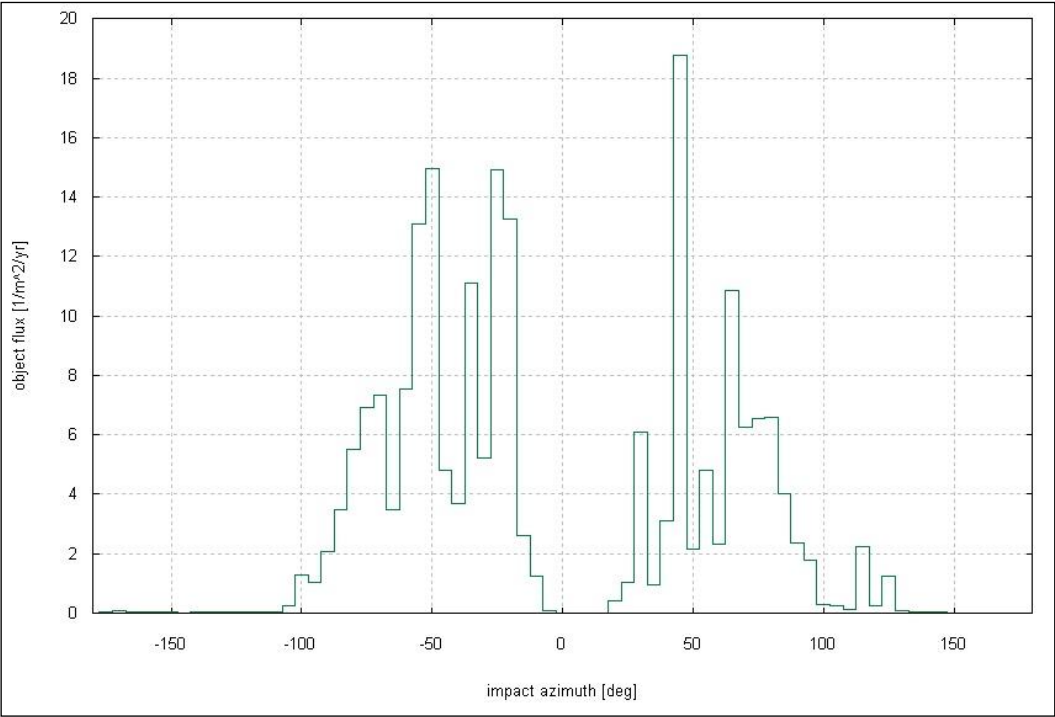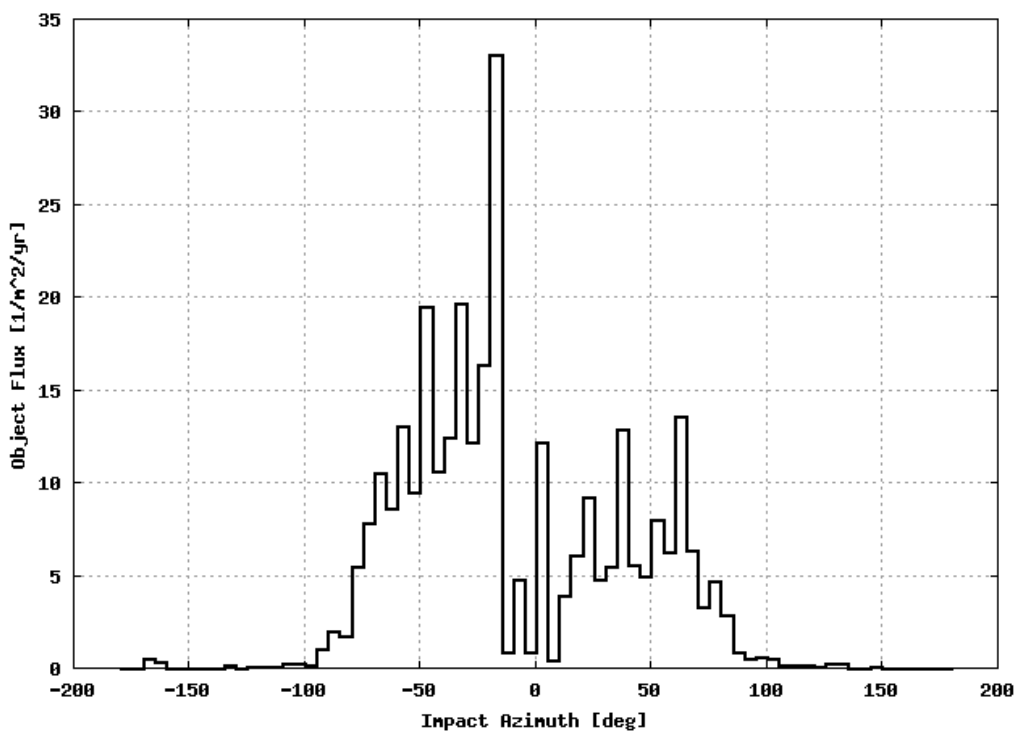
Figure 2-23   MASTER 2009 flux vs. azimuth, 400 km / 51.6° orbit / d > 1 μm
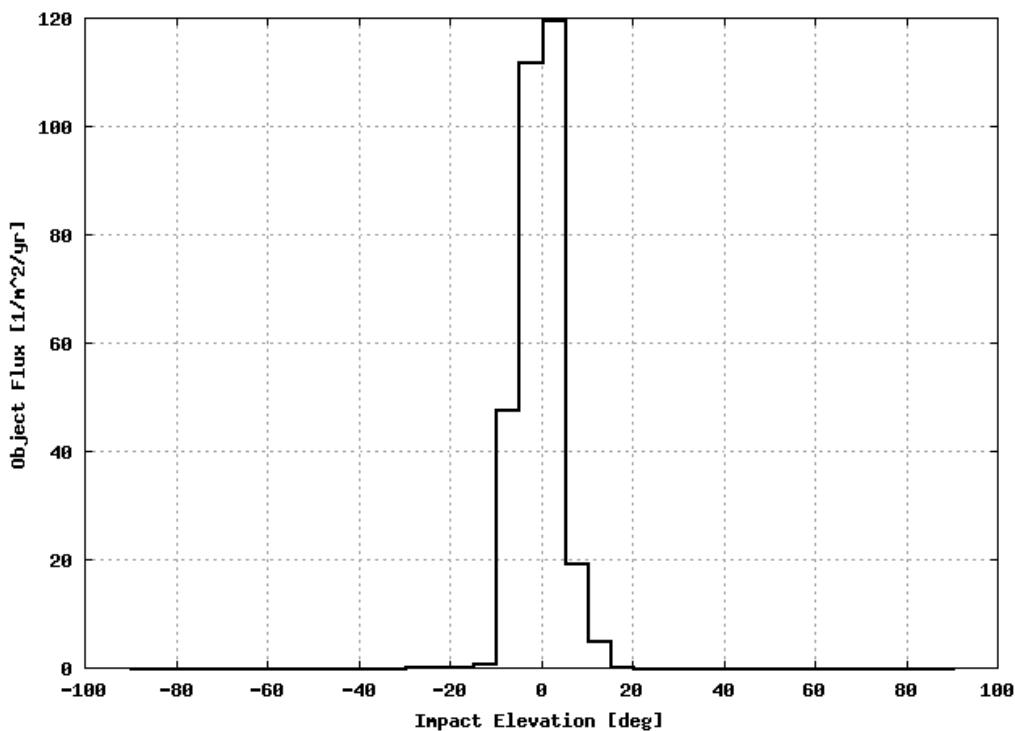
Figure 2-24   MASTER 2009 flux vs. elevation, 400 km / 51.6° orbit / d > 1 μm
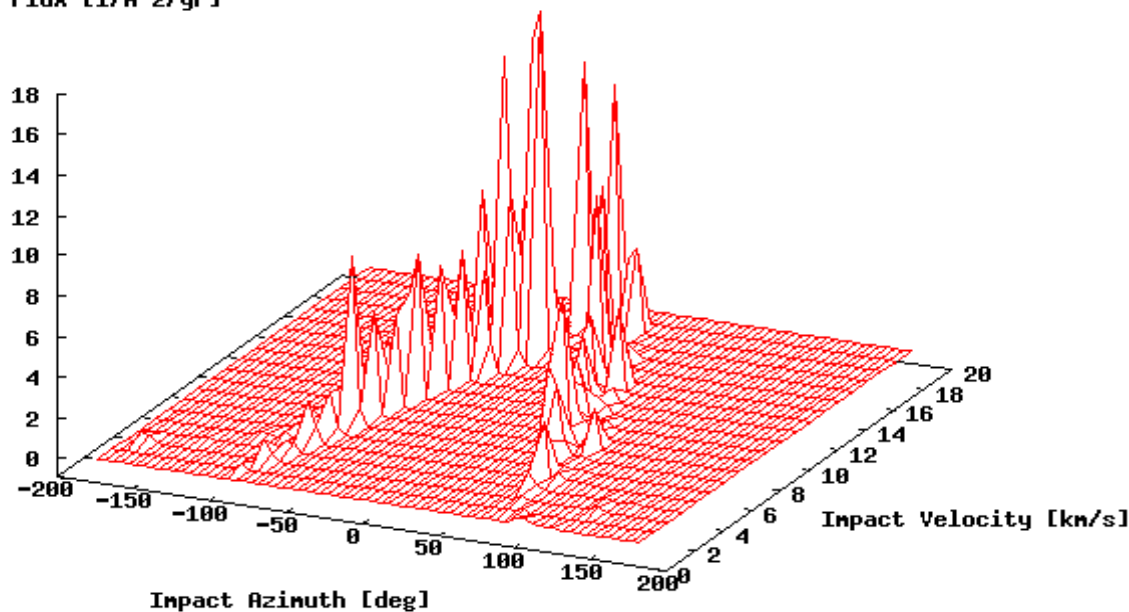
Figure 2-25   MASTER 2009 flux vs. impact velocity and azimuth, 400 km / 51.6° orbit / d > 1 µm

Although the spectra are displayed as differential distributions (except the diameter spectrum, which is cumulative) for comparability with the results of the other debris models (see section 2.1.2.1), the distributions are used in their cumulative form within the ESABASE2 analysis as described in chapter 5.

In ESABASE2/Debris the MASTER 2009 flux analysis is performed for an orbital arc spanned around the orbital point (centre of the time step) according to the time span between the points. The analysis is performed for each orbital point and covers in this way the whole orbit. Thus the flux analysis output is not limited as the output of MASTER 2005 and allows individual results for each orbital point as for MASTER 2001 or ORDEM 2000.

2.1.7 ORDEM 3.0 Model

2.1.7.1 Overview

ORDEM 3.0 is foreseen to supersede the previous NASA Orbital Debris Program Office (ODPO) model ORDEM2000. Due to the availability of new sensors, data and analytical techniques the development of a more comprehensive and sophisticated model was possible. Especially the following mandates were addressed during the development:

- extend the model to geosynchronous orbit (GEO) with the addition of Michigan Orbital Debris Survey Telescope (MODEST) data and modelling techniques to include GEO objects down to 10 cm,
- investigate and account for Molniya-type orbits with fixed arguments of perigee,
- continue to include radar detections of debris (SSN, Haystack AuXiliary radar [HAX], Haystack, and Goldstone) in the model and make use of these larger data sets to apply model fiducial points at half-decade sizes,

Project: ESABASE2/Debris Release 12.1		Date:	2024-02-19
Technical Description		Revision:	1.11
Reference: R077-231rep_01_11_Debris_Technical Description.docx		Status:	Final

FEV etamax GmbH   Page 53 / 173

- use the NASA Hypervelocity Impact Technology (HVIT) group's Space Transportation System (STS) micro-debris impact database (STS 71-135 listing over 600 impacts), which includes crater dimension, chemical composition, and derived damage equations on STS aluminium radiator panels and windows,
- assign small fragment (<10 cm) material density based on the Satellite Orbital Debris Characterization Impact Test (SOCIT) laboratory impact test results and on-orbit STS returned surface impactor analysis,
- model the Radar Ocean Reconnaissance SATellite (RORSAT) sodium potassium (NaK) coolant droplet population with radar measurements,
- include specific, major debris-producing events that have been thoroughly observed (i.e., the remnants of the FY-1C on 11 January 2007, and the accidental collision of Iridium 33 and Cosmos 2251 on 10 February 2009) and add to the general population,
- include long-term, debris-producing events that have been surmised from LEO high altitude radar data (i.e., SNAPSHOT, Transit, and 56° inclination-debris shedding activity) and add to the general population,
- fully develop the Bayesian statistical model for population derivation,
- include debris population uncertainties,
- provide "igloos" with equal-angle elements for full surrounding visualization of debris flux on spacecraft, and
- build the ORDEM 3.0 GUI to accommodate the full-angle views (i.e. 4π steradian views) of the large yearly input files.

Table 7 compares the ORDEM 3.0 features with the features of its predecessor ORDEM2000.

Parameter	ORDEM2000	ORDEM 3.0
Spacecraft & Telescope/Radar analysis modes	Yes	Yes
Time range	1991 to 2030	2010 to 2035
Altitude range with minimum debris size	200 to 2000 km (>10 µm) (LEO)	100 to 40,000 km (>10 µm)* (LEO to GTO) 34,000 to 40,000 km (>10 cm) (GEO)
Orbit types	Circular (radial velocity ignored)	Circular to highly elliptical
Model population breakdown by type & material density	No	Intacts Low-density (1.4 g/cc) fragments Medium-density (2.8 g/cc) fragments & microdebris High-density (7.9 g/cc) fragments & microdebris

Project: ESABASE2/Debris Release 12.1		Date:	2024-02-19
Technical Description		Revision:	1.11
Reference: R077-231rep_01_11_Debris_Technical Description.docx		Status:	Final

FEV etamax GmbH   Page 54 / 173

Parameter	ORDEM2000	ORDEM 3.0
		RORSAT NaK coolant droplets (0.9 g/cc)
Model cumulative size thresholds (fiducial points)	10 µm, 100 µm, 1 mm, 1 cm , 10 cm, 1 m	10 µm, 31.6 µm, 100 µm, 316 µm, 1 mm, 3.16 mm, 1 cm, 3.16 cm, 10 cm, 31.6 cm, 1 m
Flux uncertainties	No	Yes
Total input file size	13.5 MB	1.25 GB

Table 7   Feature comparison of ORDEM2000 and ORDEM 3.0

* While the geosynchronous transfer orbit (GTO) is not as well observed as LEO, the orbital dynamic forces and mechanisms for fragmentation are considered to be similar. The ODPO therefore allows for > 10 µm fluxes through GTO. For GEO the dynamics (including perturbation forces and impact velocities) as well as the size and structure of satellites are unique, though GTO and GEO physically overlap. The ODPO provides GEO debris fluxes for 10 cm and larger only. This is based on the SSN (1 m and larger), the MODEST uncorrelated target data (30 cm – 1 m) and the MODEST uncorrelated targets extended to 10 cm. Any fluxes below that 10 cm threshold at altitudes above LEO altitudes are solely due to GTO objects.

Figure 2-26 visualise the ORDEM GUI options and coding structure flowchart. Red frame indicates GUI user selections; gray background indicates the ORDEM processes and blue highlights the ESABASE2 relevant path. For orbits whose parameters overlap into LEO and GEO igloo bins, both LEO and GEO calculations are accessed. Due to the interaction between ESABASE2 and ORDEM 3.0 via command line, the user selections are written to the ORDEM 3.0 input file by ESABASE2.

The igloo bin sizes of 10° in azimuth, 10° in elevation and 1 km/sec in velocity or 30° in azimuth, 30° in elevation and 2 km/sec in velocity can be chosen. The first, higher resolution is used in ESABASE2.
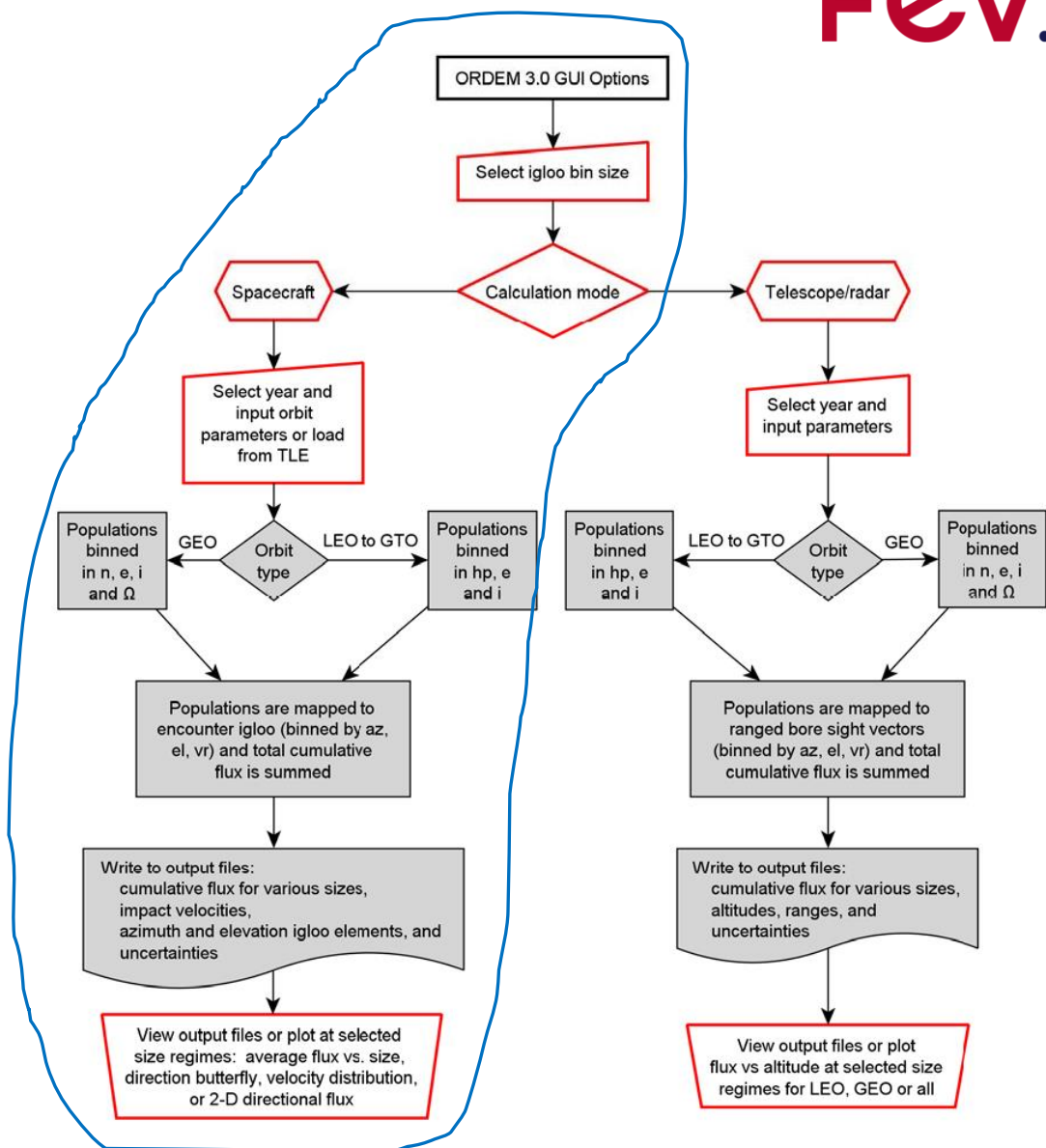
Figure 2-26   ORDEM GUI options and coding structure flowchart

2.1.7.2 Observation Data Sources and Modelling

The new model input populations are pre-derived directly from the data sources listed in Table 8. These consist of in-situ sources, for debris ranging from 10 µm to less than 1 mm, and remote sensors, for debris ranging from 1 mm to over 1 m. These data are applied to ORDEM 3.0 in a maximum likelihood estimation and a Bayesian statistical process, respectively, in which the NASA ODPO models listed in Table 9 form the a priori conditions. Those modelled debris populations are reweighted in number to be compatible with the data in orbital regions where the data are collected. By extension, model debris populations are reweighted in regions where no data are available (e.g., all sizes in low latitudes and sub-millimeter sizes at altitudes above the International Space Station [ISS]).

Observational Data	Role	Region/Approximate Size
SSN catalogue (radars, telescopes)	Intacts & large fragments	LEO > 10 cm, GEO > 1 m
HAX (radar)	Statistical populations	LEO > 3 cm
Haystack (radar)	Statistical populations	LEO > 5.5 mm
Goldstone (radar)	Statistical populations	2 mm < LEO < 8 mm
STS windows & radiators (returned surfaces)	Statistical populations	10 µm < LEO < 1 mm
MODEST (telescope)	GEO data set	GEO > 30 cm

<div align="center">

Table 8   **Contributing Data Sets**

</div>

Model	Usage	Corroborative Data
LEGEND	LEO Fragments > 1 mm GEO Fragments > 10 cm	SSN, Haystack, HAX, MODEST, SSN
Degradation/Ejecta	10 µm < LEO < 1 mm	STS windows & radiators

<div align="center">

Table 9   **Contributing Models (with Corroborative Data)**

</div>

Table 10 for non-GEO objects and in Table 11 for GEO objects. Bin sizes are chosen to complement actual population distributions. The final files are from the direct yearly input database of ORDEM 3.0.

The binned input populations are accessed via the Spacecraft and Telescope/Radar modes; where the former uses the encounter igloo method and the later uses a segmented bore-sight vector for computation of flux.

Parameter	Binning Intervals	Total No. of Bins
Perigee altitude, h_p	$100 \leq h_p < 2000$ km $\rightarrow$ 33.33 km bins $2000 \leq h_p < 10{,}000$ km $\rightarrow$ 100 km bins $10{,}000 \leq h_p < 40{,}000$ km $\rightarrow$ 200 km bins	287
Eccentricity, e	$0 \leq \sqrt{e} < 0.02666 \rightarrow 0.02666$ bin $0.02666 \leq \sqrt{e} < 1 \rightarrow 0.01333$ bins	74
Inclination, i	$0° \leq i < 180° \rightarrow 0.75°$ bins	240

<div align="center">

Table 10   **Input File Population Bins for LEO to GTO**

</div>

Parameter	Binning Intervals	Total No. of Bins
Mean Motion, n	$0.5 \leq n < 0.95 \rightarrow 0.01$ rev/day bins $0.95 \leq n < 1.05 \rightarrow 0.001$ rev/day bins $1.05 \leq n < 1.80 \rightarrow 0.01$ rev/day bins	220
Eccentricity, e	$0 \leq \sqrt{e} < 0.5 \rightarrow 0.02$ bins	25
Inclination, i	$0° \leq i < 0.2° \rightarrow 0.2°$ bins $0.2° \leq i < 1.0° \rightarrow 0.8°$ bins $1° \leq i < 25° \rightarrow 1°$ bins	26
Right ascension of ascending node, Ω	$0° \leq \Omega < 360° \rightarrow 5°$ bins	72

Table 11   Input File Population Bins for GEO

2.1.7.3 Results

The ORDEM 3.0 output files are plain text and column-separated for easy transfer into spreadsheets or other visualization programs.

ORDEM output files are generated for the two analysis modes: Spacecraft and Telescope/Radar. For the purpose of analyses with ESABASE2 the Spacecraft mode is used. Table 12 lists the output files of this mode.

File Name	Description
SIZEFLUX_SC.OUT	Average impact flux vs. size on the spacecraft per orbit. Graph input.
VELFLUX_SC.OUT	Impact velocity distribution on the spacecraft per orbit. Graph input.
BFLY_SC.OUT	Fluxes vs. yaw (collapsed in pitch) in the spacecraft frame. Graph input.
DIRFLUX_SC.OUT	Fluxes in 2-D map projection in the spacecraft frame. Graph input.
IGLOOFLUX_SC.OUT	Igloo element fluxes and velocities. Intermediate file.
IGLOO_FLUX_SIGMAPOP_SC.OUT	Correlated population uncertainty estimates.
IGLOOFLUX_SIGMARAN_SC.OUT	Random uncertainty estimates.

Table 12   Files output of ORDEM 3.0 Spacecraft mode

Project: ESABASE2/Debris Release 12.1		Date:	2024-02-19
Technical Description		Revision:	1.11
Reference: R077-231rep_01_11_Debris_Technical Description.docx		Status:	Final

FEV etamax GmbH   Page 58 / 173

Especially the *SIZEFLUX_SC.OUT* and the *IGLOOFLUX_SC.OUT* files provide the basis for the analyses with ESABASE2.

SIZEFLUX_SC.OUT provides the average cumulative flux by particle size. It contains additionally the lower and upper one-sigma uncertainties.

IGLOOFLUX_SC.OUT provides a multi-dimensional spectrum, with the flux vs. impact azimuth, impact elevation, impact velocity, and particle size and particle kind/density in the resolution 10° in azimuth, 10° in elevation and 1 km /s in velocity. The file is structured in the following way:

The first column lists the encounter igloo element number. The second through seventh columns list the lower and upper azimuth bin bounds, lower and upper elevation bin bounds, and lower and upper relative impact velocity bin bounds, respectively. Subsequent columns list the individual sub-population fluxes for the defined igloo element. The sub-population names are abbreviated using two letters for the population type and two numbers for the size (in powers of 10 µm).

Debris type codes:

NK - sodium-potassium (NaK) reactor coolant

LD - general low-density debris (<2 g/cc)

MD - general medium-density debris (2-6 g/cc)

HD - general high-density debris (>6 g/cc)

IN - intact/launched objects

Debris size bin codes, in powers of 10 µm:

"10" = $10^{1.0}$ µm = $1.00e^{-5}$ m = 10 µm

"15" = $10^{1.5}$ µm = $3.16e^{-5}$ m = 31.6 µm

"20" = $10^{2.0}$ µm = $1.00e^{-4}$ m = 100 µm

"25" = $10^{2.5}$ µm = $3.16e^{-4}$ m = 316 µm

"30" = $10^{3.0}$ µm = $1.00e^{-3}$ m = 1 mm

"35" = $10^{3.5}$ µm = $3.16e^{-3}$ m = 3.16 mm

"40" = $10^{4.0}$ µm = $1.00e^{-2}$ m = 1 cm

"45" = $10^{4.5}$ µm = $3.16e^{-2}$ m = 3.16 cm

"50" = $10^{5.0}$ µm = $1.00e^{-1}$ m = 10 cm

"55" = $10^{5.5}$ µm = $3.16e^{-1}$ m = 31.6 cm

"60" = $10^{6.0}$ µm = $1.00e^{+0}$ m = 1 m

This multi-dimensional spectrum is applied for the analysis purposes in ESABASE2/Debris.

Figure 2-27 to Figure 2-31 display the results (cross-sectional flux on a sphere) of the ORDEM 3.0 model for an LEO.

Average Cross-Sectional Flux vs. Size

Year: 2014 Perigee Altitude = 400.000 Apogee Altitude = 400.000 inc = 51.60

Figure 2-27   Spacecraft Assessment Average Flux vs. Size graph (src. /47/)

Flux vs. Local Azimuth

Year: 2014 Perigee Altitude = 400.000 Apogee Altitude = 400.000 inc = 51.60 particle size = >10um
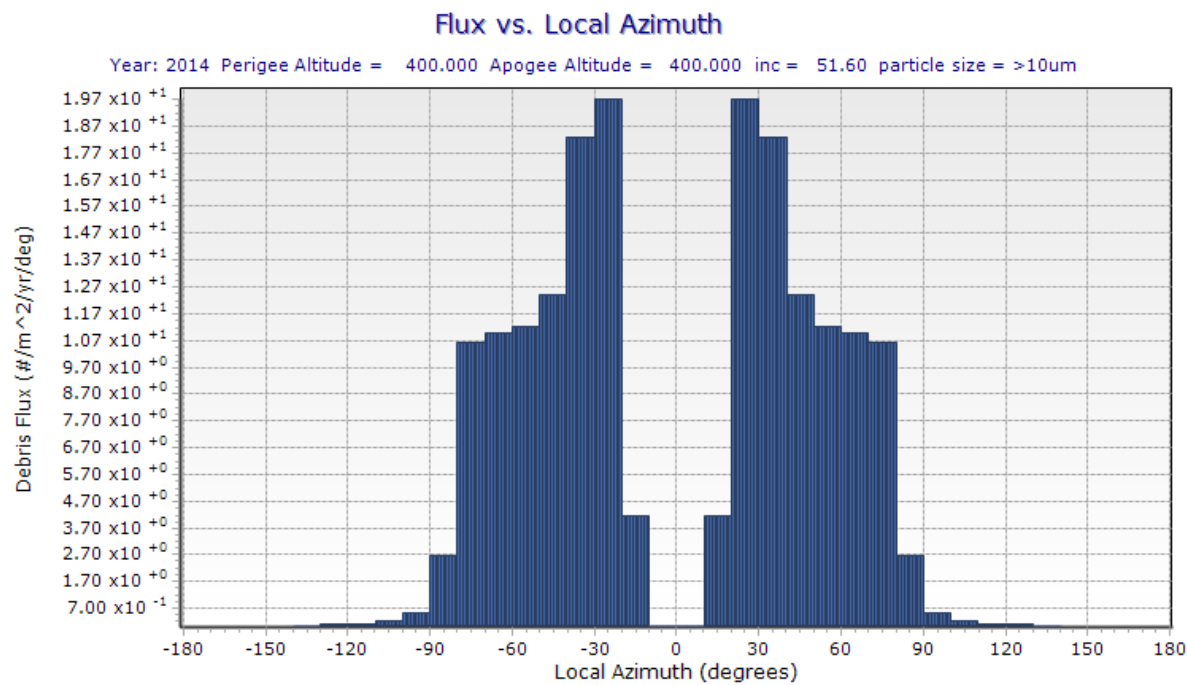
Figure 2-28   Spacecraft Assessment skyline butterfly graph (src. /47/)

Project: ESABASE2/Debris Release 12.1	Date:	2024-02-19
Technical Description	Revision:	1.11
Reference: R077-231rep_01_11_Debris_Technical Description.docx	Status:	Final

FEV etamax GmbH   Page 60 / 173

Flux vs. Local Azimuth

Year: 2014 Perigee Altitude = 400.000 Apogee Altitude = 400.000 inc = 51.60 particle size = >10um
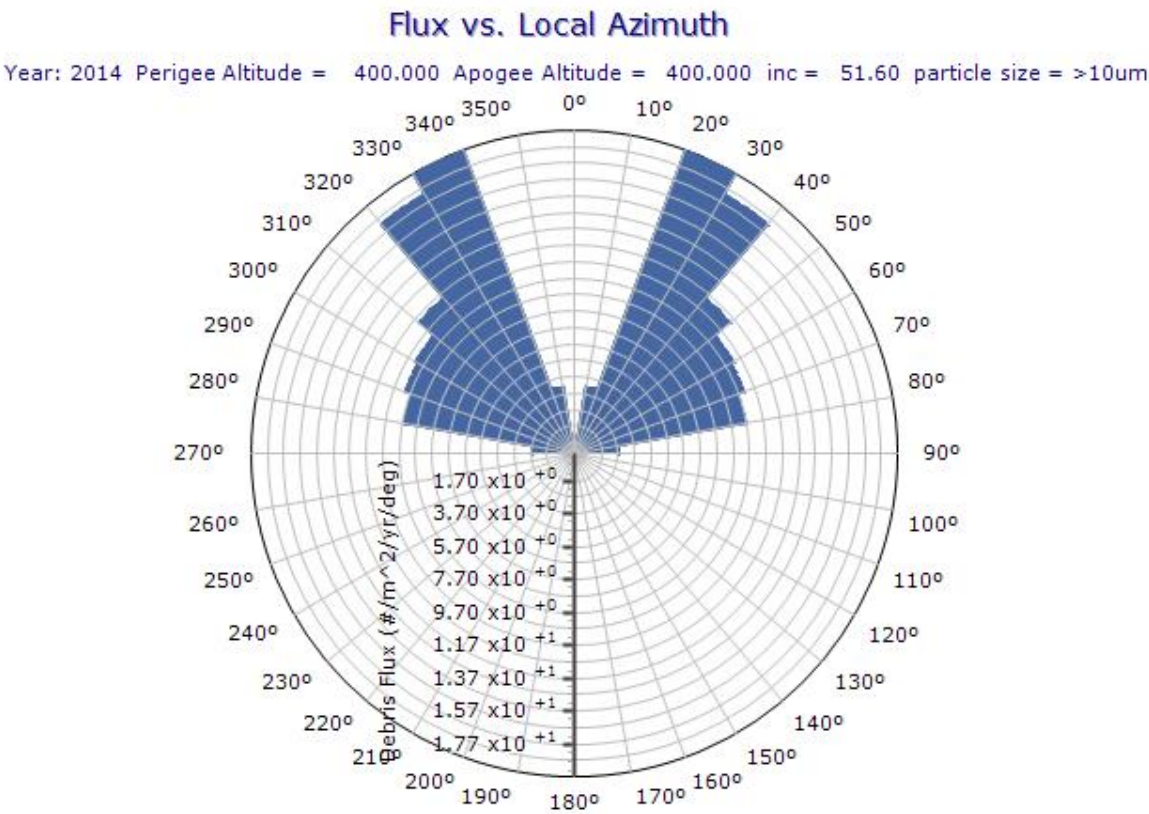
Figure 2-29   Spacecraft Assessment radial butterfly graph (src. /47/)

Velocity Distribution

Year: 2014 Perigee Altitude = 400.000 Apogee Altitude = 400.000 inc = 51.60 particle size = >10um
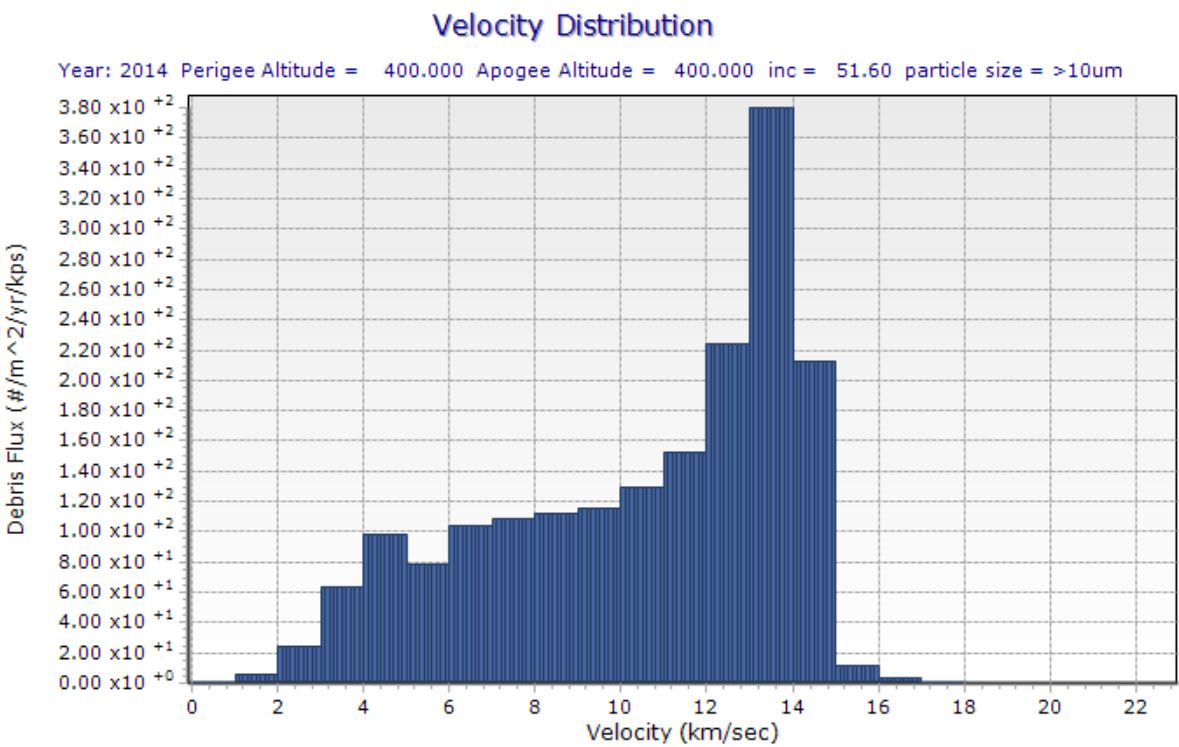
Figure 2-30   Spacecraft Assessment Velocity flux distribution (src. /47/)

Project: ESABASE2/Debris Release 12.1		Date:	2024-02-19
Technical Description		Revision:	1.11
Reference: R077-231rep_01_11_Debris_Technical Description.docx		Status:	Final

FEV etamax GmbH   Page 61 / 173

2-D Directional Flux
Year: 2014 Perigee Altitude = 400.000 Apogee Altitude = 400.000 inc = 51.60 particle size = >10um

4/8/2014 10:05:33 AM

Figure 2-31   Spacecraft Assessment 2-D Directional Flux projection (src. /47/)

Examples of the two Direction Butterfly graphs are presented in Figure 2-28 and Figure 2-29. These figures represent average directional fluxes on the spacecraft from all directions, in three dimensions. These fluxes are summed and then collapsed to the 2-D spacecraft plane defined by the velocity and angular momentum vectors. The assessment velocity flux distribution on the spacecraft is displayed in Figure 2-30. The three-dimensional average flux on the spacecraft is fully realized in the mapped 2-D directional flux projection in Figure 2-31. In the letter the direction relative to the spacecraft is noted in coordinates (local azimuth and local elevation): where azimuth runs along the horizontal from left to right and ranges from -180° to 180° and elevation runs vertically from bottom to top and ranges from -90° to 90°.

The distributions are used in their cumulative form within the ESABASE2 analysis as described in chapter 5.

In ESABASE2/Debris the ORDEM 3.0 flux analysis is performed for the whole orbit, due to the missing possibility in ORDEM 3.0 to define orbital arcs. According to this fact, the debris distributions which are provided by ORDEM 3.0 and used as basis for the analysis are equal for all orbital points.

2.1.8 MASTER 8 Model

2.1.8.1 Overview

Upgrade of the Source Models

Project: ESABASE2/Debris Release 12.1	Date:	2024-02-19
Technical Description	Revision:	1.11
Reference: R077-231rep_01_11_Debris_Technical Description.docx	Status:	Final

FEV etamax GmbH   Page 62 / 173

The following features have been upgraded in MASTER 8:

– Uncertainty indicators in altitude and diameter spectra have been implemented.

– Target orbit propagation.

– The NASA break-up model implementation has got a major upgrade.

– A major revision of the multi-layer insulation (MLI) population was performed, which lead to a validated reference population and a provided future projection.

– The sodium-potassium (NaK) droplet model is extended by a new NaK leakage sub-source.

– The SRM firing list was completely revised.

– Grün meteoroid model is now included.

– Meteoroid flux evaluations in Lagrange points is now possible.

– A new condensed population is introduced, which includes the space debris distribution of all man-made objects combined.

Update of the Reference Population

During the processing of the historical population generation non-simulated and simulated objects are combined. 'Non-simulated objects' are objects, which are published (e.g. in USSTRATCOM's Space Catalogue) and propagated until the reference date. 'Simulated objects' are objects, which are simulated based on (known) events, e.g. explosions, collisions, SRM firings and NaK droplets releases, or on a theory, e.g. surface degradation (for paint flakes or for deterioration based MLI). The ejecta population is also simulated. Objects larger than 1 μm are considered. According to the process, the population is generated and propagated up to the reference epoch of November 1, 2016, providing quarterly population snapshots. The updated list of events now comprises 258 fragmentations, 2442 SRM firings, 16 NaK droplets releases, and 2 NaK leakage events. The definition of the reference epoch is now flexible and is based on the available reference population data files, thus it can be updated in the future without updating the complete tool.

STENVI (Standard Environment Interface) Output Files

The MASTER 8 application continue to provide a possibility to activate the output of STENVI files. These files contain the flux results as a multi-dimensional distribution, with the available dimensions: impact azimuth, impact elevation, impact velocity, argument of true latitude, particle diameter and material density. One file is created for each considered debris source, or one for all sources if condensed population is used. The STENVI files provide a better description of the cross-dependencies of the parameters, compared to the 2D- or 3D-distributions, for the post processing of the data in the ESABASE2 analyses.

Flux and Spatial Density Analysis for Historic and Future Epochs

The population snapshots start with the begin of the space age 1957 and range to the future year 2036 (according to /49/ 100 years were simulated, thus up to 2116 is expected to be available). The population snapshots for past and future can, and in ESABASE2 need, to be included separately. They can be achieved from ESA's portal: https://sdup.esoc.esa.int/. The

Project: ESABASE2/Debris Release 12.1	Date:	2024-02-19
Technical Description	Revision:	1.11
Reference: R077-231rep_01_11_Debris_Technical Description.docx	Status:	Final

FEV etamax GmbH　　　　　　　　　　　　　　　　　　　　　Page 63 / 173

three different population evolution scenarios were dropped and the population evolution scenario is generated based on Monte-Carlo method. Additionally uncertainty indicators in altitude and diameter spectra are introduced.

Note: The performance of MASTER 8 is comparable (slightly better than) with MASTER 2009.

2.1.8.2 Observation Data Sources

MASTER 8 is a model of the debris environment of the Earth considering different sources and a particle diameter down to 1 μm. Figure 2-32 shows the considered debris sources and the corresponding size ranges.
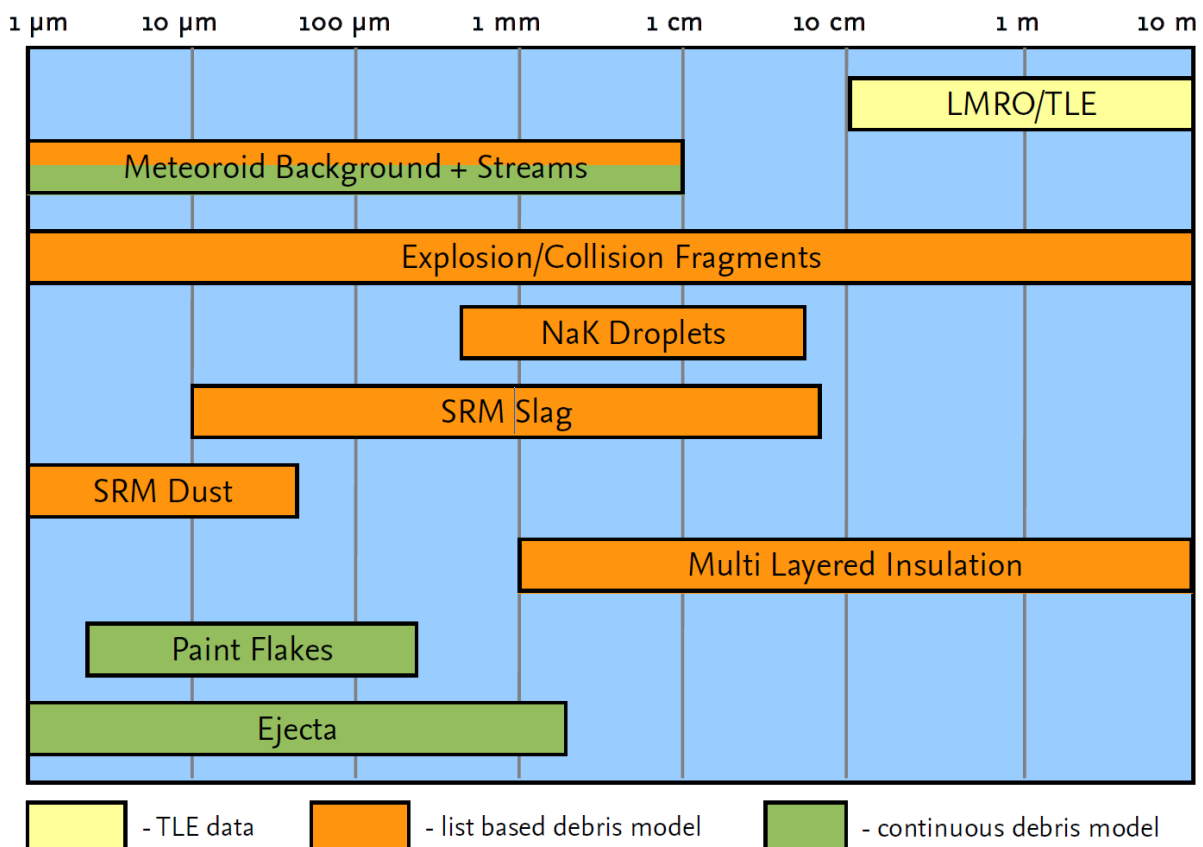
Figure 2-32: **Debris and meteoroid sources considered in MASTER 8 model (/49/)**

The MASTER 8 model provides realistic historic (quarterly) population snapshots from the beginning of spaceflight in 1957 until the reference epoch November 1st, 2016, which could change later on due to the new flexible reference date feature. Additionally, annual population snapshots for a future scenario, based on Monte-Carlo approach, for the years from 2017 until currently 2036 are provided, according to /49/ 100 years were simulated, thus results up to 2116 are expected to exist and probably made available later. More information and the descriptions can be found in /49/.

Within the ESABASE2/Debris implementation of MASTER 8, the following sub-sets of these population snapshots are available:

Project: ESABASE2/Debris Release 12.1	Date:	2024-02-19
Technical Description	Revision:	1.11
Reference: R077-231rep_01_11_Debris_Technical Description.docx	Status:	Final

FEV etamax GmbH — Page 64 / 173

Historic populations data for the reference date 2016, one snapshot (November 1st) as individual populations and as condensed population.

Future populations currently no future populations are included. Since there still not all data are finalised (ejecta and paint flakes future populations are missing at the moment of document generation), please visit ESA's portal: https://sdup.esoc.esa.int/ to download the most up-to-date available population data to be used with ESABASE2. For the integration see the following note.

Note: *Additional population snapshots can be included in the "~|Solver|DEBRIS|Master8|data" folder in the ESABASE2 installation from the MASTER 8 DVD or from ESA's portal: https://sdup.esoc.esa.int/.*

In contrary to the previous MASTER model implementation for MASTER 8 the debris analyser makes use of all population snapshot available for the mission duration and requires them to be available. This leads to an average results over the analysed time duration.

2.1.8.3 Results

This section provides a brief description of the MASTER 8 model results, which are used for flux calculation and damage assessment within ESABASE2/Debris.

The MASTER 8 model can still provide the four two-dimensional spectra, and the three-dimensional spectrum, as MASTER 2005 does. This spectra are also reflected in the 2D results of ESABASE2. The spectra definitions are given in Table 13:

Spectra	min. value	max. value	number of steps
Flux vs. diameter	as specified for the analysis		= 32
Flux vs. impact velocity	0 km/s	20 km/s (60 km/s for meteoroids)	20 (60 for meteoroids)
Flux vs. impact azimuth angle	−180°	180°	90
Flux vs. impact elevation angle	−90°	90°	45
Flux vs. impact velocity and impact azimuth angle	as specified for the corresponding 2D spectra		

Table 13   MASTER 8 flux spectra

Furthermore the MASTER 8, as MASER 2009, model can provide a seven-dimensional spectrum, with the flux vs. impact azimuth, impact elevation, impact velocity, particle diameter, argument of true latitude and particle material density. The parameters are specified as for the 2D spectra presented. The additional parameter density is considered up to 9 g/cm³ without binning and the argument of true latitude is adjusted to 360 bins each 1° and the according results to the calculated orbital point is extracted in 1°-resolution. In this configuration a five-

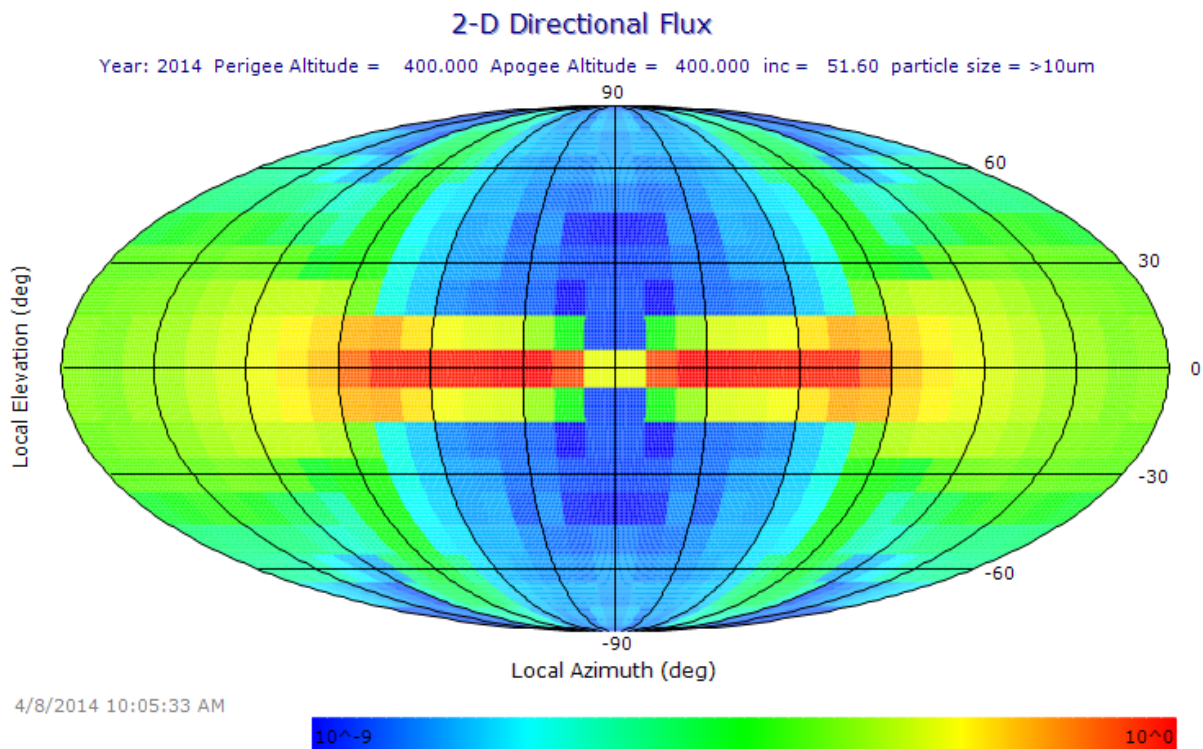| Project: ESABASE2/Debris Release 12.1	Date:	2024-02-19
Technical Description	Revision:	1.11
Reference: R077-231rep_01_11_Debris_Technical Description.docx	Status:	Final

FEV etamax GmbH | Page 65 / 173

dimensional spectrum of flux vs. impact azimuth, impact elevation, impact velocity and diameter for the orbit is provided, where the orbital points arcs can be extracted. This multi-dimensional spectrum is applied for the analysis purposes in ESABASE2/Debris.

Figure 2-33 to Figure 2-37 display the results (cross-sectional flux on a sphere) of the MASTER model for an ISS-like orbit. All spectra are given for the complete size range of the MASTER model. The cumulative population was used to generate the results.
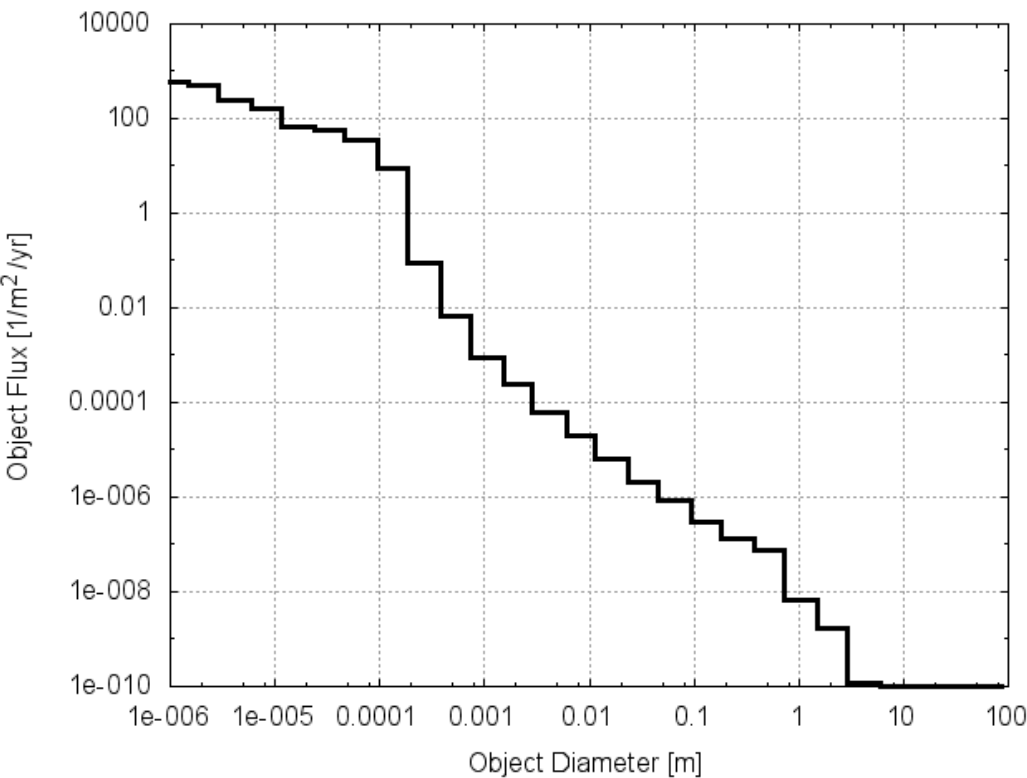
Figure 2-33   MASTER 8 flux vs. object diameter, 400 km / 51.6° orbit / d > 1 µm

Project: ESABASE2/Debris Release 12.1		Date:	2024-02-19
Technical Description		Revision:	1.11
Reference: R077-231rep_01_11_Debris_Technical Description.docx		Status:	Final

FEV etamax GmbH   Page 66 / 173
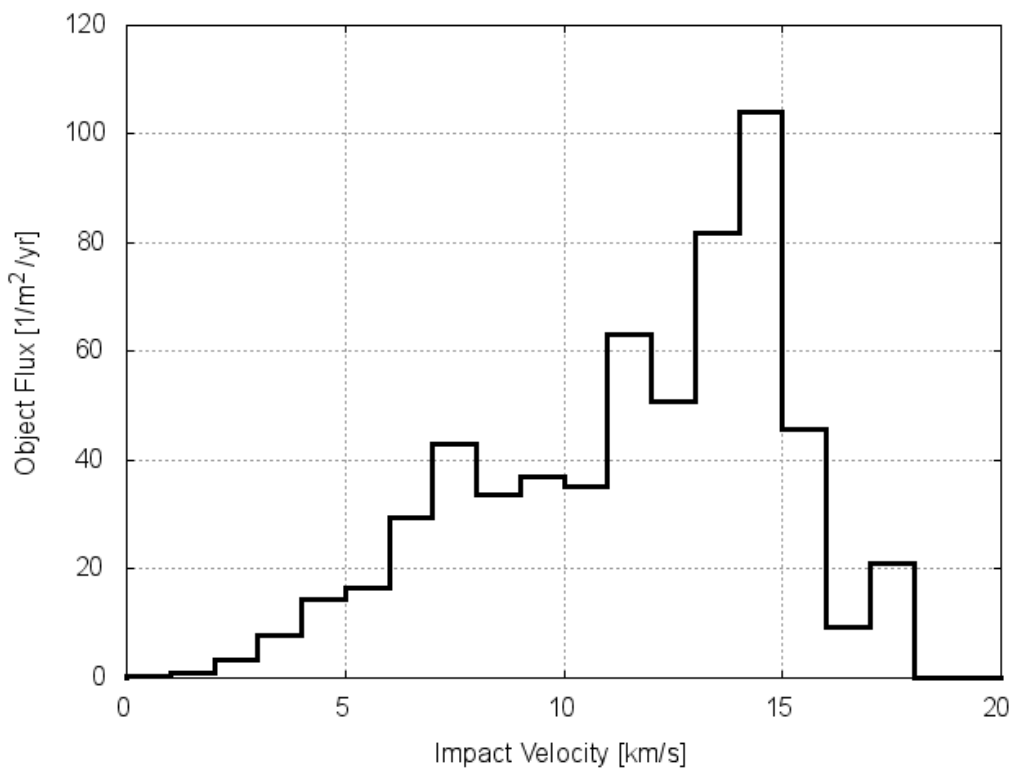
Figure 2-34   MASTER 8 flux vs. impact velocity, 400 km / 51.6° orbit / d > 1 µm
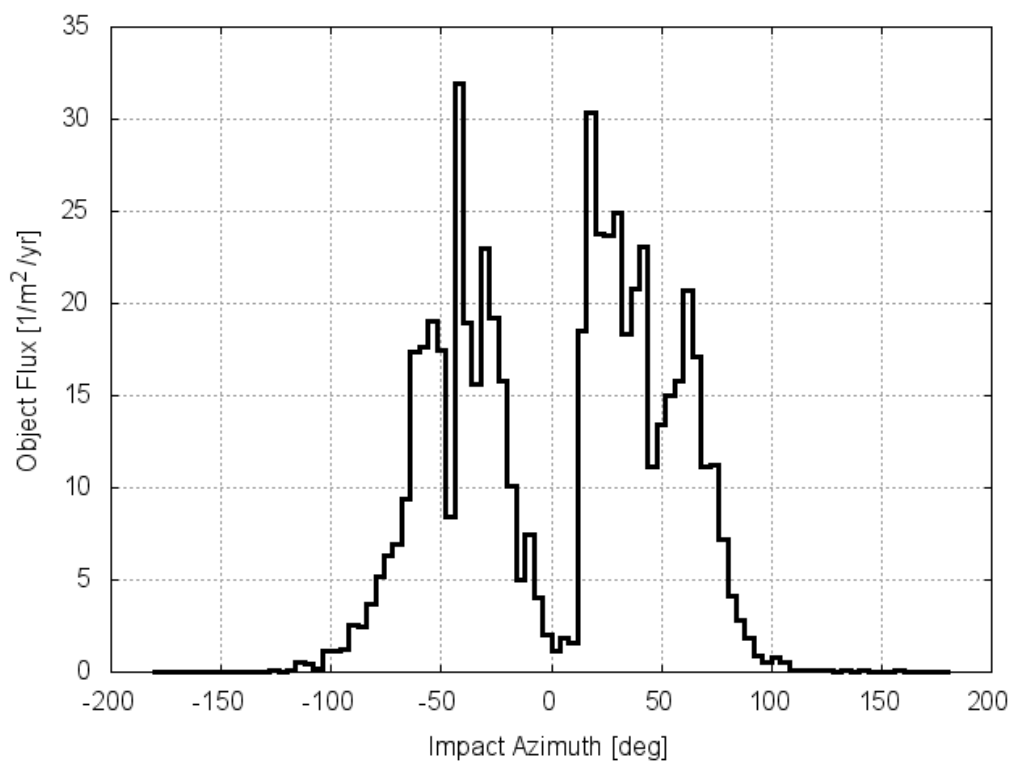
Figure 2-35   MASTER 8 flux vs. azimuth, 400 km / 51.6° orbit / d > 1 µm
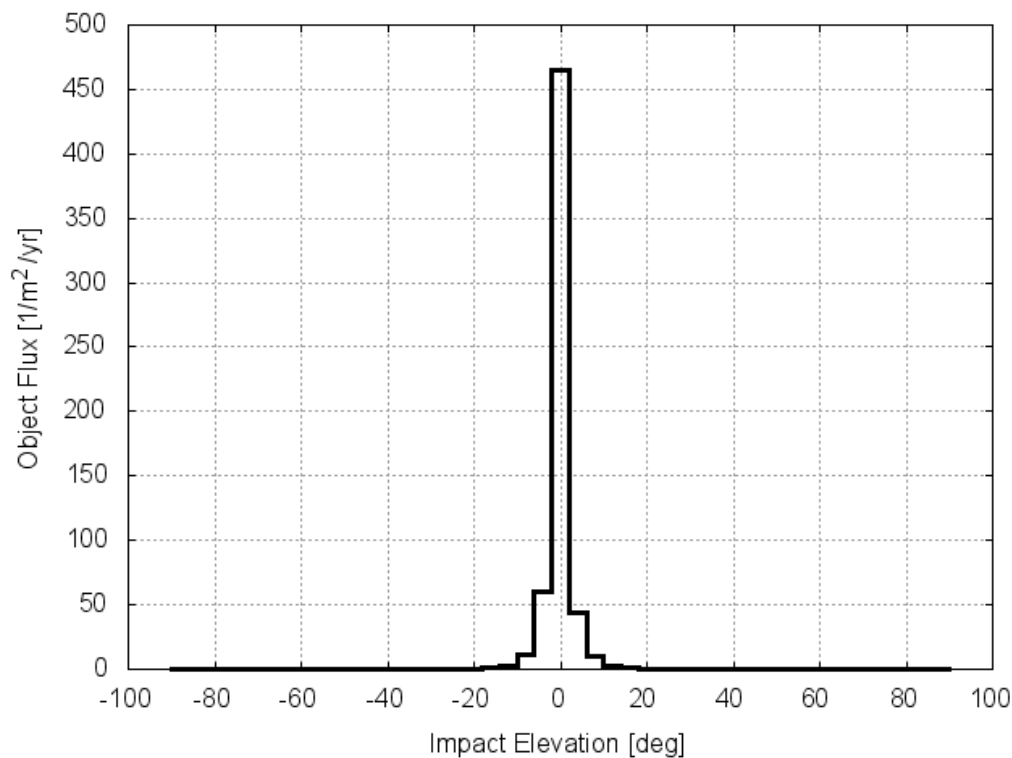
Figure 2-36   MASTER 8 flux vs. elevation, 400 km / 51.6° orbit / d > 1 μm
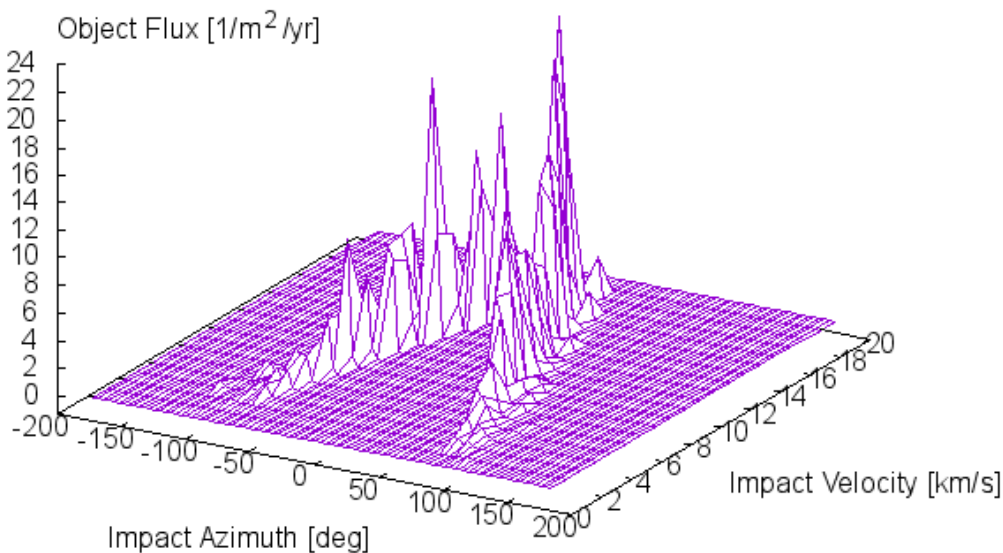
**Figure 2-37   MASTER 8 flux vs. impact velocity and azimuth,
400 km / 51.6° orbit / d > 1 μm**

Although the spectra are displayed as differential distributions (except the diameter spectrum, which is cumulative) for comparability with the results of the other debris models (see section 2.1.2.1), the distributions are used in their cumulative form within the ESABASE2 analysis as described in chapter 5.

In ESABASE2/Debris the MASTER 8 flux analysis is performed for an orbital arc spanned around the orbital point (centre of the time step) according to the time span between the points. The analysis is performed for the whole orbit considering the argument of true latitude in the results in 1° step wide. With this 1°-resolution the results for the arc for each orbital point is extracted and the arcs of all orbital points together cover the whole orbit. Thus the flux analysis output is not limited as the output of MASTER 2005 and allows individual results for each orbital point as for MASTER 2001, MASTER 2009 or ORDEM 2000.

2.1.9 ORDEM 3.2 Model

2.1.9.1 Overview

ORDEM 3.2 is most of a classical update of ORDEM 3.0 including the same capabilities as ORDEM 3.0, but updates the model populations using the most recent and highest-fidelity datasets from radar, in situ, and optical sources. For a closer look into the model please refer to ORDEM 3.0 description in *Section 2.1.7* or the corresponding user manual /61/.

Table 14 compares the ORDEM 3.2 top level output features with ORDEM 3.0.

Parameter	ORDEM 3.0	ORDEM 3.2
Spacecraft & Telescope/Radar analysis modes	Yes	Yes
Time range	2010 to 2035	**2016 to 2050**
Altitude range with minimum debris size	100 to 40,000 km (>10 µm) (non-GEO) 34,000 to 40,000 km (>10 cm) (GEO)	100 to 40,000 km (>10 µm) (non-GEO) 34,000 to 40,000 km (>10 cm) (GEO)
Orbit types	Circular to highly elliptical	Circular to highly elliptical
Model population breakdown by type & material density	Intacts Low-density (1.4 g/cc) fragments Medium-density (2.8 g/cc) fragments & microdebris High-density (7.9 g/cc) fragments & microdebris	Intacts Low-density (1.4 g/cc) fragments Medium-density (2.8 g/cc) fragments & microdebris High-density (7.9 g/cc) fragments & microdebris

Project: ESABASE2/Debris Release 12.1	Date:	2024-02-19
Technical Description	Revision:	1.11
Reference: R077-231rep_01_11_Debris_Technical Description.docx	Status:	Final

FEV etamax GmbH   Page 69 / 173

Parameter	ORDEM 3.0	ORDEM 3.2
	RORSAT NaK coolant droplets (0.9 g/cc)	RORSAT NaK coolant droplets (0.9 g/cc)
Model cumulative size thresholds (fiducial points)	10 μm, 31.6 μm, 100 μm, 316 μm, 1 mm, 3.16 mm, 1 cm, 3.16 cm, 10 cm, 31.6 cm, 1 m	10 μm, 31.6 μm, 100 μm, 316 μm, 1 mm, 3.16 mm, 1 cm, 3.16 cm, 10 cm, 31.6 cm, 1 m
Flux uncertainties	Yes	Yes
Total input file size	1.25 GB	**4 GB**

Table 14   Feature comparison of ORDEM 3.0 and ORDEM 3.2

2.1.9.2 Results

Basically, also the results/outputs of ORDEM 3.2 are the same. However, the internal approach of achieving them changed. Now, interpolation of fluxes is done for each bin individually. The logarithm of the flux is interpolated versus the logarithm of the size via the piecewise cubic Hermite interpolating polynomials (PCHIP) method. Afterwards the total fluxes are generated.

To reflect this change ORDEM 3.2 was included in ESABASE2 as an individual model. PCHIP method was introduced in ESABASE2 and is applied to the individual bins provided via *IGLOOFLUX_SC.OUT* file. Based on the results of these interpolations the total fluxes for the individual sources and the general total flux are defined. This allows for better shares consideration, which have especially effects on failure fluxes. This approach makes now the *IGLOOFLUX_SC.OUT* file the main output ESABASE2 relies on. However, for the case of using constant density for an analysis with ORDEM 3.2, still the *SIZEFLUX_SC.OUT* file is used for the flux estimation.

2.2 The Meteoroid Environment Models

2.2.1 Introduction

To describe the *sporadic* part of the meteoroid flux the Grün model remains the base. It is briefly recapitulated in section 2.2.2 .

Additionally, the **Divine-Staubach meteoroid model** /21/, /22/ as provided in the current MASTER application /49/ (no changes were performed compared to the previous MASTER implementation /34/, /39/), has been implemented into ESABASE2/Debris. A description of the main model theory is given in section 2.2.3.

Furthermore, the **Meteoroid Engineering Model (MEM)** /36/, /37/, the to the Moon orbits tailored version of it **(LunarMEM),** the Release 2.0 of it **(MEMr2)** /48/ and **MEM 3** /60/ have been implemented into ESABASE2/Debris. A brief description is given in section 2.2.4, 2.2.5, 2.2.6 and 2.2.7.

Project: ESABASE2/Debris Release 12.1		Date:	2024-02-19
Technical Description		Revision:	1.11
Reference: R077-231rep_01_11_Debris_Technical Description.docx		Status:	Final

FEV etamax GmbH   Page 70 / 173

Moreover, the **Interplanetary Meteroid Environment Model (IMEM)** /51/ and its follow-up **IMEM2** /53/ have been implemented into ESABASE2/Debris for interplanetary analyses. A brief description of the models is given in section 2.2.8 and 2.2.9.

For the *meteoroid streams*, which so far have been included in ESABASE by the Cour-Palais method (Ref. /11/) and which did not include directional information, a new approach which is based on more comprehensive and more recent observations evaluated by **P. Jenniskens**, (Ref. /5/) has been worked out by N. McBride (Ref. /6/). The first version of his contribution is dated December 1995. This version has been updated in January 1996 by including some non-symmetrical activity profiles. The latest developments are contained in (Ref. /13/). The description of the streams presented in this document is based on these latter references. For more details, please refer to the original papers or (Ref. /15/).

Some *enhancements* of the *sporadic* contribution with suggestions on how one might include the expected anisotropy in the Earth *apex* direction, the β *meteoroids* that are, because of their small size, driven away from the sun by radiation pressure, and of *interstellar* dust are discussed in a paper by N. McBride and J.A.M. McDonnell (Ref. /9/). The results for these additional directional effects which have been implemented in the software are collected in section 2.2.11 .

Also in Ref. /9/ an enhanced *velocity distribution* is given which was derived from HRMP observation data and was proposed by Taylor in 1995 (Ref. /10/). This distribution is given at 1 AU as seen from a massless Earth. This distribution is added as a new option in the enhanced tool. It is described in section 2.2.12 .

2.2.2 The Grün Model

In 1985 E. Grün et al (Ref. /4/) established an interplanetary flux model which can be considered as today's de facto standard for the modelling of the sporadic meteoroid environment. The model does not give any directional information, it assumes an isotropic environment. However, the annual streams contributions and other directional effects are implicitly contained in the Grün model.

The flux - mass distribution is defined as

$$F(m) \; = \; c_0 \{ \; (c_1\, m^{\,0.306} + c_2)^{-4.38} \; + \; c_3\, (m + c_4\, m^2 + c_5\, m^4)^{-0.36} \; + \; c_6\, (m + c_7\, m^2)^{-0.85} \; \} \quad , $$

$$\text{m} > 10^{-9}\,\text{g} \quad \rightarrow| \qquad \text{m} > 10^{-14}\,\text{g} \quad \rightarrow|10^{-18}\,\text{g} <\text{m} < 10^{-14}\,\text{g} \;\rightarrow|$$

where $F(m)$ is the cumulative flux of particles with mass m or larger in *particles/m²/year* to one side of a *randomly tumbling* plate which is assumed as *stationary* with respect to the Earth surface, m is the mass in g and the constants c_0 to c_7 are defined as follows:

c_0	=	$3.156 \cdot 10^7$	(from conversion of the units from m⁻² s⁻¹ to m⁻² year⁻¹)
c_1	=	$2.2 \cdot 10^3$	
c_2	=	15	
c_3	=	$1.3 \cdot 10^{-9}$	

$$c_4 = 10^{11}$$

$$c_5 = 10^{27}$$

$$c_6 = 1.3 \ 10^{-16}$$

$$c_7 = 10^6$$

In the line below the equation for $F(m)$ the mass contributions of the three terms are indicated. It is seen that the model covers a large mass interval from 10^{-18} to 1 g.

The Grün model represents the total meteoroid influx at the Earth's position i.e. at 1 AU distance from the sun in the ecliptic plane, but in the absence of the Earth. This requires that the flux must be corrected by the focusing effect of the gravitational field of the Earth as well as by the shielding effect of the Earth and its atmosphere. The corresponding equations are given in section 2.2.14. Due to the model independence from the Earth, it is also applicable to the Moon with modified corrections of the effects.
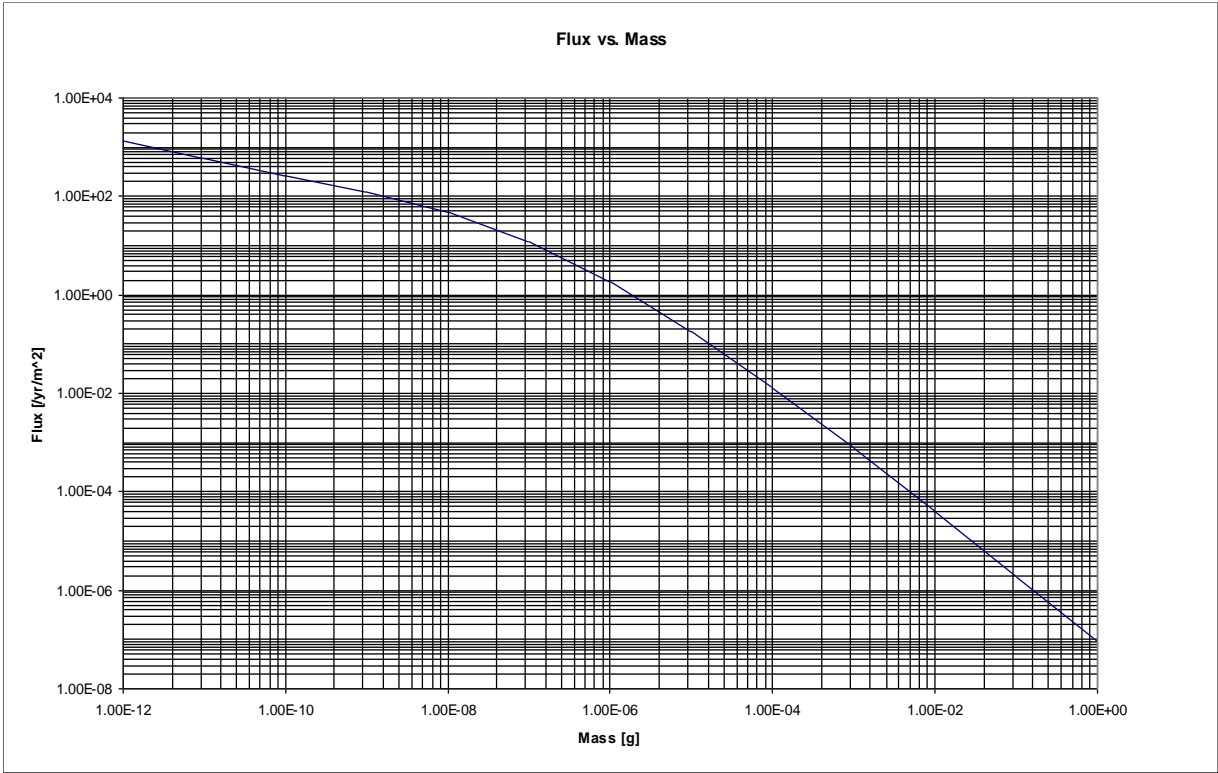
Figure 2-38   Grün flux vs. particle mass, 400 km / 51.6° orbit

Project: ESABASE2/Debris Release 12.1	Date:	2024-02-19
Technical Description	Revision:	1.11
Reference: R077-231rep_01_11_Debris_Technical Description.docx	Status:	Final

2.2.3 The Divine-Staubach Model

2.2.3.1 Implementation

As mentioned above (section 2.1.3.1), the mathematical approach developed by N. Divine originally has been applied to the interplanetary meteoroid environment. For debris flux calculation with the MASTER application the approach had to be adapted as described in section 2.1.3.2. The model is now implemented within the MASTER 8 model (no changes of Divine-Staubach model throughout the upgrade from MASTER 2009) and used through the standard environment interface (STENVI) according to the MASTER 8 debris model. The population as well as the target orbit is described in a geo-centric equatorial co-ordinate system. However, the meteoroid population is given in the helio-centric ecliptical co-ordinate system. Thus, the transformation of the target orbit from the geo-centric to the helio-centric system has been implemented for the evaluation of meteoroid flux. (This change, however, is not visible in the above given equations.)

The meteoroid population used by Divine-Staubach is divided into five sub-populations:

– asteroidal population,

– core population,

– A, B, and C population.

The population data is read from an input file as given in /22/. Figure 2-39 gives the mass distribution and the orbital element distributions of the five meteoroid populations of the Divine-Staubach model.
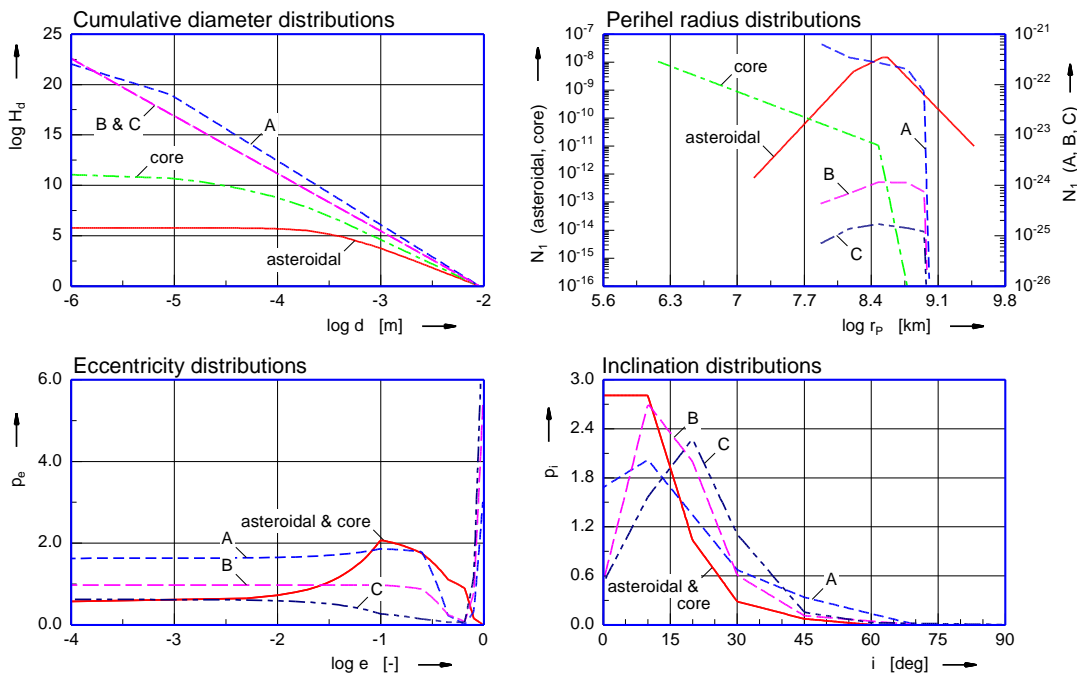
Figure 2-39   The mass and orbital element distributions of the Divine-Staubach model

Project: ESABASE2/Debris Release 12.1		Date:	2024-02-19
Technical Description		Revision:	1.11
Reference: R077-231rep_01_11_Debris_Technical Description.docx		Status:	Final

FEV etamax GmbH   Page 73 / 173

The extensions of the theory concerning Earth focussing and shielding as described in /22/ is implemented in the meteoroid branch of the Standard application. The flux equation (1) then becomes for meteoroids

$$J_M = \frac{1}{4} \sum_{dir=1}^{4} \left[N_M \cdot \left(v_{imp} \right)_{dir} \cdot \eta_F \eta_S \right] \qquad (5)$$

where η_F is the focussing factor

$$\eta_F = \left| 0,5 - \left(v_{FhE} - v_{rFhE} + \frac{2\mu_E}{r_{OhE} v_{FhE}} \right) \left(\frac{\pm 1}{4B} \right) \right| \qquad (6)$$

where

$$B = +\sqrt{ \left(\frac{v_{FhE} - v_{rFhE}}{4} \right) \left(v_{FhE} - v_{rFhE} + \frac{4\mu_E}{r_{OhE} v_{FhE}} \right) } \qquad (7)$$

with

μ_E	gravitational parameter of the Earth ($3,986*10^{-5}$ km³/s²)
v_{FhE}	heliocentric meteoroid velocity with respect to the Earth
v_{rFhE}	radial component of v_{FhE}
r_{OhE}	heliocentric object distance with respect to the Earth

The shielding factor η_S is given by

$$\eta_S = \begin{cases} 0 & \text{if } f_F > 0 \text{ and } r_{pF} < (R_E + H_A) \\ 1 & \text{in all other cases} \end{cases} \qquad (8)$$

with

f_F	meteoroid true anomaly
r_{pF}	meteoroid orbit perigee radius
R_E	mean Earth radius (6378,144 km)
H_A	height of the dense Earth atmosphere (≈ 120 km)

With these steps, the complete Divine-Staubach model is made available in the MASTER application.

2.2.3.2 Results

As for the debris population, the MASTER model provides flux results including the directional information by means of the Divine-Staubach model. Figure 2-40 to Figure 2-44 provide the resulting spectra (cross-sectional flux on a sphere) for an ISS-like orbit and a lower particle size threshold of $1\mu m$. Please note that the meteoroid flux results are depending on the analysis epoch and the orientation of the target orbit with respect to the ecliptic plane.
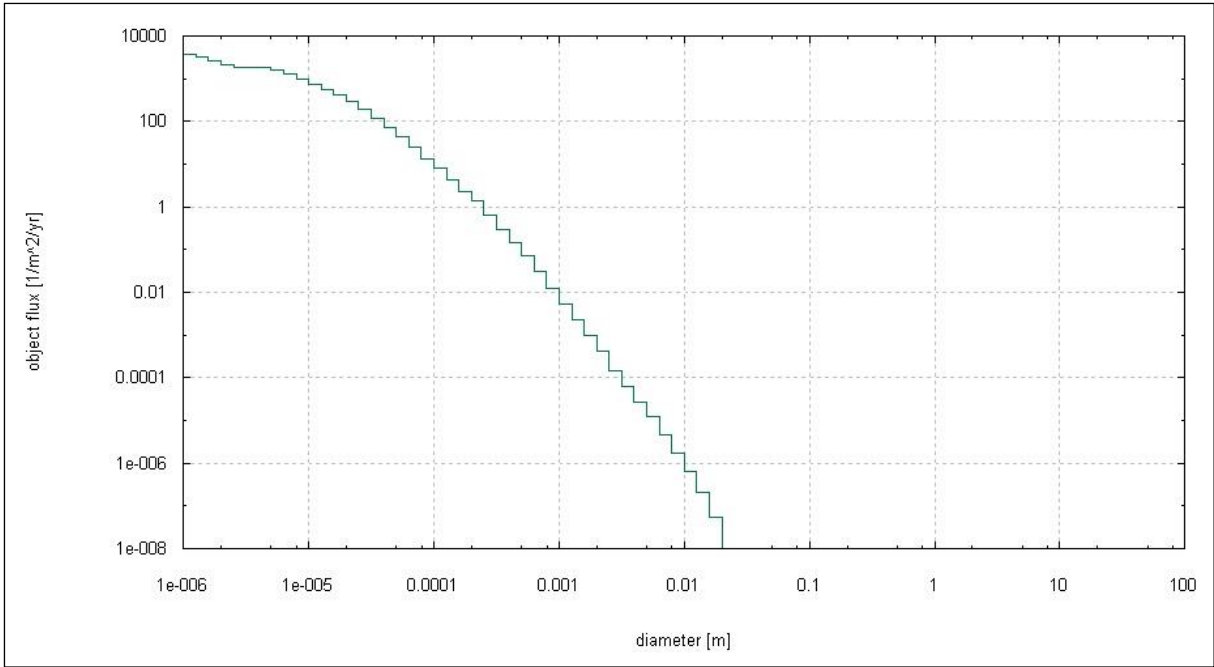
Figure 2-40   Divine-Staubach flux vs. particle diameter, 400 km / 51.6° orbit
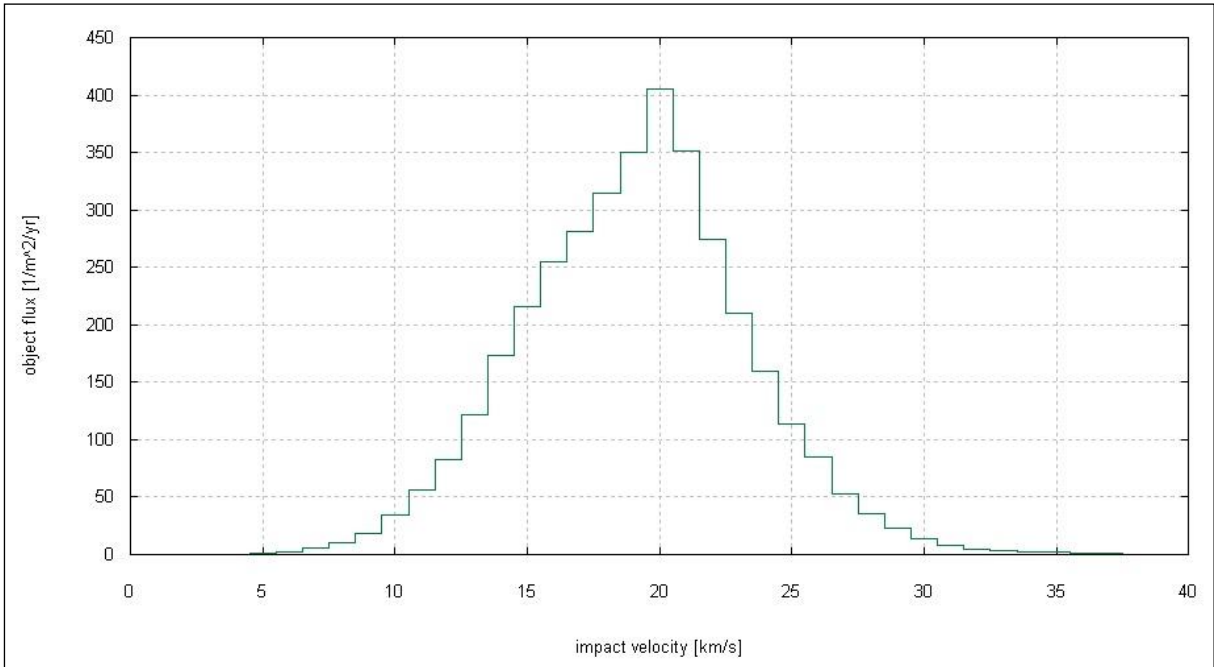
Figure 2-41   Divine-Staubach flux vs. impact velocity, 400 km / 51.6° orbit / d > 1 µm

Project: ESABASE2/Debris Release 12.1	Date:	2024-02-19
Technical Description	Revision:	1.11
Reference: R077-231rep_01_11_Debris_Technical Description.docx	Status:	Final

FEV etamax GmbH   Page 75 / 173
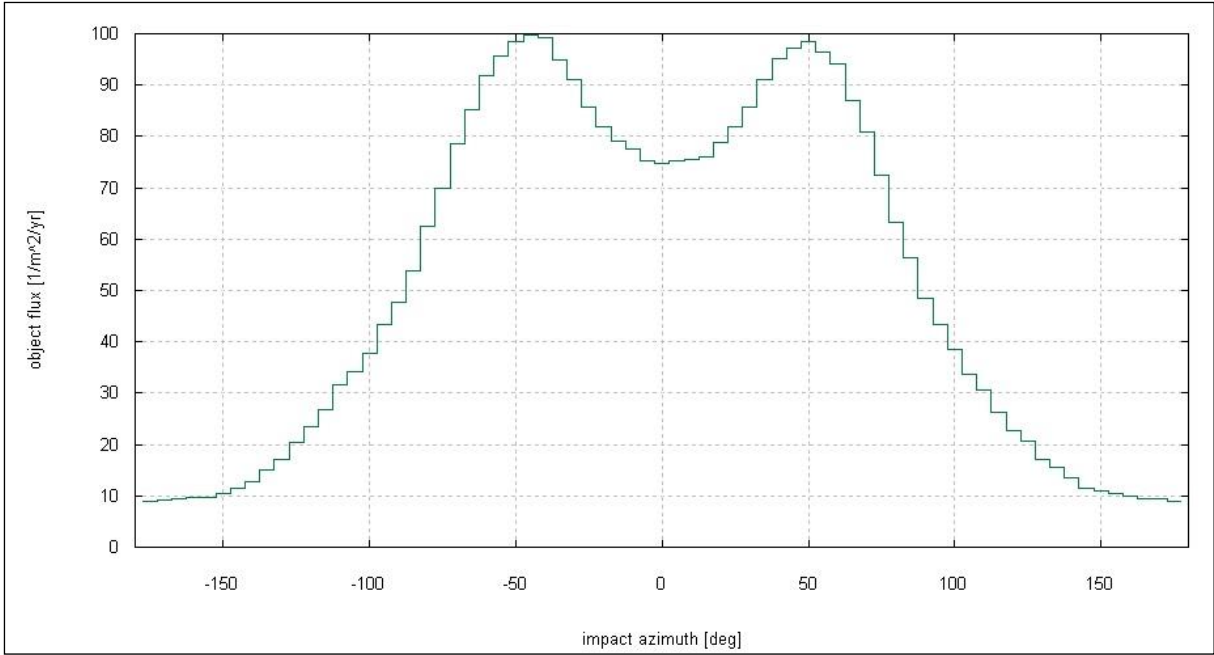
Figure 2-42   Divine-Staubach flux vs. azimuth, 400 km / 51.6° orbit / d > 1 μm
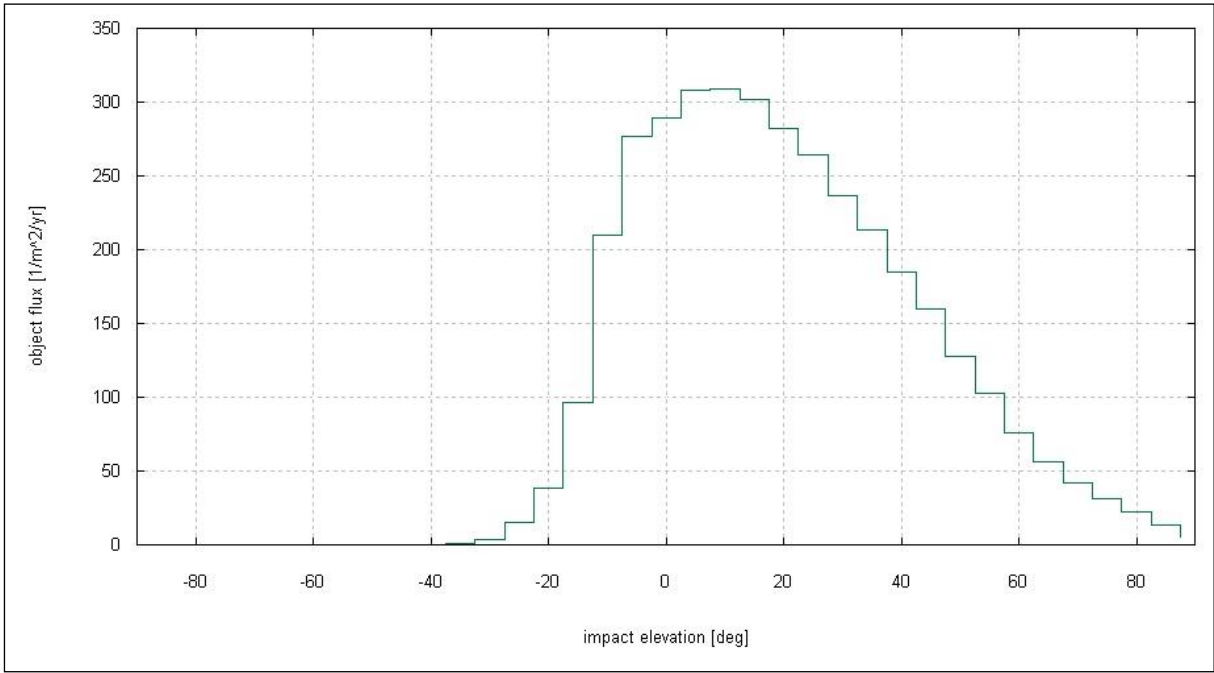
Figure 2-43   Divine-Staubach flux vs. elevation, 400 km / 51.6° orbit / d > 1 μm

Project: ESABASE2/Debris Release 12.1		Date:	2024-02-19
Technical Description		Revision:	1.11
Reference: R077-231rep_01_11_Debris_Technical Description.docx		Status:	Final
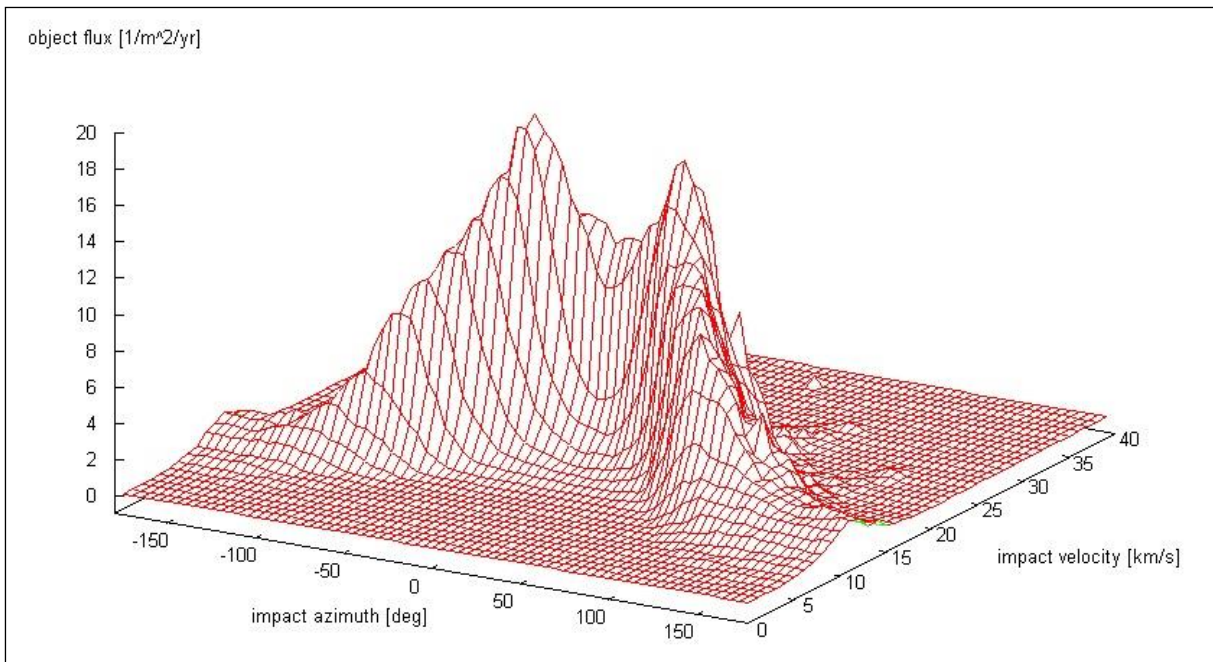
Figure 2-44   Divine-Staubach flux vs. impact velocity and azimuth, ISS orbit / d > 1 µm

Although the spectra are displayed as differential distributions – except the diameter spectrum, which is cumulative – the distributions are provided and used in their cumulative form within the ESABASE2/Debris analysis as described in chapter 5.

2.2.4 The Meteoroid Model MEM

2.2.4.1 Implementation

MEM incorporates a physics-based approach to modelling the sporadic environment, with validation against radar observations. It predicts the concentration and velocity distribution of meteoroids within the inner solar system from 0.2 to 2.0 AU, using observational measurements to constrain the physical model.

The fundamental core of the program calculates integral meteoroid fluxes and impacting speeds relative to the spacecraft. In this core, meteoroid velocities and spatial densities are derived from distributions of cometary and asteroidal meteoroid orbits. From these relative velocities and spatial densities, a meteoroid flux is calculated at the spacecraft location. This calculated meteoroid flux (including the directional information) is used as input for ESABASE2/Debris analyses. The model is capable of computing the flux of mass ranges damaging to spacecraft, 10^{-6} g to 10 g. Further details can be found in /36/ and/37/.

MEM is available as executable and the data transfer (input / output) is managed via files. This approach is similar to the one used for ORDEM 2000 or MASTER models except MASTER 2001.

2.2.4.2 Results

MEM provides flux results as multidimensional output. For each elevation/azimuth grid point a complete velocity distribution (flux vs. velocity) is provided. With this input all dependencies

Project: ESABASE2/Debris Release 12.1	Date:	2024-02-19
Technical Description	Revision:	1.11
Reference: R077-231rep_01_11_Debris_Technical Description.docx	Status:	Final

FEV etamax GmbH   Page 77 / 173

between elevation, azimuth and velocity can be considered. The used raytracing procedure is described in chapter 5. The following figures are based on an ISS like orbit.

MEM uses the same normalized flux vs. mass distribution for every orbital point. Figure 2-45 shows the normalized flux vs. mass distribution. Figure 2-46 shows the 2D flux vs. elevation spectrum generated from the multidimensional spectrum. Figure 2-47 shows the cumulated 3D flux vs. elevation/azimuth spectrum as well generated from the multidimensional spectrum. Figure 2-48 shows the flux vs. velocity as well extracted from the multidimensional spectrum.
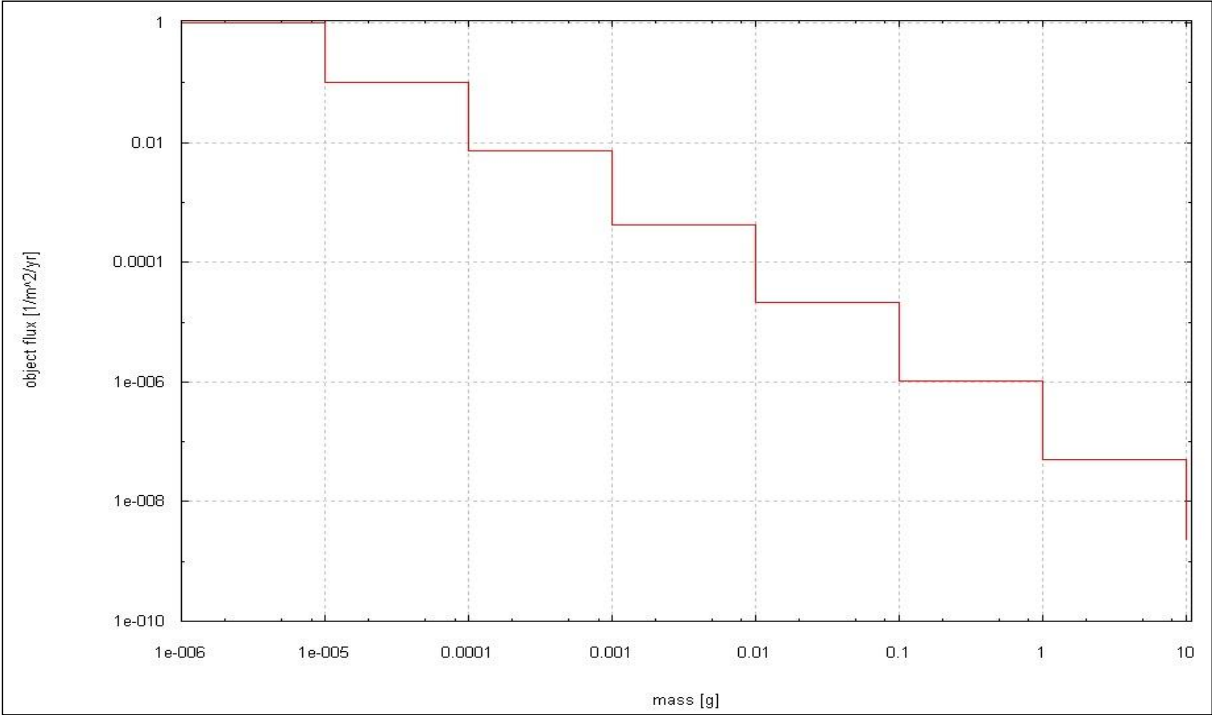
Figure 2-45:   MEM normalized flux vs. mass, ISS orbit / mass > 1*10^{-6} g

Project: ESABASE2/Debris Release 12.1	Date:	2024-02-19
Technical Description	Revision:	1.11
Reference: R077-231rep_01_11_Debris_Technical Description.docx	Status:	Final
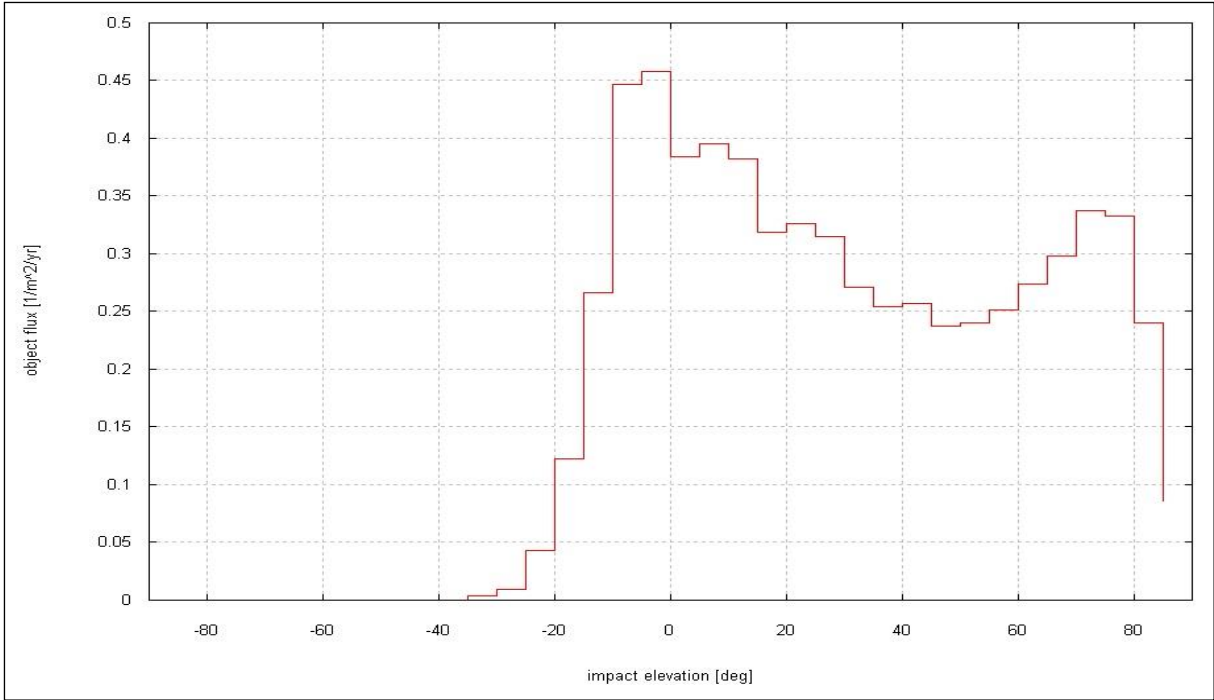
Figure 2-46: MEM flux vs. impact elevation, ISS orbit / mass > $1*10^{-6}$ g
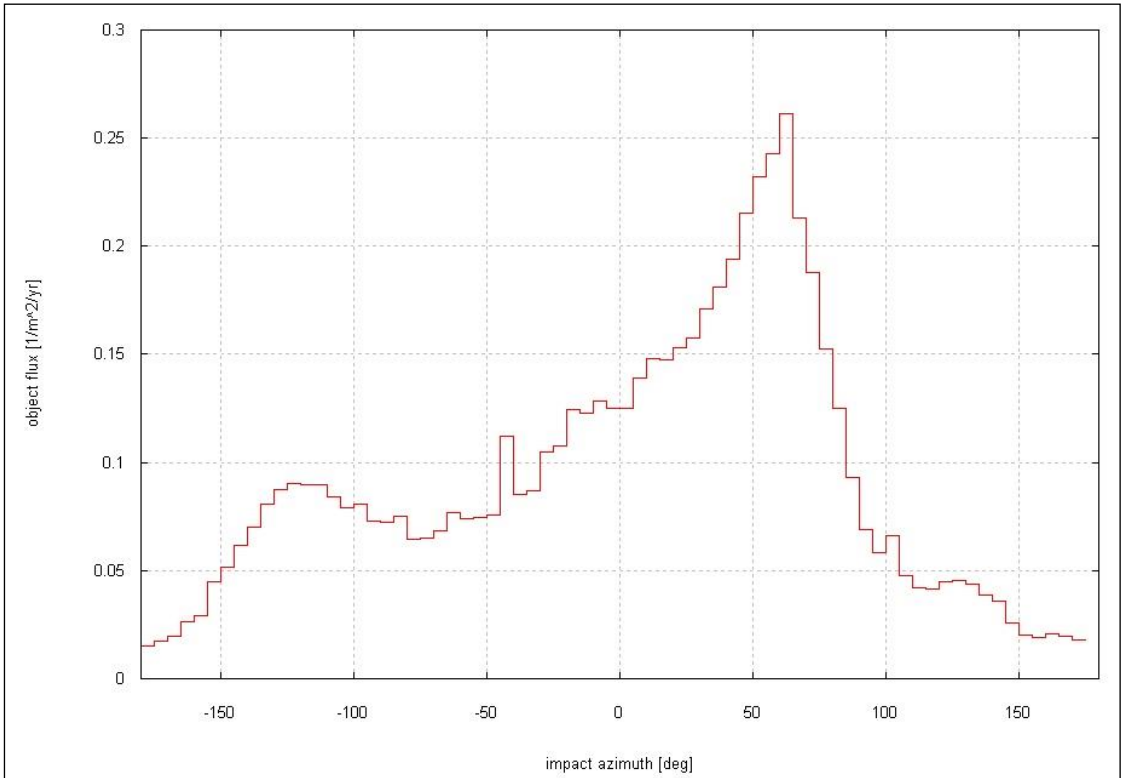
Figure 2-47: MEM cumulated flux vs. impact azimuth, ISS orbit / mass > $1*10^{-6}$ g

Project: ESABASE2/Debris Release 12.1		Date:	2024-02-19
Technical Description		Revision:	1.11
Reference: R077-231rep_01_11_Debris_Technical Description.docx		Status:	Final

FEV etamax GmbH
Page 79 / 173
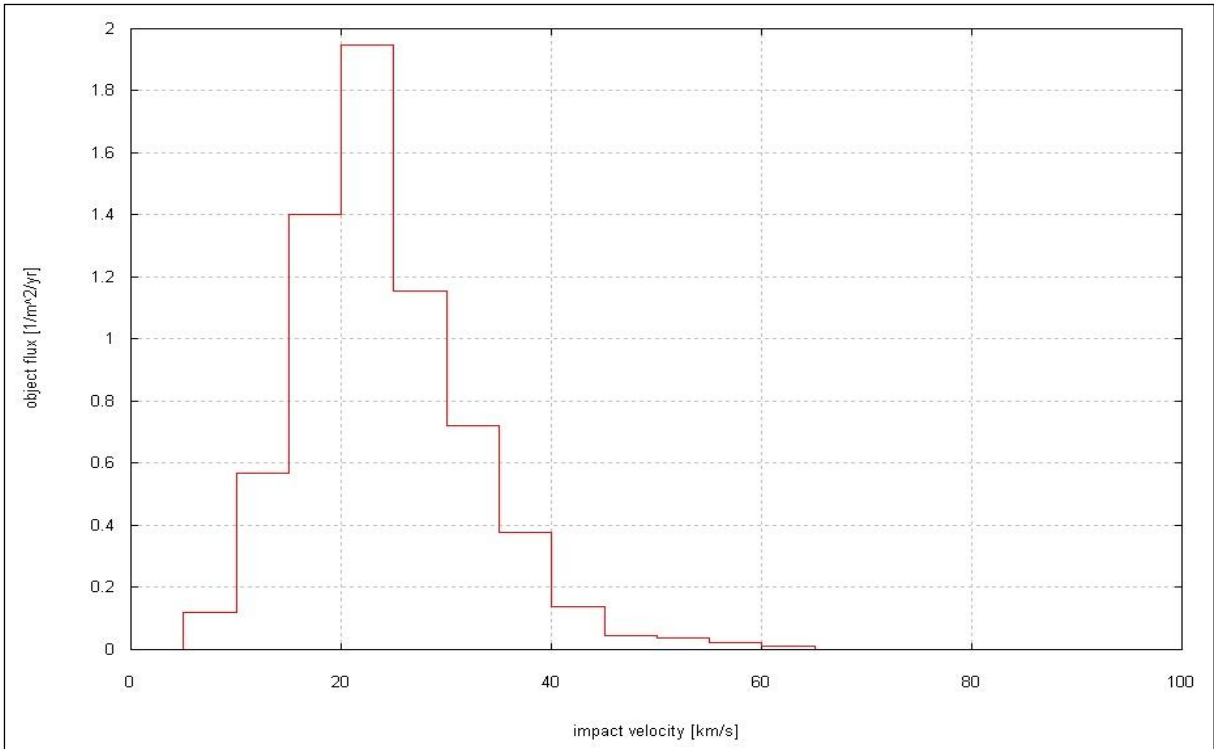
Figure 2-48: MEM flux vs. impact velocity, ISS orbit / mass > $1*10^{-6}$ g
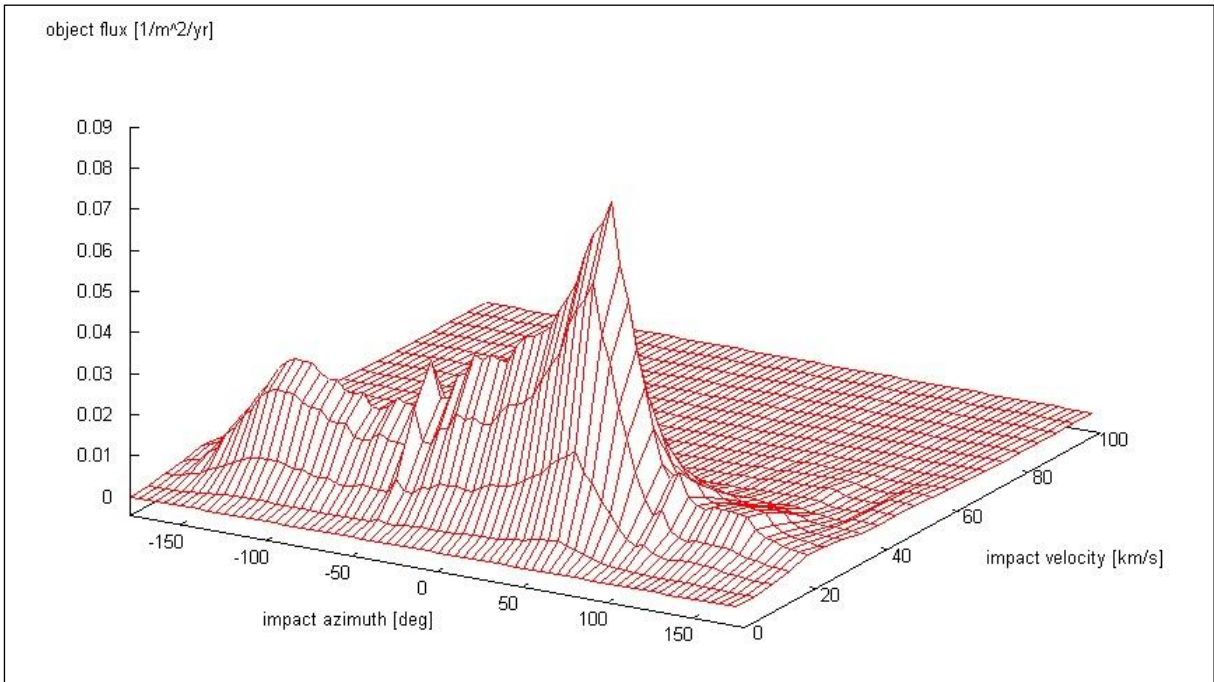
Figure 2-49: MEM flux vs. impact azimuth and velocity, ISS orbit / mass > $1*10^{-6}$ g

Although the spectra are displayed as differential distributions – except the diameter spectrum, which is cumulative – the distributions are provided and used in their cumulative form within the ESABASE2/Debris analysis as described in chapter 5.

Project: ESABASE2/Debris Release 12.1		Date:	2024-02-19
Technical Description		Revision:	1.11
Reference: R077-231rep_01_11_Debris_Technical Description.docx		Status:	Final

FEV etamax GmbH   Page 80 / 173

2.2.5 The Meteoroid Model LunarMEM

2.2.5.1 Implementation

The LunarMEM is a version of the MEM model, which is described in 2.2.4, with consistent structure and functionality. The difference of the LunarMEM is the optimisation and tailoring of the model to the lunar orbits. This tailoring leads also to the limits of applicability of up to 66000 km radius around Moon.

LunarMEM is, according to MEM, available as executable and the data transfer (input / output) is managed via files.

2.2.5.2 Results

LunarMEM provides flux results as multidimensional output. For each elevation/azimuth grid point a complete velocity distribution (flux vs. velocity) is provided. With this input all dependencies between elevation, azimuth and velocity can be considered. The used raytracing procedure is described in chapter 5. The following figures are based on a polar circular lunar orbit with a altitude of 100 km.

LunarMEM uses the same normalized flux vs. mass distribution for every orbital point, which is shown in Figure 2-50. Figure 2-51, Figure 2-52 and Figure 2-53 show the 2D flux vs. elevation respective azimuth or velocity spectrum generated from the multidimensional spectrum. Figure 2-54 shows the cumulated 3D flux vs. azimuth vs. elevation spectrum also generated from the multidimensional spectrum.
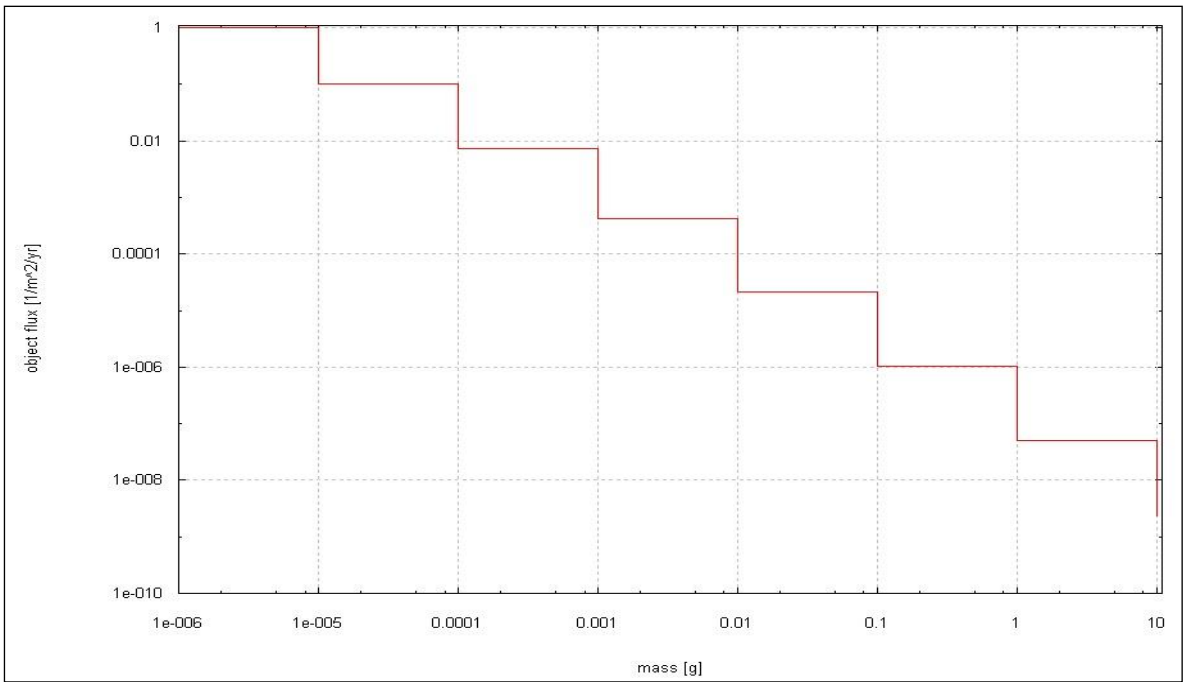
Figure 2-50: **LunarMEM normalized flux vs. mass, polar lunar orbit / mass > 1*10^-6 g**

Project: ESABASE2/Debris Release 12.1		Date:	2024-02-19
Technical Description		Revision:	1.11
Reference: R077-231rep_01_11_Debris_Technical Description.docx		Status:	Final

FEV etamax GmbH   Page 81 / 173
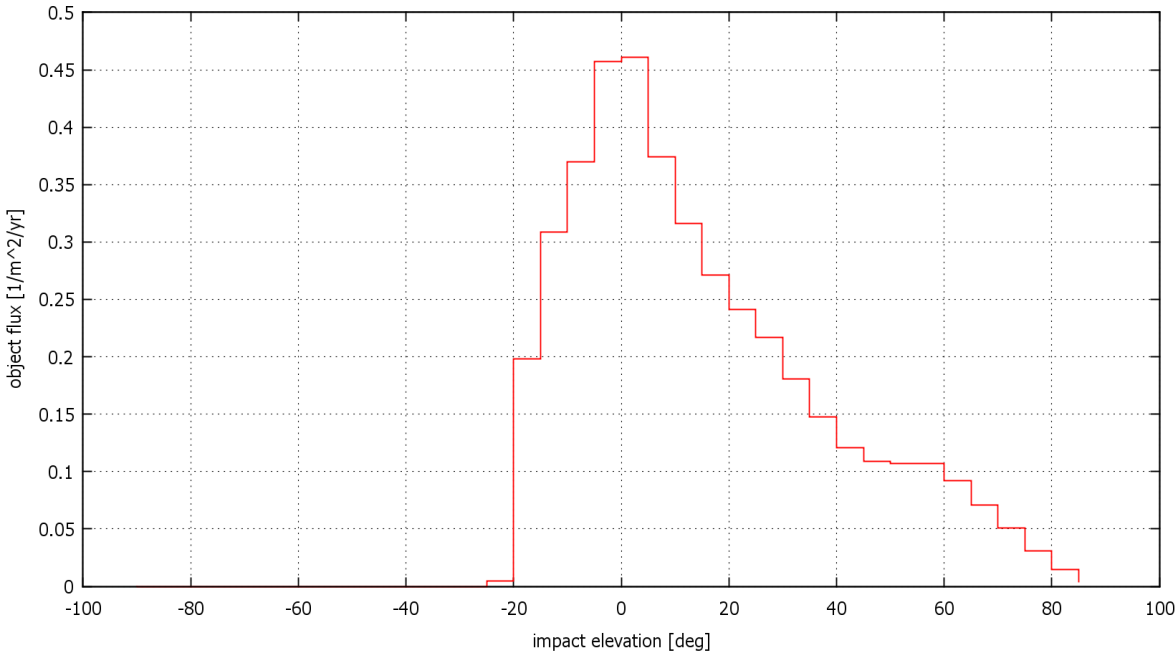
Figure 2-51: LunarMEM flux vs. impact elevation, polar lunar orbit / mass > 1*10⁻⁶ g
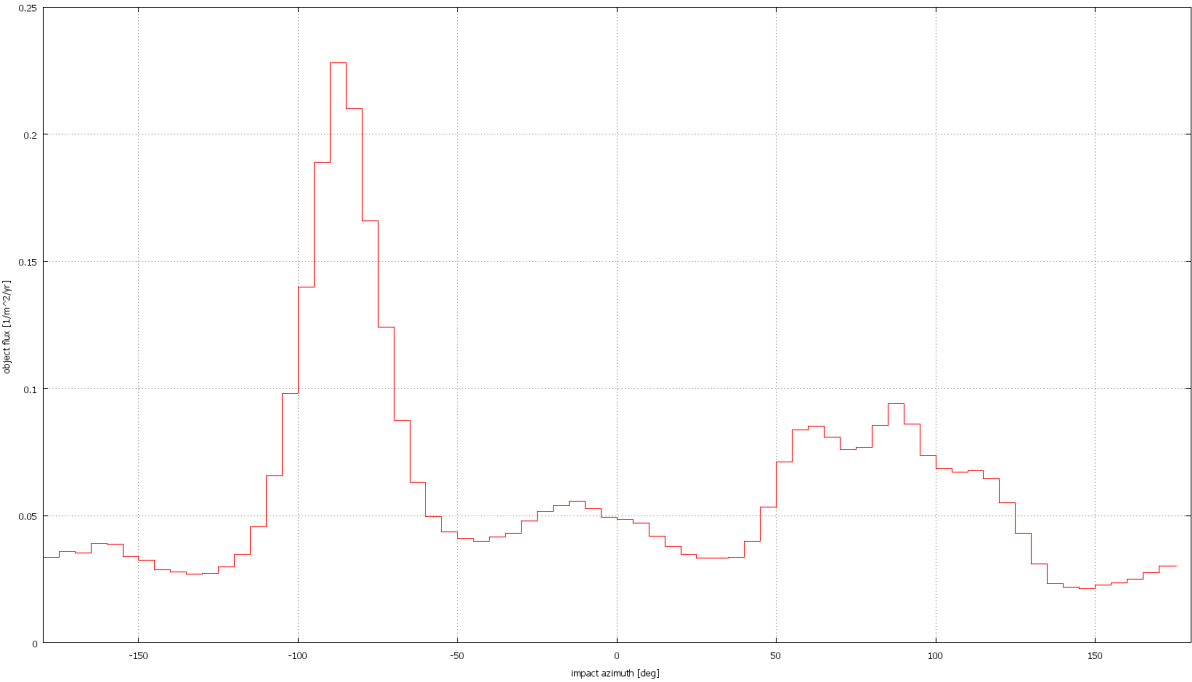
Figure 2-52: LunarMEM flux vs. impact azimuth, polar lunar orbit / mass > 1*10⁻⁶ g

Project: ESABASE2/Debris Release 12.1	Date:	2024-02-19
Technical Description	Revision:	1.11
Reference: R077-231rep_01_11_Debris_Technical Description.docx	Status:	Final

FEV etamax GmbH · Page 82 / 173
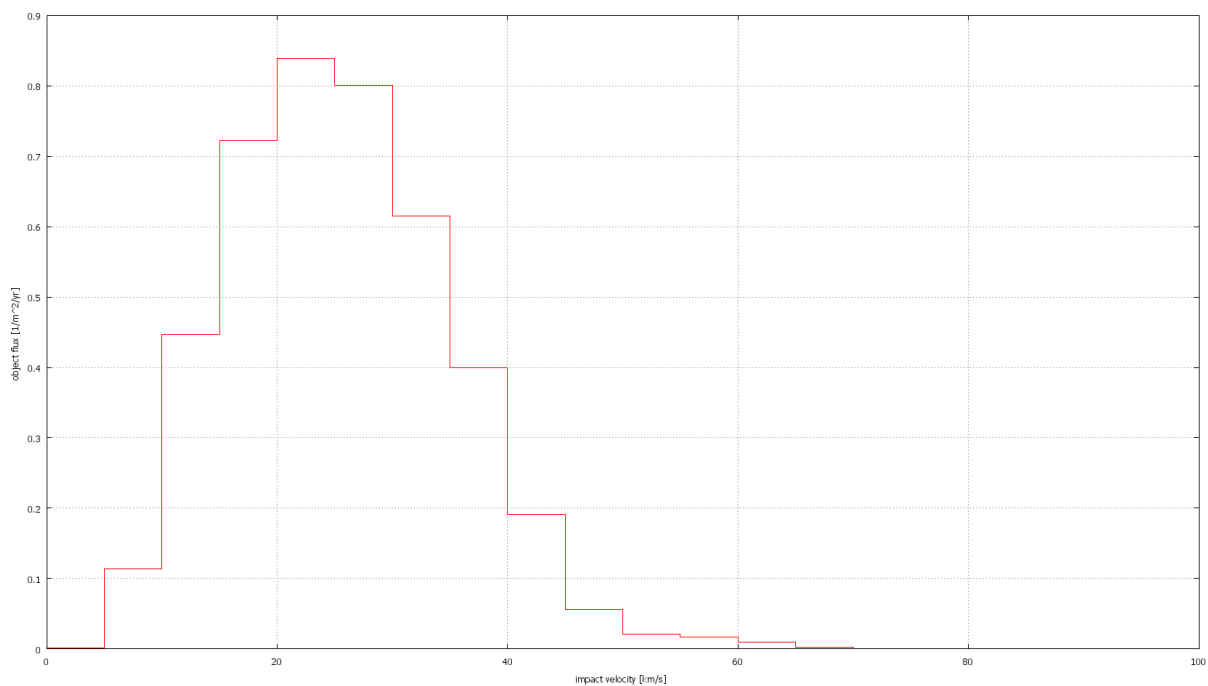
Figure 2-53: LunarMEM flux vs. impact velocity, polar lunar orbit / mass > $1*10^{-6}$ g
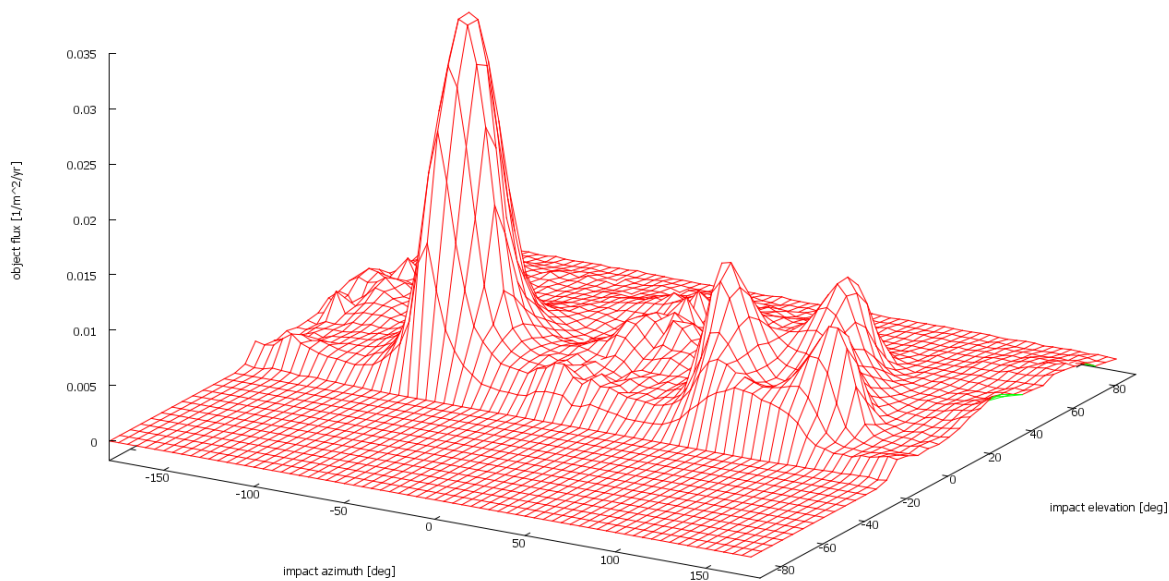
Figure 2-54: LunarMEM flux vs. impact azimuth and elevation, polar lunar orbit / mass > $1*10^{-6}$ g

Although the spectra are displayed as differential distributions – except the diameter spectrum, which is cumulative – the distributions are provided and used in their cumulative form within the ESABASE2/Debris analysis as described in chapter 5.

Project: ESABASE2/Debris Release 12.1		Date:	2024-02-19
Technical Description		Revision:	1.11
Reference: R077-231rep_01_11_Debris_Technical Description.docx		Status:	Final

FEV etamax GmbH   Page 83 / 173

2.2.6 The Meteoroid Model MEM Release 2.0 (MEMr2)

2.2.6.1 Overview

MEM incorporates a physics-based approach to modelling the sporadic environment, with validation against radar observations. It predicts the concentration and velocity distribution of meteoroids within the inner solar system from 0.2 to 2.0 AU, using observational measurements to constrain the physical model.

MEM describes the sporadic complex only. The sporadic complex is the background meteoroid environment, which is constant from year to year. The background environment described by MEM does have some average annual meteor shower statistics embedded in the overall fluxes due to MEM's reliance on the flux/mass function described in the Grün et. al (1985) paper, "Collisional Balance of the Meteoric Complex."

The MEM lower limiting mass is 10^{-6} grams (or 124 microns in diameter for a density of 1 g/cm3). In this case, the dust population is defined as anything smaller than 10^{-6} grams; MEM does not model this dust population and would not be an appropriate model choice for the development of a dust detector experiment. Similarly, predicting the degradation of sensitive external surfaces like optics or solar arrays is not possible with this model since that threat regime is below MEM's mass threshold.

MEM Release 2.0 (MEMr2) is the successor of MEM and LunarMEM. Unlike prior releases, MEMr2 is a single product containing three individual environment sub-models
- For Earth Orbiting S/C - up to approximately 925000 km from the Earth's centre
- For Moon Orbiting S/C - up to approximately 66000 km from the Moon's centre
- For Interplanetary S/C - approximately more than 925000 km from the Earth's centre

that describe the background meteoroid environment for spacecraft in orbit around the Earth, Moon, and in interplanetary space.

2.2.6.2 Implementation

MEMr2 is successor of the MEM model, which is described in 2.2.4, with consistent structure and functionality. One of the changes with MEMr2 is the comprising of EarthMEM and LunarMEM. Due to this fact MEMr2 can be used as alternative to both, the differentiation of the sub-model to be used is made internally, based on the central body applied for the analysis.

MEMr2 is available as command-line executable and the data transfer (input / output) is managed via ASCII-files. This approach is similar to the one used for previous releases MEM and LunarMEM.

2.2.6.3 Results

MEMr2 provides the multidimensional flux as output. For each elevation/azimuth grid point a complete velocity distribution (flux vs. velocity) is provided. With this input all dependencies between elevation, azimuth and velocity can be considered. The used raytracing procedure is described in chapter 5. The following figures are based on an ISS like orbit.

MEMr2 uses the same normalized flux vs. mass distribution for every orbital point, which is shown in Figure 2-55. Figure 2-56, Figure 2-57 and Figure 2-58 show the 2D flux vs. elevation respective azimuth or velocity spectrum generated from the multidimensional spectrum. Figure

Project: ESABASE2/Debris Release 12.1	Date:	2024-02-19
Technical Description	Revision:	1.11
Reference: R077-231rep_01_11_Debris_Technical Description.docx	Status:	Final

FEV etamax GmbH   Page 84 / 173

2-59 shows the cumulated (over velocity) 3D flux vs. azimuth vs. elevation spectrum also generated from the multidimensional spectrum.
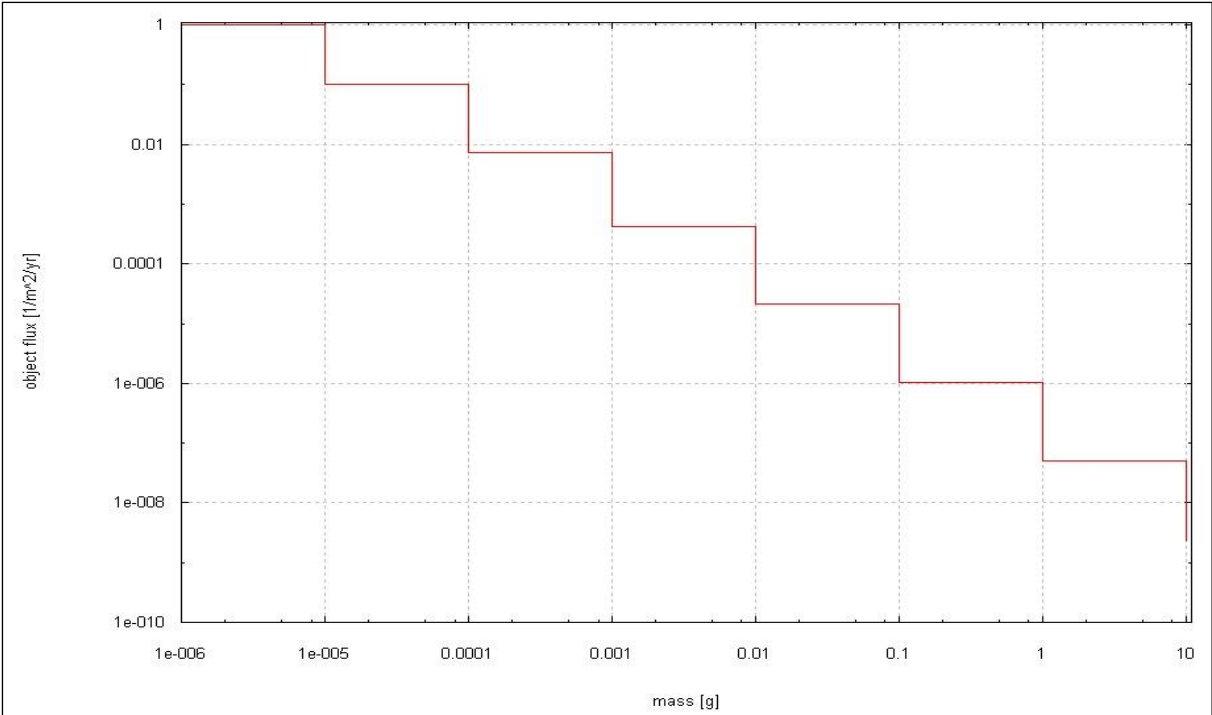
Figure 2-55:   MEMr2 normalized flux vs. mass, LEO orbit / mass > 1*10^{-6} g

Figure 2-56:   MEMr2 flux vs. impact elevation, orbital point in LEO / mass > 1*10^{-6} g
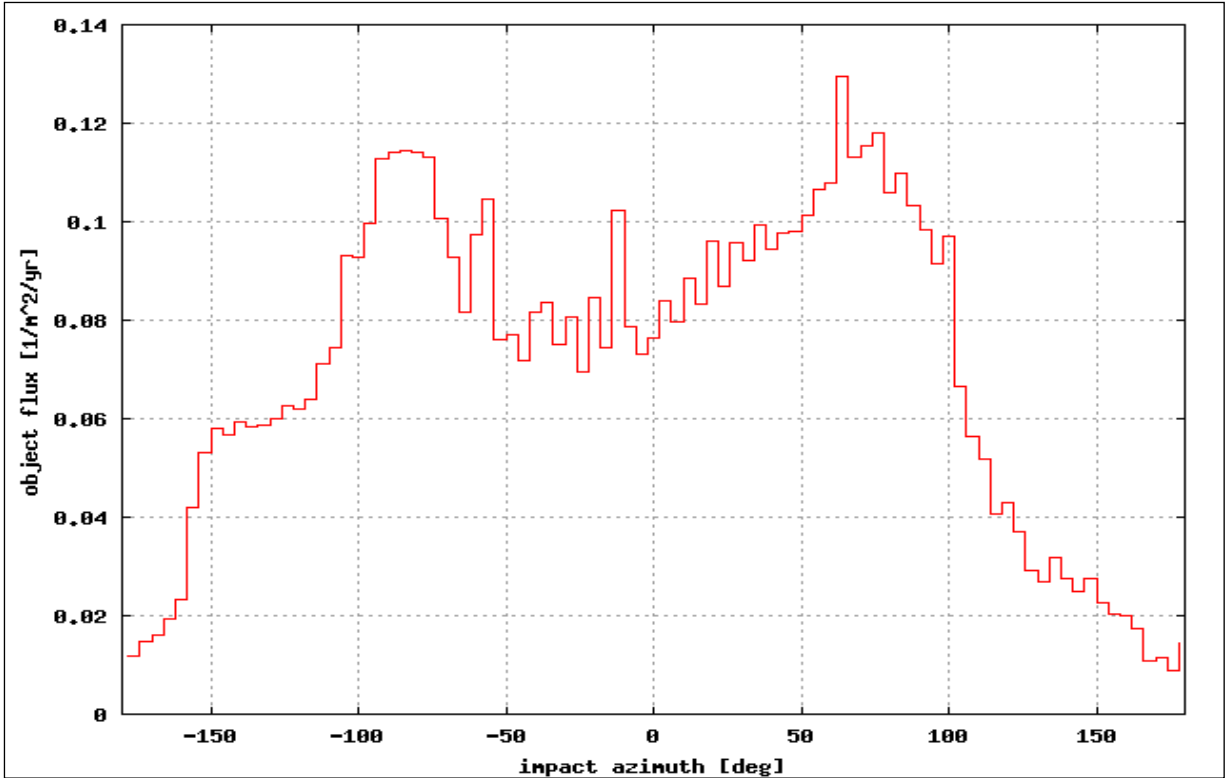
Figure 2-57: MEMr2 flux vs. impact azimuth, orbital point in LEO / mass > $1*10^{-6}$ g
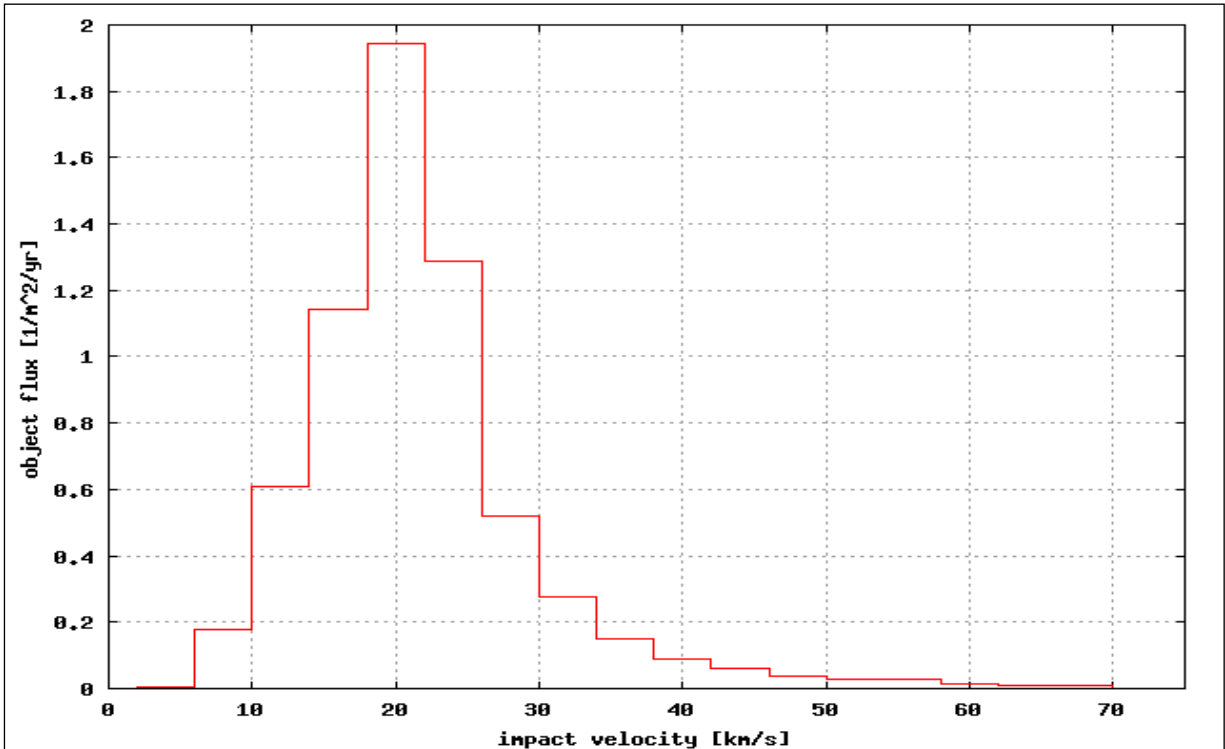
Figure 2-58: MEMr2 flux vs. impact velocity, orbital point in LEO / mass > $1*10^{-6}$ g

Project: ESABASE2/Debris Release 12.1		Date:	2024-02-19
Technical Description		Revision:	1.11
Reference: R077-231rep_01_11_Debris_Technical Description.docx		Status:	Final
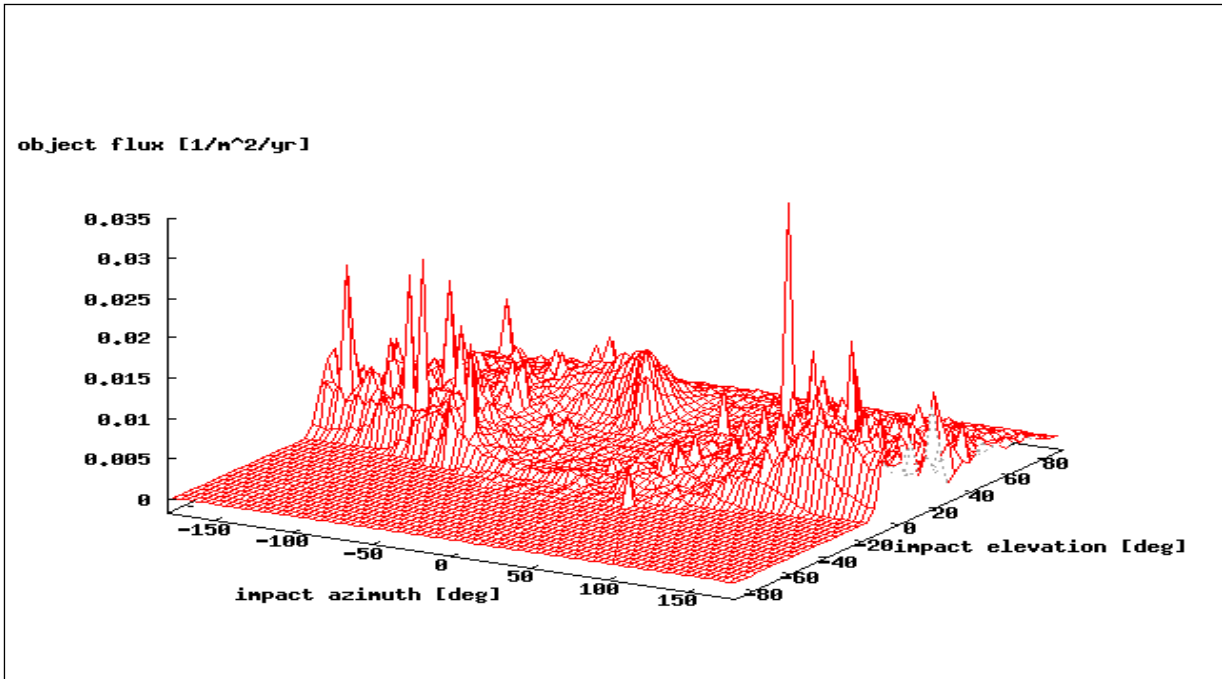
Figure 2-59: **MEMr2 flux vs. impact azimuth and velocity, orbital point in LEO / mass > 1*10^{-6} g**

In the case of MEMr2 Interplanetary usage the azimuth is defined in the orbital plane wrt. velocity direction (azimuth = 0 deg) and elevation positive to orbit impulse direction, whereas in other cases azimuth is defined in velocity-orbit impulse plane and elevation is positive away from central body, also both wrt. velocity direction (= 0 deg).

Although the spectra are displayed as differential distributions – except the diameter spectrum, which is cumulative – the distributions are provided and used in their cumulative form within the ESABASE2/Debris analysis as described in chapter 5.

2.2.7 The Meteoroid Model MEM 3

2.2.7.1 Overview

MEM incorporates a physics-based approach to modelling the sporadic environment, with validation against radar observations. It predicts the concentration and velocity distribution of meteoroids within the inner solar system from 0.2 to 2.0 AU, using observational measurements to constrain the physical model.

MEM describes the sporadic complex only. The sporadic complex is the background meteoroid environment, which is constant from year to year.

The MEM lower limiting mass is 10^{-6} grams (or 124 microns in diameter for a density of 1 g/cm^3). In this case, the dust population is defined as anything smaller than 10^{-6} grams; MEM does not model this dust population and would not be an appropriate model choice for the development of a dust detector experiment. Similarly, predicting the degradation of sensitive external surfaces like optics or solar arrays is not possible with this model since that threat regime is below MEM's mass threshold.

Project: ESABASE2/Debris Release 12.1		Date:	2024-02-19
Technical Description		Revision:	1.11
Reference: R077-231rep_01_11_Debris_Technical Description.docx		Status:	Final

FEV etamax GmbH   Page 87 / 173

MEM 3 is the successor of MEM Release 2.0 (MEMr2). However, it was substantially reworked. The code base was completely refactored and simplified. The approach was streamlined, avoiding sub-models, and the modelling algorithms were corrected. Also new density distributions were added. In the following some key upgrade/changes of MEM 3 are presented:

- More accurate environment modelling in MEM 3
    - More accurate planetary ephemerides
    - Corrected gravitational focusing model
    - Better preservation of correlations between speed and directionality
- Smoother angular distribution in MEM 3
    - Anomalous "hot pixels" sometimes produced in previous versions were traced back to a singularity in the meteoroid spatial density calculation
    - In MEM 3 it has been repaired using a small smoothing factor
- Meteoroid bulk densities considered in MEM 3
    - MEM 3 divides the meteoroid environment into low-density and high-density populations
    - MEM 3 generates two corresponding sets of environment files (output) including two density distribution files
    - Within a population, the density is independent of speed, directionality, and mass
- Independent and different velocity resolution options in MEM 3
    - MEM 3 offers 1 km/s and 2 km/s velocity resolutions
    - Velocity resolution selection is independent from the angular resolution
- Streamlined execution of MEM 3
    - MEM 3: origin and axis alignment of trajectory file only, MEM is checking for a planet (moon) vicinity and consider relevant parameters (no sub-models)
- MEM 3 includes Mercury, Venus and Mars additional to Sun, Earth and Moon
- Reduced runtime and optional high fidelity mode in MEM 3
    - Considerably run time reduction compared to MEMR2 at the same fidelity level
    - Optionally higher fidelity at similar ran times as MEMR2
- MEM 3 changes the naming scheme, content structure and file organisation
    - "Cleans up" the output files and
    - Places them in a single, user-named output directory
- MEM 3 run configuration via input file instead of interactive console
- Two-line elements are not supported in MEM 3
- Lunar coordinate system is removed in MEM 3

2.2.7.2 Implementation

MEM 3 is successor of MEMr2, which is described in 2.2.6, with similar but extended structure and functionality. Consequently the general implementation design approach in E2/D is also very similar. However, the individual components experienced significant adaptions due to the considerable changes of the MEM model and with interplanetary mode in mind. The main changes for the interfaces are:

Input for MEM 3:

Project: ESABASE2/Debris Release 12.1		Date:	2024-02-19
Technical Description		Revision:	1.11
Reference: R077-231rep_01_11_Debris_Technical Description.docx		Status:	Final

FEV etamax GmbH   Page 88 / 173

- No sub-model needs to be defined any more, however, based on the central body and the run mode or better mission definition type (e.g., trajectory, spice kernel), input origin and axes are defined. (user inputs): body fixed for Earth and inertial ecliptic for other celestial bodies
- ON/OFF trigger for the usage of the high-fidelity mode has to be defined. (user input)
- Definition of place and name of the output directory, instead of output file name. (fix)
- The output reference system is now switched to inertial ecliptic system, the velocities are always given relative to the S/C
- The angular and velocity resolution definitions are independent now and set by two parameters. (fix)
- Three triggers for desired additional output need to be defined. (fix, no special version required to achieve the intermediate files used by E2/D)

Output of MEM 3:

- Output file location: a model output folder is defined via the run name of MEM 3, which includes all output of the run, E2/D uses "eb2" run name/folder
- The intermediate files use the same structure but are re-named
- The results are provided for each source (low- and high-density) individually in separate folders
- Density shares distribution files are provided for each source

MEM 3 is available as command-line executable and the data transfer (input / output) is managed via ASCII-files. This approach is extended according to the listed changes.

2.2.7.3 Results

MEM 3 provides the multidimensional flux as output. For each elevation/azimuth grid point a complete velocity distribution (flux vs. velocity) is provided. With this input all dependencies between elevation, azimuth and velocity can be considered. This is done for both sources with additional output file comprising the distribution of the density shares of the according source. Within a source, the density is independent of speed, directionality, and mass. The used ray-tracing procedure is described in chapter 5. The following figures are based on an ISS like orbit.

E2/D relies on a scaling method for the flux vs. mass distribution definition for MEM 3 as described in /60/. Figure 2-60 and Figure 2-61 show the flux vs. mass distributions for low- and high-density, respective for an orbital point of a LEO. Figure 2-62 to Figure 2-67 show the 2D flux vs. elevation, azimuth and velocity spectra, respective, each for low- and high-density sources. The spectra are generated from the multidimensional spectrum. Figure 2-68 and Figure 2-69 show the cumulated (over velocity) 3D flux vs. azimuth vs. elevation spectrum also generated from the multidimensional spectrum.

Project: ESABASE2/Debris Release 12.1		Date:	2024-02-19
Technical Description		Revision:	1.11
Reference: R077-231rep_01_11_Debris_Technical Description.docx		Status:	Final
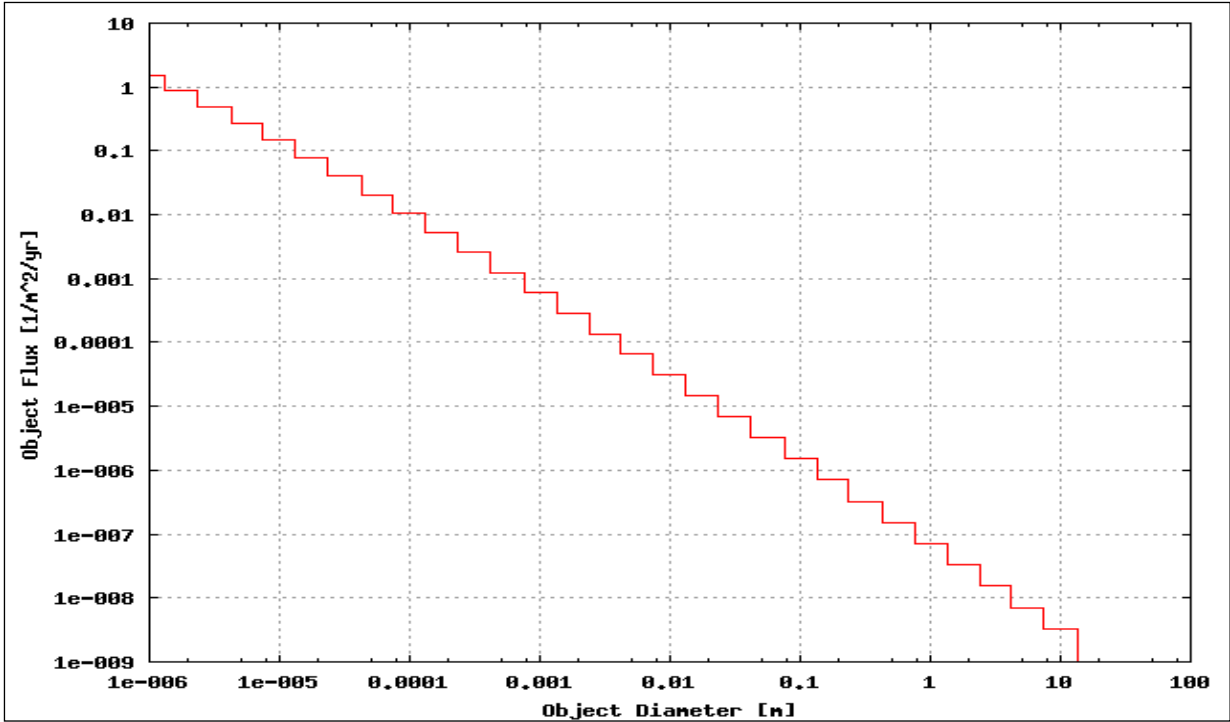
Figure 2-60:   MEM 3 low-density flux vs. mass, orbital point in LEO orbit / mass > 1*10⁻⁶ g
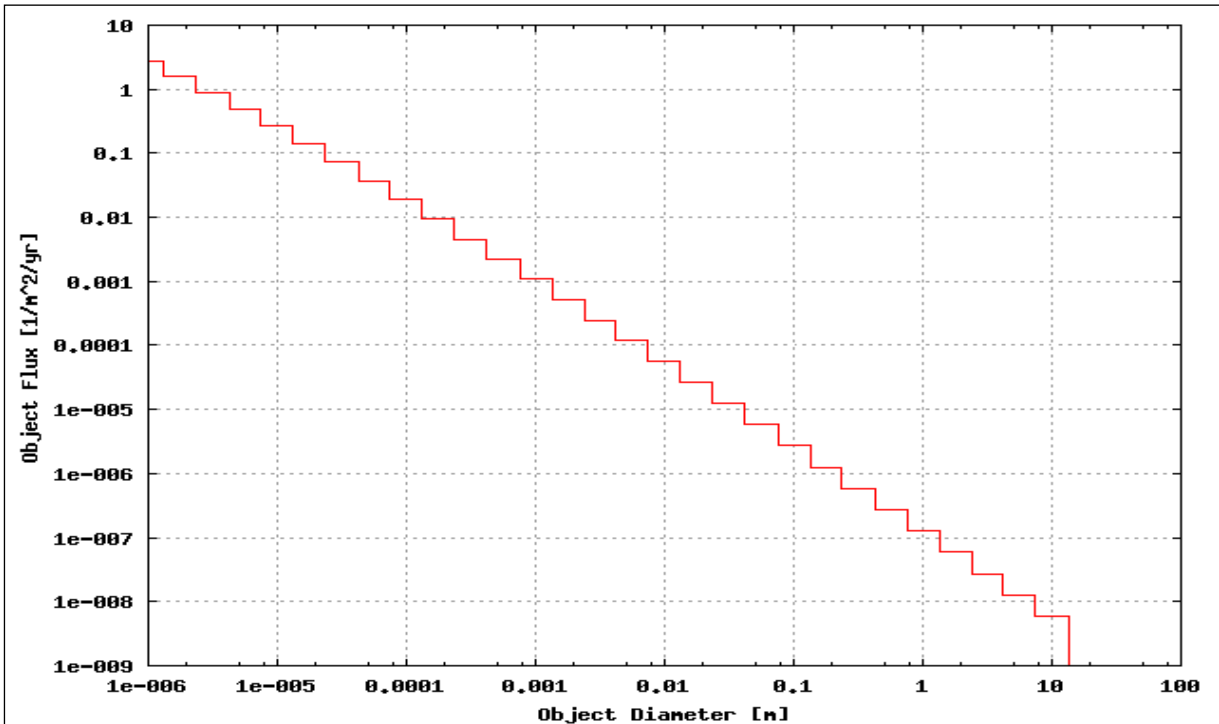
Figure 2-61:   MEM 3 high-density flux vs. mass, orbital point in LEO orbit / mass > 1*10⁻⁶ g

Project: ESABASE2/Debris Release 12.1	Date:	2024-02-19
Technical Description	Revision:	1.11
Reference: R077-231rep_01_11_Debris_Technical Description.docx	Status:	Final
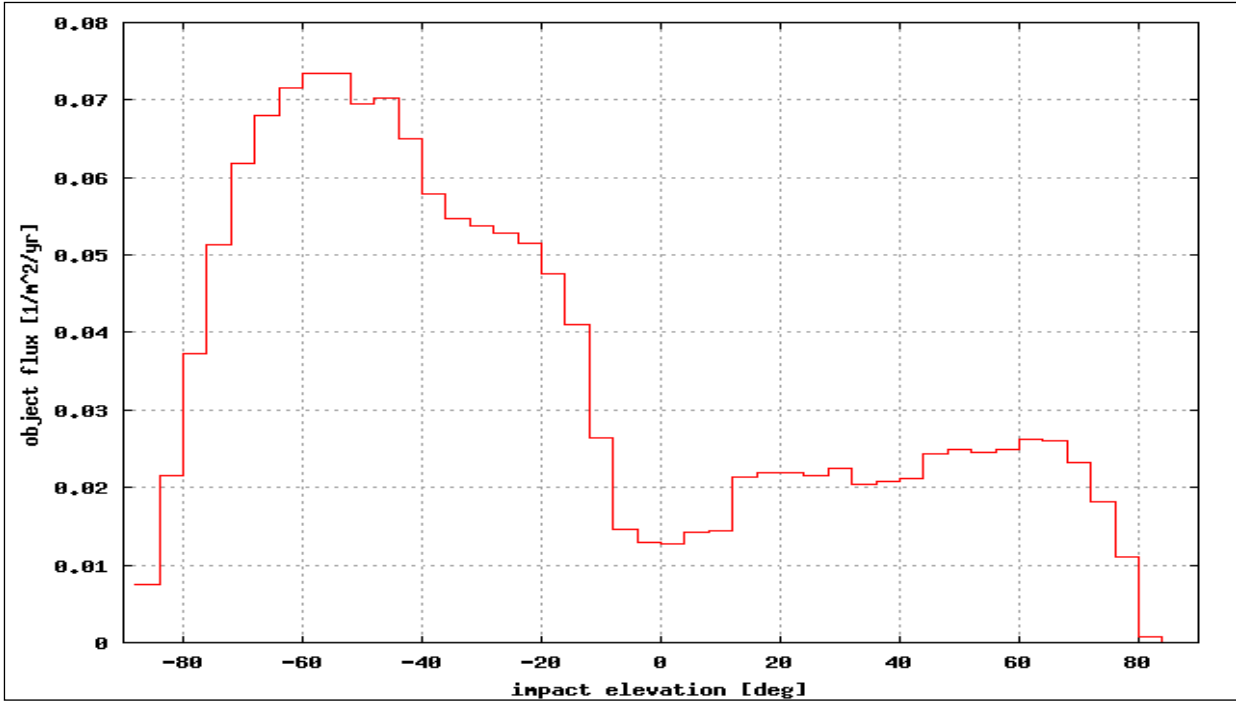
Figure 2-62: MEM 3 low-density flux vs. impact elevation, orbital point in LEO / mass > 1*10⁻⁶ g
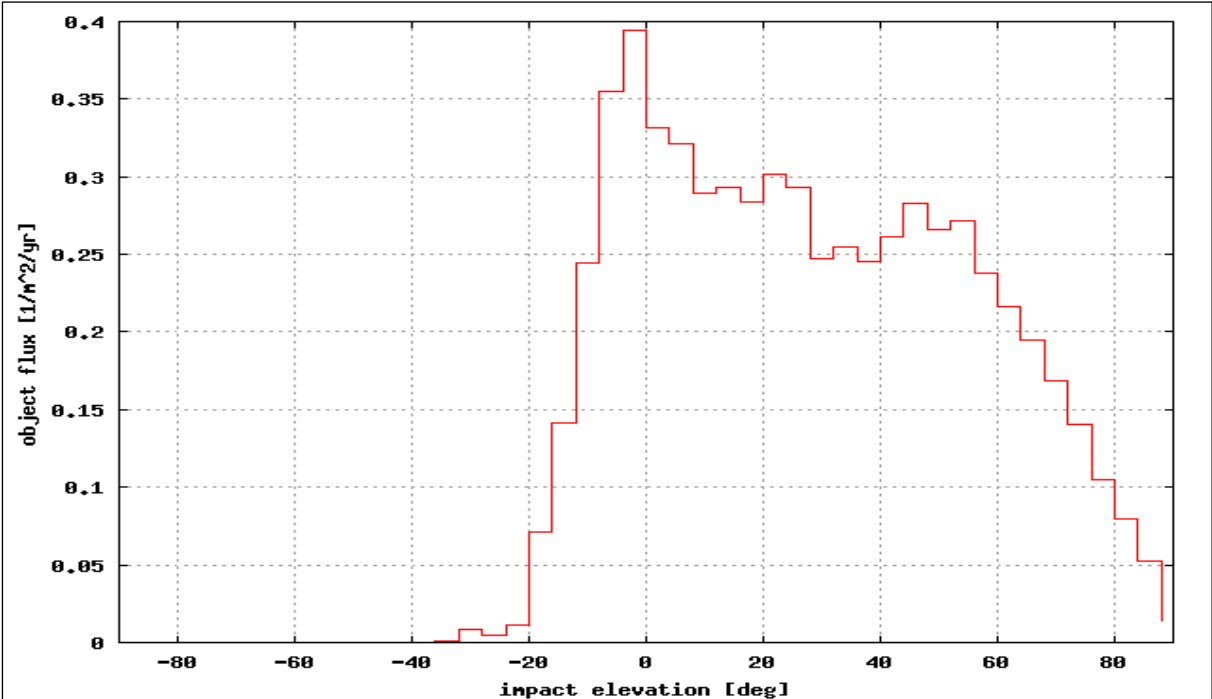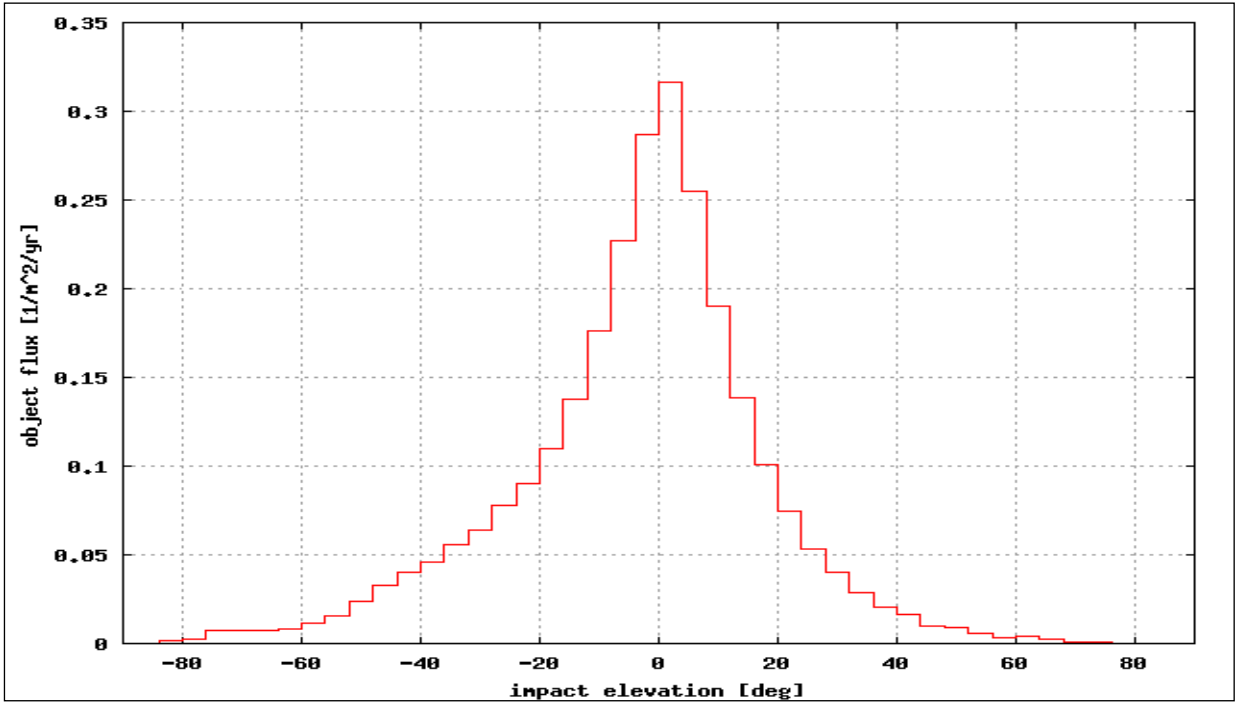

Figure 2-63: MEM 3 high-density flux vs. impact elevation, orbital point in LEO / mass > 1*10⁻⁶ g

Project: ESABASE2/Debris Release 12.1		Date:	2024-02-19
Technical Description		Revision:	1.11
Reference: R077-231rep_01_11_Debris_Technical Description.docx		Status:	Final

FEV etamax GmbH — Page 91 / 173
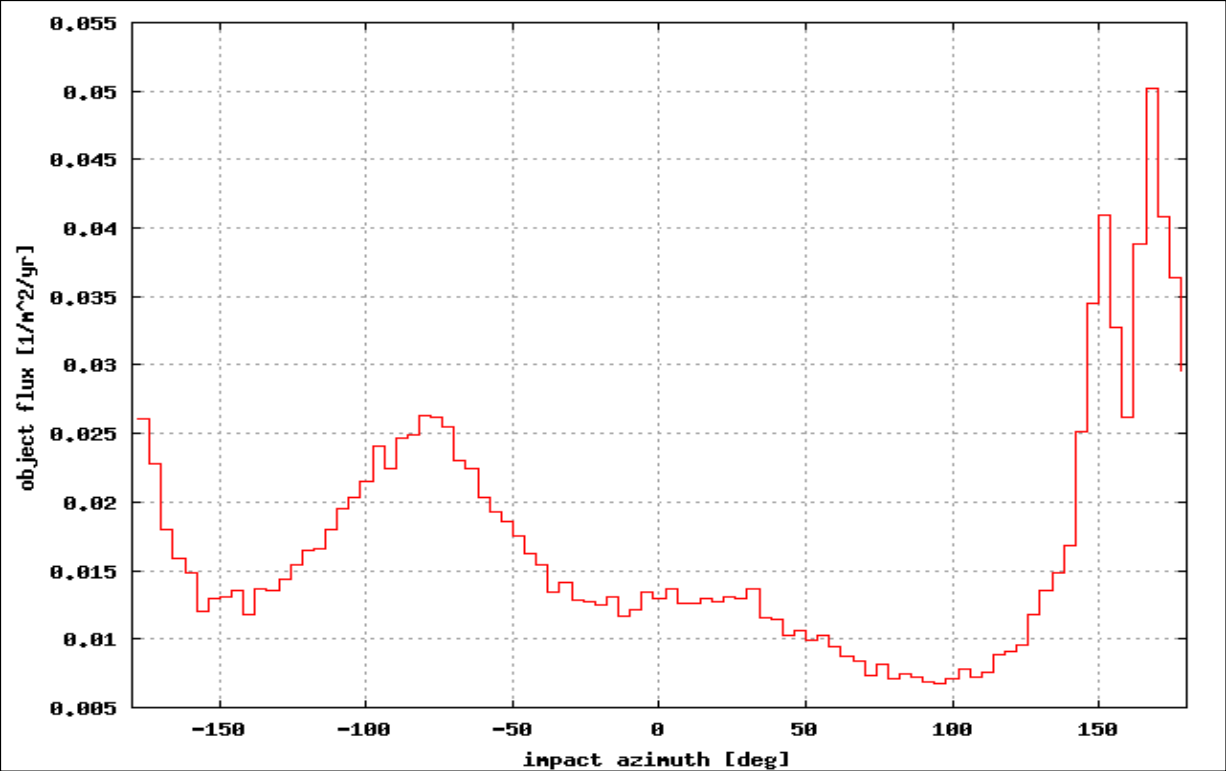
Figure 2-64: MEM 3 low-density flux vs. impact azimuth, orbital point in LEO / mass > $1*10^{-6}$ g
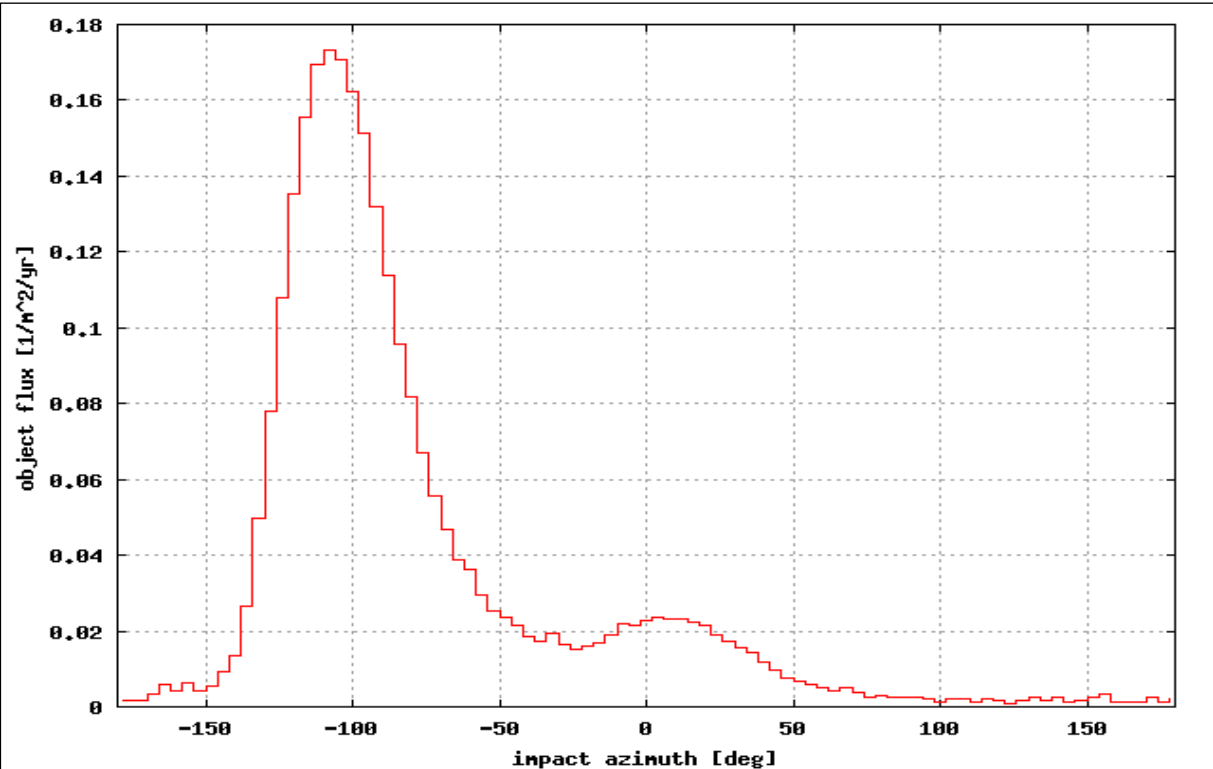
Figure 2-65: MEM 3 high-density flux vs. impact azimuth, orbital point in LEO / mass > $1*10^{-6}$ g

Project: ESABASE2/Debris Release 12.1		Date:	2024-02-19
Technical Description		Revision:	1.11
Reference: R077-231rep_01_11_Debris_Technical Description.docx		Status:	Final

FEV etamax GmbH   Page 92 / 173

Figure 2-66: **MEM 3 low-density flux vs. impact velocity, orbital point in LEO / mass > 1*10⁻⁶ g**
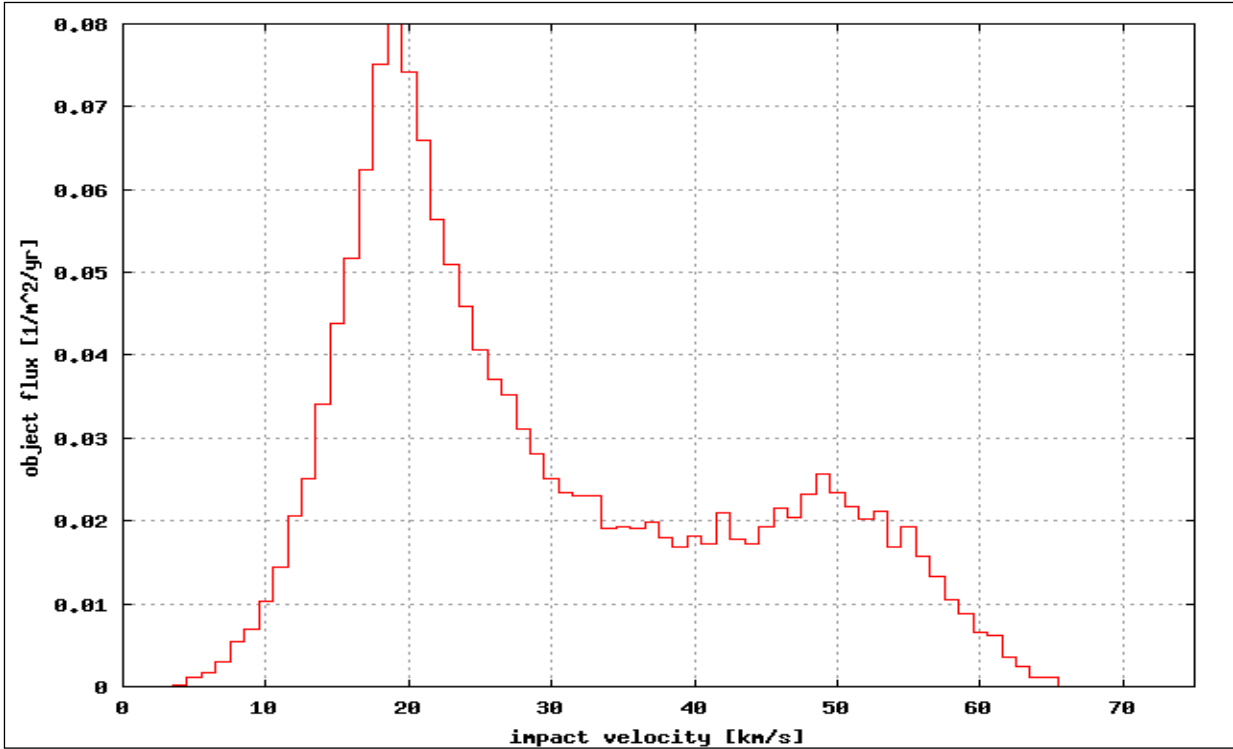
Figure 2-66: **MEM 3 low-density flux vs. impact velocity, orbital point in LEO / mass $> 1*10^{-6}$ g**
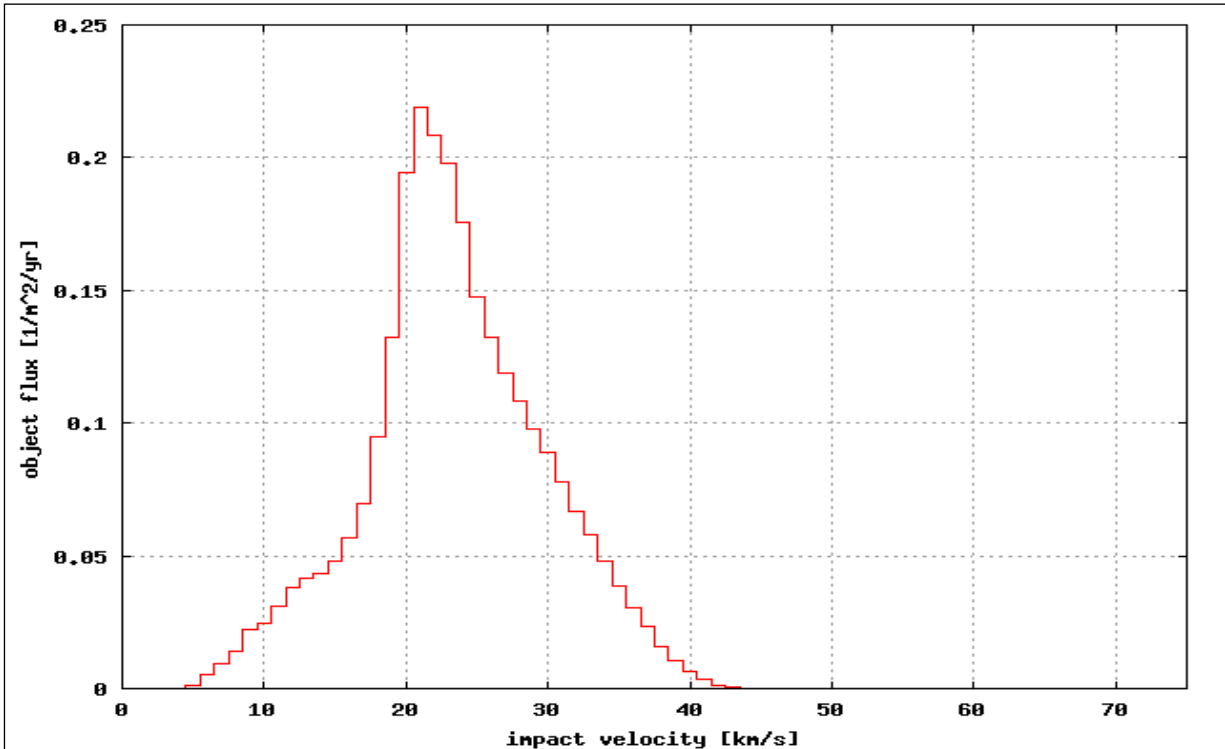
Figure 2-67: **MEM 3 high-density flux vs. impact velocity, orbital point in LEO / mass $> 1*10^{-6}$ g**
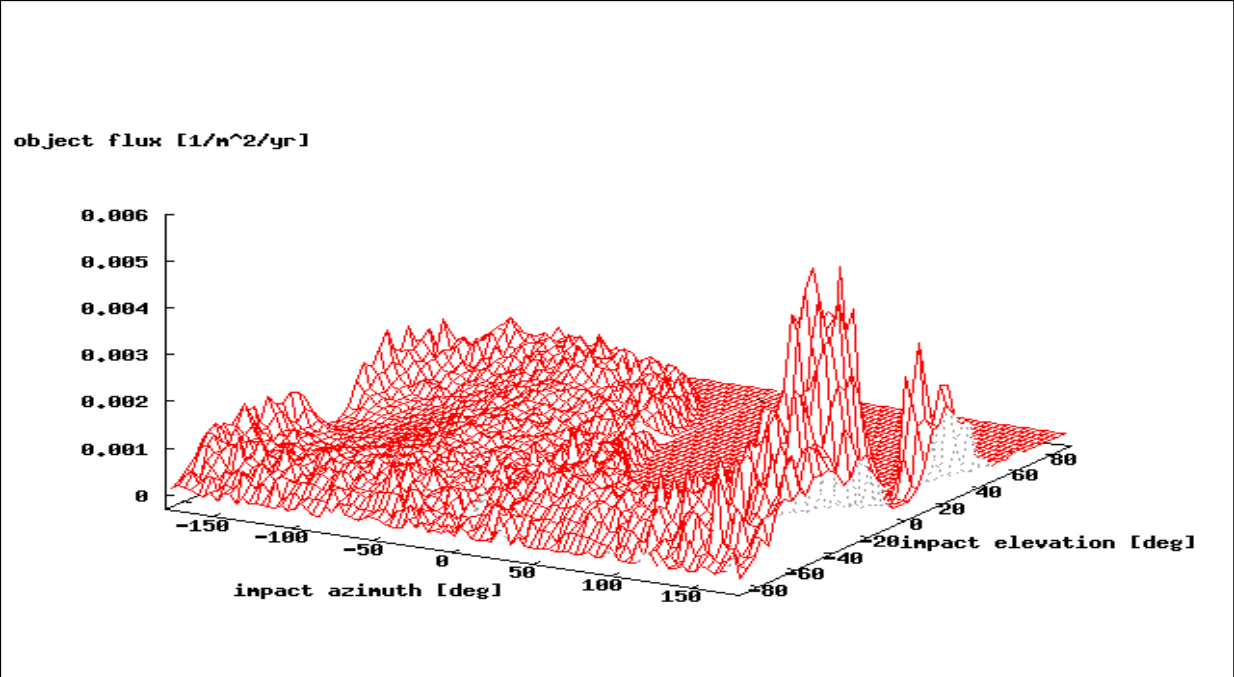
Figure 2-68: MEM 3 LoDensity flux vs. impact azi. and ele., orbital point in LEO / mass > $1*10^{-6}$ g
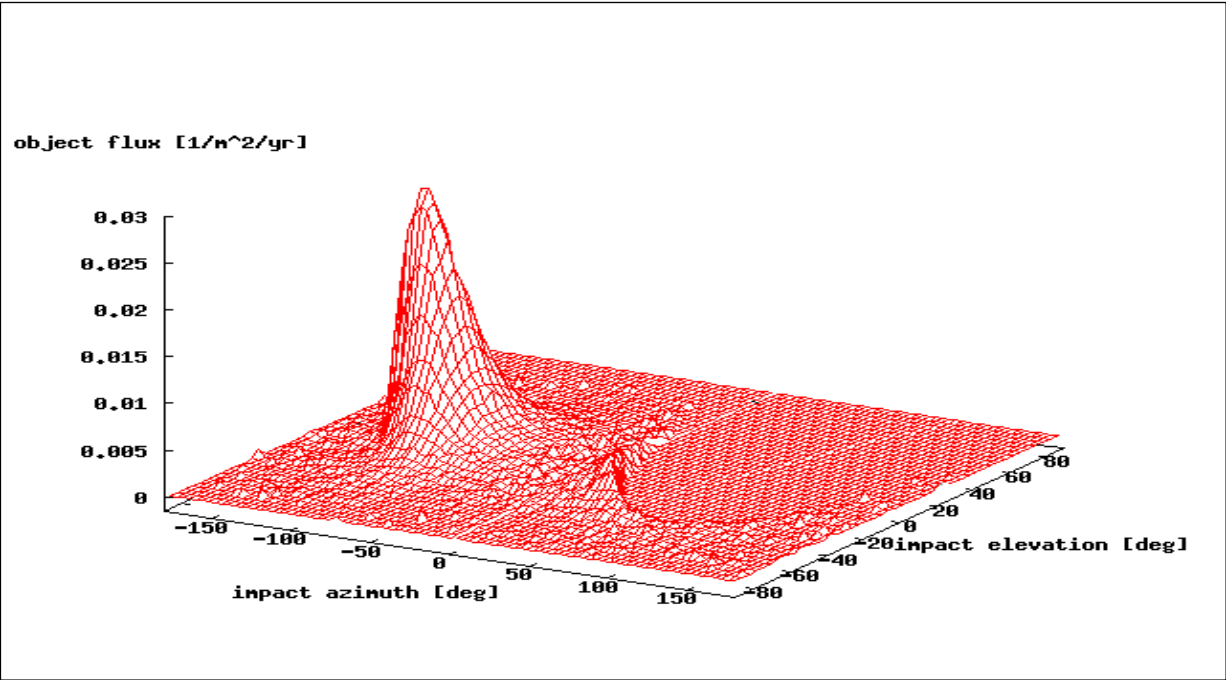
Figure 2-69: MEM 3 HiDensity flux vs. impact azi. and ele., orbital point in LEO / mass > $1*10^{-6}$ g

Although the spectra are displayed as differential distributions – except the mass spectrum, which is cumulative – the distributions are provided and used in their cumulative form within the ESABASE2/Debris analysis as described in chapter 5.

2.2.8 The Meteroid Model IMEM

2.2.8.1 Overview

ESA developed the Interplanetary Meteoroid Environment Model (IMEM), which models the orbits of particles from Jupiter-family comets and asteroids and was fitted largely to in situ data and infrared brightness measurements /51/, /52//51/. An interstellar population is parametrized as mono-directional stream. Cometary and asteroidal populations are split into heavier ("collision dominated") and lighter ("Poynting-Robertson dominated") groups. This results in a discontinuity in the mass flux at around 10^{-5} g. Modelled meteor observations were not used because they were found to be inconsistent with modelled infrared data.

The model file provided with IMEM contains data on meteoroids of mass between 10^-18 and 10^2 grams on the orbits with pericentric distances between 0.05 and 6 AU, eccentricities between 0 and 1 and inclinations between 0 and 180 degrees /52/.

With the minimum particle mass handled by the model being 10E-18 grams and the maximum being 100 grams and considering user defined density the user defined particle size/mass thresholds probably need to be adjusted. The thresholds are converted, if required, to mass and increased/decreased for scenarios where the user defines a smaller minimum particle size or larger maximum particle size, respective. The values will be adapted to the corresponding values that can be applied by the model and the user will be informed. By this, E2/Di only provides results for the mass/diameter range covered by the model itself without interpreting particles outside this range.

2.2.8.2 Implementation

The processing of the IMEM population within ESABASE2 is performed based on three individual scan options which are:

- Sky map (to obtain azimuth and declination; azimuth: split into 60 bins, 6° resolution; declination 60 bins, 3° resolution)
- Size (20 bins)
- Velocity (50 bins, 0 – 100 km/s, 2 km/s resolution)

After performing these runs separately, the resulting information will be combined to obtain an in-depth knowledge of the flux.

2.2.8.3 Results

Figure 2-70 shows an exemplary plot of the distribution from /52/. It shows the average impact velocity on a colour scale over the azimuth and declination. For the creation of such a plot combination of the sky map and velocity information is required.

Project: ESABASE2/Debris Release 12.1	Date:	2024-02-19
Technical Description	Revision:	1.11
Reference: R077-231rep_01_11_Debris_Technical Description.docx	Status:	Final

FEV etamax GmbH   Page 95 / 173
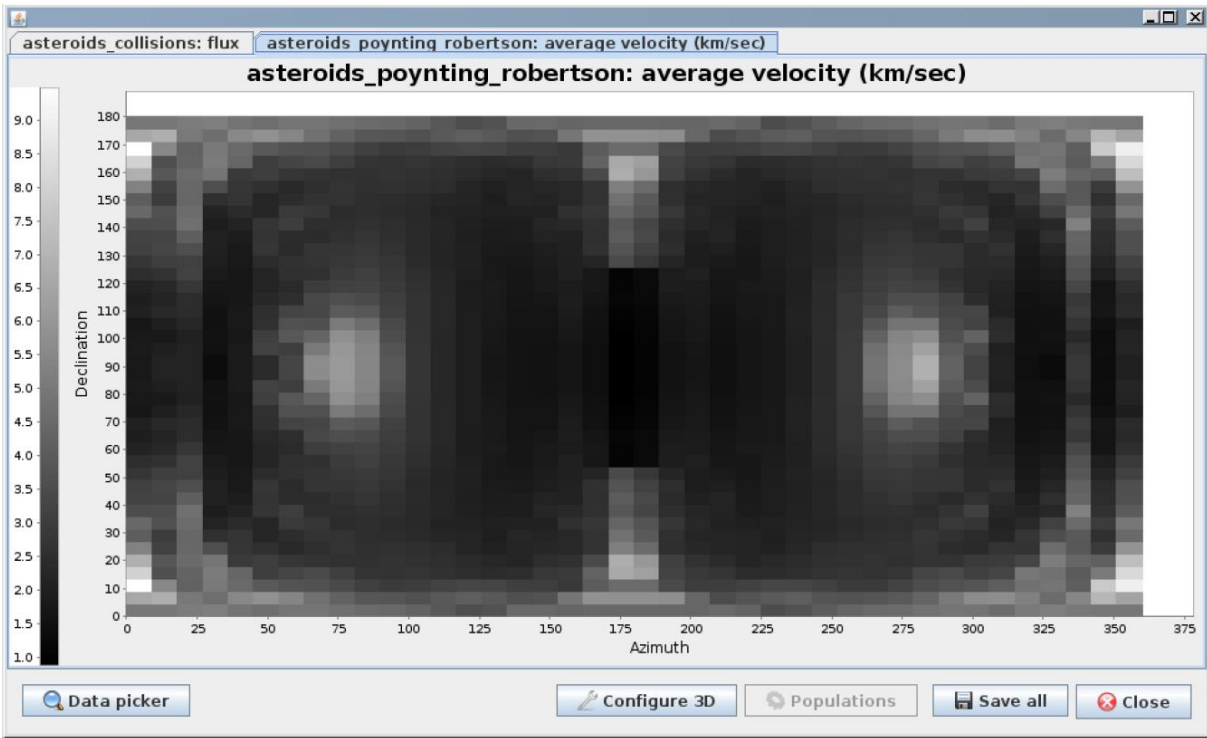
Figure 2-70:   IMEM 2-D plot example /52/.

2.2.9 The Meteoroid Model IMEM2

2.2.9.1 Overview

Interplanetary Meteoroid Environment Model 2 (IMEM2) is the follow-up approach of ESA's IMEM to model meteoroids in the Solar system.

IMEM2 contains a dynamical engineering model of the dust component of the space environment using state-of-the-art knowledge of dust cloud constituents and their development under dynamical and physical effects /53/. The aim was to improve on the IMEM model and to remove its step-wise mass flux by fully integrating the dynamics of particles of radii from 1 μm to 1 cm. The model is built based on knowledge of the orbital distributions of the dust parent bodies (cometary and asteroidal populations). The model is designed to match dust observations as closely as possible, including infrared data from the Cosmic Background Explorer (COBE), lunar microcrater counts, meteor orbit radar velocity, and orbital element distributions, as well as the flux of dust particles at the Earth.

It gives density and velocity information of asteroid and comet originated dust particles. For achieving these results, numerical integration has been applied to a period of one million years using test particles for the simulation. The particle density is divided in three different densities for the different dust populations /55/:

- HTC Halley type particles (1000 kg/m^3)
- JFC Jupiter family particles (2000 kg/m^3)
- AST asteroid particles (4000 kg/m^3)

Project: ESABASE2/Debris Release 12.1	Date:	2024-02-19
Technical Description	Revision:	1.11
Reference: R077-231rep_01_11_Debris_Technical Description.docx	Status:	Final

The model classifies the particles into 12 different sizes (1, 5, 12.5, 25, 50, 125, 250, 500, 1250, 2500, 5000 and 10000 µm). Its distance frame ranges from -6 to 6 AU which includes the inner planets up to Jupiter /55/.

Next to the GUI version released in March 2019 /54/, a command line version has been developed. It is used within this E2/Di activity to ensure a practical interface between the two applications. /55/ refers to the command line tool's interface and is also used as main source for the information given in this section.

2.2.9.2 Implementation

The processing of IMEM2 in ESABASE2 is based on the consideration of the complete 5D-Distribution (or 6D, respectively, considering IMEM2's density distribution depending on user selection) given through the STENVI format (see section 2.1.6.1 for an explanation of the STENVI format). The flux is calculated based on:

- Azimuth (split into 72 bins, 5° resolution),
- Elevation (36 bins, 5° resolution),
- Size (12 bins, fixed sizes given in Section 2.2.9.2),
- Velocity (50 bins, 0 – 100 km/s, 2 km/s resolution),
- (Density – 1/3 bins depending on user selection).

2.2.9.3 Results

An example of the particle distribution over the velocity is given in Figure 2-71: IMEM2 particle distribution over velocity example /56/.Figure 2-71.

Project: ESABASE2/Debris Release 12.1		Date:	2024-02-19
Technical Description		Revision:	1.11
Reference: R077-231rep_01_11_Debris_Technical Description.docx		Status:	Final

FEV etamax GmbH   Page 97 / 173
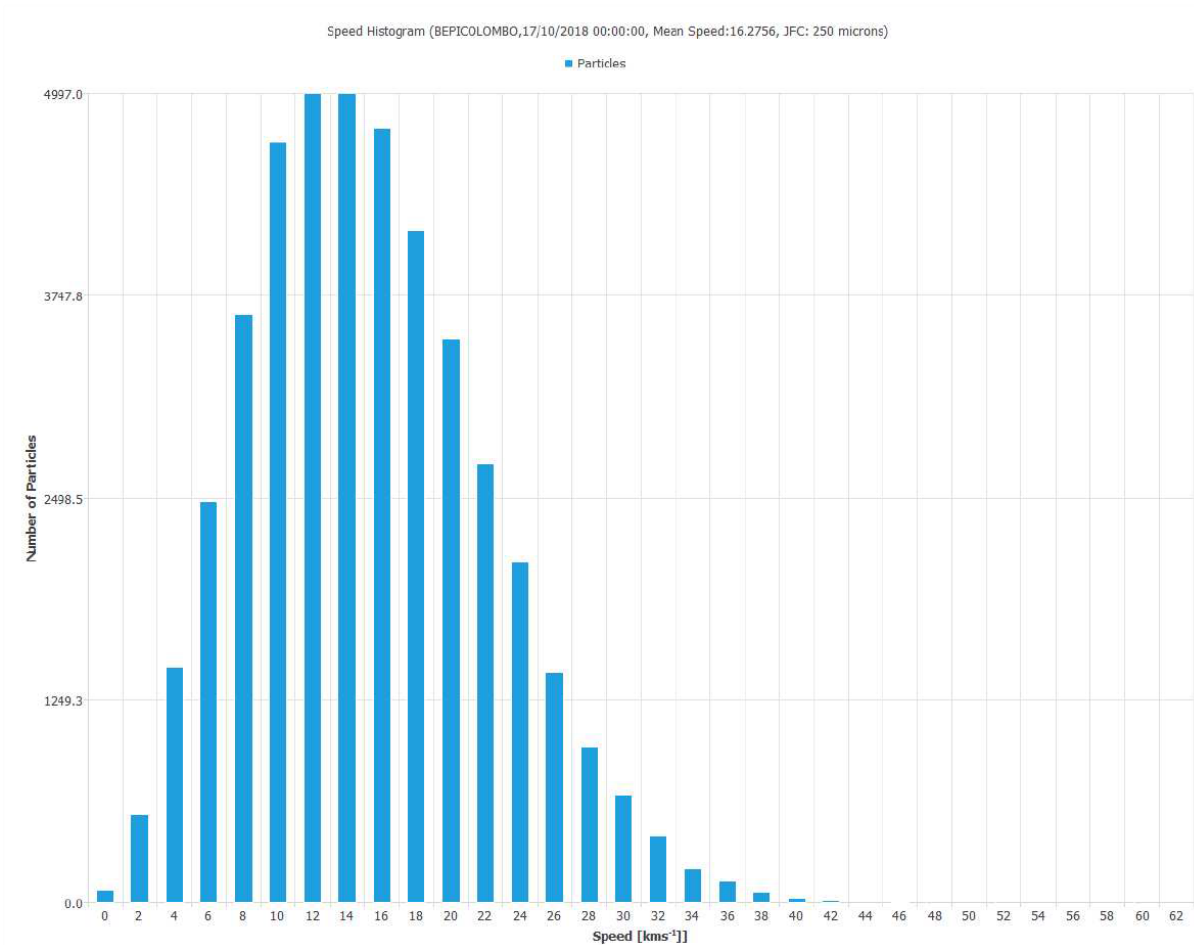
Figure 2-71: IMEM2 particle distribution over velocity example /56/.

The density grid generated for the stepping algorithm (explained in Section 6.6.3) using IMEM2 is shown in Figure 2-72. Since IMEM2 is rotationally symmetric around the z-axis pointing to ecliptic north pole only a two-dimensional grid is required.

Project: ESABASE2/Debris Release 12.1		Date:	2024-02-19
Technical Description		Revision:	1.11
Reference: R077-231rep_01_11_Debris_Technical Description.docx		Status:	Final
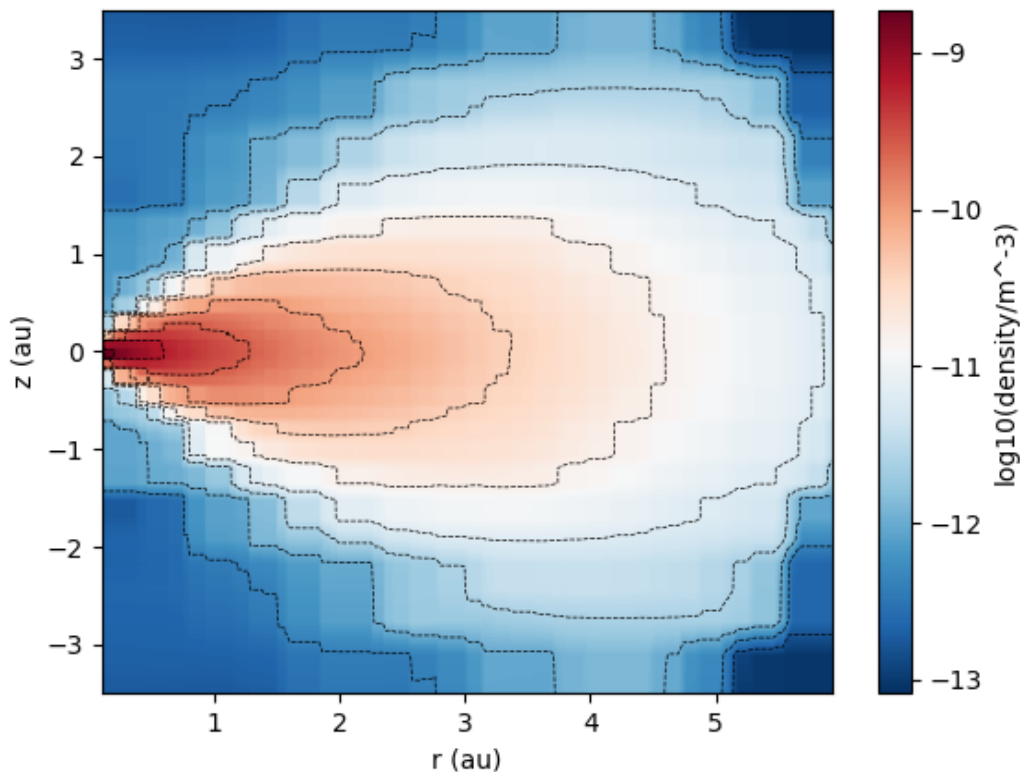
Figure 2-72:   **Contour plot of IMEM2 300x100 12.5 micron density grid**

2.2.10   Meteoroid Streams According to Jenniskens/McBride

2.2.10.1   General

In the old ESABASE/Debris software the annual meteoroid streams are implemented according to the Cour-Palais 1969 method (Ref. /11/) which does not include directional effects. This has been replaced by a new approach of P. Jenniskens (Ref. /5/, 1994) which is based on data collected by a large number of observers over a 10 year period from observation sites in both the northern and southern hemispheres. In Ref. /13/ N. McBride describes how the parameters of Jenniskens have to be implemented into a numerical application.

In summary the stream geometry and activity at shower maximum is defined by:

a) the solar longitude λ at shower maximum λ_{max}

b) the maximum zenithal hourly rate ZHR_{max} , which is the number of 'visible' meteors seen after various observer and location related corrections have been applied

c) apparent radiant position in RA (right ascension of the radiant) and Dec (declination of the radiant) . These values are tabulated in Table 15 at an epoch defined by the solar longitude λ^0

Project: ESABASE2/Debris Release 12.1	Date:	2024-02-19
Technical Description	Revision:	1.11
Reference: R077-231rep_01_11_Debris_Technical Description.docx	Status:	Final

FEV etamax GmbH   Page 99 / 173

d) the geocentric meteoroid speeds, defined as the final geocentric velocity V_∞ as the meteoroids reach the top of the atmosphere

The right ascension of the radiant and for the declination for an instantaneous value of the solar longitude λ are obtained by

$$RA(\lambda) = RA(\lambda^0) + \Delta RA\,(\lambda - \lambda^0)\,, \qquad Dec(\lambda) = Dec(\lambda^0) + \Delta Dec\,(\lambda - \lambda^0)\,.$$

The shower activity as a function of time around its maximum is described by

$$ZHR = ZHR_{max}\,10^{-B\,|\lambda - \lambda max|}\,,$$

where B is given in Ref. /5/ and describes the slopes of the activity profiles. Since most streams are found to have symmetrical profiles a single value of B is sufficient. The Geminids are the exception; this stream needs a different value of B for the inward and outward slope. Six of the streams do not have a strong enough ZHR to produce a slope, here it is suggested to use a 'typical' value of B = 0.2. Six other streams are best represented by the sum of 2 activity profiles, defined by a peak profile ZHR^p_{max} and B^p and a background profile ZHR^b_{max} with separate inward and outward slope values B^{b+} and B^{b-} respectively. This results in the following expression:

$$ZHR = ZHR^p_{max}\,10^{-B^p\,|\lambda - \lambda\,max|} + ZHR^b_{max}\,(\,10^{-B^{b-}\,(\lambda\,max - \lambda)} + 10^{-B^{b+}\,(\lambda - \lambda\,max)}\,)$$

The cumulative flux at solar longitude λ can now be expressed as

$$F(m,\lambda) = F(m)_{max}\,\frac{ZHR(\lambda)}{ZHR_{max}}$$

with

$$F(m)_{max} = k\,m^{-\alpha}$$

The total particle flux F_{TOT} is obtained by summation over all streams

$$F_{TOT} = F_{SPORADIC} + \sum F_{ST}\,.$$

Since the Grün flux models all particles, including the streams, F_{TOT} must be forced to equal the Grün flux when summed over a full year. Thus, when the stream model is used, the new sporadic flux becomes

$$F_{SPORADIC} = F_{Grün} - \sum_{1\,year} F_{ST}$$

where the sum is to be evaluated over one full year.

Note: Additional streams may be defined in place of or in addition to the Jenniskens streams by the user, using the format of Table 15, see ref. /14/.

Project: ESABASE2/Debris Release 12.1	Date:	2024-02-19
Technical Description	Revision:	1.11
Reference: R077-231rep_01_11_Debris_Technical Description.docx	Status:	Final

FEV etamax GmbH Page 100 / 173

	λ_{max}	RA_{max}	ΔRA	Dec_{max}	ΔDec	ZRH^p_{max}	B^{p+}	B^{p-}	ZHR^b_{max}	B^{b+}	B^{b-}	α	k	V_∞
Bootids	283.3	232.	0.6	45.	-0.31	10.0	2.50	2.50	20.0	.37	.45	.92	$.84\cdot10^{-16}$	43
γVelids	285.7	124.	0.5	-47.	-0.2	2.4	.12	.12	0.0	.0	.0	1.10	$.58\cdot10^{-18}$	35
αCrucids	294.5	193.	1.1	-63.	-0.4	3.0	.11	.11	0.0	.0	.0	1.06	$.19\cdot10^{-18}$	50
αHydrusids	300.0	138.	0.7	-13.	-0.3	2.0	.20	.20	0.0	.0	.0	1.03	$.34\cdot10^{-18}$	44
αCarinids	311.2	99.	0.4	-54.	0.0	2.3	.16	.16	0.0	.0	.0	.92	$.13\cdot10^{-16}$	25
δVelids	318.0	127.	0.5	-50.	-0.3	1.3	.20	.20	0.0	.0	.0	1.10	$.31\cdot10^{-18}$	35
αCentaurids	319.4	210.	1.3	-58.	-0.3	7.3	.18	.18	0.0	.0	.0	.83	$.37\cdot10^{-17}$	57
Ocentaurids	323.4	176.	0.9	-55.	-0.4	2.2	.15	.15	0.0	.0	.0	1.03	$.19\cdot10^{-18}$	51
θCentaurids	334.0	220.	1.1	-44.	-0.4	4.5	.20	.20	0.0	.0	.0	.95	$.44\cdot10^{-18}$	60
δLeonids	335.0	169.	1.0	17.	-0.3	1.1	.049	.049	0.0	.0	.0	1.10	$.19\cdot10^{-17}$	23
Virginids	340.0	165.	0.9	9.	-0.2	1.5	.20	.20	0.0	.0	.0	1.10	$.15\cdot10^{-17}$	26
γNormids	353.0	285.	1.3	-56.	-0.2	5.8	.19	.19	0.0	.0	.0	.87	$.19\cdot10^{-17}$	56
δPavonids	11.1	311.	1.6	-63.	-0.2	5.3	.075	.075	0.0	.0	.0	.95	$.51\cdot10^{-18}$	60
Lyrids	32.4	274.	1.2	33.	0.2	12.8	.22	.22	0.0	.0	.0	.99	$.20\cdot10^{-17}$	49
μVirginids	40.0	230.	0.5	-8.	-0.3	2.2	.045	.045	0.0	.0	.0	1.10	$.11\cdot10^{-17}$	30
ηAquarids	46.5	340.	0.9	-1.	0.3	36.7	.08	.08	0.0	.0	.0	.99	$.15\cdot10^{-17}$	66
βCorona Aust.	56.0	284.	1.3	-40.	0.1	3.0	.20	.20	0.0	.0	.0	1.13	$.15\cdot10^{-18}$	45
αScorpiids	55.9	252.	1.1	-27.	-0.2	3.2	.13	.13	0.0	.0	.0	.92	$.47\cdot10^{-16}$	21
Da.Arietids	77.0	47.	0.7	24.	0.6	54.0	.10	.10	0.0	.0	.0	.99	$.26\cdot10^{-16}$	38
γSagitarids	89.2	286.	1.1	-25.	0.1	2.4	.037	.037	0.0	.0	.0	1.06	$.19\cdot10^{-17}$	29
τCetids	95.7	24.	0.9	-12.	0.4	3.6	.18	.18	0.0	.0	.0	.92	$.37\cdot10^{-18}$	66
θOphiuchids	98.0	292.	1.1	-11.	0.1	2.3	.037	.037	0.0	.0	.0	1.03	$.35\cdot10^{-17}$	27
τAquarids	98.0	342.	1.0	-12.	0.4	7.1	.24	.24	0.0	.0	.0	.92	$.89\cdot10^{-18}$	63
νPhoenicids	111.2	28.	1.0	-40.	0.5	5.0	.25	.25	0.0	.0	.0	1.10	$.26\cdot10^{-18}$	48
OCygnids	116.7	305.	0.6	47.	0.2	2.5	.13	.13	0.0	.0	.0	.99	$.14\cdot10^{-17}$	37
Capricornid	122.4	302.	0.9	-10.	0.3	2.2	.041	.041	0.0	.0	.0	.69	$.83\cdot10^{-16}$	25
τAquarids N	124.1	324.	1.0	-8.	0.2	1.0	.063	.063	0.0	.0	.0	1.19	$.36\cdot10^{-19}$	42
Pisces Aust.	124.4	339.	1.0	-33.	0.4	2.0	.40	.40	0.9	.03	.10	1.16	$.15\cdot10^{-18}$	42
δAquarids S.	125.6	340.	0.8	-17.	0.2	11.4	.091	.091	0.0	.0	.0	1.19	$.36\cdot10^{-18}$	43
ιAquarids S.	131.7	335.	1.0	-15.	0.3	1.5	.07	.07	0.0	.0	.0	1.19	$.12\cdot10^{-18}$	36
Perseids	140.2	47.	1.3	58.	0.1	70.0	.35	.35	23.0	.05	.092	.92	$.12\cdot10^{-16}$	61
κCygnids	146.7	290.	0.6	52.	0.3	2.3	.069	.069	0.0	.0	.0	.79	$.30\cdot10^{-16}$	27
πEridanids	153.0	51.	0.8	-16.	0.3	40.0	.20	.20	0.0	.0	.0	1.03	$.17\cdot10^{-17}$	59
γDoradids	155.7	60.	0.5	-50.	0.2	4.8	.18	.18	0.0	.0	.0	1.03	$.11\cdot10^{-17}$	41
Aurigids	158.2	73.	1.0	43.	0.2	9.0	.19	.19	0.0	.0	.0	.99	$.29\cdot10^{-18}$	69
κAquarids	177.2	339.	0.9	-5.	0.4	2.7	.11	.11	0.0	.0	.0	1.03	$.19\cdot10^{-16}$	19
εGeminids	206.7	104.	0.7	28.	0.1	2.9	.082	.082	0.0	.0	.0	1.10	$.21\cdot10^{-19}$	71
Orionids	208.6	96.	0.7	16.	0.1	25.0	.12	.12	0.0	.0	.0	1.13	$.16\cdot10^{-18}$	67
Leo Minorids	209.7	161.	1.0	38.	-0.4	1.9	.14	.14	0.0	.0	.0	.99	$.11\cdot10^{-18}$	61
Taurids	223.6	50.	0.3	18.	0.1	7.3	.026	.026	0.0	.0	.0	.83	$.43\cdot10^{-16}$	30
δEridanids	229.0	54.	0.9	-2.	0.2	0.9	.20	.20	0.0	.0	.0	1.03	$.75\cdot10^{-18}$	31
ζPuppids	232.2	117.	0.7	-42.	-0.2	3.2	.13	.13	0.0	.0	.0	1.22	$.95\cdot10^{-19}$	41
Leonids	235.1	154.	1.0	22.	0.4	19.0	.55	.55	4.0	.025	.15	1.22	$.34\cdot10^{-19}$	71
Puppids/Vel	252.0	128.	0.8	-42.	-0.4	4.5	.034	.034	0.0	.0	.0	1.06	$.82\cdot10^{-18}$	40
Phoenicids	252.4	19.	0.8	-58.	0.4	2.8	.30	.30	0.0	.0	.0	1.03	$.25\cdot10^{-16}$	18
Monoceroti.	260.9	100.	1.0	14.	-0.1	2.0	.25	.25	0.0	.0	.0	1.25	$.33\cdot10^{-19}$	43
Geminids	262.1	113.	1.0	32.	0.1	74.0	.59	.81	18.0	.09	.31	.95	$.78\cdot10^{-16}$	36
σHydrusids	265.5	133.	0.9	0.	-0.3	2.5	.10	.10	0.0	.0	.0	1.10	$.47\cdot10^{-19}$	59
Ursids	271.0	224.	-0.2	78.	-0.3	10.0	.90	.90	2.0	.08	.2	1.22	$.81\cdot10^{-18}$	35

Table 15   The 50 Jenniskens streams

2.2.10.2   Implementation

The following symbols are used in Table 15 and in the formulas that follow:

Project: ESABASE2/Debris Release 12.1		Date:	2024-02-19
Technical Description		Revision:	1.11
Reference: R077-231rep_01_11_Debris_Technical Description.docx		Status:	Final

FEV etamax GmbH   Page 101 / 173

λ	solar longitude in degrees
λ_{max}	solar longitude in degrees at shower peak (tabled in Table 15 for 50 streams)
$ZHR^{p/b}_{max}$	Zenith Hourly Rate at shower peak / background (observer corrected)
	<u>Note</u>: the b (background) index is only relevant for streams having two profiles.
RA	right ascension of the radiant at solar longitude λ in degrees
Dec	declination of the radiant at solar longitude λ in degrees
ΔRA	variation of RA per degree of solar longitude λ
ΔDec	variation of Dec per degree of solar longitude λ
B, B^p , B^{p+}, B^{p-}, B^{b+}, B^{b-}	slopes of the shower activity profiles
V_∞	meteoroid arrival velocity in km/s, already containing gravitational enhancement
F(m)	cumulative flux in $m^{-2}\,s^{-1}$ of particles with mass greater than m (kg)
α	cumulative mass distribution index
k	cumulative mass distribution constant
$Q = ZHR / ZHR^i_{max}$	Ratio of actual ZHR to its peak value; index i = p or b

The following algorithm now applies to determine the individual streams' fluxes:

1) Given λ, choose the closest value of λ_{max} in the Table and determine the stream number

2) From $\Delta\lambda = 2/B$ determine if λ is within the range

$$(\lambda_{max} - \Delta\lambda) < \lambda < (\lambda_{max} + \Delta\lambda) \quad (\Delta\lambda \text{ determined by 1\% of } ZHR_{max})$$

if not, skip this stream. (λ_{max} to be taken from Table 15)

3) Calculate ZHR within the profile

$$ZHR = ZHR^p_{max}\ 10^{-B\,|\lambda\,-\,\lambda max\,|}$$

3a) For the six streams in Table 15 which have two activity profiles (non vanishing B^{b+} / B^{b-} values), calculate according to equation 1 and equation 10 the ratio

$$Q = ZHR / ZHR^p_{max}\ 10^{-B^p\left|\lambda - \lambda\,max\right|} + ZHR / ZHR^b_{max}\ (\ 10^{-B^{b-}(\lambda\,max-\lambda)} + 10^{-B^{b+}(\lambda-\lambda\,max)}\ )$$

4) The cumulative flux is now given by

$$F(m) = F(m)_{max}\cdot Q$$

with

$$F(m)_{max} = k \, m^{-\alpha} \qquad \text{or} \qquad dF = -\alpha \, k \, m^{-(\alpha+1)} \, dm$$

k and α are obtained from the Table according to the relevant stream number.

The *arrival velocity* V_∞ does not need gravitational corrections due to the Earth gravity because it is measured at the top of the atmosphere.

2.2.11 Further Directional Effects

2.2.11.1 Introduction

From Ref. /9/ it becomes apparent that actually very little is known about how the Grün flux should be modified to include an apex enhancement, to sort out the beta meteoroids, and to include interstellar dust. The enhancements are applicable only to Earth orbits.

2.2.11.2 Separation of α- and β-Source

In Ref. /9/ it is suggested to separate the Grün flux into an α population and an β population which has a crossover at 10^{-11} g. The β population has the direction from the Sun and is of the small particle size. The separation into the α - flux $F_\alpha(M)$ and the β - flux $F_\beta(M)$ may then be done in the following way (Ref. /9/ , eqs, 25,26,27):

$$F_\beta(M) \ = \ F_G(M) - F_\alpha(M) \qquad\qquad F_G(M) = \text{Grün flux}$$

$$F_\alpha(M) \quad = \quad \frac{F_G(M) \cdot F_H(M)}{F_G(M) + F_H(M)}$$

$$\log(F_H) \quad = \quad -a \log(M) - b \qquad\qquad a = 0.146 \qquad b = 6.427$$

Where the units are $\quad$ F: $m^{-2} \, s^{-1}$, M: g

From the above equations it is possible for each randomly generated mass value to calculate a corresponding cumulative flux value F_α and a corresponding flux value F_β from the Grün flux F_G .

The velocity of the β particles is size dependent, and according to Ref. /9/ , Eq. 28 one may assume

$$v(M) = v_0 \left(\frac{M}{10^{-11}} \right)^{-\gamma} \qquad\qquad v_0 = 20 \text{ km/s} , \qquad\qquad \gamma = 0.18$$

where v_0 and γ are user supplied.

2.2.11.3 Apex Enhancement of the α-Source

A minimum to maximum antapex to apex flux ratio R_F , which in fact is not known, is used in Ref. /9/ Eqs. 30 - 35 to define a modulation of the flux and of the velocity about the apex

Project: ESABASE2/Debris Release 12.1		Date:	2024-02-19
Technical Description		Revision:	1.11
Reference: R077-231rep_01_11_Debris_Technical Description.docx		Status:	Final

FEV etamax GmbH $\qquad\qquad\qquad$ Page 103 / 173

direction. The angular deviation from the apex direction is denoted by t, and it is assumed that a parameter δ may describe a slight deviation from the measured peak value which was observed to be about 10° off the apex direction. Thus the modulation of the α flux and of the velocity may be defined as follows:

$$F_\alpha(t) = F_\alpha{}^0 [\, 1 + \Delta_t \cos(t + \delta)]$$

$$V_\alpha(t) = V_\alpha{}^0 [\, 1 + \Delta_V \cos(t + \delta)]$$

where $\qquad \Delta_t = \dfrac{R_F - 1}{R_F + 1} \qquad$ and $\qquad \Delta_V = \dfrac{V_A - V_{AA}}{V_A + V_{AA}}$

$$V_0 = (V_A + V_{AA}) / 2$$

(subscript A for apex and AA for antapex)

From the AMOR meteor data there are some guesses for the maximum to minimum detection ratio, from which one may try to obtain some values for R_F and V_{AA}. Although R_F could be anywhere in the range of 1 to 5 , and V_A and V_{AA} are not known either, it is recommended, that for a first guess one may use the following values:

$$V_A = 17.7 \text{ Km/s} , \qquad V_{AA} = 8.3 \text{ km/s} , \qquad R_F = \frac{V_A}{V_{AA}} = 2$$

resulting in the following values for Δ_t and Δ_V:

$$\Delta_t = 0.33 \qquad \text{and} \qquad \Delta_V = 0.36$$

2.2.11.4   Interstellar Dust

Two components of interstellar dust particles have been observed according to Ref. /9/.

The *first source* concerns measurements on Ulysses and Galileo, which detected at about 5 AU particles of $3 \cdot 10^{-16}$ g with heliocentric velocities of 26 km/s. The ecliptic longitude was 252° and the latitude 2.5°. For the total particle flux at 1 AU one can estimate $5 \cdot 10^{-4}$ m^{-2} s^{-1}, and the heliocentric velocity at 1 AU would be 47 km/s . The mean particle mass detected by the Ulysses dust detector was $3 \cdot 10^{-16}$ g.

The *second source* (Ref. /12/) stems from AMOR meteor data which indicate at least two sources which would be defined by:

radiant direction: $\lambda = 243°$, $\qquad \beta = 50°, \qquad V_\infty = 40$ km/s

and

radiant direction: $\lambda = 347°$, $\qquad \beta = 60°, \qquad V_\infty = 80$ km/s

λ and β being the ecliptic longitude and latitude respectively.

Project: ESABASE2/Debris Release 12.1		Date:	2024-02-19
Technical Description		Revision:	1.11
Reference: R077-231rep_01_11_Debris_Technical_Description.docx		Status:	Final

FEV etamax GmbH   Page 104 / 173

In Ref. /12/ the mass of these interstellar meteoroids is estimated to lie between 15 and 40 μm. As of today no flux is known for these contributions.

The implementation of the interstellar source in the ESABASE2/Debris tool is lined out below:

The interstellar contributions are given in the ecliptic system where the velocity, the ecliptic longitude and the ecliptic declination of the interplanetary inward direction are input (by the user, see ref. /14/). By using two-body dynamics these quantities are transformed to the Earth reference frame. Unlike the streams contributions, these showers are changing over time in their direction and velocity due to the moving Earth.

2.2.12 Velocity Distributions

2.2.12.1 Constant Velocity

The ESABASE2/Debris tool includes the option of a constant meteoroid velocity, which is input by the user. The mean velocity of 17 km/s of the NASA 90 distribution (see 2.2.5.2 below) yields good results with the Grün flux model.

2.2.12.2 NASA 90 Meteoroid Velocity Distribution

This normalised distribution is defined in Ref. /3/ and covers a non-vanishing velocity range from 11.1 to 72.2 km/s with a mean velocity of v =17 km/s .
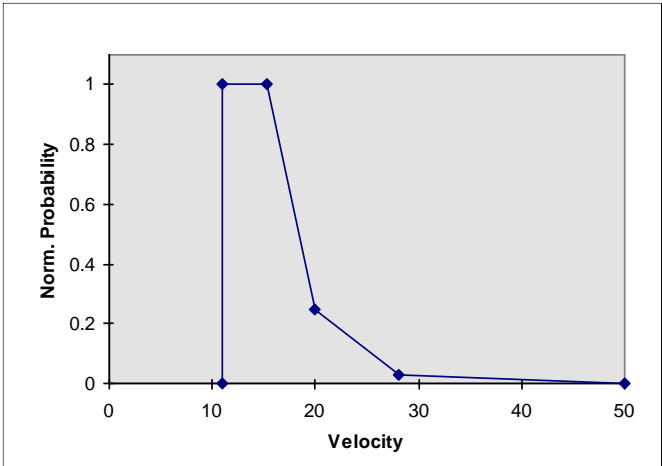
Figure 2-73　　**NASA 90 velocity distribution**

$$g(v) = 0.112 \qquad \text{for} \qquad 11.1 \leq v < 16.3 \text{ km/s}$$

$$g(v) = 3.328 \cdot 10^5 \ v^{-5.34} \qquad \text{for} \qquad 16.3 \leq v < 55 \text{ km/s}$$

$$g(v) = 1.695 \cdot 10^{-4} \qquad \text{for} \qquad 55 \leq v < 72.2 \text{ km/s}$$

2.2.12.3 Velocity and Flux Distribution According to Taylor

In Ref. /9/ several velocity distributions are discussed. The velocity distribution of meteoroids at 1 AU (i.e. as viewed from a massless Earth) has generally been derived from ground based observations of photographic meteors, which are then corrected for the effect of the Earth

gravity. Distributions by Erickson, Sekania and Southworth and by Taylor are compared. It is concluded that the most statistically reliable published data set comes from the Harvard Radio Meteor Project (HRMP) where about 20000 meteor observations were evaluated. Taylor re-evaluated and corrected the original measurement data in Ref./10/ which leads finally to the normalised distribution which is tabulated below at 1 AU, i.e. as seen from a massless Earth. The velocity is in km/s and describes the middle of the 1 km/s wide bin. Each value of $n(v_\infty)$ describes the relative flux of particles within the corresponding bin of 1 km/s width.

v_∞	$n(v_\infty)$	v_∞	$n(v_\infty)$	v_∞	$n(v_\infty)$	v_∞	$n(v_\infty)$
0.5	$0.722 \cdot 10^{-03}$	18.5	$0.447 \cdot 10^{-01}$	36.5	$0.491 \cdot 10^{-02}$	54.5	$0.345 \cdot 10^{-03}$
1.5	$0.227 \cdot 10^{-02}$	19.5	$0.422 \cdot 10^{-01}$	37.5	$0.403 \cdot 10^{-02}$	55.5	$0.326 \cdot 10^{-03}$
2.5	$0.515 \cdot 10^{-02}$	20.5	$0.394 \cdot 10^{-01}$	38.5	$0.330 \cdot 10^{-02}$	56.5	$0.298 \cdot 10^{-03}$
3.5	$0.944 \cdot 10^{-02}$	21.5	$0.363 \cdot 10^{-01}$	39.5	$0.267 \cdot 10^{-02}$	57.5	$0.266 \cdot 10^{-03}$
4.5	$0.149 \cdot 10^{-01}$	22.5	$0.329 \cdot 10^{-01}$	40.5	$0.214 \cdot 10^{-02}$	58.5	$0.238 \cdot 10^{-03}$
5.5	$0.209 \cdot 10^{-01}$	23.5	$0.297 \cdot 10^{-01}$	41.5	$0.168 \cdot 10^{-02}$	59.5	$0.215 \cdot 10^{-03}$
6.5	$0.268 \cdot 10^{-01}$	24.5	$0.266 \cdot 10^{-01}$	42.5	$0.131 \cdot 10^{-02}$	60.5	$0.193 \cdot 10^{-03}$
7.5	$0.322 \cdot 10^{-01}$	25.5	$0.239 \cdot 10^{-01}$	43.5	$0.103 \cdot 10^{-02}$	61.5	$0.168 \cdot 10^{-03}$
8.5	$0.368 \cdot 10^{-01}$	26.5	$0.215 \cdot 10^{-01}$	44.5	$0.817 \cdot 10^{-03}$	62.5	$0.142 \cdot 10^{-03}$
9.5	$0.405 \cdot 10^{-01}$	27.5	$0.194 \cdot 10^{-01}$	45.5	$0.653 \cdot 10^{-03}$	63.5	$0.118 \cdot 10^{-03}$
10.5	$0.434 \cdot 10^{-01}$	28.5	$0.173 \cdot 10^{-01}$	46.5	$0.535 \cdot 10^{-03}$	64.5	$0.954 \cdot 10^{-04}$
11.5	$0.456 \cdot 10^{-01}$	29.5	$0.153 \cdot 10^{-01}$	47.5	$0.465 \cdot 10^{-03}$	65.5	$0.747 \cdot 10^{-04}$
12.5	$0.472 \cdot 10^{-01}$	30.5	$0.133 \cdot 10^{-01}$	48.5	$0.433 \cdot 10^{-03}$	66.5	$0.557 \cdot 10^{-04}$
13.5	$0.483 \cdot 10^{-01}$	31.5	$0.115 \cdot 10^{-01}$	49.5	$0.419 \cdot 10^{-03}$	67.5	$0.398 \cdot 10^{-04}$
14.5	$0.488 \cdot 10^{-01}$	32.5	$0.987 \cdot 10^{-02}$	50.5	$0.405 \cdot 10^{-03}$	68.5	$0.281 \cdot 10^{-04}$
15.5	$0.487 \cdot 10^{-01}$	33.5	$0.842 \cdot 10^{-02}$	51.5	$0.386 \cdot 10^{-03}$	69.5	$0.193 \cdot 10^{-04}$
16.5	$0.479 \cdot 10^{-01}$	34.5	$0.712 \cdot 10^{-02}$	52.5	$0.368 \cdot 10^{-03}$	70.5	$0.118 \cdot 10^{-04}$
17.5	$0.466 \cdot 10^{-01}$	35.5	$0.594 \cdot 10^{-02}$	53.5	$0.356 \cdot 10^{-03}$	71.5	$0.486 \cdot 10^{-05}$

Table 16   Taylor altitude dependent velocity distribution

2.2.12.4   Flux Enhancement and Altitude Dependent Velocity Distribution

In Ref /9/ it is explained how the above velocity distribution may be adjusted to reflect its altitude dependence. The velocity correction which is used to increase the flux with decreasing

Project: ESABASE2/Debris Release 12.1		Date:	2024-02-19
Technical Description		Revision:	1.11
Reference: R077-231rep_01_11_Debris_Technical Description.docx		Status:	Final

FEV etamax GmbH   Page 106 / 173

distance from the Earth (or Moon) is used to adjust the velocity distribution which is then re-binned accordingly.

In case of a single velocity value the flux increase due to Earth/Moon gravity at a given distance r of the centre of the Earth/Moon is described by the factor G which is given by

$$G = 1 + \frac{v_{esc}^2}{v_\infty^2} \qquad \text{or} \qquad G = \frac{v^2}{v^2 - v_{esc}^2} \qquad ,$$

with

$$v^2 = v_{esc}^2 + v_\infty^2 \qquad .$$

Using the product μ of the constant of gravitation with Earth's (respective Moon's) mass, the escape velocity at distance r can be written as

$$v_{esc} = \sqrt{\frac{2\mu}{r}} \quad ,$$

and v_∞ is the velocity in free space, i.e. in the absence of Earth's gravity which is tabulated in Table 16, and v is the 'enhanced' meteoroid velocity at distance r.

To obtain the correct flux enhancement in case a velocity *distribution* is given we must realise that G is a function of v_∞. Thus the enhanced flux F_E is obtained from the Grün flux F_G by

$$F_E = \overline{G} \cdot F_G \qquad \text{with} \qquad \overline{G} = \int_0^\infty n(v_\infty) G(v_\infty) dv_\infty \qquad .$$

This assumes that the velocity distribution $n(v_\infty)$ has been normalised:

$$\int_0^\infty n(v_\infty) dv_\infty = 1$$

The above formulas contain the necessary information to calculate the altitude dependence of the velocity distribution, since we can write

$$\overline{G} = \int_0^\infty n(v_\infty) G(v_\infty) dv_\infty \quad \approx \quad \sum_{k=1}^N n_k G_k \quad = \quad \sum_{k=1}^N n_k' \quad ,$$

with $n_k = n(v_{\infty,k})$ and $n_k' = n(v_k)$ representing the tabulated values for the original distribution function and for the distribution function at distance r respectively.

Given the escape velocity at distance r, v_{esc} and the tabulated values of $n(v_\infty)$ in 1 km/s bins n_k, we calculate the values n_k' for the distribution n'(v) at distance r by

$$n_k' = G_k n_k$$

with

$$G_k = \frac{v_k^2}{v_k^2 - v_{esc}^2}$$

and

$$v_k = \sqrt{v_{esc}^2 + v_{\infty,k}^2} \ .$$

If we now tabulate the values of n'_k we need to change the bin limits by inserting the values of v at the places of the given values of v_∞ which is done by using again the formula

$$v = \sqrt{v_{esc}^2 + v_\infty^2} \ .$$

As a result the bin widths will now no longer be equidistant in v, which is the independent variable of the new distribution function $n'(v)$, so re-binning will be necessary by interpolating the values of $n'(v)$. This completes the calculation procedure of the new table for the velocity distribution $n'(v)$ at the given distance r.

2.2.13 Particle Densities and Flux-mass Functions

2.2.13.1 Particle Densities

There is little knowledge on the densities of meteorite particles, and today's estimate has not improved over the model assumed in the existing ESABASE (Ref. /1/), which is either a user defined constant with a default density of $\rho = 2.5$ g/cm^3, or it is calculated by the following decreasing and discontinuous function of the meteoroid mass m:

$$\rho\,(m) \ = \ 2.0 \text{ g/cm}^3 \qquad \text{for} \qquad m \ < 10^{-6} \text{ g}$$

$$\rho\,(m) \ = \ 1.0 \text{ g/cm}^3 \qquad \text{for} \qquad 10^{-6} \text{ g} \ \leq m \ \leq 10^{-2} \text{ g}$$

$$\rho\,(m) \ = \ 0.5 \text{ g/cm}^3 \qquad \text{for} \qquad m \ > 10^{-2} \text{ g}$$

2.2.13.2 Flux-size to Flux-mass Function

In some cases it will be necessary to convert a flux which is given by its $F(d)$ function to the $F(m)$ function or vice versa. With the meteoroid mass density ρ and its particle diameter d and an assumed spherical shape the relation

$$m = 1/6 \ \rho \ \pi \ d^3$$

is used.

2.2.14 Shielding and Gravitational Effects

A description of the consideration of gravitational focussing and Planet shielding effects of the omni-directional meteoroid models is given in the following subsections.

Within the Divine-Staubach model these effects are treated as given in /20/ or /22/. The corresponding equations are given in section 2.2.3.1.

Project: ESABASE2/Debris Release 12.1		Date:	2024-02-19
Technical Description		Revision:	1.11
Reference: R077-231rep_01_11_Debris_Technical Description.docx		Status:	Final

FEV etamax GmbH   Page 108 / 173

2.2.14.1 Gravitational Focusing

With the exception of the streams contributions of Jenniskens, which are derived from measurements at the meteoroids entry into the Earth's atmosphere, the fluxes are given in the models at a distance of 1 AU from the Sun at the Earth's position but in absence of the Earth. Thus the change of the particle trajectories due to Earth/Moon attraction needs to be taken into account. This will change the flux by a flux increase factor which is denoted by $G_e(h)$ and is a function of the target altitude h above the Earth/Moon surface.

When the Grün sporadic flux model is used, the flux is corrected by the factor

$$G_e(h) = 1 + \frac{R_e + 100}{R_e + h} \quad ,$$

which is given in Ref. /3/. $R_e + 100 = 6478$ km, which is the Earth radius augmented by 100 km atmosphere height. In the case of a lunar orbit $R_e + 0 = 1738$ km, which is Moon's radius without any atmospheric augmentation.

If the altitude dependent velocity distribution of section 2.2.12.3 is used, the gravitational flux increase must be calculated as described in 2.2.12.4 .

2.2.14.2 Planet Shielding

Earth/Moon shielding is accounted for by excluding all arrival directions which are within an angle θ subtended with the direction of the Earth's (respective Moon's) centre, the 'Planet-shielding cone'. By subtracting the corresponding solid angle element from the unit sphere the shielding factor η

$$\eta = \frac{1 + \cos\theta}{2}$$

is obtained for the case of a *randomly tumbling* plate. The angle θ is then geometrically given by

$$\sin\theta = \frac{R_e + 100}{R_e + h}$$

where R_e is the mean Earth/Moon radius in km and h is the target orbiter altitude in km. The atmosphere height is accounted for by the constant 100 km for Earth orbits and 0 km for lunar orbits.

Taking into account that all the meteoroid orbits which have velocities higher than the escape velocity at the Earth's atmosphere will be 'seen' at the top of the atmosphere, the determination of the angle θ needs to be made in a more precise way, by using the formula

$$v = \sqrt{v_{esc}^2 + v_\infty^2}$$

which was mentioned in section 2.2.12.4. This yields a modified expression for the angle θ

$$\sin\theta = \frac{(R_e + 100)\sqrt{v_\infty^2 + v_{esc}^2(R_e + 100)}}{(R_e + h)\sqrt{v_\infty^2 + v_{esc}^2(R_e + h)}}$$

which gives 5% to 10% better results. If a velocity distribution is used, the mean value

$$\overline{\theta} = \int_0^\infty n(v_\infty)\theta(v_\infty)dv_\infty$$

needs to be calculated by integrating over the normalised velocity distribution $n(v_\infty)$.

For an oriented plate the above relation between η and θ is no longer correct. The collision probability is then strongly dependent on the angle between the normal to the plate and the Earth direction. This problem can be geometrically formulated, but unfortunately the solution becomes unwieldy in the general case and contains an elliptical integral at one place. For the strict application of the ray tracing technique this is however not a problem, because only the angle θ (and in some cases possibly $\overline{\theta}$) will be used to determine if a ray must be fired or not in a certain direction.

2.2.15   Ray Tracing and k-Factor

As it has been discussed in the previous sections, most of the particle fluxes which are calculated with the presented models are quantified with respect to a "randomly tumbling plate" or even a "virtual randomly tumbling plate which is stationary with respect to the Earth's surface".

The analysis of the debris / micrometeoroid environment hazard acting upon a spacecraft requires the computation of particle fluxes on oriented surfaces. The method chosen for this uses a ray tracing technique, which enables to account for the mutual shading between different surfaces of the orbiting structure.

The relative relation between the flux on a virtual randomly tumbling plate which is stationary with respect to the Earth surface above Earth, the flux on a randomly tumbling plate in orbit and the flux on an oriented plate in orbit has been discussed in several papers in the past.

In the review phase of the study, the topic was thoroughly investigated, also with respect to the implementation of the ray tracing technique for the analysis in the enhanced ESABASE/Debris tool. The analytical assessment was backed up by numerical analysis using ray tracing. This work is documented in Annex C of (Ref. /15/).

The main finding in Ref. /15/, Annex C is that a properly implemented ray tracing fully renders the true situation, without the necessity to include an additional k factor. This result also encourages the use of ray tracing to account for the Earth shielding, as it has been lined out in paragraph 2.2.7.2.

An abstract of the investigation documented in (Ref. /15/) is included in Annex A.

Project: ESABASE2/Debris Release 12.1		Date:	2024-02-19
Technical Description		Revision:	1.11
Reference: R077-231rep_01_11_Debris_Technical Description.docx		Status:	Final

FEV etamax GmbH   Page 110 / 173

3 The Damage Equations

This chapter describes the equations used for the modelling of the interaction between micro-particles and satellite structures. The satellite structure can be either a single wall (e.g. aluminium) or a multiple wall, typically in the case when a specific micro-particle shielding or thermal protection (MLI) is applied to the basic structure.

Due to the increasing concern of the risk posed by the micro-particle environment of long term missions (above all the international space station), special micro-particle shields have been developed.

The particle / wall interaction models - in this document referred to as damage equations - describe the phenomena of high and hyper velocity impacts on structures. The typical impact velocity for space debris is 8 to 10 km/s, for meteoroids about 20 km/s. The equations are largely derived from experiments.

The damage equations are treated in two separate groups:

- The *ballistic limit equations*, which yield the critical impacting particle size above which the structure fails. Different equations are used for single and multiple wall structures.
- The *damage size equations*, which yield the crater size of semi-infinite targets and the hole diameter of punctured targets (generally thin walls).

In this chapter, the 5 classes of damage equations which are implemented in the ESABASE2/ DEBRIS analysis tool are described:

- *The single wall ballistic limit equation*
- *The multiple wall ballistic limit equation*
- *The crater size equation*
- *The generic clear hole equation*
- *The advanced hole equation*

ESABASE2/Debris further offers the option to integrate a user defined subroutine for the damage equation. This requires a FORTRAN 77 compiler and linker and is only advised for the advanced user and hyper velocity impact expert. For details, refer to (Ref. /14/).

3.1 The Parametric Formulation of the Damage Equations

To provide the necessary flexibility in the usage of currently available and possible future damage equation formulations, the 5 classes of damage equations have been formulated in a parametric form, allowing the user to adapt the equation to his needs.

It must be clearly stated however, that parameter variations of the damage equations should only be performed by the experienced user and hypervelocity impact specialist. For the beginner, the standard equations, activated by key words in the software, are recommended, see (Ref. /14/).

Project: ESABASE2/Debris Release 12.1	Date:	2024-02-19
Technical Description	Revision:	1.11
Reference: R077-231rep_01_11_Debris_Technical Description.docx	Status:	Final

FEV etamax GmbH Page 111 / 173

The parameters of the standard equations of each class are tabled in the respective sub chapters.

In the software, the ballistic limit equations are used to compute the critical particle diameter, and the damage size equations to compute the crater or hole diameter. The damage equations are presented in these formulations in the following sub-sections.

In the equations, the following general symbols are used:

Symbol	Unit	Description
t_t, t_B, t_s	[cm]	Thickness of Target, Back-up wall, Shield
K	[-]	Characteristic Factor
d_p	[cm]	Particle (impactor) Diameter
ρ_t, ρ_p, ρ_s, ρ_B	[g/cm³]	Density of Target, Particle, Shield, Back-up wall
v	[km/s]	Impact velocity
α	[--]	Impact angle
S	[cm]	Spacing between shielding and back-up wall
D	[cm]	Crater or Hole diameter
F_{mx}	[cm]	Ballistic Limit

3.2 The Single Wall Ballistic Limit Equation

The parametric formulation of the equation is

$$d_{p,\lim} = \left[\frac{t_t}{K_f \cdot K_1 \cdot \rho_p^{\beta} \cdot v^{\gamma} \cdot (\cos\alpha)^{\xi} \cdot \rho_t^{\kappa}} \right]^{\frac{1}{\lambda}}$$

The K_f factor allows specifying what type of damage is considered a failure for the ESABASE2 thick plate equation and the glass target equations. In the other equations it is not used. The K_1 factor includes other parameters particular to each of equation (e.g. target yield strength σ_t).

It is also often found in the following form:

$$F_{mx} = K_o \cdot K_{mat} \cdot d_p^{\lambda} \cdot \rho_p^{\beta} \cdot v^{\gamma} \cdot (\cos\alpha)^{\xi} \cdot \rho_t^{\kappa}$$

The K_{mat} factor is material dependent. Compared to the first formulation, $K_0 \cdot K_{mat} = K_1$. In the second formulation, the failure specification does not appear explicitly.

Project: ESABASE2/Debris Release 12.1		Date:	2024-02-19
Technical Description		Revision:	1.11
Reference: R077-231rep_01_11_Debris_Technical Description.docx		Status:	Final

FEV etamax GmbH   Page 112 / 173

The values of the parameters for standard equations are given below. For this group of equations, the yield strength σ_t of the target material is to be input in ksi.

Equation	K_f [1)	K_1 2)	λ	β	γ	ξ	κ
ESABASE Thick Plate	1.8 ÷ 3	0.2 ÷ 0.33	1.056	0.519	2/3	2/3	0
ESABASE Thin Plate	1.0	0.26 ÷ 0.64	1.056	0.519	0.875	0.875	0
MLI 3)	1.0	0.37	1.056	0.519	0.875	0.875	0
Pailer-Grün	1.0	0.77	1.212	0.737	0.875	0.875	-0.5
McDonnell & Sullivan	1.0	$0.756\left[\dfrac{\sigma_{Al}}{\sigma_t}\right]^{0.134}$	1.056	0.476	0.806	0.806	-0.476
Gardner	1.0	$0.608\sigma_t^{-0.093}$	1.059	0.686	0.976	0.976	-0.343
Gardner, McDonnell, Collier	1.0	$0.85\sigma_t^{-0.153}$	1.056	0.763	0.763	0.763	-0.382
Frost	1.0	0.43	1.056	0.519	0.875	0.875	0
Naumann, Jex, Johnson	1.0	0.65	1.056	0.5	0.875	0.875	-0.5
Naumann	1.0	0.326	1.056	0.499	2/3	2/3	0
McHugh & Richardson Thick glass target	1.85 ÷ 7	0.64	1.2	0.5	2/3	2/3	0
Cour-Palais Thick glass target	1.85 ÷ 7	0.53	1.06	0.5	2/3	2/3	0

Table 17   Single wall ballistic limit equation typical parameter values. In this table, all yield strengths are assumed to be given in ksi.

Notes

1)   Failure factors K_f:

-    ESABASE Thick Plate: $K_f \geq 3$ Crater generation without spall

$2.2 \leq K_f < 3$ Spallation of the plate

$1.8 \leq K_f < 2.2$ Spall breaks away

$K_f < 1.8$ Perforation of the plate

- Thick Glass Targets: $K_f \geq 7$ — Crater generation without spall

$1.85 \leq K_f < 7$ — Spallation of the plate

$K_f < 1.85$ — Perforation of the plate

2) K_1 factors:

- ESABASE Thick Plate: Aluminium alloys: $K_1 = 0.33$

Stainless steel: $K_1 = 0.2$

- ESABASE Thin Plate: Aluminium alloys: $K_1 = 0.43 - 0.454$

Stainless steel: $K_1 = 0.255$ — AISI 304, AISI 306

$K_1 = 0.302$ — 17-4 PH annealed

Magnesium lithium: $K_1 = 0.637$

Columbium alloys: $K_1 = 0.271$

- McDonnell & Sullivan: Reference σ_t-values are given in Table 18

- Gardner: σ_t shall be input in Pa for this equation

3) The single wall ballistic limit equation for MLI assesses the failure of the thermal blanket, and was derived by tests and hydro-code simulations using the ESABASE thin plate equation as starting point, see ref. /2/. The equation is expressed as

$$F_{mx} = 0.37 \cdot d_p^{1.056} \cdot \rho_p^{0.519} \cdot (v \cdot \cos\alpha)^{0.875}$$

Some reference values for the 0.2 yield strength σ is given below (used in the McDonnell & Sullivan and Gardner equations):

Material	[ksi] [1]	[MPa]
Aluminium pure	10	70
Aluminium alloys (superior)	30 - 65	200 - 450
Silver	22	150
Gold	17.5	120
Beryllium copper	120	830
Copper	32	220
Stainless steel	110	760
Titanium	140	980

Table 18   Some values of yield strength

Note: [1]   ksi = kilo.lb/sq.-inch = 1000 lb / inch^2 = 6.895 MPa

3.3 The Multiple Wall Ballistic Limit Equation

The parametric form of this equation is

$$d_{p,\lim} = \left[\frac{t_B + K_2 \cdot t_s^{\mu} \cdot \rho_s^{\upsilon_2}}{K_1 \cdot \rho_p^{\beta} \cdot v^{\gamma} \cdot (\cos\alpha)^{\xi} \cdot \rho_B^{\kappa} \cdot S^{\delta} \cdot \rho_s^{\upsilon_1}} \right]^{\frac{1}{\lambda}}$$

It is also often formulated as:

$$F_{mx} = K_1 \cdot d_p^{\lambda} \cdot \rho_p^{\beta} \cdot v^{\gamma} \cdot [\cos\alpha]^{\xi} \cdot \rho_B^{\kappa} \cdot S^{\delta} \cdot \rho_s^{\upsilon_1} - K_2 \cdot t_s^{\mu} \cdot \rho_s^{\upsilon_2}$$

Three velocity regions are defined, delimited by the two limit velocities $v_{\lim1}$ and $v_{\lim2}$. The governing parameters mostly have different values for velocities below $v_{\lim1}$ and above $v_{\lim2}$. For velocities between $v_{\lim1}$ and $v_{\lim2}$, a linear interpolation is performed.

The limit velocities may vary with the impact angle:

$$v_{\lim 1} = v_{\lim 1,0} \cdot (\cos\alpha)^{\varphi_1}$$

$$v_{\lim 2} = v_{\lim 2,0} \cdot (\cos\alpha)^{\varphi_2}$$
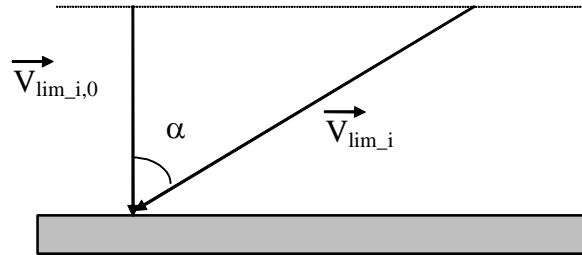
Where the normal velocity component is used (which is generally the case), i.e. $\gamma = \xi$, the cosine exponent in the equations above is $\varphi_1 = \varphi_2 = -1$.

The values of the parameters for typical multiple wall equations are given in Table 17 and Table 20 below (here the limit velocities are defined as function of the impact angle).

For the Cour-Palais, MLI and Maiden-McMillan equations, only one velocity domain is used.

Equation	K_1	K_2	λ	β	γ	κ	δ	ξ	ν_1/ν_2	μ
Cour-Palais	$0.044\left[\sigma_{y,ref}/\sigma_{y,t}\right]^{0.5}$	0	1	0.5	1	0.167	-0.5	1	0 / 0	0
MLI [3]	$0.034\left[\sigma_{y,ref}/\sigma_{y,t}\right]^{0.5}$	0	1	0.5	1	0.167	-0.5	1	0 / 0	0
Maiden-McMillan [1]	$K_f \bullet \dfrac{\pi}{6}\left[\sigma_{y,ref}/\sigma_{y,t}\right]^{0.5}$	0	3	1	1	0	-2	1	0 / 0	0
ESA [2] $v < 3$	$0.255 \div 0.637$	1	1.056	0.519	0.875	0	0	0.875	0 / 0	1
$v > 9.5$	$\dfrac{\pi}{6}\left[\sigma_{y,ref}/\sigma_{y,t}\right]^{0.5}$	0	3	1	1	0	0	1	0 / 0	0

Table 19   Standard Double wall ballistic limit equation parameter values

Notes

[1]   *Failure factors* K_f for the Maiden-McMillan equation:

$K_f \geq 41.5$ No damage

$8.2 \leq K_f < 41.5$ Incipient yield zone

$7.1 \leq K_f < 8.2$ Fracture zone

$K_f < 7.1$ Penetration zone

The K_f factor flows into the K_1 factor, see Table 19.

[2]   *ESA Equation*:

Project: ESABASE2/Debris Release 12.1		Date:	2024-02-19
Technical Description		Revision:	1.11
Reference: R077-231rep_01_11_Debris_Technical Description.docx		Status:	Final

FEV etamax GmbH   Page 116 / 173

- The Boeing-ESA equation described in chapters 1 and 2 has the same form as the ESA equation, but with $v_{lim1} = 1.4$ km/s and $v_{lim2} = 7.83$ km/s.
- The reference yield strength $\sigma_{y,ref} = 70'000$ lb/in^2 = 482.8 MPa.

3)   *MLI Equation*

The multiple wall ballistic limit equation for MLI assesses the debris / meteoroid protection of the thermal blanket, and was derived by tests and hydro-code simulations using the Cour-Palais equation as starting point, see ref. /2/.

The equation is expressed as $F_{mx} = 0.034 \cdot \left(\frac{70000}{\sigma_w}\right)^{0.5} \cdot \rho_p^{0.5} \cdot \rho_w^{0.167} \cdot d_p \cdot (v \cdot \cos\alpha) \cdot S^{-0.5}$ with σ_w in lb/in^2.

Equation		K_1	K_2	λ	β	γ	κ	δ	ξ	ν_1/ν_2	μ
ESA	$v < 3$ km/s	$0.312(\tau_1^*/\tau)^{0.5}$	$1.667 \bullet K_1$	1.056	0.5	2/3	0	0	5/3	0/0	1
Triple	$v > 7$ km/s	$0.107(\tau_2^*/\tau)^{0.5}$	0	1.5	0.5	1	0	-0.5	1	0.167/0	0
NASA	$v < 3$ km/s	$0.6\,(\sigma_w/40)^{-0.5}$	$(\sigma_w^*/40)^{-0.5}$	1.056	0.5	2/3	0	0	5/3	0/0	1
ISS	$v > 7$ km/s	$[3.918(\sigma_w/70)^{1/3}]^{-1.5}$	0	1.5	0.5	1	0	-0.5	1	0.167/0	0
NASA	$v < 3$ km/s	$0.3\,(\tau_1^*/\tau)^{0.5}$	$1.233 \bullet K_1$	1.056	0.5	2/3	0	0	5/3	0/1	1
Shock	$v > 6$ km/s	$22.545(\tau_1^*/\tau)^{0.5}$	0	3	1	1	-1	-2	1	0/0	0
NASA	$v < 3$ km/s	$0.4(\tau_1^*/\tau)^{0.5}$	$0.925 \bullet K_1$	1.056	0.5	2/3	0	0	5/3	0/1	1
Bumper	$v > 6$ km/s	$18.224(\tau_1^*/\tau)^{0.5}$	0	3	1	1	-1	-2	1	0/0	0

Table 20   Standard Multiple wall ballistic limit equation parameter values

Notes: τ_1^*, τ_2^* are the yield stresses of a reference material (higher quality aluminium)

$\tau_1^* = 40'000$ lb/in^2 = 276E6 Pa.

$\tau_2^* = 70'000$ lb/in^2 = 483E6 Pa.

$\sigma_w = 47$ ksi for the reference equation used for system tests. σ_w to be input in ksi

3.4 The Crater Size Equation

The parametric form of the equation is:

$$D = K_1 \cdot K_c \cdot d_p^{\lambda} \cdot \rho_p^{\beta} \cdot v^{\gamma} \cdot (\cos\alpha)^{\xi} \cdot \rho_t^{\kappa}$$

It is basically the same as that of the single wall ballistic limit equation, see section 3.2.

Project: ESABASE2/Debris Release 12.1		Date:	2024-02-19
Technical Description		Revision:	1.11
Reference: R077-231rep_01_11_Debris_Technical Description.docx		Status:	Final

The crater factor K_c is the ratio of the crater radius D/2 to the crater depth p, see sketch.

Strictly speaking, the crater size equation is only valid when no failure occurs.

For ductile targets, the crater is more or less spherical, and $K_c \approx 1$.

For brittle targets, an interior crater with diameter D_h may form, the outer crater (with diameter D_c) being much larger. For brittle targets, K_c may be as high as 10.
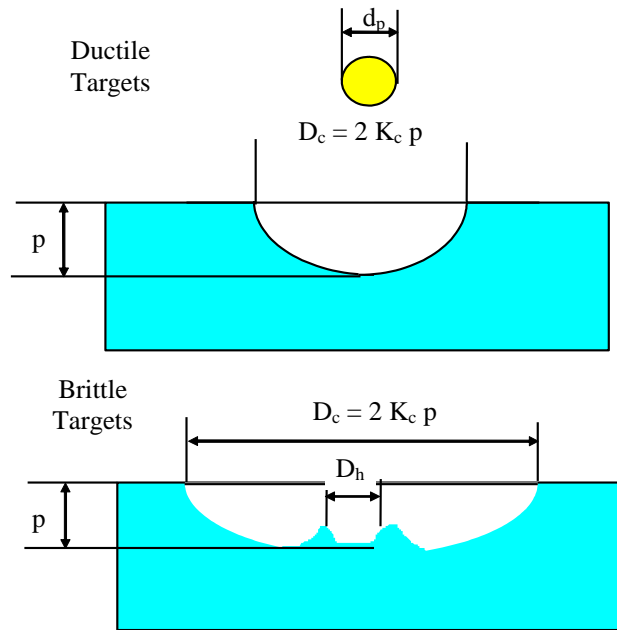
The crater size equation assumes a semi-infinite target and should only be used for cases where the wall thickness is much larger than the particle diameter.

The values of the parameters for typical equations are given in Table 21.

Equation	K_c	K_1	λ	β	γ	ξ	κ
Ductile targets							
ESABASE Thick Plate [1]	2	$0.4 \div 0.66$	1.056	0.519	2/3	2/3	0
Shanbing et al	n/d [2]	$0.54\left(\sigma_{y,t}\right)^{-\frac{1}{3}}$	1	2/3	2/3	2/3	-1/3
Sorensen	n/d [2]	0.622 $\left(\tau_t\right)^{-0.282}$	1	0.167	0.564	0.564	0.115
Christiansen for $\dfrac{\rho_p}{\rho_t} < 1.5$	n/d [2]	$10.5\ H_t^{-\frac{1}{4}} \cdot c_s^{\frac{2}{3}}$	1.056	0.5	2/3	2/3	-0.5
Christiansen for $\dfrac{\rho_p}{\rho_t} > 1.5$	n/d [2]	$10.5\ H_t^{-\frac{1}{4}} \cdot c_s^{\frac{2}{3}}$	1.056	2/3	2/3	2/3	-2/3
Brittle targets							
Gault	n/d [2]	1.08	1.071	0.524	0.714	0.714	-0.5

Project: ESABASE2/Debris Release 12.1		Date:	2024-02-19
Technical Description		Revision:	1.11
Reference: R077-231rep_01_11_Debris_Technical Description.docx		Status:	Final

FEV etamax GmbH   Page 118 / 173

Equation	K_c	K_1	λ	β	γ	ξ	κ
Fechtig	n/d [2]	6.0	1.13	0.71	0.755	0.755	-0.5
McHugh & Richardson	n/d [2]	1.28	1.2	0	2/3	2/3	0.5
Cour-Palais	n/d [2]	1.06	1.06	0.5	2/3	2/3	0

Table 21   Standard Crater size equation parameter values

Notes

[1] K_1 factors:

- ESABASE Thick Plate: Aluminium alloys: $K_1 = 0.66$

  Stainless steel: $K_1 = 0.4$

[2]   "n/d" means not defined in the equation reference.

The software uses a default value of 1 for ductile targets and 10 for brittle targets.

[3]   Christiansen equations

- Ht is the target Brinell hardness. A typical value is 90.

- c_s is the velocity of sound in the target material. For steel, $c_s = 5.85$ km/s.

3.5 The Generic Clear Hole Equation

The parametric form of the equation is:

$$D = \left\{ K_0 \cdot \left(\frac{t_s}{d_p} \right)^{\lambda} \cdot \rho_p^{\beta} \cdot v^{\gamma} \cdot (\cos\alpha)^{\xi} \cdot \rho_s^{\nu} + A \right\} \cdot d_p$$

The clear hole equation is only valid for a full perforation, i.e. mainly for thin foils (typically bumper shields or similar).

The limit of validity is given by the relation $\frac{t_s}{d_p} < 10$

The values of the parameters for the common standard equations are given in Table 22 below:

Equation	K_0	λ	β	γ	ξ	ν	A
Maiden	0.88	2/3	0	1	1	0	+0.9
Nysmith-Denardo	0.88	0.45	0.5	0.5	0.5	0	0
Sawle	0.209	2/3	0.2	0.2	0.2	-0.2	+1

Project: ESABASE2/Debris Release 12.1		Date:	2024-02-19
Technical Description		Revision:	1.11
Reference: R077-231rep_01_11_Debris_Technical Description.docx		Status:	Final

FEV etamax GmbH   Page 119 / 173

Equation	K_0	λ	β	γ	ξ	ν	A
Fechtig	5.24E-5	0	1/3	2/3	2/3	0	0

Table 22   Standard Classical hole size equation parameter values

3.6 The Advanced Hole Equation

The advanced form of the hole size equation is based on the equations derived at UniSpace Kent by Dr. Gardner, Prof. McDonnell and Dr. Collier.

The equation is derived for the computation of the particle size from the impact velocity and the hole size on the back side of the target shield.

The equation is only valid for ductile targets. Dimensionless hole and particle diameters are used:

$$d'_p = \frac{d_p}{t_s}$$

$$D'_h = \frac{D_h}{t_s}$$

d_p is the particle diameter, D_h is the perforated hole diameter, t_s is the target thickness.
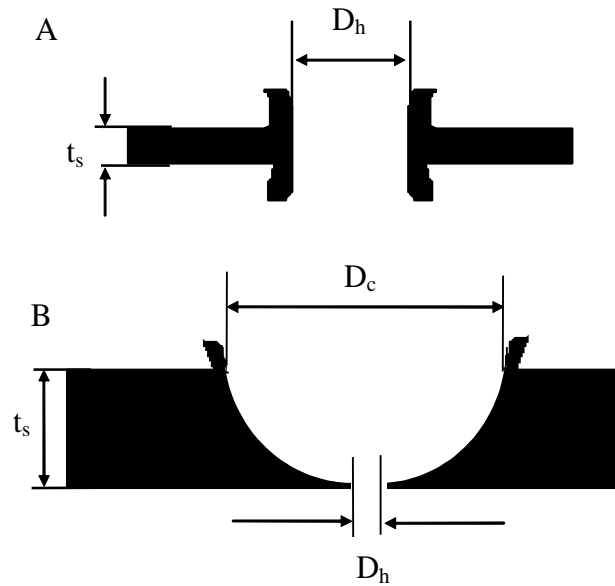
The general form of the equation is

$$d'_p = A \cdot \left(\frac{10}{9 + \exp\left[D'_h / B \right]} \right) + D'_h \left(1 - \exp\left[-D'_h / B \right] \right)$$

$$A = \frac{d_p}{F_{mx}} = 6.97 \cdot \left(\frac{V_n \cdot \rho_p}{\sqrt{\sigma_s \cdot \rho_s}} \right)^{-0.723} \cdot \left(\frac{\sigma_s}{\sigma_{Al}} \right)^{-0.217} \cdot t_s^{-0.053}$$

F_{mx} is the ballistic limit, $V_n = V \cdot \cos\alpha$ the normal impact velocity, ρ_p the particle density, t_s, ρ_s and σ_s the target thickness, density and yield stress. σ_{Al} is the yield stress of Aluminium.

In the above equation, all units are uniform (e.g. SI), except for t_s which is in μm.

Project: ESABASE2/Debris Release 12.1		Date:	2024-02-19
Technical Description		Revision:	1.11
Reference: R077-231rep_01_11_Debris_Technical_Description.docx		Status:	Final

FEV etamax GmbH   Page 120 / 173

An alternative form of the equation of A is:

$$A = 2.35 \cdot \left(\frac{V_n \cdot \rho_p}{\sqrt{\rho_s}} \right)^{-0.723} \cdot \sigma_s^{0.145} \cdot t_s^{-0.053}$$

with V_n in km/s, ρ in kg/m³, σ in Pa and in μm

Using the standard units of ESABASE/Debris, i.e. km/s for velocity, cm for thickness, g/cm³ for densities and MPa for stresses, the constant of the second equation for A above becomes 0.88 (in the place of 2.35).

$$B = B_1 + B_2 \bullet V_n = B_1 + B_2 \bullet V \bullet \cos \alpha$$

B_1 and B_2 are taken from Table 23.

The equation for A can be used as a ballistic limit equation.

For the computation of the hole size in the target or shield, the basic equation cannot be used directly, since it is a function of $d_p(D_h)$. The form of this equation does not allow an analytical inversion. Thus a numerical scheme must be used (e.g. Newton method).

For the starting value of D_h, the Carey, McDonnell, Dixon equation is used:

$$\frac{D_h}{d_p} = 1 + 2.9 \left(\frac{\rho_s}{\rho_p} \right)^{0.6} \cdot \left(\frac{t_s}{d_p} \right) \cdot V_n \left[\frac{1}{1 + 2.9 \left(\frac{\rho_s}{\rho_p} \right)^{0.6} \cdot \left(\frac{t_s}{d_p} \right)^2 \cdot V_n^{-m}} \right]$$

$V_n = V \bullet \cos \alpha$

For $2 < V_n < 20$ km/s: $1.02 - 4 \cdot \exp(-0.9 V_n^{0.9}) - 0.003(20 - V_n)$

For $V_n \geq 20$ km/s: $m = 1.02$

The equations for the parameters A and B can be parametrised as follows:

$$A = K_1 \cdot V^{\gamma} \cdot (\cos \alpha)^{\xi} \cdot \rho_p^{\beta} \cdot \rho_s^{\nu} \cdot t_s^{\lambda}$$

$$B = B_1 + B_2 \cdot V \cdot (\cos \alpha)^{u}$$

$$K_1 = 0.88 \cdot \sigma_s^{0.145}, \gamma = -0.723, \xi = -0.723, \beta = -0.723, \nu = 0.362, \lambda = -0.053$$

B_1 and B_2 are to be taken from Table 23, $u = 1 + (\xi - \gamma)$.

Project: ESABASE2/Debris Release 12.1		Date:	2024-02-19
Technical Description		Revision:	1.11
Reference: R077-231rep_01_11_Debris_Technical Description.docx		Status:	Final

FEV etamax GmbH   Page 121 / 173

For more flexibility, one could also use the formulation $V_n = V \cdot (\cos \alpha)^u$ in the Carey, McDonnell, Dixon equation.

Material		Velocity V_n (km/s)	Density ρ_s (kg/m³)	Yield stress σ_s (MPa)	B_1 (-)	B_2 (s/km)
Al	Aluminium	1.2 - 6.0	2780	69	-0.004	1.85
Al	Aluminium	6.0 - 10.7	2780	69	6.66	0.74
Ag	Silver	2.9 - 5.6	10500	150	7.92	3.14
Au	Gold	2.1 - 7.5	19300	120	6.65	2.77
BeCu	Beryllium Copper	3.7 - 6.4	8240	828	-26.3	10.3
Cu	Copper	2.0 - 6.9	8950	220	3.2	2.62
SS	Stainless Steel	2.2 - 3.7	7840	759	0.11	2.34
Ti	Titanium	2.3 - 6.6	4720	986	0.618	2.26

Table 23   Typical values of B_1 and B_2

Note: The experimental data has shown a rather important scatter for the samples of material other than aluminium. For velocity regions outside the given ranges, the 0.74 figure for aluminium may also be used. Of the Al parameter sets, only the one in the lower velocity regime is implemented in the software. For the higher velocity regime, the user specified input option has to be used.

Project: ESABASE2/Debris Release 12.1		Date:	2024-02-19
Technical Description		Revision:	1.11
Reference: R077-231rep_01_11_Debris_Technical Description.docx		Status:	Final

FEV etamax GmbH   Page 122 / 173

4   The Secondary Ejecta Model

This chapter describes the secondary ejecta module which has been implemented in the ESABASE2/ DEBRIS analysis tool. This model permits to evaluate the effect of ejecta produced by primary impacts (from space debris or meteoroids) on surrounding faces of the analysed structure.

4.1 Ejecta Phenomenon

4.1.1 Normal Impacts

Material ejection under hypervelocity impact is divided in three processes corresponding to different physical and mechanical phenomena: jetting phase, debris cone formation and spallation.

In general, no spalls are observed on ductile targets.

The jetting phase:

During the first times of projectile penetrating into the target, both target and projectile undergo partial or complete melting and vaporisation. A certain amount of material is ejected from the impact interface. The physical state of the ejected material is mainly liquid and the ejection angle is approximately 20° measured from the target surface. The ratio of jetted mass to total ejected mass is very small, less than 1%.

The debris cone:

Later in the crater formation, the target material is finely commuted in fine solid fragments by compression or tensile failure, these fragments are ejected in a thin debris cone. The physical state of the ejected material is mainly solid. The ejection angle is between 60° and 80° measured from the target surface and depends on target characteristics. The ratio of ejected mass to total ejected mass is estimated between 50% and 70%. The ejection velocity from a few m/s to a few km/s is inversely proportional to fragment size. The minimum size depends mainly on target characteristics and should be sub-micron sized. The maximum size can be evaluated by empirical relations. The size distribution is inversely proportional to the square of the fragment size.

The spallation phase:

In general, no spallation is observed on ductile targets.

Near the free surface, rarefaction waves produce tensile stress. In brittle material, tensile failure leads to the formation of spall fragments that are ejected. The physical state of the ejected material is mainly solid. The ejection direction is normal to the surface. The ejection velocity is less than 1 km/s and is 10 to 100 times less than impact velocity. The fragment size is large, about 10 times the size of debris cone fragments. These fragments have plate shape

Project: ESABASE2/Debris Release 12.1	Date:	2024-02-19
Technical Description	Revision:	1.11
Reference: R077-231rep_01_11_Debris_Technical Description.docx	Status:	Final

whose dimensions are difficult to evaluate because large plate fragments are likely to fragment themselves into smaller particles. The ratio of spalled mass total mass is estimated between 30% and 50%.
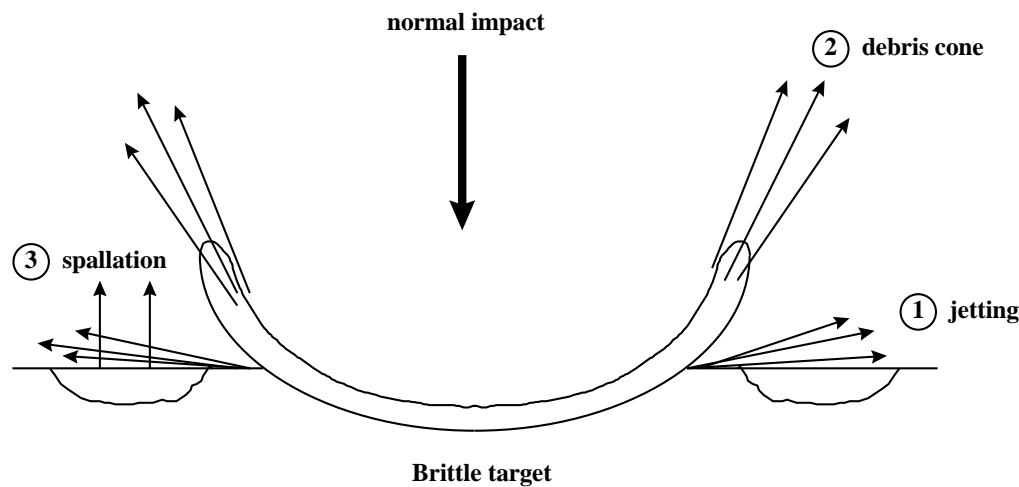
Figure 4-1   Schematic summary of ejection processes under normal impact.

4.1.2 Oblique Impacts

Oblique impacts with impact angles > 60° (measured from the target surface normal) are considered separately.
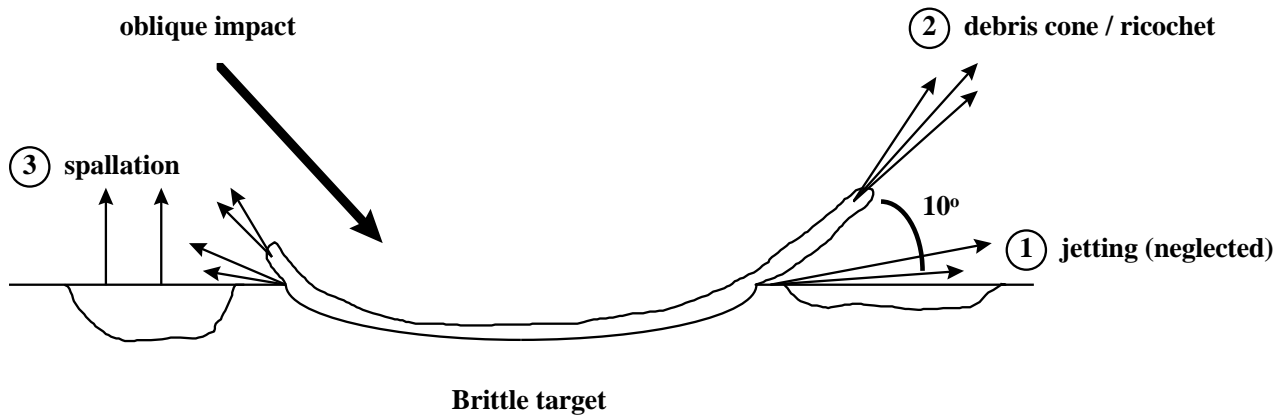
Figure 4-2   Schematic summary of ejection processes under oblique impact.

The phenomena involved in ejecta formation are similar to those observed for normal impacts: jetting phase, debris cone formation and spallation phase.

The main differences are:

- the total ejected mass decreases with decreasing impact angle,

Project: ESABASE2/Debris Release 12.1	Date:	2024-02-19
Technical Description	Revision:	1.11
Reference: R077-231rep_01_11_Debris_Technical Description.docx	Status:	Final

- the debris cone central axis remains vertical but the cone is flattened. The debris cone ejection angle decreases with decreasing incidence angle,

- the problem is not any more axisymmetric as the obliquity of impact favours the azimuth direction downstream the incidence angle.

4.2 Enhanced Ejecta Model

4.2.1 General Description

The ejecta model distinguishes between ductile and brittle targets. Calculations are made in the satellite frame. Therefore, the target is considered as immobile and the impact velocity is the relative velocity between the projectile and the target surface.

The **model inputs** are then:

- target characteristics: ductile or brittle, density (ρ_t) ;

- projectile characteristics: mass (m_i), density (ρ_i) ;

- impact characteristics: relative impact velocity vector determined by the scalar velocity (v) and the impact direction (φ_i, Θ_i).

A description of the model input is given in section 4.2.2.2.

The **model outputs** consist of an analytical function providing the number $n(\varphi,\theta,\delta,v)$ of fragments of size (δ) ejected at velocity (v) in the spatial direction (φ, θ), by solid angle unity. It is basically assumed that $n(\varphi,\theta,\delta,v)$ is the sum of independent terms corresponding to the different ejection processes:

- $n_{cone}(\varphi,\theta,\delta,v)$ + $n_{spalls}(\varphi,\theta,\delta,v)$ for brittle targets ;

- $n_{cone}(\varphi,\theta,\delta,v)$ only for ductile targets.

The *jetting phenomenon is neglected* since the proportion of material involved is less than 1% of the total ejected mass.

The model (Ref. /16/) provides a continuous ejecta distribution in the geometrical space around the impact and has thus to be adapted for an implementation into ESABASE/Debris. The recent upgrade of the ejecta model as described in the following sections considers the conservation of the momentum and the energy of the impacting particle and the ejected particles, as well as the latest upgrade of the mathematical theory (Ref. /24/).

4.2.2 Software Model

The introduction of an ejecta model into ESABASE2/Debris allows assessing the influence of secondary impacts in terms of flux and penetration. The ejected fragments of material resulting from the particle primary impact shall thus be treated in the same way as the primary particle impacting the surface and thus shall be characterised by the same parameters:

Project: ESABASE2/Debris Release 12.1	Date:	2024-02-19
Technical Description	Revision:	1.11
Reference: R077-231rep_01_11_Debris_Technical Description.docx	Status:	Final

FEV etamax GmbH   Page 125 / 173

- particle size (or mass),
- number of particles,
- particle density,
- particle velocity.

4.2.2.1 Description of the Ejecta model

4.2.2.1.1 Total ejected mass

The basic equation is taken from Gault (1973), valid for brittle target and for an incident particle with a diameter larger than 10 μm:

$$\theta_i \leq 60°: \qquad M_{Gault} = 7.41 \cdot 10^{-6} \sqrt{\frac{\rho_p}{\rho_t}} \, E_i^{1.133} \left(\cos\theta_i\right)^2 \qquad \text{(SI units)}$$

$$\theta_i > 60°: \qquad M_{Gault} = 7.41 \cdot 10^{-6} \sqrt{\frac{\rho_p}{\rho_t}} \, E_i^{1.133} \left(\cos 60°\right)^2 \qquad \text{(SI units)}$$

with:
- E_i impact kinetic energy
- ρ_p projectile density
- ρ_t target density
- θ_i impact incidence angle (from normal direction)

For other cases, we introduce a corrective coefficient K:

$$M_e = K \, M_{Gault}$$

	$d_p < 10$ μm	$d_p \geq 10$ μm
ductile target	$K = 10^{-2} - 10^{-3}$	
brittle target	$K = d_p/10^{-5}$	$K = 1$

with: d_p projectile diameter

4.2.2.1.2 Mass partitioning

The total ejected mass is partitioned in three components:

$$M_e = M_{jet} + M_{cone} + M_{spalls}$$

$$M_{jet} \approx 0$$

$$M_{cone} = \beta \, M_e$$

$$M_{spalls} = (1 - \beta) \, M_e$$

	$d_p \leq 1 \ \mu m$	$1 \ \mu m < d_p \leq 10 \ \mu m$	$10 \ \mu m < d_p \leq 100 \ \mu m$	$d_p > 100 \ \mu m$
ductile target	$\beta = 1$			
brittle target	$\beta = 1$	$\beta = -0.3 \log d_p - 0.8$		$\beta = 0.4$
solar cell	$\beta = 1$	$\beta = -0.3 \log d_p - 0.8$	$\beta = -0.6 \log d_p - 2.3$	$\beta = 0.1$

4.2.2.1.3 Cone Fragments Modelling

For each primary particle with a velocity v_i, an impact direction (θ_i, φ_i) and a size (δ_i), the debris cone and secondary particle impacts are modelled using analytical formulation and ray-tracing technique. The software model calculates the number of secondary particle ($n(\varphi, \theta, \delta, v)$) in function of size ($\delta$, in N_δ intervals) and the velocity (v) in randomly distributed directions. Each direction, characterising a ray, is determined by its elevation (θ) and its azimuth (φ). The number of rays in ($\theta \in [0, \pi/2]$, $\varphi \in [0, 2\pi]$) is fixed by the user.

We suppose that δ (ejecta diameter), θ (ejecta zenith) and φ (ejecta azimuth) are independent variables and that V (ejecta velocity) is a function of these 3 variables:

$$n_{cone}(\delta, \theta, \varphi, V) = K_{cone} \, f_{cone}(\delta) \, g_{cone}(\theta) \, h_{cone}(\varphi) \, \Delta\big(V - V_{cone}(\delta, \theta, \varphi)\big)$$

Note: In the following equations, $\mathbf{1}$ is the interval function, whose value is 1, if the parameter (e.g. δ) is within the range given in squared brackets (e.g. $[\delta_1, \delta_{max}]$) and 0 elsewhere.

Size distribution

$$f_{cone}(\delta) = \frac{1 - \alpha 1}{\delta_{max}^{1-\alpha 2} \delta_1^{\alpha 2 - \alpha 1} - \delta_{min}^{1-\alpha 1}} \delta^{-\alpha 1} \mathbf{1}[\delta_{min}, \delta_1] + \frac{1 - \alpha 2}{\delta_{max}^{1-\alpha 2} - \delta_{min}^{1-\alpha 1} \delta_1^{\alpha 1 - \alpha 2}} \delta^{-\alpha 2} \mathbf{1}[\delta_1, \delta_{max}]$$

$$\delta_{min} = 0.1 \ \mu m$$

$$\delta_{max} = \sqrt[3]{\frac{6 \, m_b}{\pi \, \rho_t}}$$

$$m_b = \lambda \, M_e$$

Project: ESABASE2/Debris Release 12.1	Date:	2024-02-19
Technical Description	Revision:	1.11
Reference: R077-231rep_01_11_Debris_Technical Description.docx	Status:	Final

FEV etamax GmbH · Page 127 / 173

if $\quad \delta_{max} > 10\ \mu m \qquad\qquad \delta_1 = 10\ \mu m$

else $\qquad\qquad\qquad\qquad \delta_1 = \delta_{max}$

	$\theta_i \leq 60°$	$\theta_i > 60°$
ductile target	$\alpha 1 = \alpha 2 = 2.6$; $\lambda = 0.02$	$\alpha 1 = \alpha 2 = 2$; $\lambda = 0.05$
brittle target	$\alpha 1 = 2.6$; $\alpha 2 = 3.5$; $\lambda = 0.1$	$\alpha 1 = \alpha 2 = 2$; $\lambda = 0.5$

Zenith density

$$g_{cone}(\theta) = \frac{1}{\sigma\sqrt{2\pi}} \exp\left(-\frac{(\theta - \theta_{max})^2}{2\sigma^2} \right) \mathbf{1}[0, 2\pi]$$

for $\theta_i \leq 60°$: $\quad \theta_{max} = \dfrac{\theta_{max\,60} - \theta_{max\,0}}{\pi/3}\theta_i + \theta_{max\,0} \qquad$ radian units

for $\theta_i > 60°$: $\quad \theta_{max} = \theta_{max\,60}$

$\qquad\qquad \theta_{max\,60} = 80°$

$\qquad\qquad \theta_{max\,0} = 30°$

$\qquad\qquad \sigma = 3°$

Azimuth density

for $\theta_i \leq 60°$: $\quad h_{cone}(\varphi) = \dfrac{1}{2\pi}\left(\dfrac{3\theta_i}{2\pi - 3\theta_i}\cos(\varphi - \varphi_i) + 1 \right)\mathbf{1}[0, 2\pi]$

for $\theta_i > 60°$: $\quad h_{cone}(\varphi) = \dfrac{1}{\sigma'\sqrt{2\pi}} \exp\left(-\dfrac{(\varphi - \varphi_{max})^2}{2\sigma'} \right)\mathbf{1}[0, 2\pi]$

$\qquad\qquad \sigma' = 5°$

Normalisation

$$M_{cone} = \iiiint_{\delta\ \theta\ \varphi\ V} \frac{\pi\ \rho_t\ \delta^3}{6}\ n_{cone}(\delta, \theta, \varphi, V)\ d\delta\ d\theta\ \sin\theta\ d\varphi\ dV$$

By developing sinθ at order 0 (i.e.: sinθ = sinθmax), we obtain:

$$K_{cone} = \frac{6\,M_{cone}}{\pi\,\rho_t}\,\frac{(4-\alpha1)(4-\alpha2)\left(\delta_{max}^{1-\alpha2}\,\delta_1^{\alpha2} - \delta_{min}^{1-\alpha1}\,\delta_1^{\alpha1}\right)}{(4-\alpha1)(1-\alpha2)\delta_{max}^{4-\alpha2}\,\delta_1^{\alpha2} + 3(\alpha2-\alpha1)\delta_1^4 - (4-\alpha2)(1-\alpha1)\delta_{min}^{4-\alpha1}\,\delta_1^{\alpha1}}\,\frac{1}{\sin\theta_{max}}$$

Velocity

There is an inverse proportionality between diameter and velocity of ejecta:

$$V(\delta,\theta,\varphi) = D(\varphi)/\delta + E(\varphi)$$

$$D(\varphi) = \frac{V_{max}(\varphi) - V_{min}}{\delta_{max} - \delta_{min}}\,\delta_{max}\,\delta_{min}$$

$$E(\varphi) = \frac{V_{min}\,\delta_{max} - V_{max}(\varphi)\,\delta_{min}}{\delta_{max} - \delta_{min}}$$

$$V_{min} = 10\,m/s$$

for θi ≤ 60°: $V_{max}(\varphi) = \frac{V_i}{\cos\theta_i}\left(1 - \frac{3\theta_i}{4\pi}\left(1 - \cos(\varphi - \varphi_i)\right)\right)$

for θi > 60°: $V_{max}(\varphi) = 3\,V_i$

4.2.2.1.4 Spallation Process Modelling

No spallation is considered on ductile targets.

We propose a formulation with separated variables:

$$n_{spalls}(\delta,\theta,\varphi,V) = K_{spalls}\,f_{spalls}(\delta)\,g_{spalls}(\theta)\,h_{spalls}(\varphi)\,j_{spalls}(V)$$

Size distribution

We assume that all the spall particles have the same mass. Spalls have a plate-like shape, so we define an equivalent diameter:

$$\delta_{spalls} = \sqrt[3]{\frac{6\,M_{spalls}}{N_{spalls}\,\pi\,\rho_t}}$$

Project: ESABASE2/Debris Release 12.1		Date:	2024-02-19
Technical Description		Revision:	1.11
Reference: R077-231rep_01_11_Debris_Technical Description.docx		Status:	Final

FEV etamax GmbH   Page 129 / 173

We suggest: $N_{spalls} = 20$

$$f_{spalls}(\delta) = \Delta(\delta - \delta_{spalls})$$

Zenith distribution

$$g_{spalls}(\theta) = \frac{1}{\theta_{spalls}} \mathbf{1}\left[0, \theta_{spalls}\right]$$

$$\theta_{spalls} = 5°$$

Azimuth distribution

$$h_{spalls}(\varphi) = \frac{1}{2\pi} \mathbf{1}[0, 2\pi]$$

Velocity distribution

$$V_{spalls} = 10\,m/s$$

$$j_{spalls}(V) = \Delta(V - V_{spalls})$$

Normalisation

$$N_{spalls} = \iiiint_{\delta\,\theta\,\varphi\,V} n_{spalls}(\delta, \theta, \varphi, V)\,d\delta\,d\theta\,\sin\theta\,d\varphi\,dV$$

$$K_{spalls} = N_{spalls}\,\frac{\theta_{spalls}}{1 - \cos\theta_{spalls}}$$

4.2.2.2 Model Inputs, Parameters and Outputs

This section summarises all inputs, parameters, and outputs used in the ejecta model.

Model inputs:

- particle density (ρ_p)
  (constant, or as specified in the sections 2.1.2.3 and 2.2.13.1)

- particle mass   (m_p)
  (within the particle mass range to be considered according to the debris or meteoroid model mass distribution)

- target density   (ρ_t)
  (user input for ESABASE2/Debris, s. |25|, |26|)

- magnitude of the impact velocity   (v_i)
  (meteoroid or debris model output)

- incidence of the impact direction with respect to the surface   (θ_i)
  (determined from meteoroid or debris model output)

- azimuth of the impact direction   (φ_i)
  (Meteoroid or debris model output)

- type of target   (brittle) or (ductile)
  *(determined by ESABASE2/Debris based on the selected damage size equation k_c-factor:
  if $k_c > 5 \;\wedge\;$ brittle target, else ductile target)*

- number of directions for the modelling of the debris cone   (N_{cone})
  (user input)

Model outputs:

The ray-tracing technique is used for debris cone and spallation phenomena.

For each ray (i), outputs are:

- azimuth (φ_i),
- elevation (θ_i),

  concerning debris cone

  – size of the fragments (δ_i) in width interval ($\Delta\delta_i$),

  – number of fragments (n_i) of size (δ_i),

  – velocity of fragments (v_i) of size (δ_i),

  concerning spallation

  – fragment mass (m_{spall}),

  – fragment velocity (v_{spall}) .

The model parameters and limit angles are described in the notes Ref. /16/, /17/, /24/.

4.2.2.3 Software Limits

This model should be used under following conditions:

- projectile diameter between 1 µm and 1 mm,
- impact velocity between 1 km/s and 20 km/s,
- thick target [1],
- ductile and brittle homogenous targets.

Some uncertainties remain concerning the size and velocity of ejecta fragments. Results are in fact very different from one author to another, as they used different measurement techniques. A direct relation between fragment size and its velocity is proposed.

<u>Notes</u>: 1) In the software implementation, the ejecta model is only available for objects with single wall design.

4.2.3 Conclusion

A complete improved ejecta model is implemented, based on the review of existing publications on various experiments and on theoretical considerations. Normal and oblique impacts are taken into account.

Different phases of projectile impacts are studied: jetting phase, debris cone phase and spallation phase.

The model inputs are the projectile and target properties and the impact characteristics. The output is the ejecta distribution in the geometrical space around the impact by solid angle unity, in term of fragment size and velocity.

5 The Impact and Damage Probability Analysis

This chapter describes the methodology of the probability analysis for impacts and damage which is implemented in the ESABASE2/Debris analysis tool. It also briefly describes the software tool. For more details on the tool itself and its usage, refer to the software user manual (Ref. /14/).

5.1 General

The analysis of the micro-particle risk is based on the integration of the impact probabilities delivered by the space debris and micro meteoroid models over area and time of the spacecraft mesh. The spacecraft mesh and object orientation is delivered by the ESABASE2 framework, defined in the *.geometry* file. The spacecraft orbit is generated by the ESABASE2 SAPRE module, which together with the mesh and kinematics define spacecraft velocity and orbital position, as well as the orientation and all spacecraft model elements at each orbital point of the analysis. For more details on the modelling in ESABASE2, the user is invited to consult the general ESABASE and ESABASE2 documentation.

5.2 The Weighted Ray-tracing Method

The integration of the impacts probabilities is performed using the flux models and a Monte Carlo raytracing method available in the ESABASE2 framework. The raytracing analysis method consists of the following main steps:

For each ray:

1) Generation of the micro particle impact velocity vector V.

2) Generation of a random impact point P on the element.

3) Generation of an emitting ray, launched from the point P and in the opposite direction of V.

4) Check if the emitted ray reaches free space; if so, a particle from this direction may hit the element and the ray is retained for further processing.

5) Computation of the damage related entities (ballistic limit, crater / hole diameter).

6) Computation of the weighted probabilistic data for the ray (see below)

For the summed results of all rays

7) Computation of flux, fluence and total quantity of impact and damage data

8) Computation of averaged impact data (impact velocity and angle, Ks factor [see below])

The weighted ray tracing technique method is based on the following facts:

Project: ESABASE2/Debris Release 12.1	Date:	2024-02-19
Technical Description	Revision:	1.11
Reference: R077-231rep_01_11_Debris_Technical Description.docx	Status:	Final

- The particle flux from a certain direction is proportional to the projection of the element surface onto a plane perpendicular to this direction, i.e. to the cosine of the impact angle α.

- For fluxes related to particle velocities, the flux is proportional to the ratio between impact velocity and particle velocity; this is the case for meteoroids.

- The element data is obtained by dividing the summed weighted ray data with the number of emitted rays[1], corrected with a factor depending on the ray flux model; for flux models generating fluxes on a random tumbling plate from a spherical direction generation, this factor is 4.

For the surface, the flux computation is expressed by the following equation:

$$FLUX = \int_{m_{min}}^{m_{max}} \int_{sphere} Flux(m) \cdot (v_i \cos\alpha) \cdot d\alpha \cdot dm$$

On ray level, this is equivalent to the summing up of the individual ray data.

$$DATA = \frac{\sum_{i=1}^{n_{ray}} F_s \cdot data_{ray-i} \cdot \cos\alpha_i}{n_{ray}}$$
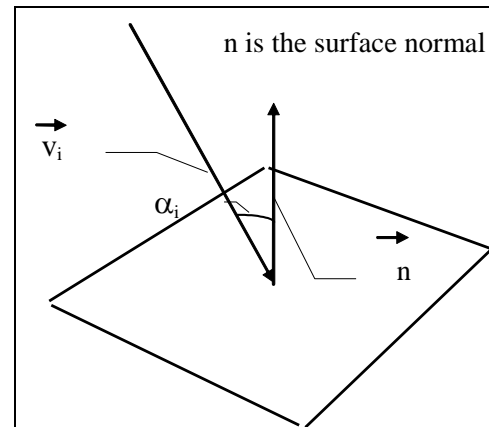
F_s is the shading factor: Fs =1 no shading,

F_s = 0: ray totally shaded. Fs is delivered by the ray tracing

The above described raytracing method automatically generates the k factor of the surface element (which depends on element orientation and spacecraft velocity [for meteoroids]); this is described in detail in annex C of ref. (Ref. /15/). The Earth shielding is treated as a surface of the geometric model: if the emitted ray lies within the Earth cone, it is considered as shaded.

The following results are computed and summed for all non-shaded rays:

- $\cos\alpha$ cosine impact angle
- $\alpha (\cos\alpha)$ impact angle times cosine impact angle
- $v_i (\cos\alpha)$ impact velocity times cosine impact angle

---

[1] The sum of the rays contains the weighting factor from the point seeding process of the raytracing library.

- Fflx $(\cos \alpha)$ Failure flux times cosine impact angle
- Crflx $(\cos \alpha)$ Crater flux times cosine impact angle
- Flx $(\cos \alpha)$ Impact flux times cosine impact angle

The flux related data is computed with the difference of the flux of the considered particle size minus the flux of the maximum particle size of the analysis (the limit particle sizes are user input). This is a consequence of the cumulated flux formulation of the environment models, i.e. a flux for a given size s is given as the number of impacts of particles of equal or larger size then s per year and m^2.

For impact fluxes, the minimum particle size is used. For ballistic limits, the critical or limit particle size (computed for the impact velocity vector with the ballistic limit equation). For cratered areas, a loop over particle size with the associated impact flux is run over the damage size equation and the data summed up.

5.3 Generation of Micro-Particle Impact Velocities

All the geometric features of the models, described in chapter 2, are simulated with raytracing. An essential part of the method relies on the proper generation of particle arrival directions. Depending on the particle type and model, a different type of particle generation is applied. The different methods implemented in the software and their applications are briefly explained in the following sections.

5.3.1 Particle Velocity Generation

Basically two impact direction schemes are used in the software: 1 for the NASA 90 model and one for the MASTER models, MEM models and IMEM(2) models. The difference relies on the fact that the NASA 90 model impact direction generation is performed in the plane normal to the Earth direction, the other named models impact direction generation is performed in 3D space.

Both impact direction schemes rely on the use of cumulated direction probabilities and a random number generator. The scheme is visualised in the example below.

Project: ESABASE2/Debris Release 12.1		Date:	2024-02-19
Technical Description		Revision:	1.11
Reference: R077-231rep_01_11_Debris_Technical Description.docx		Status:	Final

FEV etamax GmbH   Page 135 / 173

For a distribution function, the cumulated function is generated.

A random number is generated between Y(X = Xmin) and Y-cumulated(X=Xmax), in the case of the example between 0 and 5.

For the randomly generated value of Y-cumulated, the corresponding X-value is extracted: this is the sought value.

In the case of impact velocity, the direction and amplitude is thus generated from the velocity distribution function(s) of the space debris environment model.
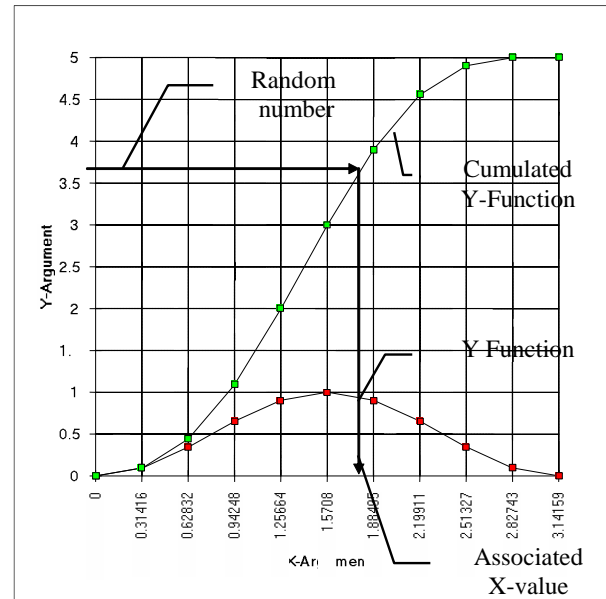
For the NASA 90 model, the cumulated velocity amplitude and arrival angle are function of the orbit inclination. In the NASA 90 model, the debris orbits are assumed circular, thus the altitude dependent debris velocity component is given directly by the spacecraft velocity. Two random number generator calls are used for the impact velocity vector generation.

For the ORDEM models, the MASTER models, MEM models and IMEM models, the flux vs. elevation and azimuth data and impact velocity is computed by the corresponding model with the spacecraft orbit and a sphere as spacecraft. The results of this analysis are stored on scratch files in case of ORDEM models, MEM models, IMEM models and MASTER models except MASTER 2001 or provided via *COMMON* in case of MASTER 2001.

For the space debris impact velocity, the data is tabulated. For the MASTER 2001 and MASTER 2005 models two independent data sets are created: the flux vs. elevation angle and the flux vs. azimuth angle. Associated with the azimuth angle is the impact velocity. Two independent random number generator calls are used to extract the impact velocity vector (amplitude, azimuth angle, elevation angle). Similar approach applies to IMEM, however, the independent data sets are impact velocity and azimuth-elevation associated sky-map.

For MEM models, IMEM2, MASTER models since MASTER 2009 and ORDEM 3.0/3.2 only one independent random number generator call is used to extract the impact velocity vector (amplitude, azimuth angle, elevation angle). Once the impact elevation angle is determined from cumulated 2D spectrum (as described above), the corresponding impact azimuth angle and the impact velocity can be determined from the multidimensional output of the models (proprietary, STENVI).

5.3.2 Grün Particle Velocity Generation

Contrary to the space debris, the micro meteoroid velocities are generated relatively to Earth. Two different schemes are used, depending on the meteoroid model used.

Project: ESABASE2/Debris Release 12.1		Date:	2024-02-19
Technical Description		Revision:	1.11
Reference: R077-231rep_01_11_Debris_Technical Description.docx		Status:	Final

FEV etamax GmbH

Page 136 / 173

Grün sporadic omni-directional model

In this model, the meteoroids may arrive from any direction. This random arrival is generated with two random number generator calls:

- For the azimuth angle between 0 and 2π
- For the cosine of the elevation angle between -1 and 1.

The velocity amplitude is generated from the chosen velocity distribution scheme:

- For constant velocity, the input amplitude is used
- For the NASA 90 velocity distribution, the amplitude is extracted from the distribution function with a random number generator call.
- For the Taylor HRMP, the velocity / flux function is used to generate the velocity amplitude

For more details, see chapter 2.

Meteoroid streams and β particles

For these enhanced options, the meteoroid velocity vector (arrival direction and velocity amplitude) is derived from the meteoroid enhancement model itself, see chapter 2. In the case these options are activated, the meteoroid ray is split into different classes:

- The main Grün portion ray, derived as described above
- In case the α/β-separation is activated, the Grün ray is split into the α part (of random direction) and the β with a fixed direction from the sun.
- In case the streams / interstellar source option is activated, each stream or interstellar source is provided with a ray of the corresponding velocity vector.

As can be seen, the enhanced meteoroid options may lead to noticeable increases in computing time. If the Grün model is switched off, the analysis can be performed with a smaller number of rays (50 is generally enough).

For both meteoroid velocity generation methods, the impact velocity is computed as a vector sum of the meteoroid velocity and the spacecraft velocity.

5.3.3 Implementation of the Stream & Interstellar Contribution

The stream velocity vector is extracted from the streams file for the specific time corresponding to the orbital step being analysed. The relative flux contribution is checked according to the scheme lined out in section 2.2.10.2. For missions which are longer than one orbit, the flux contribution is checked for all calendar times corresponding to the orbital point over the mission.

Project: ESABASE2/Debris Release 12.1		Date:	2024-02-19
Technical Description		Revision:	1.11
Reference: R077-231rep_01_11_Debris_Technical Description.docx		Status:	Final

FEV etamax GmbH

Page 137 / 173

E.g. for a 10 day mission on a geostationary orbit, 10 calls to the stream file extraction routine will be performed, and the stream contribution of all active streams averaged for all these time steps. Depending on the mission duration, some streams may only be active for certain time steps. The number of calls to the stream extraction routine is echoed during analysis execution.

With this scheme, it is obvious that the directional information from the stream contribution will be lost for long mission durations. Also, for low Earth orbits, a large number of calls to the stream extraction routine will be performed for extended mission times (160 calls for an orbit with 90 minutes period and 10 days mission time).

The active stream numbers are echoed to the analyser listing file. The summed stream contribution over mission time is stored in the model view file, see ref. /14/.

The interstellar sources are treated as streams for velocity vector generation and flux contribution.

5.4 Damage and Impact Probability Computations

On ray level, the impact, failure and crater fluxes are computed as follows for un-shaded rays:

Impact flux:

$$i_{flx} = \left[flux(s_{min}) - flux(s_{max}) \right] \cdot \cos\alpha$$

s is the impactor size, diameter or mass.

Failure Flux:

$$f_{flx} = \left[flux(s_{crit}) - flux(s_{max}) \right] \cdot \cos\alpha$$

s_{crit} is delivered by the damage equation.

The crater flux is obtained by looping over the impactor size bins, summing the binned fluxes (flux of bin minimum size - flux of bin maximum size) multiplied with the crater / hole size produced by an impactor of logarithmic mean size of the bin.

Impact angle: $\qquad \alpha_i = \alpha \cdot \cos\alpha$

Impact velocity: $\qquad v_{imp,i} = v_{imp} \cdot \cos\alpha$

The impact and damage fluxes are computed with the following equations of the ray data:

Impact Flux: $\qquad I_{flx} = \dfrac{4\sum \zeta \cdot i_{flx}}{n_{ray}} \qquad$ n_{ray} is the total number of rays fired per element.

$\zeta=1$ for non-shaded ray, $\zeta=0$ for shaded ray.

Failure Flux: $\qquad F_{flx} = \dfrac{4\sum \zeta \cdot f_{flx}}{n_{ray}} \qquad$ The crater flux is obtained similarly.

Fluence and number of impacts / failures are computed from the flux data:

Fluence = Flux x Time $\qquad$ Orbital arc: time of one revolution;

Mission: mission time

Nb. of (impacts / failures / craters) = Fluence x Element area

The probability of no failure is extracted from the number of failures with the following equation:

$$P_{no\_failure} = \exp\left[-N_{failures} \right] \qquad$$ $N_{failures}$ is the number of failures.

Project: ESABASE2/Debris Release 12.1		Date:	2024-02-19
Technical Description		Revision:	1.11
Reference: R077-231rep_01_11_Debris_Technical Description.docx		Status:	Final
FEV etamax GmbH			Page 139 / 173

The probability of no failures is computed on object and spacecraft level.

Additionally, the average impact velocity data and the Ks factor are computed as follows:

Average impact angle: $\quad \overline{\alpha} = \dfrac{\sum \alpha_i}{n_{hit}} \quad$ n_{hit} is the number of non-shaded rays per element.

Average impact velocity: $\quad \overline{v}_{imp} = \dfrac{\sum v_{imp}}{n_{hit}} \quad$ Only non-shaded rays are processed.

The Ks factor: $\quad Ks = \dfrac{4 \sum \zeta \cdot \cos \alpha_i}{n_{ray}}$

Note

The Ks factor is the combined value of the k factor (i.e. the impact flux ratio of the element to the flux of a random tumbling plate [for meteoroids: a fixed random tumbling plate, i.e. with $V_{s/c} = 0$]) and the shading of the plate of Earth and neighbouring surfaces of the spacecraft.

Thus for a simple box, the Ks factor of the faces correspond to the k factor. This type of result can also be obtained with the fixed plate option, see ref. (Ref. /14/).

The above data is computed for each orbital point. The result is averaged for the orbital arc level output, which is appropriate for the flux computation over an orbit. The mission level results are simply the orbital arc flux results multiplied by the mission time.

5.5 Use of FAME Algorithm for Highlighting Weak Spots

Within the results of an geometrical analysis it is possible to indicate/highlight "weak spots" of the spacecraft. This significates the representation of the impact velocity in colour and the impact elevation and azimuth are represented as weak spot arrows on the surface elements of the spacecraft. The statistical representation takes place by using the median, the minimum, the maximum and Q1 as well as Q3 quantile. The calculation is performed by the Fast Algorithm for Median Estimation (FAME).

The median divides a sorted data set into two equal halves. The median is the value that stands exactly in the middle of the record. Equivalent to the standard deviations in the normal distribution, the quartiles are used here. Quartiles divide the dataset into four equally sized regions, with the second quartile boundary Q2 equal to the median. Exactly 50% of the measured values lie between the first quartile boundary Q1 and the third quartile boundary Q3.

The basic idea of the FAME algorithm is to determine the median of a data set without having to use all acquired measurement data, see /59/. The median is determined only by the old median, the new measured value and a step size. The advantage of this is that less memory is needed, and that the computing time is lower. The disadvantage is that the median is only approximated and not exact. In order to determine the median exactly, all values would have to be considered. How well the result matches the real median depends on the quality of the measurements and the size of the data set. This means that if the measured values do not

Project: ESABASE2/Debris Release 12.1		Date:	2024-02-19
Technical Description		Revision:	1.11
Reference: R077-231rep_01_11_Debris_Technical Description.docx		Status:	Final

FEV etamax GmbH   Page 140 / 173

show too much variation, a smaller amount of data is needed to approximate the median well. For higher scatter readings, a larger amount of data is needed for a good approximation. For sufficiently large data sets, each distribution can be well approximated.

The algorithm proceeds as follows. First, it is initialized with the first measured value. That is, the first measured value is first set equal to the median M and it is defined a step, which is initially set equal to half of the first measured value. For each new data value d, M is incremented by step if d is greater than M. If d is smaller, M is decreased by step. If the new data value is close to M, the step is halved. Expressed in formulas: $M = M \pm step$ and $d \in (M - step, M + step)$: $step = step/2$.

Algorithm 1 : Fast Algorithm for Median Estimation

1: **Initialization:**
2: $M = data(1)$
3: $Step = max(|data(1)/2|, b)$ // b is a minimal initial step

4: **For each new item i:**
5: **if** $M > data(i)$ **then**
6:    $M = M - step$
7: **else if** $M < data(i)$ **then**
8:    $M = M + step$
9: **end if**
10: **if** $|data(i) - M| < step$ **then**
11:    $step = step/2$
12: **end if**

Figure 5-1   Pseudocode of the FAME algorithm, ref. /59/.

The same algorithm applies to derive the quartiles Q1 and Q3. The initialisation is the same for all quartiles Q1, Q2 and Q3. If the new data set d is smaller than the median M, it is considered for the determination of Q1. Consequently, if d is larger than M, it is considered for the determination of Q3.

Project: ESABASE2/Debris Release 12.1	Date:	2024-02-19
Technical Description	Revision:	1.11
Reference: R077-231rep_01_11_Debris_Technical Description.docx	Status:	Final

FEV etamax GmbH   Page 141 / 173

6 Orbit Generation

6.1 Introduction

Many ESABASE applications, and the pointing facility, need to know the position of a spacecraft on its orbit at successive times during an analysis. For the purpose of generating this information in a standard form, an orbit generator is provided with ESABASE2. The orbit propagator in use is SAPRE.

The SAPRE orbit generator uses a 4th order Runge-Kutta routine with fixed step size to integrate the equations of motion, expressed in terms of osculating orbital elements. It is a general purpose orbit generator and can be used for different orbit types.

The structure and functionality of the orbit generator are described in detail in ref. /40/. This section will introduce the modifications and extensions performed to allow the application to lunar orbits. The following topics will be discussed:

- General propagation;
- Consideration of 3rd body perturbation;
- Consideration of spherical harmonics.

Furthermore the generation of vectors for L1/L2 orbits will be described. It is integrated in the structure of SAPRE and uses some of its functionality, but does not follow the regular orbit generation of SAPRE.

6.2 General Propagation

The first step, the propagation without the consideration of perturbations has a general approach. To adapt the orbit generation to other celestial bodies than the Earth, the corresponding constants, e.g. gravitational constant and radius, of the bodies have to be used. To achieve this, a module was introduced containing the required constants for Earth and Moon, as well as Mercury, Venus and Mars. The module contains also a routine *setOrbitCon*, which adjusts the provided constants to the parameters used in the orbit generator based on the central body (centre of motion) ID. At begin of the orbit generation the constants are defined by using *setOrbitCon* according the user definition of the orbit central body.

The central body ID is defined according the NAIF ID definition (used for SPICE), refer to /46/. The ID's are defined by three-digit numbers. The plain numbers identifies the barycentre of a planet system, e.g. 300 for the barycentre of the Earth-Moon system. The highest number identifies the planet itself, e.g. 399 for Earth and the other numbers indicates the moons of the planet, e.g. 301 for Moon. The first digit of the number identifies the planet of the solar system, thus Mercury is 199, Venus is 299, Earth is 399, Mars is 499, etc.

6.3 Consideration of 3rd Body Perturbation

The calculation of the 3rd body perturbation is based on generic code, but it requires the position of the celestial bodies, which are to be considered, in the 'planeto'-centric coordinate frame as input. I.e. if Sun and Earth shall be considered for a lunar orbit, the position of them

Project: ESABASE2/Debris Release 12.1		Date:	2024-02-19
Technical Description		Revision:	1.11
Reference: R077-231rep_01_11_Debris_Technical Description.docx		Status:	Final

FEV etamax GmbH   Page 142 / 173

in the selenocentric inertial frame is needed. The 3rd body perturbations can be applied for orbits around Earth and Moon, only.

Due to the existing options to account for the perturbations, caused by Sun and Moon, for Earth orbits, the functionalities exist to calculate the positions of the both celestial bodies in the (geocentric) equatorial inertial frame (ICRF equator, vernal equinox frame). These calculations are used as basis for the position definition of Earth and Sun in the selenocentric inertial system.

The idea of the position definition is to calculate the position vectors in the ICRF equator vernal equinox frame so that they originate at Moon. Subsequent the coordinate system is rotated to the Moon inertial coordinate system. The Moon coordinate system is defined according /41/ with the z-axis in the direction of the Moon's mean axis of rotation. The x-axis is along the intersection of the ICRF and Moon's equators directed at the ascending node. The Figure 6-1 illustrates the used reference system for the definition of the orientation.

158   P. K. Seidelmann et al.

Fig. 1 Reference system used to define orientation of the planets and their satellites
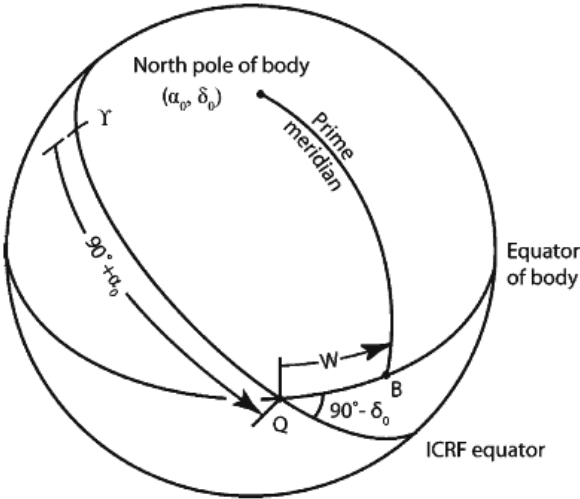
Figure 6-1   Reference system for the planet coordinate system definitions, ref. /41/.

The Figure 6-2 lists the recommended values and calculations of the rotation angles to the Moon coordinate system.

Table 2 Recommended values for the direction of the north pole of rotation and the prime meridian of the satellites

α_0, δ_0, T, and d have the same meanings as in Table 1 (epoch JD 2451545.0, i.e. 2000 January 1 12 hours TDB)

Earth	Moon				
		$\alpha_0 = 269°.9949$	$+0°.0031 T$	$-3°.8787 \sin E1$	$-0°.1204 \sin E2$
			$+0.0700 \sin E3$	$-0.0172 \sin E4$	$+0.0072 \sin E6$
			$-0.0052 \sin E10$	$+0.0043 \sin E13,$	
		$\delta_0 = 66.5392$	$+0.0130 T$	$+1.5419 \cos E1$	$+0.0239 \cos E2$
			$-0.0278 \cos E3$	$+0.0068 \cos E4$	$-0.0029 \cos E6$
			$+0.0009 \cos E7$	$+0.0008 \cos E10$	$-0.0009 \cos E13,$
		$W = 38.3213$	$+13.17635815 d$	$-1.4 \times 10^{-12} d^2$	$+3.5610 \sin E1$
			$+0.1208 \sin E2$	$-0.0642 \sin E3$	$+0.0158 \sin E4$
			$+0.0252 \sin E5$	$-0.0066 \sin E6$	$-0.0047 \sin E7$
			$-0.0046 \sin E8$	$+0.0028 \sin E9$	$+0.0052 \sin E10$
			$+0.0040 \sin E11$	$+0.0019 \sin E12$	$-0.0044 \sin El3$

where $E1 = 125°.045 - 0°.0529921 d$, $E2 = 250°.089 - 0°.1059842 d$, $E3 = 260°.008 + 13°.0120009 d$,
$E4 = 176.625 + 13.3407154 d$, $E5 = 357.529 + 0.9856003 d$, $E6 = 311.589 + 26.4057084 d$,
$E7 = 134.963 + 13.0649930 d$, $E8 = 276.617 + 0.3287146 d$, $E9 = 34.226 + 1.7484877 d$,
$E10 = 15.134 - 0.1589763 d$, $E11 = 119.743 + 0.0036096 d$, $E12 = 239.961 + 0.1643573 d$, $E13 = 25.053 + 12.9590088 d$

Figure 6-2 **Reference values for the calculation of the rotation angles, ref. /41/.**

The calculation process of the positions is described in the following.

6.3.1 Earth Position

The first step for the calculation of Earth's position in the selenocentric system is the estimation of the Moon position in the geocentric coordinate system using the available functionality. Than the unit vector and the norm are generated from the vector. Because of the vector connecting both bodies the unit vector can originates in both of them without translation. The vector is inverted, so that starting in the centre of the Moon it defines now the position of the Earth relative to Moon. But the vector is still in the ICRF equator vernal equinox system and has to be rotated to the Moon equator ICRF intersection (ascending node of lunar equator) system. The rotation angles:

- α, the angle along the ICRF equator, from vernal equinox (x-axis) to the ascending node of the lunar equator;

- δ, the inclination of the lunar equator to the ICRF equator;

are calculated to

$$\alpha = 90 + \alpha_0$$

$$\delta = 90 - \delta_0$$

with α_0 and δ_0 defined in Figure 6-2. The first rotation is performed around the z-axis of the ICRF equator vernal equinox system with the angle α. The second rotation is performed around the new x-axis with the angle δ. After the rotation the unit vector is combined with the norm again and can be used in further calculations.

6.3.2 Sun Position

At the beginning of the estimation of the Sun position in the Moon coordinate system the positions of Sun and Moon are calculated in the geocentric coordinates by the available routines. Subsequent the vector from Moon to Sun is calculated by subtracting Moon's vector from Sun's vector. The result is a vector from Moon to Sun (originating in Moon) in the ICRF equator vernal equinox system. The Figure 6-3 illustrates the described relation.
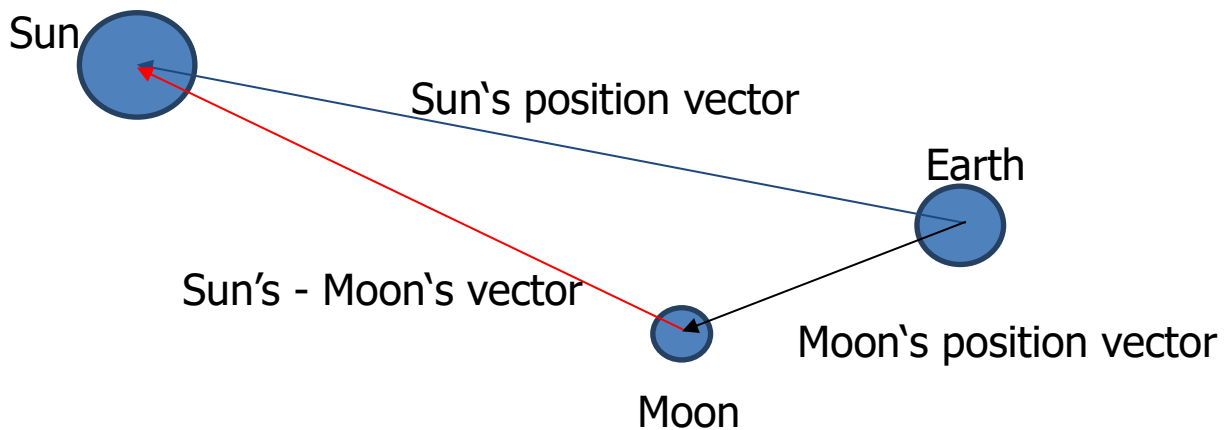
Figure 6-3   **Relation between the Sun-Moon, Sun and Moon vectors**.

After the calculation of the vector from Moon to Sun, the unit vector is rotated from the ICRF equator vernal equinox system to the Moon equator ICRF intersection (ascending node of lunar equator) system as depicted in 6.3.1. After the rotation the unit vector is combined with the norm and can be used in further calculations.

6.4 Consideration of Spherical Harmonics

The perturbation due to the spherical harmonics is applied by considering the additional acceleration caused by them. It is clear that the effect of the spherical harmonics is individual for each celestial body; therefore a calculation of the acceleration caused by the non-spheric form of the Moon has been implemented.

The theory is described in the section 8.6.1 of /43/. The important equations are introduced in the following.

The acceleration is described by:

$$\vec{a} = \frac{\partial U}{\partial r}\left(\frac{\partial r}{\partial \vec{r}}\right)^{T} + \frac{\partial U}{\partial \phi_{sat}}\left(\frac{\partial \phi_{sat}}{\partial \vec{r}}\right)^{T} + \frac{\partial U}{\partial \lambda_{sat}}\left(\frac{\partial \lambda_{sat}}{\partial \vec{r}}\right)^{T}$$

with $\vec{a}$ as the acceleration, U as the aspherical potential function, $\vec{r}$ as the position, ϕ_{sat} as the latitude of the spacecraft and λ_{sat} as the longitude of the spacecraft.

The aspherical potential function derivatives are defined as:

$$\frac{\partial U}{\partial r} = -\frac{\mu}{r^2} \sum_{l=2}^{\infty} \sum_{m=0}^{l} \left(\frac{R_\oplus}{r}\right)^l \cdot (l+1) \cdot P_{l,m} \cdot [\sin(\phi_{sat})] \cdot \{C_{l,m} \cdot \cos(m\lambda_{sat}) + S_{l,m} \cdot \sin(m\lambda_{sat})\}$$

$$\frac{\partial U}{\partial \phi_{sat}} = \frac{\mu}{r} \sum_{l=2}^{\infty} \sum_{m=0}^{l} \left(\frac{R_\oplus}{r}\right)^l \cdot \{P_{l,m+1} \cdot [\sin(\phi_{sat})] - m \cdot \tan(\phi_{sat}) \cdot P_{l,m} \cdot [\sin(\phi_{sat})]\}$$
$$\cdot \{C_{l,m} \cdot \cos(m \cdot \lambda_{sat}) + S_{l,m} \cdot \sin(m \cdot \lambda_{sat})\}$$

$$\frac{\partial U}{\partial \lambda_{sat}} = \frac{\mu}{r} \sum_{l=2}^{\infty} \sum_{m=0}^{l} \left(\frac{R_\oplus}{r}\right)^l \cdot m \cdot P_{l,m} \cdot [\sin(\phi_{sat})] \cdot \{S_{l,m} \cdot \cos(m \cdot \lambda_{sat}) - C_{l,m} \cdot \sin(m \cdot \lambda_{sat})\}$$

with μ as the gravitational constant and $R_\oplus$ as the mean radius of the celestial body. l and m are degree and order of the gravitational potential. $P_{l,m}$ are the Legendre polynomials and $C_{l,m}$ as well as $S_{l,m}$ are the gravitational coefficients.

The derivatives of the position vector are (unit vectors):

$$\frac{\partial r}{\partial \vec{r}} = \frac{\vec{r}^T}{r}$$

$$\frac{\partial \phi_{sat}}{\partial \vec{r}} = \frac{1}{\sqrt{r_x^2 + r_y^2}} \left(-\frac{\vec{r}^T \cdot r_z}{r^2} + \frac{\partial r_z}{\partial \vec{r}}\right)$$

$$\frac{\partial \lambda_{sat}}{\partial \vec{r}} = \frac{1}{r_x^2 + r_y^2} \left(r_x \cdot \frac{\partial r_y}{\partial \vec{r}} + r_y \cdot \frac{\partial r_x}{\partial \vec{r}}\right)$$

The equations results in the following individual acceleration components:

$$a_x = \left\{\frac{1}{r} \cdot \frac{\partial U}{\partial r} - \frac{r_z}{r^2 \cdot \sqrt{r_x^2 + r_y^2}} \cdot \frac{\partial U}{\partial \phi_{sat}}\right\} \cdot r_x - \left\{\frac{1}{r_x^2 + r_y^2} \cdot \frac{\partial U}{\partial \lambda_{sat}}\right\} \cdot r_y$$

$$a_y = \left\{\frac{1}{r} \cdot \frac{\partial U}{\partial r} - \frac{r_z}{r^2 \cdot \sqrt{r_x^2 + r_y^2}} \cdot \frac{\partial U}{\partial \phi_{sat}}\right\} \cdot r_y + \left\{\frac{1}{r_x^2 + r_y^2} \cdot \frac{\partial U}{\partial \lambda_{sat}}\right\} \cdot r_x$$

$$a_z = \frac{1}{r} \cdot \frac{\partial U}{\partial r} \cdot r_z + \frac{\sqrt{r_x^2 + r_y^2}}{r^2} \cdot \frac{\partial U}{\partial \phi_{sat}}$$

The calculated acceleration components are used to consider the perturbation caused by the spherical harmonics.

Project: ESABASE2/Debris Release 12.1		Date:	2024-02-19
Technical Description		Revision:	1.11
Reference: R077-231rep_01_11_Debris_Technical Description.docx		Status:	Final

Due to the arranging of the functionality with the legacy implementation, the degree and order are limited to 8. An order of 8, however, must be considered as sufficient for the purpose of meteoroid analysis.

The gravitational coefficients are taken from the Goddard Lunar Gravity Model (GLGM-3) co-efficient table. The normalised values were un-normalized for the use with the theory by adapting the equation 8-22 of /43/.

The normalisation is described as:

$$\bar{S}_{l,m} = \Pi_{l,m} \cdot S_{l,m}$$

$$\bar{C}_{l,m} = \Pi_{l,m} \cdot C_{l,m}$$

with $\bar{C}_{l,m}$ and $\bar{S}_{l,m}$ as normalised coefficients and the transformation defined as:

$$\Pi_{l,m} = \sqrt{\frac{(l+m)!}{(l-m)! \cdot k \cdot (2l+1)}}$$
$$\text{with } k = 1 \text{ if } m = 0$$
$$k = 2 \text{ if } m \neq 0$$

The un-normalisation is then:

$$S_{l,m} = \frac{\bar{S}_{l,m}}{\Pi_{l,m}}$$

$$C_{l,m} = \frac{\bar{C}_{l,m}}{\Pi_{l,m}}$$

Consideration of spherical harmonics can be applied for orbits around Earth and Moon, only.

6.5 L1/L2 State Vector Generation

The definition of the state vectors of the L1/L2 orbits is based on a simplified approach. The simplification defines that a satellite is not moving on the complicated Lissajous orbit, which can only be numerically propagated by consideration of maintaining manoeuvres, but is directly at the L1/L2 position on the Sun-Earth connecting line. Furthermore it orbits the Earth with a period of 1 year. This allows analytically compute a state vector for the satellite. The method is listed in the following.

Position Vector:

- The simplification for the position vector is the assumption that the satellite position is equal to the position of the according libration point L1 respective L2.
- For the calculation of the position SAPRE functionality is used to define the Sun position in the geocentric equatorial coordinate system.

Project: ESABASE2/Debris Release 12.1		Date:	2024-02-19
Technical Description		Revision:	1.11
Reference: R077-231rep_01_11_Debris_Technical Description.docx		Status:	Final

FEV etamax GmbH   Page 147 / 173

- The norm of the vector is scaled with the factor 0.01, due to the fact that the Earth-L1/L2 distances are each ca. 1.5 millions of kilometres, which is roughly 1/100 of the Sun-Earth distance.
- In the case of L2 the vector is inverted, due to the L2 position on the opposite side of the Earth than the Sun.

Velocity Vector:

- The simplifications for the calculation of the velocity vector are the following;
    - The orbit is in the ecliptic plane, which results from the equivalence of the L1/L2 and the satellite positions.
    - The orbit is considered as circular.
    - The period of the orbit is 1 year and the rotation is positive around the z-axis of the ecliptic system. This is due to Earth's positive rotation around Sun and its period duration of 1 year.
- The previously calculated position vector is converted to the geocentric ecliptic coordinate system.
- The z-axis of the system is cross multiplied with the converted position vector.
- The resulting vector shows in the direction of the velocity. It is converted back to the geocentric equatorial coordinate system and normalised. This results in the normalised velocity vector.
- Based on the angular velocity ($\omega = 2\pi/P$, period duration P = 1 year) and the calculated L1 respective L2 distance (r), the norm of the velocity vector (v) is calculated to $v = \omega r$, since the orbit is assumed to be circular.
- The combination of the normalised vector and the norm provides the searched velocity vector.

After the calculation of the position and velocity vectors they can be combined to a state vector.

The Figure 6-4 shows a schematic not to scale illustration of the calculated state vector. For the reason of better understanding it is represent in the ecliptic coordinate system only, without the transformation to the equatorial coordinate system performed in the application. The difference of the magnitude of the "calculated velocity direction" and the "Velocity vector (ecliptic)" indicates the two steps of calculating the velocity vector; the calculation of the normalised velocity vector (Z_{ECL} X position vector, normalisation of the result) and the calculation of the velocity norm.

The Figure 6-5 illustrates the positions of the Sun-Earth libration points.

Project: ESABASE2/Debris Release 12.1		Date:	2024-02-19
Technical Description		Revision:	1.11
Reference: R077-231rep_01_11_Debris_Technical Description.docx		Status:	Final

FEV etamax GmbH   Page 148 / 173

Figure 6-4   **Schematic illustration of the calculated state vector in ecliptic coordinate system***.*

Figure 6-5   **Position of the Sun-Earth libration points (not to scale; credit: NASA/WMAP Science Team)***.*

Project: ESABASE2/Debris Release 12.1	Date:	2024-02-19
Technical Description	Revision:	1.11
Reference: R077-231rep_01_11_Debris_Technical Description.docx	Status:	Final

FEV etamax GmbH   Page 149 / 173

6.6 Interplanetary Analyses Trajectory Generation

For the use of ESABASE2 in interplanetary micrometeoroid risk assessments, the trajectory input can be given in two formats. These are a Consultative Committee for Space Data Systems' Orbit Ephemeris Message (CCSDS OEM) files and SPICE kernels, which will be introduced in the following. The SPICE application program interface (API) is used as common trajectory interface, which results in the necessity of converting the information from the OEM file to SPICE kernels. Furthermore, the stepping algorithm for the use of the new trajectory in the application of meteoroid environment models and the analyses in ESABASE2 is explained.

6.6.1 SPICE

ESABASE2 is able to handle trajectory information given via SPICE. SPICE is a toolkit developed by NASA's Navigation and Ancillary Information Facility (NAIF). It is mainly used to plan and interpret space-based observations as well as to overcome the engineering challenges for such observation missions /50/. This includes the possibility to analyse spacecraft trajectories.

In general, the toolkit offers APIs in FORTRAN, C, IDL and MATLAB. Within this activity, the C and FORTRAN API will be used. More concrete, the toolkit has libraries which offer several functions of data exchange and processing. In SPICE, the data itself is stored in different kind of kernels, e.g. spacecraft, planet, time or reference frame related kernels. For using SPICE in ESABASE2 the user is supposed to give the probe kernel while necessary supporting kernels will be loaded using a meta kernel. Also, these probe kernels are binary files. By using the SPICE API functions, the required trajectory points can be obtained from the kernel.

However, being able to create own kernels using OEM2SPK conversion (see Section 6.6.2.1) or bringing non-plausible trajectory kernels, the user has to ensure these trajectory files contain plausible data. For example, the user could generate new positional data for the Sun using an OEM file. As a result, this could fatally affect interplanetary analyses as well as pointing options within ESABASE2.

6.6.2 CCSDS/OEM

OEM was developed by the CCSDS along some other formats within the frame of defining standardized Orbit Data Messages /57/. An OEM file contains ephemeris information in form of Cartesian state vectors at given points of time. By additionally interpolating these state vectors positional as well as velocity information can be obtained for the whole trajectory.

For a better understanding Figure 6-6 shows the condensed version of the OEM example given in /57/, which will be used to briefly explain its structure and contents. In this context, only the most relevant aspects will be explained. For more detailed information, please refer to /57/.

The given example consists of three main parts:

- a header (lines one to three),
- meta-information (lines four to 14),
- the ephemeris information (lines 17 to 29).

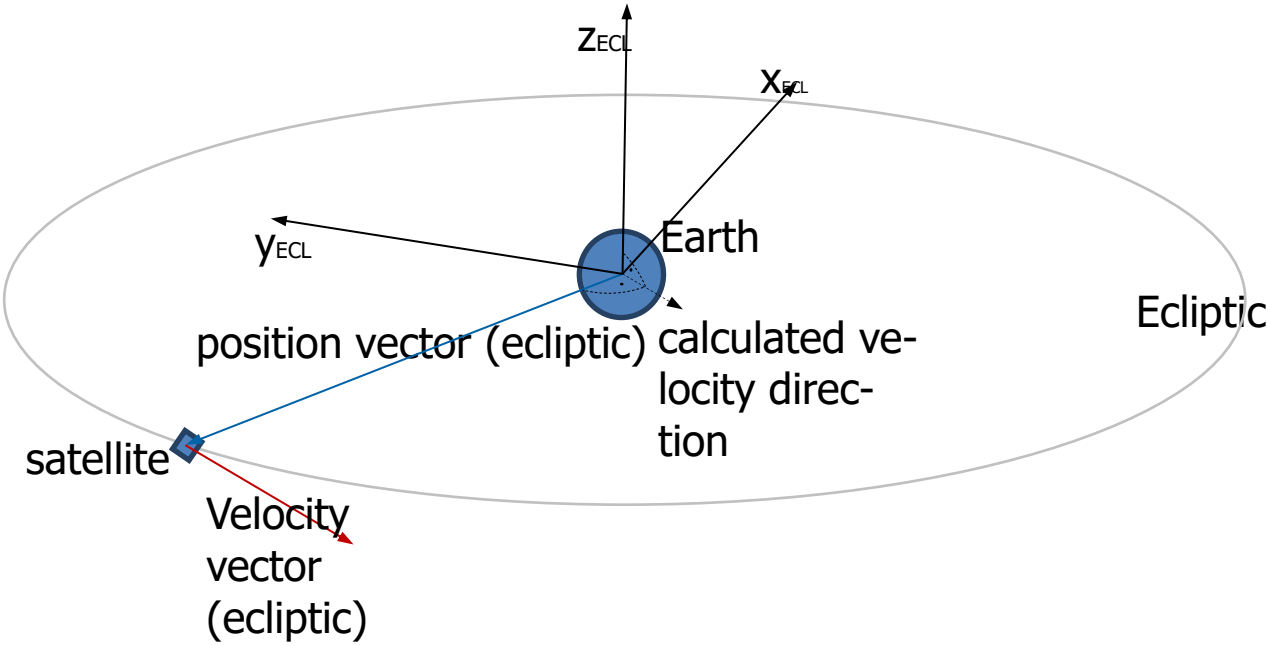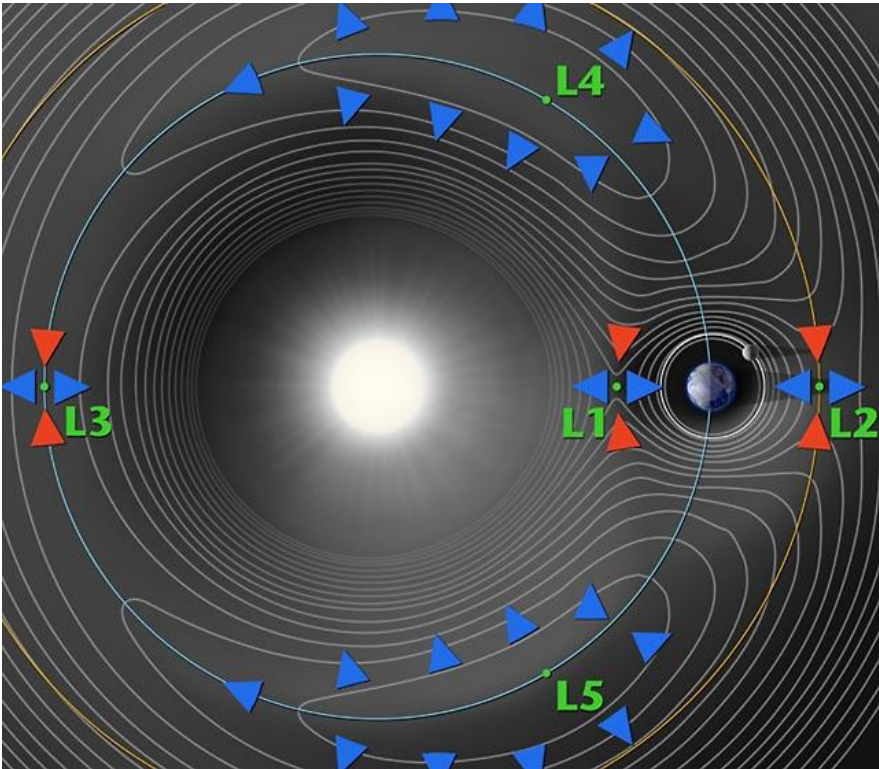| Project: ESABASE2/Debris Release 12.1 | Date: | 2024-02-19 |
| Technical Description | Revision: | 1.11 |
| Reference: R077-231rep_01_11_Debris_Technical Description.docx | Status: | Final |

FEV etamax GmbH   Page 150 / 173

The header indicates information about the file itself which is the OEM version applied as well as the creator and the creation date.

The block of metadata gives context information about the following ephemeris. This includes the object as well as the trajectory's centre name. For using the state vectors the reference system needs to be known and therefore, it has to be provided. Also, the time frame of the upcoming data as well as its format is specified. Further, for interpolating the state vectors a suggestion for the interpolation method and degree is given.

The ephemeris data is given in form of a time stamp plus position and velocity information in x, y and z direction, respectively.

Moreover, it has to be mentioned that it is possible to define more than one pair of metadata and ephemeris. This can be used to indicate changing the reference frame of the state vectors, e.g. when the central body changes.

```
 1  CCSDS_OEM_VERS = 2.0
 2  CREATION_DATE = 1996-11-04T17:22:31
 3  ORIGINATOR = NASA/JPL
 4  META_START
 5  OBJECT_NAME          = MARS GLOBAL SURVEYOR
 6  OBJECT_ID            = 1996-062A
 7  CENTER_NAME          = MARS BARYCENTER
 8  REF_FRAME            = EME2000
 9  TIME_SYSTEM          = UTC
10  START_TIME           = 1996-12-18T12:00:00.331
11  STOP_TIME            = 1996-12-18T12:12:00.331
12  INTERPOLATION        = HERMITE
13  INTERPOLATION_DEGREE = 7
14  META_STOP
15  COMMENT  This file was produced by M.R. Somebody, MSOO NAV/JPL, 1996NOV 04. It is
16  COMMENT  to be used for DSN scheduling purposes only.
17  1996-12-18T12:00:00.331  2789.619 -280.045 -1746.755  4.73372 -2.49586 -1.04195
18  1996-12-18T12:01:00.331  2783.419 -308.143 -1877.071  5.18604 -2.42124 -1.99608
19  1996-12-18T12:02:00.331  2776.033 -336.859 -2008.682  5.63678 -2.33951 -1.94687
20  1996-12-18T12:03:00.331  2776.033 -336.859 -2008.682  5.63678 -2.33951 -1.94687
21  1996-12-18T12:04:00.331  2776.033 -336.859 -2008.682  5.63678 -2.33951 -1.94687
22  1996-12-18T12:05:00.331  2776.033 -336.859 -2008.682  5.63678 -2.33951 -1.94687
23  1996-12-18T12:06:00.331  2776.033 -336.859 -2008.682  5.63678 -2.33951 -1.94687
24  1996-12-18T12:07:00.331  2776.033 -336.859 -2008.682  5.63678 -2.33951 -1.94687
25  1996-12-18T12:08:00.331  2776.033 -336.859 -2008.682  5.63678 -2.33951 -1.94687
26  1996-12-18T12:09:00.331  2776.033 -336.859 -2008.682  5.63678 -2.33951 -1.94687
27  1996-12-18T12:10:00.331  2776.033 -336.859 -2008.682  5.63678 -2.33951 -1.94687
28  1996-12-18T12:11:00.331  2776.033 -336.859 -2008.682  5.63678 -2.33951 -1.94687
29  1996-12-18T12:12:00.331  2776.033 -336.859 -2008.682  5.63678 -2.33951 -1.94687
```

Figure 6-6: **Example of a CCSDS OEM file (based on /57/)**

6.6.2.1 Use of OEM2SPK

For the conversion of the OEM file to a valid SPICE kernel, the publically available SPICE utility tool OEM2SPK is used (/58/). For detailed information on how to define OEM2SPK setup files, see /58/. An example file specifically used for E2/Di is shown in Figure 6-7. Here, the |*begindata* identifier introduces the block of setup parameter. First, the leapseconds file (*LEAPSECONDS_FILE*) path gets defined.

Project: ESABASE2/Debris Release 12.1		Date:	2024-02-19
Technical Description		Revision:	1.11
Reference: R077-231rep_01_11_Debris_Technical Description.docx		Status:	Final

FEV etamax GmbH   Page 151 / 173

```
 1
 2
 3    \begindata
 4
 5       LEAPSECONDS_FILE      = 'metaKernel.tm'
 6
 7       INTERPOLATION_METHOD = 'HERMITE'
 8
 9       INTERPOLATION_DEGREE = 11
10
11       STRING_MAPPING        = ( 'EME2000',  'J2000',
12                                 'TT',        'TDT'   )
13
14       NAIF_BODY_NAME        += ( 'JUICE' )
15       NAIF_BODY_CODE        += ( -28 )
16
17    \begintext
```

Figure 6-7:   Example setup file for the OEM2SPK utility tool.

Both *INTERPOLATION_METHOD* and *INTERPOLATION_DEGREE* define default interpolation parameters (interpolation method and degree, respectively). Being default parameters, they will only be used in case, they are not defined in the given OEM input file. When interpolation settings are given in the OEM file, those values will be used.

STRING_MAPPING is responsible for mapping terms which are differently defined in OEM and SPICE. For E2/Di, there are mainly two relevant terms that have to be mapped. As shown in the example, the OEM standard uses the term *EME2000* for the same reference system which is called *J2000*. Also, OEM's Terrestrial Time (*TT*) is known as Terrestrial Dynamical Time (*TDT*).

With *NAIF_BODY_NAME* and *NAIF_BODY_CODE*, it is possible to add additional pairs of NAIF bodies and IDs to the internal catalogue which is hard coded in the SPICE API.

6.6.3 Stepping Algorithm

With SPICE, a trajectory is described for a given time and the description with computed state vectors for the required epochs within the period of the trajectory. However, for the application of the meteoroid environment models and the analyses in ESABASE2 a set of orbital points including state vector and epoch needs to be defined.

The Stepping Algorithm automatically selects orbital points along the spacecraft trajectory. Changes in the expected impact fluxes are of interest for the impact risk assessment. The impact flux is highly depending on the spatial dust density of the passed space thus the variation of the spatial dust density is used as the basis for the step size modification. Orbital points may be inserted or removed to find a balance between acknowledging local spatial dust density variations and runtime optimization. After the Stepping Algorithm the user can manually add additional and/or remove single/multiple orbital points.

6.6.3.1 Default Step Size

SPICE trajectories do not provide any leads on a reasonable definition of dedicated orbital points. Without such reference points it was decided to generate orbital points with default

Project: ESABASE2/Debris Release 12.1		Date:	2024-02-19
Technical Description		Revision:	1.11
Reference: R077-231rep_01_11_Debris_Technical Description.docx		Status:	Final

FEV etamax GmbH   Page 152 / 173

equidistant temporal step size, at first. Since the time periods of the trajectories can vary between seconds (e.g. only one orbital point) and tens of years, the default time step needs to be adapted to the trajectory duration. Table 24 lists the default step sizes depending on the different trajectory durations. The step sizes end at 100 years trajectory duration, which appears to be a reasonable duration for an absolute maximum of a spacecraft trajectory.

Table 24: **Default step sizes for different trajectory durations**

Considered trajectory duration up to:	Default step size
10 hours	10 minutes
10 days	1 hour
1 year	1 day
2 years	2 days
5 years	5 days
20 years	10 days
40 years	20 days
60 years	30 days
80 years	40 days
100 years	50 days

6.6.3.2 Density Grid

In order to retrieve density information for a given trajectory a density grid based on the IMEM2 meteoroid model (r=0.1 - 5.93 AU; z=-3.5 - 3.5 AU) is used. It stores pairs of fixed positions and the associated spatial number density as a simple ASCII table. Figure 6-8 depicts a contour plot of the density grid. The densities are colour-coded.

Project: ESABASE2/Debris Release 12.1		Date:	2024-02-19
Technical Description		Revision:	1.11
Reference: R077-231rep_01_11_Debris_Technical Description.docx		Status:	Final

FEV etamax GmbH   Page 153 / 173
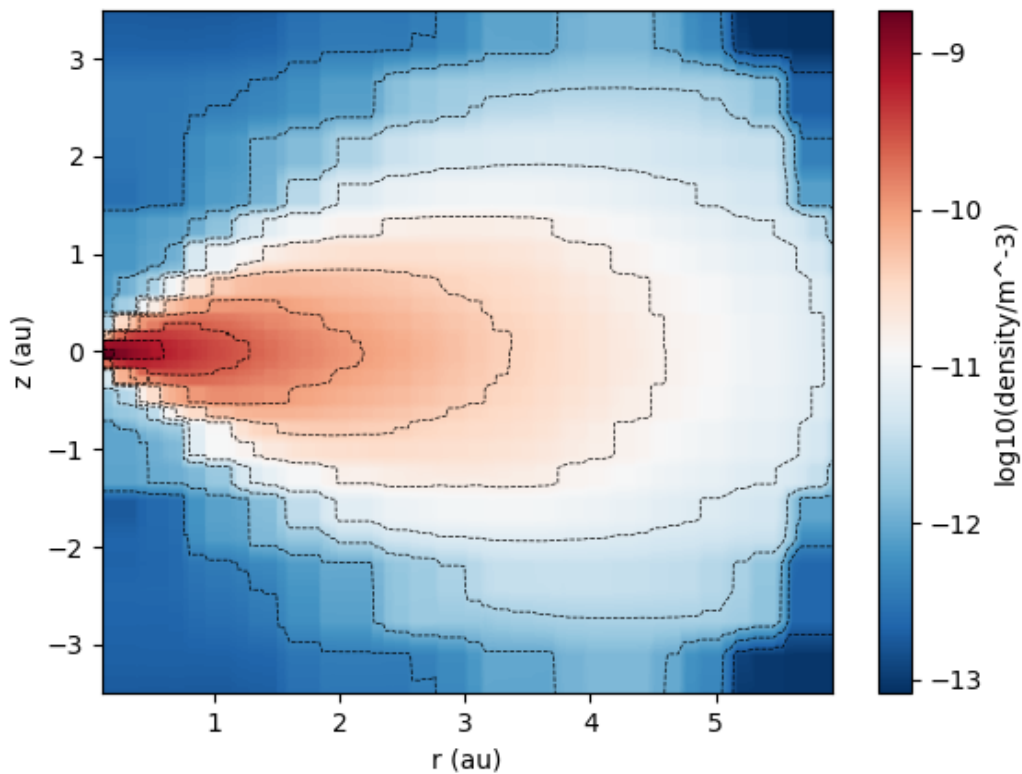
Figure 6-8: **Contour plot of IMEM2 300x100 12.5 micron density grid**

For establishing the density grid, 30000 regular logarithmic distributed grid points were considered. The spatial resolution in r is set to 300 and in z to 100 points acknowledging the grid size and different spatial density distributions in the two directions. Figure 6-9 displays the logarithmic density grid point distribution.

Project: ESABASE2/Debris Release 12.1	Date:	2024-02-19
Technical Description	Revision:	1.11
Reference: R077-231rep_01_11_Debris_Technical Description.docx	Status:	Final

FEV etamax GmbH   Page 154 / 173
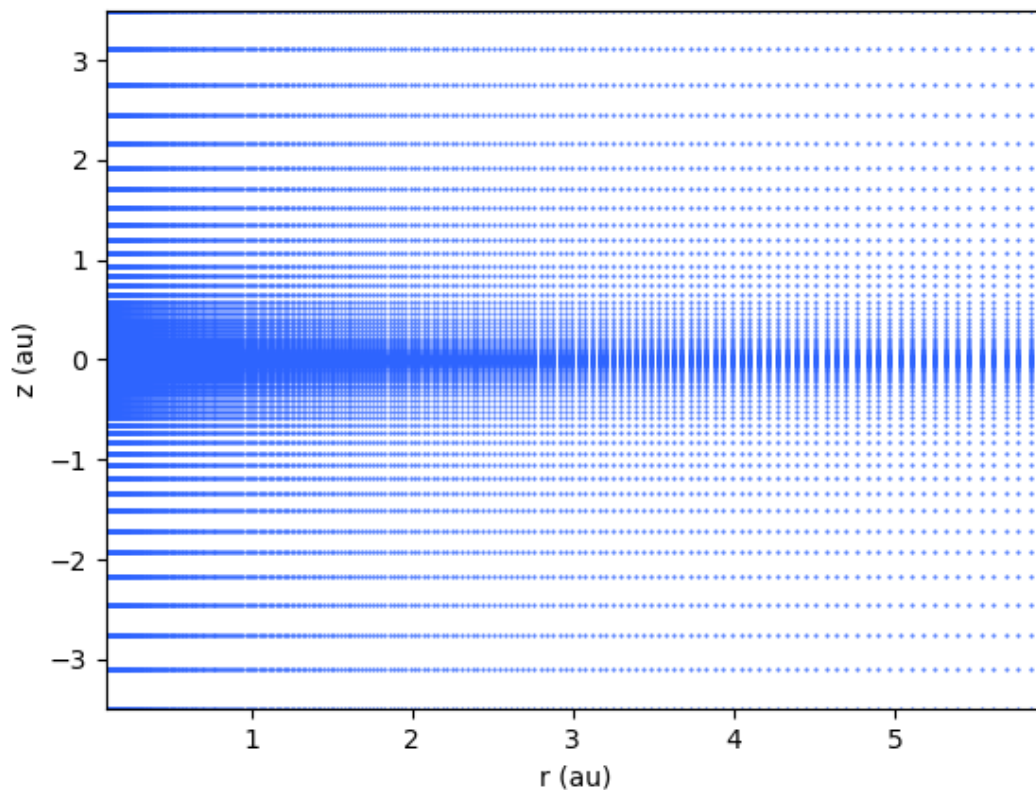
Figure 6-9: Logarithmic density grid point distribution (300x100)

The grid points were processed by IMEM2 in order to obtain number densities of the 12.5 micron size group for each point of the grid. Testing showed that using the 12.5 micron size group results in a smooth spatial dust density distribution across multiple orders of magnitude resulting in a conservative step size variation. Since IMEM2 is rotationally symmetric around the z-axis pointing to ecliptic north pole only a two-dimensional grid is required.

IMEM2 stores information on different sizes and object types in an octree bin structure. Each octree bin has a different size. Therefore, density values are obtained by a bilinear interpolation from a regular logarithmic grid yielding the IMEM2 spatial dust density information.

6.6.3.3 Obtaining densities

In order to obtain densities for orbital points of a given trajectory a bilinear interpolation between the densities of the nearest four surrounding grid points is applied. Figure 6-10 depicts a sample trajectory inside the density grid. The densities of the four grid points are displayed by n_{11}, n_{12}, n_{21}, n_{22}. They are weighted by the distance between the evaluated orbital point and the grid point on the opposite side in each direction.

Project: ESABASE2/Debris Release 12.1		Date:	2024-02-19
Technical Description		Revision:	1.11
Reference: R077-231rep_01_11_Debris_Technical Description.docx		Status:	Final
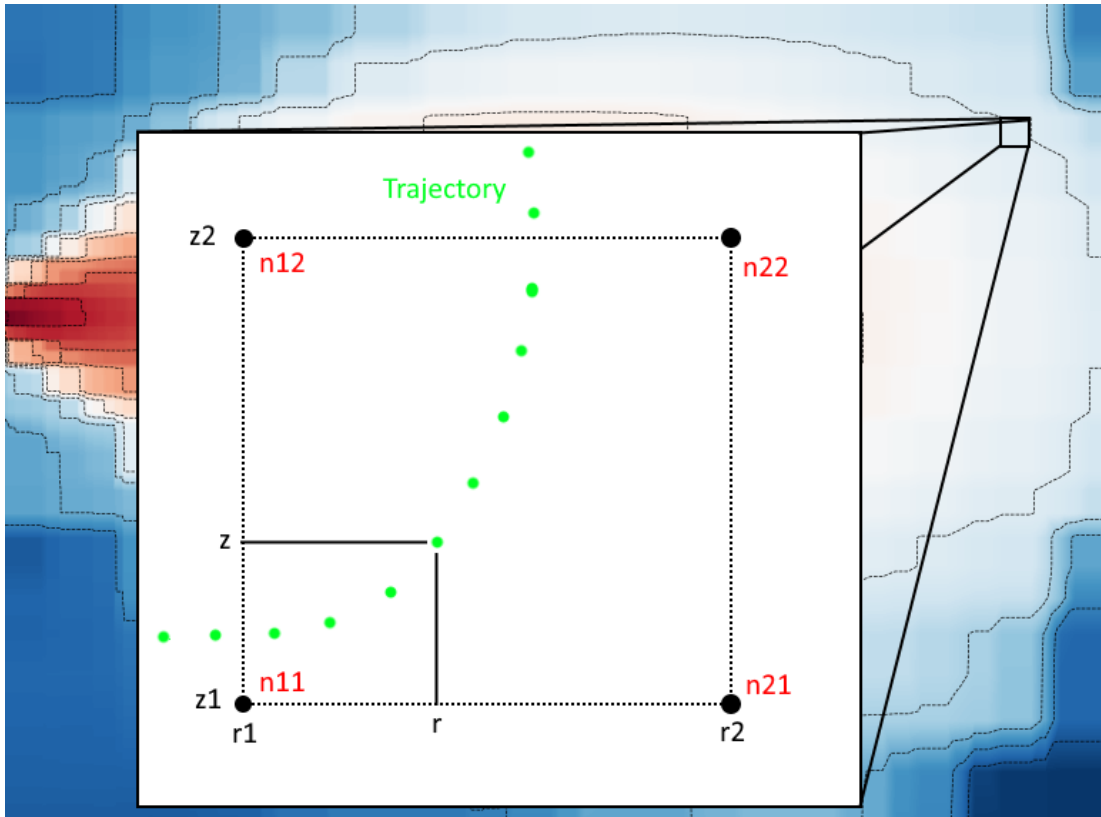
Figure 6-10:   Bilinear interpolation between density grid points

6.6.3.4 Thresholds

The Stepping Algorithm evaluates local density gradients between two consecutive orbital points and decides by two thresholds whether to insert or remove further orbital points. There is a removal (< 5%) and an insertion threshold (> 50%) meaning that orbital points with local density gradients lower than 5% are removed from the stepped trajectory and where local density gradients are higher than 50% a new OP is inserted.

$$\left|1 - \frac{n_{i,\,12.5\mu m}}{n_{i-1,\,12.5\mu m}}\right| = n_{\text{gradient}} = \begin{cases} n_{\text{gradient}} > 0.50, insert\ OP\ at\ t_{\text{new}} = t_i - \dfrac{(t_i - t_{i-1})}{2} \\ 0.05 < n_{\text{gradient}} < 0.50, do\ nothing \\ n_{\text{gradient}} < 0.05, remove\ \text{i-th}\ OP \end{cases}$$

Project: ESABASE2/Debris Release 12.1		Date:	2024-02-19
Technical Description		Revision:	1.11
Reference: R077-231rep_01_11_Debris_Technical Description.docx		Status:	Final

FEV etamax GmbH   Page 156 / 173

7 Pointing Facility

7.1 Introduction

A system (for example, a spacecraft) in orbit is subject to various environmental effects, such as solar illumination, the gravitational field, the atmosphere and so on. These effects appear as forces and torques which affect the orbital position and attitude of the system (e.g. aerodynamic, radiation effects) or as material degradation (e.g. surface recession due to the atomic oxygen fluence) and depend strongly on the geometrical configuration of the system, on its orbital orientation and on the orbital position and velocity of the system.

In order to compute these effects accurately, the articulating capabilities of the bodies of the system have to be properly modelled. For example, a central body(Earth, Moon)-oriented system may assume a solar array articulating capability within angular constraints in order to track the direction of the Sun. With such a system, changes in the solar panel orientation with respect to the velocity vector and/or the sun significantly alter the resulting effects (e.g. torques, forces, surface degradation) on the system.

The orientation of the various bodies of an articulated system along an orbital trajectory is computed by the ESABASE2 pointing facility. The pointing facility computes the best possible pointing of each body of a configuration of an articulated system to be oriented in its required pointing direction starting with the prime body.

The pointing facility is described in detail in ref. /40/. This section will introduce the modifications and extensions performed to allow the application to lunar orbits.

7.2 Modification of the Pointing Facility for Lunar Missions

The majority of the transformation matrices in the pointing facility are generated based on the spacecraft state vector. Due to this fact they can be used for the different celestial bodies, centre of motions, as long as the state vectors are given in the according coordinate system. Also the pointing to Earth was calculated. To allow the use of a geometry for both, Earth and lunar missions, the pointing EARTH was redefined in pointing CENTRALBODY. The calculation was kept due to the general approach.

The pointing to Earth, which is for Earth orbits equal to pointing to central body, is nevertheless a direction of interest. Thus, also a pointing EARTH is introduced again, but it is calculated in a different way.

For the analysis of lunar missions, the pointing directions: NONE, CENTRALBODY, EARTH, SUN, VELOCITY and FIXED are available. According to the previous information EARTH and SUN are pointing options, which depending on the position relative to the centre of motion and thus need to be handled individually.

To define the pointing to Earth the following new reference frame was introduced:

EARTHLEQ: selenocentric/planetocentric, Earth-fixed, tilted lunar/planet equator system:

Project: ESABASE2/Debris Release 12.1	Date:	2024-02-19
Technical Description	Revision:	1.11
Reference: R077-231rep_01_11_Debris_Technical Description.docx	Status:	Final

FEV etamax GmbH   Page 157 / 173

- x within the orbital plane, towards the true Earth position of date
- z perpendicular to x in the direction of the north
- y within the equatorial plane, completes the right hand system x, y, z

The frame is deduced from the selenocentric/planetocentric inertial by rotating the x-axis by α_S around z to the intersection of the meridian of the true Earth with lunar/planet equator, and the subsequent rotation by δ_S around y' to the true Earth position of date. The transformation is depicted in Figure 7-1.
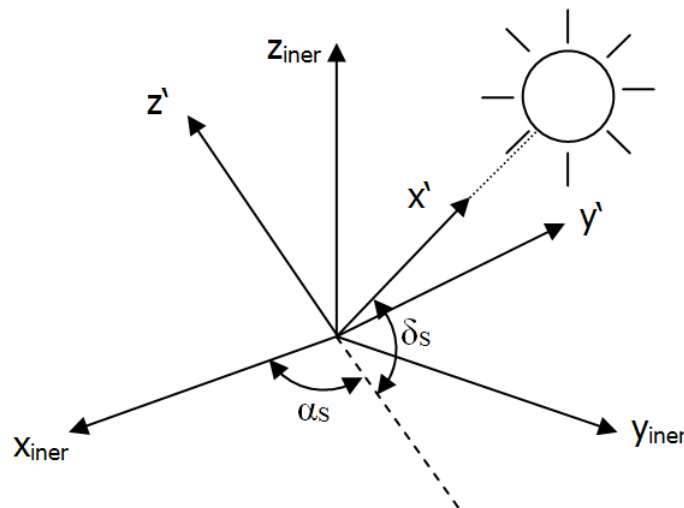
Figure 7-1   Selenocentric inertial ($_{iner}$) to EARTHLEQ (').

The position vectors of Sun and Earth, which are used to generate the transformation matrices, are calculated for lunar orbits according to the process described in section 6.3. In this way the both pointing possibilities are individualised for the different centres of motion.

7.3 Modification of the Pointing Facility for Interplanetary Missions

To realize a pointing to further reference objects (e.g. planets) for interplanetary missions (only available in this mission mode), the user is able to select the new pointing option NAIFID. This option allows to give the NAIF ID of reference objects. It is essential that this reference object is existing in the meta-kernel provided for the meteoroid analysis.

Since SPICE is already used for interplanetary missions, it will be also used for pointing applications. During ESABASE2's pointing algorithm, the pointing direction is determined in Gamma-50's inertial, equatorial reference frame first with the reference epoch of 1/1/1950 0:00. Afterwards, it gets transformed into system coordinates. Hence, SPICE was implemented to get necessary object positions to calculate the pointing direction. Since SPICE does not naturally offer Gamma-50 positions, positions in the J2000 reference frame are used. This neglects the precession difference between the two reference frames (tool internal comparison shows deviation of relative rotation to be clearly less than 1%). However, considering this use case, it

Project: ESABASE2/Debris Release 12.1		Date:	2024-02-19
Technical Description		Revision:	1.11
Reference: R077-231rep_01_11_Debris_Technical Description.docx		Status:	Final

FEV etamax GmbH   Page 158 / 173

is an acceptable approach. This inertial information will then be transformed to the system reference frame like it is done for the other pointing options.

The J2000 pointing direction can be obtained by using the following the following equation:

$$r_{J2000,pdir} = r_{J2000,probe} - r_{J2000,rObj},$$

where $r_{J2000,pdir}$ is the pointing direction vector, $r_{J2000,probe}$ the position of the probe and $r_{J2000,rObj}$ the position of the pointing reference object, each in the J2000 reference frame.

8 Trajectory File Handling

The use of a trajectory file allows providing the track of a mission by a list of state vectors with according epochs. In this way the generation/propagation of one defined orbit is not necessary and the trajectories can be more complex. Beside the state vectors the file provides also the starting and targeted celestial body for the trajectory. The description of the structure and an example of a trajectory file can be found in /44/.

After the parsing of the file, the retrieved information is analysed, the according central body (centre of motion) is defined and if required the state vector is transformed to the central body coordinate frame.

The definition of the according centre of motion is based on the sphere of influence (SOI) of the corresponding celestial body. The SOI express an abstracted spherical space where the gravity of a body has effect of other objects in space. The SOIs are designed as constants for the used celestial bodies. They are calculated according to the equation from /45/:

$$R_S = D \cdot \left(\frac{m}{M} \right)^{2/5}$$

where R_S is the radius of the sphere of influence, m is the mass of the smaller body in the system, which SOI is calculated, M is the mass of the bigger body in the system and D is the distance between the bodies. For the SOI of the Moon the Earth-Moon system is considered, which means m = mass of the Moon and M = mass of the Earth. For the SOI of the Earth the Sun-Earth system is examined, which means m = mass of the Earth and M = mass of the Sun. To have a little buffer for the model application (LunarMEM) the calculated values of SOIs are slightly lowered and defined to:

- Lunar SOI: 66000 km radius around Moon
- Earth SOI: 924000 km radius around Earth.

To define the centre of motion the SOIs of the start and target celestial bodies are compared and the lower SOI is used for the first check. This ensures that objects in the SOI of the Moon are mapped to Moon and not to Earth, which could happen because the Moon and also the object on a lunar orbit are in the SOI of the Earth. If the object is outside of both SOIs (Earth's and Moon's) the program currently stops because interplanetary missions are not implemented.

In case of the analysis of L1/L2 orbits the Earth SOI is virtually extended to 3 Mio km. The reason is that the libration points have a distance of ca. 1.5 Mio km from Earth, and thus are outside of the "normal" Earth SOI. The application of doubled distance should allow more flexibility for the provided trajectory. L1 and L2 orbits are only applicable with Earth as the origin celestial body.

The estimation of the presence in a SOI is performed by the check of the distances between the object and the both bodies. If the distance to the body with the smaller SOI is lower than the according radius, the centre of motion is the checked body; else if the object is in the bigger SOI than the according body is the centre of motion.

For the distance check the state vectors of the bodies are calculated in the coordinate frame that is used for the state vectors of the spacecraft in the trajectory file. This is done by the calculation of the body position in the ecliptical vernal equinox frame of J2000.0 according to /42/, which allows calculating the classical orbital elements of the celestial body by providing time dependant reference values for the different planets and the Moon. The classical elements are converted using legacy functionalities to a state vector. Afterwards the state vector is rotated to the used coordinate frame as described in 6.3 exemplarily for the Moon frame. The calculated celestial body state vectors are stored for possible later transformation of the S/C vectors.

After the definition of the centre of motion (central body) to a point it is checked if the frame of the S/C state vectors is the frame of the central body, if not the vector is transformed. To achieve the state vector of the S/C relative to the central body, the stored state vector of the central body in the frame of trajectory file is subtracted from the state vector of the S/C in the same frame. The Figure 8-1 illustrates the process; the red state vector is the achieved result.
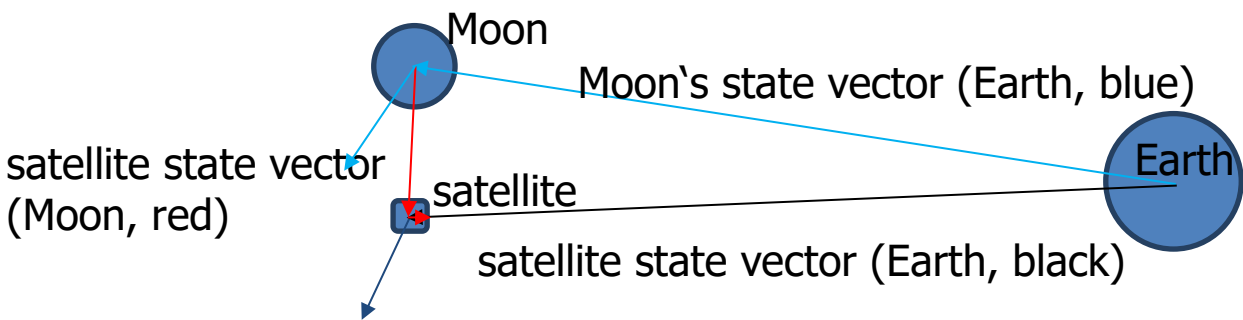
Figure 8-1 **Calculation of the S/C state vector relative to the central body**.

After the calculation of the S/C state vector relative to the centre of motion it is rotated in the corresponding frame of the central body according the exemplarily description in 6.3.

The calculated state vectors in the according central body frame are stored and provided to the data model of ESABASE2/Debris for the further use in the analysis.

Annex A   Particle Flux on Orbiting Structures

A.1   Introduction

Two factors interfere with the particle impact flux computation on an orbiting spacecraft, namely:

1) The influence of the spacecraft velocity on the impacting flux, referred to as the „k" or "f_t" factor in several papers, and

2) The Earth shielding of the omni-directional particle flux.

The presented results are implemented in the upgraded ESABASE2/DEBRIS software.

It is assumed that the particle flux is omni-directional, i.e. no direction is preferential. This corresponds to the Grün sporadic meteoroid flux model.

The influence of the spacecraft velocity will first be investigated for two factors:

1) The "f_t" factor describing the relation between the flux on a moving oriented surface element and the flux on a virtual stationary surface element.

2) The "k_f" factor describing the relation between the flux on the forward side of a moving, oriented surface (or plate) to the average flux on the surface (average = 0.5·[forward + lee fluxes]).

As will be seen, these two factors are linked and depend on the orientation of the surface element. Drawn from the above two factors, two additional factors can be defined:

3) The "f_t" factor, which is obtained by evaluating the f_t factor on three perpendicular planes, which corresponds to the ratio between the flux on a moving "random tumbling" surface element and the flux on a virtual stationary surface element. This factor can also be used for the total flux increase on a symmetric spacecraft.

4) The "k" factor, which is the ratio between the flux on the forward side of a surface element (or plate) to the flux on a virtual stationary randomly oriented surface element.

A.2   Theoretical Description of the Particle Impact Flux on a Moving Plate

A.2.1   General Description

For the general case, we need to consider an omni-directional particle flux and an arbitrary direction of motion of the plate.

Project: ESABASE2/Debris Release 12.1		Date:	2024-02-19
Technical Description		Revision:	1.11
Reference: R077-231rep_01_11_Debris_Technical Description.docx		Status:	Final

FEV etamax GmbH   Page 162 / 173

Let us first consider the situation depicted in fig. A-1 of a particle hitting the moving plate under an angle α_i. The plate is moving with a velocity $\vec{v}_s$. $\vec{v}_s$ makes an angle β with the surface normal vector $\vec{s}$.

The impacting flux from the particles impinging with the velocity $\vec{v}_i$ on the plate is obtained by the product between the particle probability, the scalar impact velocity and the cosine of the angle between impact velocity and surface normal. The latter can be described by the scalar product between the impact velocity $\vec{v}_i$ and the surface element normal vector $\vec{s}$:

Figure A-1 Oblique flux on a plate moving in an arbitrary direction

$i = n(v_m) \cdot \vec{s} \cdot \vec{v}_i$ where n(v_m) is the probability of a particle arriving with a velocity v_m, taken from the velocity distribution.

The impact velocity can be expressed as: $\vec{v}_i = \vec{v}_m + \vec{v}_s$, where $\vec{v}_s$ is chosen positive in the direction towards the plate.

Using the distributivity of the vector sum with respect to the scalar product, we obtain:

$$i = n(v_m) \cdot \vec{s} \cdot (\vec{v}_m + \vec{v}_s) = n(v_m) \cdot (\vec{s} \cdot \vec{v}_m + \vec{s} \cdot \vec{v}_s) = n(v_m) \cdot s \cdot (v_m \cos\alpha + v_s \cos\beta) \quad (9)$$

In order to assess the complete situation, we must evaluate the integration limits of the particle angle α of the whole „captured" spherical portion seen by the plate. The situation is best illustrated with a 2D sketch, see fig. A-2 below.
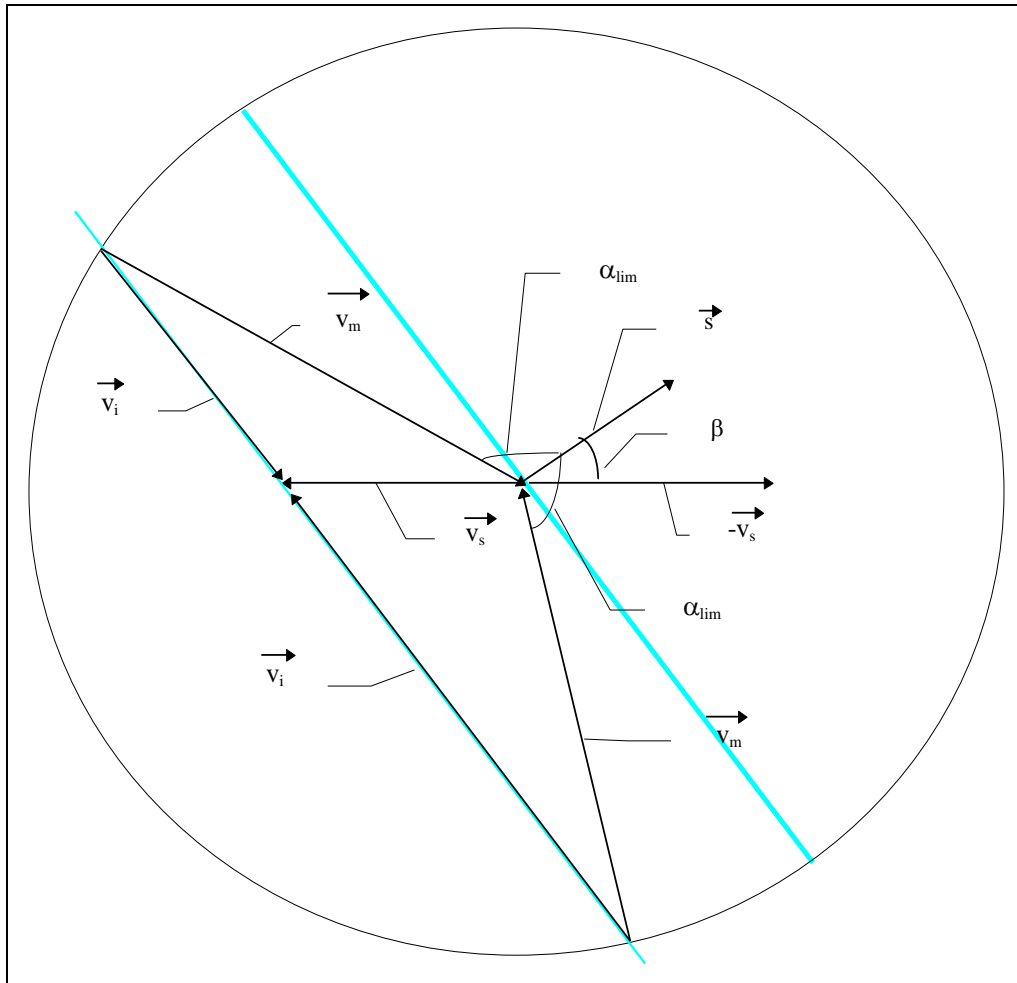
Figure A-2 Integration limits for an arbitrary direction of motion

As can be seen in the figure above, the grazing impact directions allow computing the limit particle directions knowing that the scalar product in this case is zero:

$$\vec{v}_i \cdot \vec{s} = \vec{v}_m \cdot \vec{s} + \vec{v}_s \cdot \vec{s} = 0 \quad .$$

The numerical expression of the limit angle, which is constant around the whole captured sphere, is:

$$\cos \alpha_{\text{lim}} = \frac{- v_s \cdot \cos \beta}{v_m} \qquad\qquad (\ 10 \ )$$

In order to obtain the total impact flux I on the plate, we must integrate over the sphere captured by the plate and the velocity distribution:

$$I = \int\limits_{0}^{\infty} \int\limits_{0}^{\alpha_{\text{lim}}(v_m)} di$$

$$di = i(v_m, \alpha) \cdot ds = n(v_m) \cdot (\vec{v}_i \cdot \vec{s}) \cdot 2\pi \sin \alpha \cdot d\alpha \cdot dv_m$$

$$di = 2\pi \cdot n(v_m)(v_m \cos \alpha + v_s \cos \beta) \sin \alpha \cdot d\alpha \cdot dv_m$$

Project: ESABASE2/Debris Release 12.1		Date:	2024-02-19
Technical Description		Revision:	1.11
Reference: R077-231rep_01_11_Debris_Technical Description.docx		Status:	Final

FEV etamax GmbH · Page 164 / 173

$2\pi \sin\alpha \bullet d\alpha$ is the surface integration argument computed from the integration over φ of the spherical surface differential $\sin\alpha \bullet d\varphi \bullet d\alpha$.

We thus obtain the following integral:

$$I = \int_0^\infty \int_0^{\alpha_{lim}} 2\pi \cdot n(v_m) \cdot \left(v_m \cos\alpha + v_s \cos\beta\right) \cdot \sin\alpha \cdot d\alpha \cdot dv_m \qquad (11)$$

α_{lim} is obtained from equation (17).

A.2.2 Particle Flux on a Plate with Unique Particle Velocity

We shall first consider the situation where the particles have a unique velocity.

With a unique particle velocity, equation (18) boils down to a single integral:

$$I = 2\pi \cdot n_0 \int_0^{\alpha_{lim}} \left(v_m \cos\alpha + v_s \cos\beta\right) \cdot \sin\alpha \cdot d\alpha$$

with n_0 being the probability of a particle arriving from a random direction. This integral can easily be solved analytically:

$$I = 2\pi \cdot n_0 \int_0^{\alpha_{lim}} \left(v_m \cos\alpha + v_s \cos\beta\right) \cdot \sin\alpha \cdot d\alpha$$

Substituting and solving the equations, we finally obtain:

$$I = \frac{\pi \cdot n_0}{v_m} \left(v_m + v_s \cos\beta\right)^2$$

The above expression for I permits the analytical computation of the k and f_t factors. The f_t factor needs the total flux on an orbiting structure:

For an oriented plate:
$$I_{tot} = \frac{\pi \cdot n_0}{v_m} \left[\left(v_m + v_s \cos\beta\right)^2 + \left(v_m - v_s \cos\beta\right)^2\right]$$

For the case with $v_s = 0$: $I_{tot} = 2\pi n_0 v_m$.

We can now derive the analytical expressions of the two factors:

$$k_f = \frac{2 \cdot I\left(+v_s\right)}{I\left(+v_s\right) + I\left(-v_s\right)} \qquad (12)$$

$$f_t = \frac{I_{tot}\left(v_s\right)}{I_{tot}\left(v_s = 0\right)} \qquad (13)$$

A spacecraft can be symbolised by a regular box, moving with one side normal to the flight direction, i.e. two sides with β = 0 and four sides with β = 90°. This of course implies a symmetrical spacecraft structure. We can now derive the f_t^t factor for the whole spacecraft:

$$f_t^{\,t} = \frac{1}{6v_m^2}\left[4v_m^2 + (v_m + v_s)^2 + (v_m - v_s)^2\right] = \frac{6v_m^2 + 2v_s^2}{6v_m^2}$$

We finally obtain:

$$f_t^{\,t} = 1 + \frac{v_s^2}{3v_m^2} \qquad\qquad (\,14\,)$$

In the same way one can compute the k factor:

$$k = \frac{I(+v_s)}{I(v_s = 0)} = \frac{2 \cdot I(+v_s)}{I(+v_s) + I(-v_s)} \cdot \frac{I(+v_s) + I(-v_s)}{2 \cdot I(v_s = 0)} = f_t \cdot k_f \qquad (\,15\,)$$

Tables A-1 and A-2 below show the f_t, k_f and k factors for two velocity values and a set of values of β.

$$I^{*+} = \frac{I(+v_s)}{\pi n_0 v_m}$$

$$I^{*}_{\,tot} = \frac{I_{tot}(+v_s)}{\pi n_0 v_m}$$

Case 1: $v_s = v_m$

β [deg]	0	15	30	45	60	75	90
I^{*+}	4	3.86	3.48	2.91	2.25	1.58	1
I^{*}_{tot}	4	3.87	3.5	3.0	2.5	2.13	2
k_f	2.0	1.99	1.99	1.94	1.8	1.49	1.0
k	4.0	3.84	3.48	2.91	2.25	1.59	1.0
f_t	2.0	1.93	1.75	1.5	1.25	1.07	1.0

Table A-1   Analytical values for k and f_t with $v_s = v_m$

f_t^t = 1.333

Case 2: v_s = 7.6 km/s; v_m = 16.8 km/s

β [deg]	0	15	30	45	60	75	90

Project: ESABASE2/Debris Release 12.1		Date:	2024-02-19
Technical Description		Revision:	1.11
Reference: R077-231rep_01_11_Debris_Technical Description.docx		Status:	Final

FEV etamax GmbH   Page 166 / 173

I^{*+}	2.11	2.06	1.94	1.74	1.5	1.25	1
I^{*}_{tot}	2.41	2.38	2.31	2.2	2.1	2.03	2
k_f	1.75	1.73	1.68	1.58	1.43	1.23	1.0
k	2.1	2.06	1.93	1.74	1.5	1.24	1.0
f_t	1.2	1.19	1.15	1.1	1.05	1.01	1.0

Table A-2   Analytical values for k and f_t with v_s = 7.6 km/s; v_m = 16.8 km/s

$f_t^t = 1.068$

A.2.3 Particle Flux on a Plate with a given Velocity Distribution

The general expression of I is given by equation (18) in paragraph A.2.1 Proceeding as in the previous section, we can solve the first integration step (over α). We now have the following equation:

$$I = \int_0^\infty \frac{\pi}{v_m} n(v_m) \cdot (v_m + v_s \cos\beta)^2 \, dv_m \qquad (16)$$

In order to proceed further, we need to define the form of the velocity distribution $n(v_m)$.

An easy way to approach the velocity distribution is to define a function composed of a series of straight curves as depicted in figure A-3. Actually most velocity distributions can be approximated with such a function.

To derive the general formulation for I, let's integrate the portion of the velocity function between v_1 and v_2:

$$v_1 < v_m < v_2 \qquad n(v_m) = n_2 + (n_1 - n_2)\frac{v_2 - v_m}{v_2 - v_1}$$
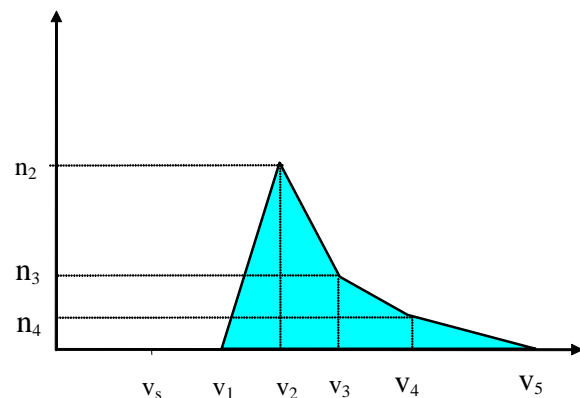
Figure A-3 Generalised velocity distribution

In fig. A-3, one can split the integration into four steps.

An integration step I_2 between v_1 and v_2 becomes:

$$I_2 = \pi \int_{v_1}^{v_2} (n_2 + \frac{(n_1 - n_2)(v_2 - v_m)}{v_2 - v_1}) \frac{(v_m + v_s \cos\beta)^2}{v_m} \cdot dv_m$$

The above expression can be analytically solved. This process is described in (Ref /15/). One finally obtains:

$$I = \pi \sum_{i=2}^{m} \left\{ \frac{2n_i + n_{i-1}}{6} v_i^2 - \frac{2n_{i-1} + n_i}{6} v_{i-1}^2 + \frac{n_{i-1} - n_i}{6} v_i v_{i-1} + (n_{i-1} + n_i) v_s \cos \beta (v_i - v_{i-1}) \right. $$

$$\left. + (n_i - n_{i-1}) v_s^2 \cos^2 \beta + \frac{n_{i-1} v_i - n_i v_{i-1}}{v_i - v_{i-1}} v_s^2 \cos^2 \beta \cdot \ln \left(\frac{v_i}{v_{i-1}} \right) \right\} \quad (17)$$

Equation (24) above is easily programmable. The two standard meteoroid velocity distributions, the NASA 90 model and the Cour-Palais model were approximated with 5 (n;vm) points and computed with equation (24). The results are presented in tables A-3 and A-4.

For comparison with the data in chapters A.2.2 and A.3, the plate velocity was set at 7.6 km/s.

Analytical flux computation of the NASA 90 model

The NASA 90 velocity distribution can be approximated as follows:

Velocity	Normalised Probability
11.0	1.0
15.2	1.0
20.0	0.25
28.0	0.03
50.0	0.0
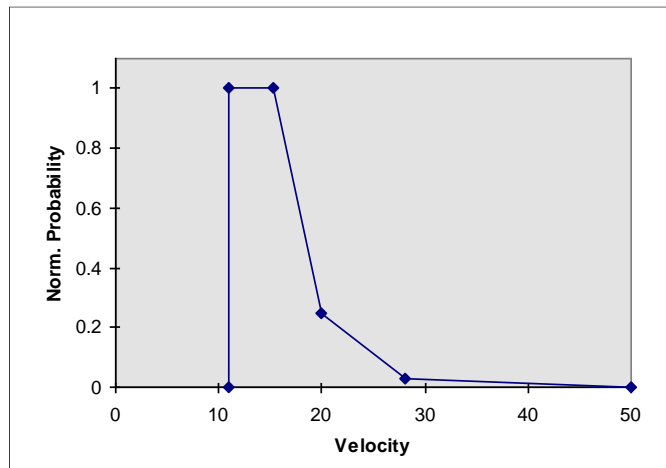
The analysis over the above velocity distribution with equation (24) gives the following results:

	$v_s = 0$	$v_s = 7.6$						
β [deg]	N/A	0	15	30	45	60	75	90
Flux positive	451.6	966	945.1	885.3	794.3	683.5	565.3	451.6
Flux total	903.2	1106	1092	1055	1005	953.8	916.8	903.2
k_f factor	1.0	1.75	1.73	1.68	1.58	1.43	1.23	1.0

Project: ESABASE2/Debris Release 12.1		Date:	2024-02-19
Technical Description		Revision:	1.11
Reference: R077-231rep_01_11_Debris_Technical Description.docx		Status:	Final

FEV etamax GmbH   Page 168 / 173

	$v_s = 0$	$v_s = 7.6$						
β [deg]	N/A	0	15	30	45	60	75	90
k factor	N/A	2.14	2.09	1.97	1.75	1.52	1.25	1.0
f_t factor	N/A	1.22	1.21	1.17	1.11	1.06	1.015	1.0

<p style="text-align:center">Table A-3   Results with $v_s = 7.6$, NASA 90 Velocity distribution</p>

The f_t^t factor amounts to 1.075.

Comparing table A-3 to table A-2, the results are very close.

A.3 Validation of the numerical Approach with Ray Tracing

A.3.1 General

In order to assess the behaviour of the ray tracing technique implemented in ESABASE and also to double-check the analytical derivations of chapter A.2, two computer programs were written to numerically simulate the effects of an omni-directional particle flux environment on a moving plate:

-   The first program simulated the true environment, firing rays randomly from a sphere onto a plate
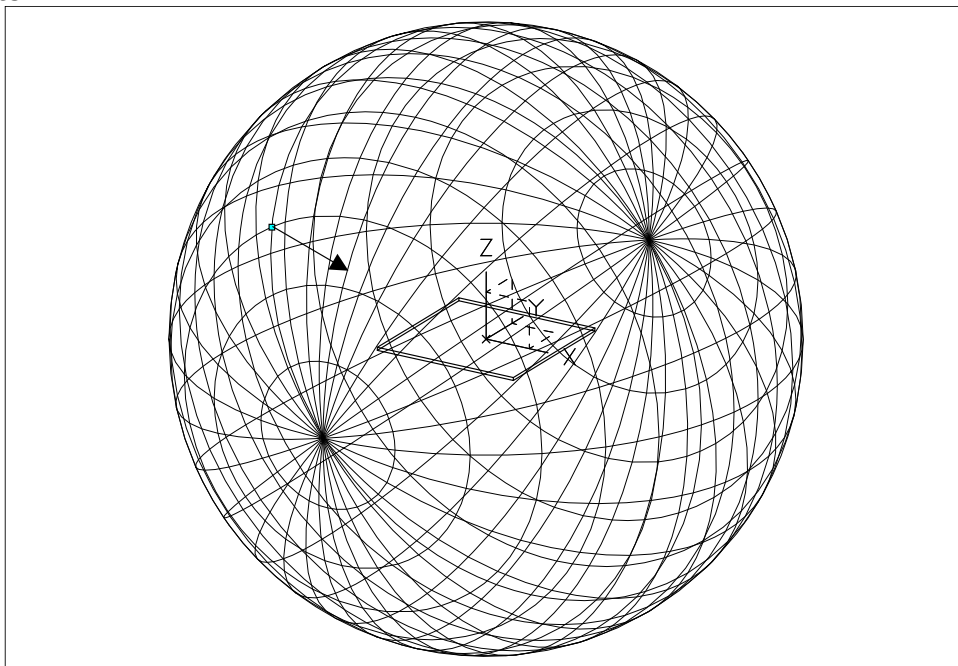
Project: ESABASE2/Debris Release 12.1	Date:	2024-02-19
Technical Description	Revision:	1.11
Reference: R077-231rep_01_11_Debris_Technical Description.docx	Status:	Final

FEV etamax GmbH   Page 169 / 173

- The second program corresponds to the raytracing technique implemented in the enhanced software, firing the rays from the plate and weighting the ray data with the cosine of the impact angle.

The ray hits were recorded and the factors computed analytically in the previous section evaluated. The results are shown in the following two subsections.

The ray hits were counted on both sides of the plate. The case for a box was derived from the single plate results.

A.3.2 Results when the Rays are fired from a Unit Sphere

The program K_SPHERE was run with 2.0E6 rays, with two velocity configurations. The first is the extreme case where the plate velocity equals the particle velocity, the second the case treated in the previous chapter, i.e. with 16.8 particle velocity and 7.6 plate velocity. The ray scaling factor is 0.001.

The results are presented in tables A-5 and A-6.

Case 1: $v_s = v_m = 9.25$

	$v_s = 0$	$v_s = 9.25$						
β [deg]	N/A	0	15	30	45	60	75	90
Nhit positive	12911	34090	32996	29836	25839	20468	15577	10898
Nhit negative	13050	0	68	489	1679	3702	6836	10737
Nhit total	25961	34090	33064	30325	27518	24170	22413	21635
Flux positive	119.4	473.9	457.1	409.6	346.0	262.7	186.6	119.3
Flux negative	120.7	0	0.15	2.1	10.1	29.4	65.3	116.8
Flux total	240.1	473.9	457.2	411.8	356.1	292.1	251.9	236.1
Flux total 3 plates	717.3	945.0	943.2	938.8	950.1	938.8	943.2	946.3
Imp. angle positive	44.9	38.0	34.5	36.6	40.2	44.9	50.3	51.9
Imp. angle negative	45.0	--	84.5	79.3	73.5	67.9	62.1	51.6
k_f factor	0.995	2.0	2.0	1.99	1.94	1.8	1.48	1.01
f_t factor	N/A	1.97	1.9	1.72	1.48	1.22	1.05	0.98
k factor	N/A	3.94	3.8	3.42	2.87	2.2	1.55	0.99
f_t^t factor	N/A	1.32	1.32	1.31	1.33	1.31	1.32	1.32

Table A-5　　　　Results from K_SPHERE with $v_s = v_m = 9.25$

Case 2: $v_s = 7.6$; $v_m = 16.8$

	$v_s = 0$	$v_s = 7.6$						
β [deg]	N/A	0	15	30	45	60	75	90
Nhit positive	12893	21278	21071	20071	18555	16835	14563	12510
Nhit negative	12787	5855	6091	6567	7544	8890	10719	12567
Nhit total	25680	27133	27162	16638	26099	25725	25282	25077
Flux positive	216.6	455.6	448.5	420.0	377.5	328.5	269.1	215.8
Flux negative	214.8	65.5	69.5	80.2	99.8	129.1	170.7	216.6
Flux total	431.4	521.1	518.0	500.2	477.2	457.6	439.7	432.4
Flux total 3 plates	1301	1386	1389	1390	1387	1390	1389	1386
Imp. angle positive	44.9	39.4	39.8	40.7	41.9	43.5	45.3	47.2
Imp. angle negative	45.3	52.5	52.0	52.4	51.6	50.5	49.3	47.4
k_f factor	1.004	1.75	1.73	1.68	1.58	1.44	1.22	1.0
f_t factor	N/A	1.21	1.20	1.16	1.11	1.061	1.02	1.0
k factor	N/A	2.12	2.08	1.95	1.75	1.53	1.24	1.0
f_t^t factor	N/A	1.065	1.068	1.068	1.066	1.068	1.068	1.065

Table A-6   Results from K_SPHERE with $v_s = 7.6$ $v_m = 16.8$

A.3.3 Results when the Rays are fired from plate centre

The program K_PLATE simulates the ESABASE approach by firing particles from the plate (centre) in random directions. The impact flux is computed.

The program K_PLATE was run with 26000 rays and with two velocity configurations. The same cases are studied as in the previous section. The flux scaling factor is 0.001.

The results are presented in tables A-7 and A-8.

Case 1: $v_s = v_m = 9.25$

	$v_s = 0$	$v_s = 9.25$						
β [deg]	N/A	0	15	30	45	60	75	90
Nhit positive	12929	26000	25531	24291	22108	19563	16247	13107

	$v_s = 0$	$v_s = 9.25$						
β [deg]	N/A	0	15	30	45	60	75	90
Nhit negative	13071	0	469	1709	3892	6437	9753	12893
Nhit total	26000	26000	26000	26000	26000	26000	26000	26000
Flux positive	59.71	238.7	231.8	209.1	174.2	136.7	94.61	60.43
Flux negative	60.0	0	0.1	1.01	5.2	15.0	33.2	59.38
Flux total	119.7	238.7	231.9	210.2	179.5	151.7	127.8	119.8
Flux total 3 plates	361.1	478.8	479.9	481.9	481.6	481.9	479.9	478.8
Imp. angle positive	45.1	33.9	34.5	36.9	40.4	44.8	50.3	56.2
Imp. angle negative	45.4	--	84.6	79.1	73.7	67.8	62.2	56.0
k_f factor	1.0	2.0	2.0	1.99	1.94	1.8	1.48	1.01
f_t factor	N/A	1.99	1.94	1.76	1.5	1.27	1.07	1.0
k factor	N/A	3.98	3.88	3.5	2.91	2.29	1.58	1.01
f_t^t factor	N/A	1.33	1.33	1.34	1.33	1.34	1.33	1.33

Table A-7   Results from K_PLATE with $v_s = v_m = 9.25$

Case 2: $v_s = 7.6$; $v_m = 16.8$

	$v_s = 0$	$v_s = 7.6$						
β [deg]	N/A	0	15	30	45	60	75	90
Nhit positive	12913	18894	18585	18054	17179	16027	14542	12979
Nhit negative	13087	7106	7415	7946	8821	9973	11458	13021
Nhit total	26000	26000	26000	26000	26000	26000	26000	26000
Flux positive	108.1	230.2	224.3	211.0	190.4	165.1	136.6	109.0
Flux negative	109.6	32.7	35.0	40.5	51.1	65.3	84.4	109.2
Flux total	217.7	292.8	259.3	251.5	241.4	230.4	221.0	218.2
Flux total 3 plates	654.9	700.3	698.5	700.0	699.9	700.0	698.5	700.3
Imp. angle positive	45.0	39.6	39.7	40.8	42.0	43.4	45.3	47.5

	$v_s = 0$	$v_s = 7.6$						
β [deg]	N/A	0	15	30	45	60	75	90
Imp. angle negative	45.0	52.8	52.1	52.4	51.2	50.5	49.3	47.3
k_f factor	0.99	1.75	1.73	1.68	1.58	1.43	1.24	1.0
f_t factor	N/A	1.21	1.19	1.16	1.11	1.058	1.02	1.0
k factor	N/A	2.12	2.06	1.95	1.75	1.51	1.26	1.0
f_t^t factor	N/A	1.069	1.067	1.069	1.069	1.069	1.067	1.069

Table A-8   **Results from K_PLATE with v_s = 7.6 v_m = 16.8**

A.4 Conclusions and Discussion

The numerical results presented in the previous sections prove full agreement between the *k* and f_t factors computed analytically or numerically.

The main conclusions are:

- For a plate, the flux is strongly dependent on the orientation of the plate with respect to the flight direction. Also the total flux (i.e. the f_t factor) depends on this. For a plate in LEO, the flux increase when the plate is normal to the flight direction compared to the flux when parallel to the flight direction amounts to *20%.*

- The ray tracing technique used in ESABASE perfectly captures the true particle flux situation, provided that the cosα term (angle between impact direction and surface normal) is introduced in the flux computation.